*Chemical Studies on Wood Hemicelluloses. I. On the Hemicellulose of Japanese Beech Wood. I**

By Seishi MACHIDA, Mitsumasa INANO and Yasuo MATSUMURA

(Received September 8, 1956)

Introduction

Concurrently with the development of an improved type of chemical pulp has appeared the need for still more minute knowledge of the carbohydrates associated with wood cellulose[1].

Generally speaking, more hemicelluloses, which are said to have undesirable influences upon the manufacture and qualities of viscose or acetate rayon[2], are contained in the chemical pulp from deciduous wood than from coniferous. But the chemical structure of wood hemicellulose is not yet clear. The deciduous woods, for all that, have recently appeared to be used increasingly for the dissolving pulp in Japan, owing to unavoidable circumstances of natural sources.

This research was designed to find out a suitable method of analysing wood hemicellulose by paper chromatography; and the behaviour of hemicelluloses in Japanese beech wood (*Fagus crenata* Blume) during the pulping processes was analysed. The state of hemicelluloses in wood pulp was also investigated.

Experimental Results and Discussion

(1) Preparation of Samples.—Beech wood grown in Hokkaido was employed in the present study. The normal analysis is shown in Table I.

TABLE I
THE COMPOSITION OF THE JAPANESE BEECH WOOD

	(%)
Ash	0.55
Extract with alcohol-benzene	1.50
Lignin	22.76
Pentosan	19.86
Uronic acid	0.76
Total cellulose	54.80
α-cellulose	40.61
β-cellulose	6.74
γ-cellulose	7.45

a. Wood.—Sawdust (40 mesh) of the wood was air-dried.

b. Unbleached Pulp.—Chips of the wood were cooked by sulfite pulping process using calcium base.

Cooking liquor: total SO_2 7%, combined SO_2 0.8%, liquor ratio 1 : 5. Time to 100°C, 2; time from 100°C to 110°C, 2; time from 110°C to 140°C, three hours. Maximum temperature, 140°C; maximum pressure, 7 atm. Cooking time at maximum temperature, five hours.

The pulp resulting from the procedure was washed and air-dried. Cuprammonium viscosity:** 4.20.

c. Bleached Pulp at the First Step.—Fifty grams of the unbleached pulp were treated with 1665 ml. of water containing 5.65 g. of chlorine for an hour. After the bleaching, the sample was washed with water until the filtrate indicated no reaction with potassium iodide-starch test paper, and air-dried.

d. Bleached Pulp at the Second Step.—Thirty grams of the said pulp were secondly treated with 600 ml. of NaOH solution at 90–95°C for an hour. The amount of NaOH used was 7% of that of the pulp. The pulp was washed and dried. Cuprammonium viscosity, 4.24.

e. Bleached Pulp at the Third Step.—Sixteen gram of the pulp were subsequently bleached with 300 ml. of water containing 1 g. of NaClO and 0.1 g. NaOH at 50°C for four hours. Cuprammonium viscosity, 4.06.

(2) Analytical Procedure of Hemicellulose.—As the hemicellulose was not satisfactorily extracted with alkali directly from the wood[3], holocellulose was prepared from each sample by Wise's method[4].

About 4 g. of the holocellulose was mixed with 72% sulfuric acid at room temperature. After 17.5 hours, the solution was diluted with water to a concentration of 4% sulfuric acid, heated in a bath of boiling water, neutralized with barium carbonate using congo-red test paper and filtered. The filtrate was evaporated to 50 ml.

The component sugars in each hydrolysate of the sample were detected by paper chromatography.

As much work has been done on the paper

* Read before the 9th Annual Meeting of the Chemical Society of Japan on April 5, 1956 at Kyoto.

1) W. J. Polglase; "Advances in Carbohydrate Chemistry," Vol **10**, (1955), p. 283.

2) G. Jayme and U. Schench *Mell. Textilber.*, **31**, 153 (1950).

** Cuprammonium viscosity means the specific viscosity of the solution of 50 mg. sample in 100 ml. Schweizer's reagent at 20°C.

3) H. Sobue and A. Hatano, *J. Chem. Soc. Japan. Ind. Chem. Sec.*) **55**, 131 (1952).

4) L. E. Wise and E. K. Ratliff, *Anal. Chem.*, **19**, 459 (1947).

...STRY HALL LIBRARY

chromatography of carbohydrates[5], various solvents were tested to find the most suitable method for the present research. After many preliminary experiments, it became clear that the use of circular chromatograms which were reported by Buurman[6] would have certain advantages. R_f values of reference-sugars obtained are shown in Table II.

TABLE II

R_f VALUE OF REFERENCE-SUGARS

Sugars	Butanol-acetic acid-water (4 : 5 : 1)	Butanol saturated with water	Phenol saturated with water	Butanol-pyridine-water (4 : 1 : 2)
Arabinose	0.46	0.15	0.58	0.41
Xylose	0.47	0.17	0.49	0.46
Glucose	0.38	0.10	0.40	0.36
Galactose	0.35	0.09	0.45	0.33
Mannose	0.44	0.15	0.47	0.40

(3) Composition of Beech Pulp Hemicellulose.—Referring to the results mentioned above, the chromatographic separations were carried out on a sheet of Toyo-Roshi No. 2 filter-paper with the solvent mixture of *n*-butanol-pyridine-water (4 : 1 : 2).

Aniline hydrogen phthalate in *n*-butanol was used as a spray to reveal the sugars[7]. In every case where a sugar was indicated by R_f value, the identity was established by running further chromatograms with reference-sugar spots. And each component sugar was analysed quantitatively according to Buurman[6]. The results obtained are shown in Table III.

TABLE III

COMPOSITION OF HEMICELLULOSE OF BEECH WOOD

	Xylan	Araban	Mannan	Uronic acid
Wood	19.7	1.0	0.1	0.76
Unbleached pulp	5.7	trace	trace	0.26
Bleached pulp at the 1st step	5.0	—	trace	0.44
Bleached pulp at the 2nd step	3.1	—	trace	0.49
Bleached pulp at the 3rd step	2.8	—	trace	0.58

Uronic acid is perhaps 4-O-methyl-D-glucuronic acid. Rhamnose was not found in the hemicellulose, which differs from that of European beech wood (*Fagus sylvatica*) reported by Aspinall et al[8].

It is found, as is shown in Table III, that the greater part of xylan is removed from the wood during the sulfite cooking. Oxidative bleaching is less effective for the removal of the remaining xylan than the alkali treatment. About 3% of xylan still remains in the final pulp, which is so-called resistant xylan.

Mannan is contained in the original wood in small amount, but a trace of it is found to remain still in the final pulp without being removed in each step of the pulping process.

Both xylan and mannan, having similar chemical structure to cellulose, are considered to exist not only in the amorphous but also in the crystalline region of cellulose.

Araban contained originally in small quantity in the wood is almost completely removed during the sulfite cooking and chlorine-bleaching.

Uronic acid, which is probably 4-O-methyl-D-glucuronic acid, is found to be ruptured during the sulfite cooking, but D-glucuronic acid is formed again in the subsequent oxidative treatments of the pulp. Koike[9] found that most of the carboxyl group is distributed in the outer secondary lamellae. The fact that two-thirds of the carboxyl group is removed during the sulfite cooking indicates that the cooking liquor penetrates tolerably into the cell walls.

It was found by electron microscopy that these bleaching reactions proceed topochemically***. At any rate, the hemicellulose consisting mainly of xylan, mannan and uronic acid was found to be contained in the beech wood pulp for all the bleaching reactions; further treatment is needed to remove the residual xylan and mannan from the wood cellulose.

It is a characteristic of wood hemicellulose that it is very firmly associated with cellulose. The studies of the molecular structure of the Japanese beech wood hemicellulose will be published in subsequent papers.

Summary

1. A suitable method of analysing wood hemicelluloses by paper chromatography was studied.

2. The behavior of hemicellulose in Japanese beech wood (*Fagus crenata* Blume) during the chemical pulping processes was studied; the state of the hemicelluloses in wood pulp was investigated.

The beech wood used in this work was generously provided by Dr. H. Okada of Kokusaku Pulp Ind. & Co. Ltd.

Chemical Laboratory of Textile Fibers
Kyoto University of Industrial
Arts and Textile Fibers, Kyoto

5) G. N. Kowkabany, "Advances in Carbohydrate Chemistry," Vol. 9, 303 (1954).
6) A. Buurman, *Text. Res. J.*, **23**, 888 (1953).
7) S. M. Partridge, *Nature*, **164**, 443 (1949); S. Machida, M. Inano, This Bulletin, **28**, 630 (1955).
8) G. O. Aspinall, E. L. Hirst and R. S. Mahomed, *J. Chem. Soc.*, **1954**, 1734.
9) R. Koike and S. Nagatomo, *J. Tappi*, **9**, 375 (1955).
*** The results will be published elsewhere.

Molecular Rotations of Glucides in Relation to their Structures. I. The Absolute Configuration of γ-Lactones

By Shukichi YAMANA

(Received September 29, 1956)

Introduction

About the problem of the absolute configuration of an optically active molecule, several studies were undertaken from the standpoint of X-ray analysis of a substance[1], or by calculation of the signs of optical rotatory powers of appropriate molecules[2].

Referring to the hypothesis that the sign of the optical rotatory power of a molecule under investigation is determined by Kirkwood's term $g^{(0)}$, Wood, Fickett and Kirkwood presumed the absolute configuration of the enantiomorph of 2,3-epoxybutane[2]. They first divided the molecule of 2,3-epoxybutane into the following unit groups; a three-membered ring with attached hydrogen atoms and two methyl groups which combine with the ring. Next, by using experimental data, they calculated the partial rotations caused by dynamical coupling effects between these unit groups. However, for lack of experimental data in relation to the three-membered ring, they could not calculate the partial rotations caused by the dynamical coupling effects with which the three-membered ring is concerned. Therefore, they resorted to a quasi-empirical evaluation of them, by using the experimental datum of the optical rotatory power of configurationally related 1,2-epoxypropane. Formerly, Kirkwood proposed a convenient method of calculation of the partial rotation caused by the dynamical coupling effect of OH group, in calculating the optical rotatory power of secondary butyl alcohol[3],*1. To evaluate the optical rotatory powers of polypeptides of alanine, Murakami used a concept of bond-interaction in place of the idea of group-interaction and proposed a method of calculation of the partial rotation caused by the dynamical coupling effect of C=O bond. He demonstrated also that the observed values of optical rotatory power were proportional to the values calculated by Kirkwood's polarizability theory[4]. It was explained that the contribution of the one-electron effect[5] is much smaller than that of the dynamical coupling effect[6].

The author presumed the absolute configuration of γ lactones of a five-membered ring, by using a method*2 which was devised by adopting the conception of Freudenberg's Verschiebungssatz[7] on the basis of Kirkwood's group-interaction method[3] and Murakami's bond-interaction method[4]. In order to avoid the difficulty caused by the impossibility of calculation of the terms with which the five-membered ring is concerned, a new method, different from Kirkwood's, was proposed*3.

Theoretical Formulae

The molecular rotation of plane polarized light of wave-length λ by an optically active substance is given as follows[3],

$$[\mathrm{M}]=\frac{288\pi^2 N}{\lambda^2}\cdot\frac{n^2+2}{3}g. \qquad (1)$$

where N is Avogadro's number and n is the refractive index of the medium (solution or pure liquid). If every one of the substituent groups of the molecule—strictly speaking, unit groups made by division of the molecule—has its own optical axis of cylindrical symmetry,

$$g\fallingdotseq g^{(0)}=\frac{1}{6}\sum_{i}^{N}\sum_{k=1}^{N}\alpha_i\alpha_k\beta_i\beta_k G_{ik}\boldsymbol{R}_{ik}(\boldsymbol{b}_i\times\boldsymbol{b}_k)^{*4}$$

1) A. F. Peerdeman, A. J. van Bommel and J. M. Bijvoet, *Koninkl. Ned. Akad. Wetensckap. Proc.*, B. **54**, 16 (1951).

2) W. W. Wood, W. Fickett and J. G. Kirkwood, *J. Chem. Phys.*, **20**, 561 (1952).

3) J. G. Kirkwood, *J. Chem. Phys.*, **5**, 479 (1937).

*1 Ref. "Molecular Model and Data Used" in this article.

4) H. Murakami, This Bulletin, **27**, 246 (1954), **28**, 583 (1955).

In these papers, the author presumed that the proportional constant depends upon the quantitative ratio between various isomers in the equilibrium state.

5) W. J. Kauzmann, J. E. Walter and H. Eyring, *Chem. Rev.*, **26**, 339 (1940).

6) W. Kuhn, *Z. Electrochem.*, **56**, 506 (1952).

*2 The idea of this method had already been demonstrated in the previous paper, (S. Yamana, This Bulletin, **23**, 259 (1950)).

7) K. Freudenberg und W. Kuhn, *Ber.*, **64**, 726 (1931).

*3 Ref. "Method Proposed" in this paper.

*4 The error of signs in reference (3) is corrected in reference 2).

$$G_{ik}=\frac{1}{R^3_{ik}}\left[\vec{b_i}\cdot\vec{b_k}-3\frac{(\vec{b_i}\cdot\vec{R_{ik}})(\vec{b_k}\cdot\vec{R_{ik}})}{R^2_{ik}}\right]$$

$$\vec{R_{ik}}=\vec{R_k}-\vec{R_i}$$

where α_i (mean polarizability of group or bond i) $=(3/4\pi N)\cdot\sum_s^{(i)} A_s$, but A_s is atomic refraction; β_i (anisotropy ratio of the polarizability of group or bond i) $=\alpha_{11}^{(i)}-\alpha_{22}^{(i)}/\alpha_i$, but $\alpha_{11}^{(i)}$ and $\alpha_{22}^{(i)}$ are components of α_i parallel and perpendicular to $\vec{b_i}$ and β_i can be calculated from the depolarization-degree Δ of light, scattered by vapor; $\vec{b_i}$ (unit vector along the optical symmetry axis of group or bond i) and $\vec{R_i}$ (vector distance from the center of mass of the molecule to the center of mass of group or bond i) are determined from the geometry of the molecule.

Molecular Model and Data Used

γ-Lactones to which the calculations were applied and their corresponding molecular rotations, are as follows,

Name	Unit Groups	$[M]_D^{20}$(W)	Lit.
D-erythronic γ-lactone	[CO, $(OH)^{2\alpha}$,*5, $(OH)^{3\alpha}$, Ring]*6	−86.5°	(a)
D-threonic γ-lactone	[CO, $(OH)^{2\beta}$, $(OH)^{3\alpha}$, Ring]	−36.6°	(b)
L-threonic γ-lactone	[CO, $(OH)^{2\alpha}$, $(OH)^{3\beta}$, Ring]	36.6°	(b)

Square brackets [ ], written on the right side of these names imply unit groups of the corresponding γ-lactone molecules, and any two members of these unit groups in the same square bracket couple together to produce their own partial molecular rotation. (ref. Fig. 1). Haworth's perspective formulae of these γ-lactones are shown in Fig. 1.

It was concluded that all of four carbon atoms and one oxygen atom of the aldo-

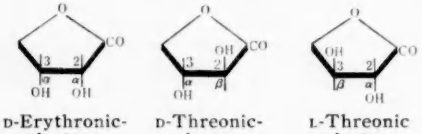

D-Erythronic-γ-lactone D-Threonic-γ-lactone L-Threonic γ-lactone

Fig. 1. Haworth's perspective formulae

furanose ring lie on one plane — namely, the γ-lactone ring plane — from the results of investigations measuring the dipole moment[8] of an aldofuranose molecule and examining its crystal with X ray[9].

In order to simplify the calculations, the values of bond lengths and valency angles were assumed as follows*7,

(1) The lengths of C—C and C—O bonds in the γ-lactone ring are all 1.54Å, that is to say, the γ-lactone ring plane is a regular pentagon and the length of its side is 1.54Å.

(2) C=O bond (its length is 1.24Å)[c] projects out from C^1-atom*8, in the direction of the extension line from the center of the ring to C^1-atom.

(3) The hydroxyl oxygen atom (represented by O^k) and H atom combine with C atom of the γ-lactone ring and the angle $\angle O^kCH$ (tetrahedral angle = 109°28′) is bisected by the γ-lactone ring plane. The length of $C\text{-}O^k$ bond is 1.42 Å*9. The refractive indices of aqueous solutions of three γ-lactones given in Fig. 1, whose concentrations are suitable for measurement of the optical rotatory power, can be considered equal*10.

Concerning the experimental data and the manner of treatment of OH groups and of C=O bond, the following two methods of treatment were employed.

Kirkwood's Treatment[3].— It is supposed that OH group has its optical axis of cylindrical symmetry directed along its bond to C atom, and the optical center of OH group is located at O atom*11. Values of mean polarizability α and of anisotropy

*5 $(OH)^{2\alpha}$ means OH group, which combines with 2-position of the ring in α-orientation. (ref. L. F. Fieser, *J. Am. Chem. Soc.*, **72**, 623 (1950)).

*6 Because of the small polarizabilities of H atom and C-H bond, they can be neglected.

a) Ruff, *Ber.*, **32**, 3679 (1899).

b) K. Gätzi and T. Reichstein, *Helv. Chim. Acta.*, **20**, 1298 (1937).

8) H. Hilbert and J. S. Allen, *J. Am. Chem. Soc.*, **54**, 4115 (1932).

9) E. G. Cox and T. H. Goodwin, *J. Chem. Soc.*, **1932**, 1844.

*7 In the calculation of the optical rotatory power by Kirkwood's polarizability theory, a small deviation in atomic distance or in valency angle causes only a small deviation in the calculated value of optical rotatory power. Concerning a concrete example of the magnitude of this deviation, refer to the next paper "Molecular Rotations of Glucides in Relation to their Structures. II."

c) M. Kimura and Y. Kurita, *J. Chem. Soc. Japan*, **72**, 396 (1951).

*8 C^1-atom means the C atom at 1-position of the ring.

*9 The mean value of lengths of C-O bonds in α-D-glucose. (ref. T. R. R. Mc Donald and C. A. Beevers, *Acta Cryst.*, **5**, 654 (1952)).

*10 For determination of optical rotatory power of a sugar-group substance, about 2% aqueous solution is used in general, and the value of n of it is about 1.34.

*11 This manner of treatment was rejected by Gorin, J. Walter and H. Eyring (*J. Chem. Phys.*, **6**, 824 (1938)), because it regards a single OH group as isotropic. The author of this paper, however, thought that this was very convenient and useful for approximate estimation of partial rotation of the OH group, especially when optical rotatory power of such a substance which has many OH groups in its molecule as a sugar was the subject. Besides, for lack of data for C-O and O-H bonds, OH group cannot be divided into its component bonds.

ratio β of OH group are 1.04×10^{-24} (cc)[d] and 0.35[e] respectively.

Murakami's Treatment.[f]—It is supposed that C=O bond has its optical axis of cylindrical symmetry directed along itself. The optical center of C=O bond is located at its center of mass. Value of $\alpha\beta$ of C=O bond is $(19.4-8.0)\times10^{-25}=1.14\times10^{-24}$ (cc)[f].

Method Proposed

Partial molecular rotations of the plane polarized light of wave-length of D line at 20°C, represented by the notation $[\mu]^{20}_{D}$, caused by the dynamical coupling effect between any two members of unit groups in the molecular model of γ-lactone, were calculated by using Eq. (1). Of course, the molecular rotation is the sum of the partial molecular rotations, namely

$$[M]^{20}_{D}=\sum[\mu]^{20}_{D}$$

where $\sum$ means the summation over all $[\mu]^{20}_{D}$s possible. Therefore, for the calculated values, the following equation can be obtained.

$$[M]^{20}_{Dcalcd}=\sum[\mu]^{20}_{Dcalcd} \qquad (2)$$

where the suffix calcd means the calculated value. For the observed values,

$$[M]^{20}_{Dobs}=\sum[\mu]^{20}_{Dobs}{}^{*12} \qquad (3)$$

The results of calculation are given in Table I.

TABLE I

$[\mu]^{20}_{Dcalcd}$ $(3/n^2+2)$, CAUSED BY THE DYNAMICAL COUPLING EFFECT BETWEEN ANY TWO MEMBERS OF UNIT GROUPS (EXCEPT RING), WITH REGARD TO HAWORTH'S PERSPECTIVE FORMULAE

	3β	3α	2β	2α
CO	4.9	−4.9	21.0	−21.0
2α	4.4	0		
2β	0	−4.4		

Note: 2α is an abbreviated symbol of $(OH)^{2\alpha}$, and so on.

If the theory used for the calculation of optical rotatory power is perfect and data which are used in calculation are satisfactory, the calculated value, $[M]^{20}_{Dcalcd}$, must be equal to the observed value, $[M]^{20}_{Dobs}$, in sign and magnitude. However, in fact, they are not equal, owing to the imperfectness of the theory, and of assumptions and to the errors of data used. Generally, $[M]^{20}_{Dcalcd}$ by Kirkwood's polarizability theory is equal to $[M]^{20}_{Dobs}$ in sign, and the magnitude of the former can be made equal to that of the latter by multiplying by a proportionality-constant[f],*13. Therefore,

$$[M]^{20}_{Dobs}=\kappa[M]^{20}_{Dcalcd} \qquad (4)$$

where κ is always positive. If the orientation of one unit group in a molecular model changes, $[M]^{20}_{Dobs}$ and $[M]^{20}_{Dcalcd}$ change to $[M']^{20}_{Dobs}$ and $[M']^{20}_{Dcalcd}$ respectively. By the change of the orientation of a unit group, a new molecule appears. For this new molecule,

$$[M']^{20}_{Dobs}=\kappa[M']^{20}_{Dcalcd} \qquad (5)$$

where $[M']^{20}_{D}$ means the molecular rotation of a new substance. From Eq. (5) minus Eq. (4),

$$[M']^{20}_{Dobs}-[M]^{20}_{Dobs}=\kappa([M']^{20}_{Dcalcd}-[M]^{20}_{Dcalcd})$$

or
$$\Delta[M]^{20}_{Dobs}=\kappa\Delta[M]^{20}_{Dcalcd} \qquad (6)$$

In (6), as κ is always positive, if, concretely speaking, the orientation of a unit group changes in a molecule, the observed value of its optical rotatory power changes toward the same direction as the calculated value. Accordingly, in calculation, with regards to a definite molecular model, of $\Delta[M]^{20}_{D}$ due to the orientation-change of a unit group, if $\Delta[M]^{20}_{Dcalcd}$ has the same sign as $\Delta[M]^{20}_{Dobs}$ this molecular model must be a structurally correct representation of the absolute configuration. On the other hand, if they are different in sign, the model used must be incorrect. In short, the problem of the absolute configuration becomes the problem of the sign of κ of Eq. (6) or (4). The author will illustrate the above-described principle, by using concrete examples. As is seen in Fig. 1, if the ori-

d) Landolt-Börnstein, Physikalisch-Chemische Tabellen, Hw. 2. p. 985.

e) Values obtained by Ramakrishna-Rao; see Landolt-Börnstein, Physikalisch-Chemische Tabellen, 5th Ed., Eg. 2. p 90, 91.

f) Sheng-Nien Wang, *J. Chem. Phys.*, **7**, 1012 (1939).

*12 In the actual experiments, $[\mu]$ can not be observed. Then strictly speaking, $[\mu]^{20}_{Dobs}$ is of hypothetical character.

*13 In this case, the value of the proportionality-constant depends upon various factors, chiefly owing to the effect of solvation.

entation of OH group which combines with 2-position of the ring in the molecular model of D-erythronic γ-lactone changes from α to β, the molecular model of D-threonic γ-lactone can be obtained, and if the orientation of OH group, which combines with 3-position of the ring in the molecular model of D-erythronic γ-lactone changes from α to β, the molecular model of L-threonic γ-lactone can be obtained. Therefore, by calculation, with regards to Haworth's perspective formulae, of $\Delta[M]^{20}_{D}$ caused by the above-described two orientation-changes we can presume the absolute configuration of γ-lactones. That is to say, if $\Delta[M]^{20}_{D\text{calcd}}$ is in the same direction as that of $\Delta[M]^{20}_{D\text{obs}}$, Haworth's perspective formula (accordingly, Fischer convention)[10] is presumed to be a structurally correct representation of absolute configuration, and if the change is in the opposite direction, the formula is presumed to be incorrect. This method of presumption of the absolute configuration can be easily subjected to calculation with regards to D-erythronic- and D-threonic-γ-lactones, as follows; $[\mu]^{20}_{D\text{calcd}}(3/n^2+2)$, caused by the dynamical coupling effects between OH group which combines with 2-position of the ring and the other unit groups in these molecules are given below. (ref. Table I)

	CO	3α	Ring	Sum
2α	-21.0	0	$(2\alpha)\times$Ring*14	$-21.0+(2\alpha)\times$Ring
2β	21.0	-4.4	$(2\beta)\times$Ring	$16.6+(2\beta)\times$Ring

From Eq. (2), $\Delta[M]^{20}_{D\text{calcd}}=\sum\Delta[\mu]^{20}_{D\text{calcd}}$

Therefore, $\Delta[M]^{20}_{D\text{calcd}}$ (namely, $\sum\Delta[\mu]^{20}_{D\text{calcd}}$) due to the orientation-change of OH group which combines with 2-position from α to β in this case is $\{(16.6+(2\beta)\times\text{Ring})-(-21.0+(2\alpha)\times\text{Ring})\}(n^2+2)/3=\{37.6+(2\beta)\times\text{Ring}-(2\alpha)\times\text{Ring}\}(n^2+2)/3$

The corresponding $\Delta[M]^{20}_{D\text{obs}}$ is given by ($[M]^{20}_{D\text{obs}}$ of D-Threonic γ-lactone) minus ($[M]^{20}_{D\text{obs}}$ of D-Erythronic γ-lactone). This is, $-36.6-(-86.5)=49.9$

By using these values, Eq. (6) becomes as below,

$$49.9=\kappa\{37.6+(2\beta)\times\text{Ring}-(2\alpha)\times\text{Ring}\}(n^2+2)/3. \quad (7)$$

The author's purpose was to know the sign of κ, but to his regret, he was unable to calculate $(2\alpha)\times$Ring and $(2\beta)\times$Ring, owing to lack of data for α, β and $\vec{b}$ etc. of Ring. Kirkwood used a quasi-empirical method in order to avoid the difficulty of calculating $[\mu]_D$ due to a three-membered ring*15, but the author devised a new quasi-empirical method, different from that of Kirkwood, as follows.

The same treatment was tried at 3-position of the ring, in the molecular model of D-erythronic γ-lactone as that which was carried out at 2-position, above, and the following equation was obtained.

$$123.1=\kappa\{14.2+(3\beta)\times\text{Ring}-(3\alpha)\times\text{Ring}\}(n^2+2)/3 \quad (8)$$

On the other hand, owing to the symmetry of the γ-lactone ring plane

$$(2\alpha)\times\text{Ring}=(3\beta)\times\text{Ring}$$

and $$(2\beta)\times\text{Ring}=(3\alpha)\times\text{Ring}$$

Combining these two conditional equations with Eqs. (7) and Eq. (8)

$$\kappa=10.02/n^2+2$$

where n^2 is always positive, then $\kappa>0$*16. This result indicates that the Fischer convention is a structurally correct representation of absolute configuration, and this is consistent with those of Bijvoet[1] and Kirkwood[2].

Summary

The changes in optical rotatory power of γ-lactone due to orientation-changes of a unit group in the molecule were calculated by using the Kirkwood's polarizability theory with regard to molecular model, derived from Haworth's perspective formula. The Fischer convention was presumed to be the structurally correct representation of absolute configuration.

10) Wohl and Freudenberg, *Ber.*, **56**, 309 (1923).

*14 $(2\alpha)\times$Ring means $[\mu]^{20}_{D\text{calcd}}(3/n^2+2)$, caused by the dynamical coupling effect between $(OH)^{2\alpha}$ group and ring.

*15 Ref. "Introduction" of this paper.

*16 By using n=1.34 (ref. *10), $\kappa=2.64$. That is to say, $[M]^{20}_{D\text{obs}}$ is about 2.64 times as large as $[M]^{20}_{D\text{calcd}}$.

The value of κ(2.64) happens to be very consistent with the value of $\kappa=3.97/1.43=2.78$, obtained by T. C. Kwoh and H. Eyring (*J. Chem. Phys.*, **18**, 1186 (1950)) for the optical rotatory power of the acetone solution of benzoin.

The author wishes to express his sincere gratitude to Professor S. Tanaka (Kyoto University) for his valuable advice and kind encouragement throughout the course of this study.

Department of Chemistry
Kyoto Gakugei University
Fushimi-ku, Kyoto

Molecular Rotations of Glucides in Relation to their Structures. II. The Conformation and the Absolute Configuration of Aldopyranoses. Physical Meaning of Hudson's Isorotation Rule

By Shukichi YAMANA

(Received October 1, 1956)

Introduction

The problem of stereochemical structure of the aldopyranose-ring in its aqueous solution is not yet solved. By x-ray analysis of the crystals of aldopyranoses, Cox, Goodwin and Wagstaff concluded that the aldopyranose-ring is composed of five coplanar C atoms and one O atom (the ring-O-atom) situated outside the plane. Such a ring is called Cox's flat ring. They presumed, moreover, that aldopyranose molecules retain Cox's flat ring even in aqueous solutions[1].

From the results of the studies on cuprammonium-glycoside complexes, Reeves concluded that an aldopyranose molecule has a slightly distorted hexagonal structure oriented in one of the Sachse strainless ring[2] conformations, and that all of D-galactose, D-glucose and D-mannose have a chair-form ring of special type (according to Reeves' symbol, C 1 conformation[3],*1.

On the other hand, Hudson reported of the quantitative relation between the structure of pyranoses and the value of their molecular rotations, and found Hudson's isorotation rule, but he could not explain the fact that the magnitude of the anomeric difference*2 of mannose is smaller than those of other pyranoses[4]. Freudenberg explained the above-described fact, paying attention to the orientation of the OH group, which combines with C^2-atom, but his explanation did not imply any physical or mathematical equations[5]. Kauzmann, Walter and Eyring discussed this rule from the standpoint of the one-electron theory, but they insisted upon the fact that the OH group is not isotropic and the orientations of O—H bonds are complex, and they did not give any decisive explanation for this rule[6]. In short, the physical meaning of Hudson's isorotation rule and of the deviation of mannose from this is not yet determined. The author discussed in the preceding article[7] the absolute configuration of γ lactones by using Kirkwood's treatment of OH group, regarding it as nearly isotropic. By using this treatment, the absolute configuration of aldopyranoses was examined as follows*3; The method of investigation was quite similar to that used for the study of γ-lactones. It was, first, to assume a molecular model, and next, to calculate the variation of the molecular rotation of the plane polarized light of the wave-length of D line at 20°C, ($\Delta[M]_D^{20}$), caused by the orientation-change of one unit group in the molecule by using Kirkwood's polarizability theory[8]; lastly, to examine the sign of the proportionality-constant κ, by making the

1) E. G. Cox, T. H. Goodwin and (Miss) A. I. Wagstaff, *J. Chem. Soc.*, **1953**, 1495, part 2.
2) U. Sachse, *Z. Phys. Chem.*, **10**, 203 (1892).
3) R. E. Reeves, *J. Am. Chem. Soc.*, **72**, 1499 (1950).
*1 By X-ray analysis, T. R. R. McDonald and C. A. Beevers came to the conclusion that the structure of α-D-glucose molecule in crystalline state is almost the same as that of Reeves' C 1 conformation, but its bond lengths and valency angles are not simple (ref. T. R. R. Mc Donald and C. A. Beevers, *Acta. Cryst.*, **5**, 654 (1952)).
*2 This is the difference in optical rotation of α and β aldoses.
4) C. S. Hudson and K. P. Monroe, *J. Am. Chem. Soc.*, **41**, 1141 (1919).
5) K. Freudenberg and W. Kuhn, *Ber.*, **64**, 703 (1931).
6) W. J. Kauzmann, J. E. Walter and H. Eyring, *Chem. Rev.*, **26**, 339 (1940).
7) S. Yamana, This Bulletin, **30**, 203 (1957).
*3 Then, unexpectedly, it became possible to presume the conformation of the aldopyranose-ring, and moreover, to understand the physical meaning of Hudson's isorotation rule.
8) J. G. Kirkwood, *J. Chem. Phys.*, **5**, 479 (1937).

Name	Unit Groups	$[M]_D^{20}$(w)	Lit.
α-D-Galactose	[$(OH)^{1\alpha}$, $(OH)^{2\alpha}$, $(OH)^{3\beta}$, $(OH)^{4\beta}$, $(CH_2OH)^{5\beta}$, Ring]	261.0°	(a)
β-D-Galactose	[$(OH)^{1\beta}$, $(OH)^{2\alpha}$, $(OH)^{3\beta}$, $(OH)^{4\beta}$, $(CH_2OH)^{5\beta}$, Ring]	97.6°	(a)
α-D-Glucose	[$(OH)^{1\alpha}$, $(OH)^{2\alpha}$, $(OH)^{3\beta}$, $(OH)^{4\alpha}$, $(CH_2OH)^{5\beta}$, Ring]	198.2°	(a)
β-D-Glucose	[$(OH)^{1\beta}$, $(OH)^{2\alpha}$, $(OH)^{3\beta}$, $(OH)^{4\alpha}$, $(CH_2OH)^{5\beta}$, Ring]	34.7°	(a)
α-D-Mannose	[$(OH)^{1\alpha}$, $(OH)^{2\beta}$, $(OH)^{3\beta}$, $(OH)^{4\alpha}$, $(CH_2OH)^{5\beta}$, Ring]	53.8°	(b)
β-D-Mannose	[$(OH)^{1\beta}$, $(OH)^{2\beta}$, $(OH)^{3\beta}$, $(OH)^{4\alpha}$, $(CH_2OH)^{5\beta}$, Ring]	−29.3°	(b)

calculated value of $\Delta[M]_D^{20}$ proportional to its observed value. However, as it was impossible to calculate the terms concerning the aldopyranose-ring, a new method was applied*1.

Molecular Model and Data Used

Reeves' C 1 conformation and Cox's flat ring were used as the molecular model of the aldopyranose-ring for calculation. These are shown in Fig. 1.

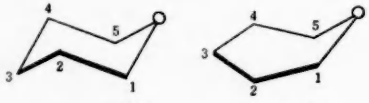

Reeves' C 1 conformation Cox's flat ring

Fig. 1. Aldopyranose-ring
○, ring-O-atoms.

In order to simplify the calculations, the values of bond lengths and valency angles are assumed as follows, by referring to the data in the original papers. That is to say, as for Reeves' C 1 conformation[3], the lengths of C—C and C—O bonds in the ring are assumed to be all 1.54 Å, and that of C—O bond which projects out of the ring to be 1.42 Å*5. The valency angles of C and O atoms are assumed to be a tetrahedral angle (109° 28′). According to Cox's investigations, the geometry of Cox's flat ring is as follows[1]. The lengths of C—C and C—O bonds in the molecule are 1.54 Å and 1.46 Å respectively. As for the corner-angles of the ring, the valency angles of C atoms lie between 113° and 116°, the corresponding limits of the valency angle of O atom being 90° and 106°. Then the author used 114° as the valency angle of C atom which is the mean value of 113° and 116°, therefore the valency angle of O atom became 92°*6. If the hydroxyl oxygen is symbolized by O^h, O^h atom and H atom combine with the same C atom of the ring and the angle $\angle HCO^h$ which is tetrahedral angle, 109° 28′, must be bisected by the plane which is determined by three atoms, namely, C atom and the two atoms besides H- and O^h- atoms attached to this C atom. The unit groups of the aldopyranose molecules were given in square brackets, as shown on the top of this page*7.

It is assumed that the orientation of OH group in $(CH_2OH)^{5\beta}$ as regards the aldopyranose-ring is definite and similar in all of the above-described aldopyranoses. The values of the optical properties of OH group and H atom, used in the preceding article[7] were used without any correction. The refractive indices of aqueous solutions of D-galactose, of D-glucose and of D-mannose, whose concentrations are suitable for measurement of the optical rotatory power, are nearly equal (1.34)*8.

Method Proposed

Partial molecular rotations of the plane polarized light of wave-length of D line at 20°C, represented by $[\mu]_D^{20}$, caused by the dynamical coupling effect between any two members of unit groups (except $(CH_2OH)^{5\beta}$ and Ring) in the aldopyranose molecule, were calculated according to Kirkwood's polarizability theory[8]. The results of the calculation with regard to Reeves' C 1 conformation are given in Table I.

*1 Concerning this method, refer to "Method Proposed" in this article.

*5 This is the mean value of lengths of C-O bonds in α-D-glucose. (ref. *1).

*6 In order to see the magnitude of deviation of $[\mu]_{D\,calcd}^{20}(3/n^2+2)$, caused by a small deviation in bond length or in valency angle, the author tried the other type of Cox's flat ring. In this ring, the valency angle of C atom and of O atom is 116° and 101.5° respectively, and lengths of C-C and C-O bonds in the molecule are 1.54 Å and 1.48 Å (ref. M. Kimura, *J. Chem. Soc. Japan.* **71**, 18 (1950)), respectively. $[\mu]_{D\,calcd}^{20}(3/n^2+2)$, caused by the dynamical coupling effect of the unit groups in this molecular model is given in each parenthesis in Table II.

*7 $(OH)^{1\alpha}$ means OH group which combines with 1-position of the aldopyranose-ring, in α orientation. (ref. L. F. Fieser, *J. Am. Chem. Soc.*, **72**, 623 (1950).)

a) C. N. Riiber, J. Minsaas and R. T. Lyche, *J. Chem. Soc.*, **1929**, 2173.

b) C. N. Riiber und J. Minsaas, *Ber.*, **60**, 2402 (1927).

*8 ref. *10 in the preceding paper (7) cf. "International Critical Tables of Numerical Data," Vol. 2, p 351,347.

	2α	3β	4β	$(CH_2OH)^{5\beta}$	Ring	Sum
1α	6.5	1.7	0	$(1\alpha)\times(CH_2OH)^{5\beta}$,*10	$(1\alpha)\times$Ring	$8.2+(1\alpha)\times(CH_2OH)^{5\beta}+(1\alpha)\times$Ring
1β	−6.5	0	0	$(1\beta)\times(CH_2OH)^{5\beta}$	$(1\beta)\times$Ring	$-6.5+(1\beta)\times(CH_2OH)^{5\beta}+(1\beta)\times$Ring

TABLE I

$[\mu]^{20}_{D\text{calcd}}(3/n^2+2,)$ CAUSED BY THE DYNAMICAL COUPLING EFFECT BETWEEN ANY TWO MEMBERS OF UNIT GROUPS (EXCEPT $(CH_2OH)^{5\beta}$ AND RING), WITH REGARD TO REEVES' C 1 conformation*9

	4β	4α	3β	3α	2β	2α
1α	0	0	1.7	0	0	6.5
1β	0	0	0	−1.7	6.5	−6.5
2α	1.7	0	6.5	−6.5		
2β	0	−1.7	−6.5	0		
3α	0	6.5				
3β	6.5	−6.5				

Note: 1α is an abbreviated symbol of $(OH)^{1\alpha}$, and so on.

Then, $[\mu]^{20}_{D\text{calcd}}(3/n^2+2)$, caused by the dynamical coupling effects between OH group situated in the 1-position of D-galactose molecule and the other unit groups in this molecule are as shown on the top of this page.

If the orientation of $(OH)^1$ group of D-galactose molecule changes from β to α, then the calculated value of the optical rotatory power of this molecule changes and the value of this change is as follows,

$$\Delta[M]^{20}_{D\text{calcd}}=\sum\Delta[\mu]^{20}_{D\text{calcd}}=[\{8.2+(1\alpha)\times(CH_2OH)^{5\beta}+(1\alpha)\times\text{Ring}\}\ \text{minus}\ \{-6.5+(1\beta)\times(CH_2OH)^{5\beta}+(1\beta)\times\text{Ring}\}]\ (n^2+2)/3,$$
$$=(14.7+L)\ (n^2+2)/3$$

where

$$L\equiv(1\alpha)\times(CH_2OH)^{5\beta}-(1\beta)\times(CH_2OH)^{5\beta}+(1\alpha)\times\text{Ring}-(1\beta)\times\text{Ring}.$$

The corresponding $\Delta[M]^{20}_{D\text{obs}}$ is given by, $\{[M]^{20}_{D\text{obs}}$ of α-D-galactose$\}$ minus $\{[M]^{20}_{D\text{obs}}$ of β-D-galactose$\}$. This is (261.0−97.6) =163.4. These two values must be made equal to each other by using a proportionality-constant κ. Then

$$163.4=\kappa(14.7+L)\ (n^2+2)/3. \qquad (1)$$

Of course, the left side and the right side of Eq. (1) show the observed value and the calculated value of the anomeric difference of D-galactose, respectively. By using the method like that mentioned above, two other equations are obtained.

From D-glucose,

$$163.5=\kappa(14.7+L)\ (n^2+2)/3 \qquad (2)$$

and from D-mannose,

$$83.1=\kappa(-4.8+L)\ (n^2+2)/3 \qquad (3)$$

The left side of (1) is nearly equal to that of (2), and this fact is well known as Hudson's isorotation rule[9]. The right side of (1) is equal to that of (2). In other words, the calculated value of the anomeric difference of D-galactose and that of D-glucose is equal. Now, the above-described calculation can be said to bear satisfactory results to explain Hudson's isorotation rule. On the other hand, the anomeric difference of D-mannose is given by Eq. (3), but it is apparent that these values are different from those in Eqs. (1) and (2). Namely, the anomeric difference of D-mannose is different from those of D-galactose and D-glucose. From Eq. (2) minus Eq. (3), $\kappa=12.37/n^2+2$, where n^2 is always positive, then $\kappa>0$. This result means that the Fischer convention from which Reeves' C 1 conformation is derived, is a structurally correct representation of the absolute configuration.

Next, the author applied the method which is analogous to that used in the case of Reeves' C 1 conformation above, to the

TABLE II

$[\mu]^{20}_{D\text{calcd}}(3/n^2+2)$, CAUSED BY THE DYNAMICAL COUPLING EFFECT BETWEEN ANY TWO MEMBERS OF UNIT GROUPS (EXCEPT $(CH_2OH)^{5\beta}$ AND RING), WITH REGARD TO COX'S FLAT RING*11

	4β	4α	3β	3α	2β	2α
1α	−1.1 (−0.9)	1.3 (1.0)	−0.2 (0.2)	2.9 (2.4)	1.4 (2.0)	6.0 (5.5)
1β	0.3 (0.4)	−0.1 (−0.2)	1.8 (1.6)	−2.1 (−2.1)	6.0 (5.5)	−6.4 (−6.2)
2α	1.4 (1.4)	0 (0)	4.5 (4.5)	0 (0)		
2β	0 (0)	−1.4 (−1.4)	0 (0)	−4.5 (−4.5)		
3α	4.5 (4.5)	0 (0)				
3β	0 (0)	−4.5 (−4.5)				

*9 When 1.48 Å (ref. *6) is used as the value of length of C-O bond, the values 6.1 and 1.6 appears in Table 1, instead of 6.5 and 1.7 respectively.

*10 $(1\alpha)\times(CH_2OH)^{5\beta}$ means $[\mu]^{20}_{D\text{calcd}}(3/n^2+2)$, caused by the dynamical coupling effect between $(OH)^{1\alpha}$ and $(CH_2OH)^{5\beta}$.

9) C. S. Hudson, *J. Am. Chem. Soc.*, **31**, 66 (1909).

*11 Concerning the values in parentheses, refer to *6.

case of Cox's flat ring. The results of calculation of $[\mu]_D^{20}(3/n^2+2)$ are given in Table II.

By using these values three equations are obtained.

From D-galactose,

$$163.4=\kappa'(9.0+L')(n^2+2)/3 \quad (4)$$

from D-glucouse,

$$163.5=\kappa'(11.8+L')(n^2+2)/3 \quad (5)$$

and from D-mannose,

$$83.1=\kappa'(-5.2+L')(n^2+2)/3 \quad (6)$$

where κ' is a proportionality-constant and

$$L'\equiv(1\alpha)\times(CH_2OH)^{5\beta}-(1\beta)\times(CH_2OH)^{5\beta}+(1\alpha)\times\text{Ring}-(1\beta)\times\text{Ring}$$

in this case. From Eq. (5) minus Eq. (6),

$$\kappa'=14.19/n^2+2^{*12}$$

where n^2 is always positive; then $\kappa'>0$. That is to say, it is concluded from the result of calculation with regard to Cox's flat ring that the Fischer convention is a structurally correct representation of the absolute configuration. But the right side of Eq. (4) is different from that of Eq. (5). In other words, the calculated value of the anomeric difference of D-galactose is different from that of D-glucose, and this is not consistent with the fact that the observed value of the anomeric difference of D-galactose is equal to that of D-glucose. In short, Hudson's isorotation rule can not be explained by using Cox's flat ring.

*12) By using the values given in the parentheses in Table II, $\kappa''=15.87/n^2+2$, where κ'' is a proportionality-constant for this case.

Conclusion

The results of calculation and presumption in this paper are as follows,

(1) The Fischer convention is a structurally correct representation of the absolute configuration.

(2) If D-galactose, D-glucose and D-mannose are of the same type of ring structure in aqueous solution, and this type should be either Reeves' C 1 conformation or Cox's flat ring, then this common type must be the former and not the latter.

(3) Hudson's isorotation rule can be explained easily, by calculation of the anomeric difference adoption Kirkwood's polarizability theory of optical rotatory power with regard to Reeves' C 1 conformation of an aldopyranose molecule.

The author wishes to express his deepest gratitude to Professor S. Tanaka (Kyoto University) for his valuable advice and kind encouragement throughout this work.

Department of Chemistry
Kyoto Gakugei University
Fushimi-ku, Kyoto

Studies on Meso-ionic Compounds. III[1]. *Reactions of 3-Phenyl-4-bromosydnone*

By Hiroshi KATO and Masaki OHTA

(Received August 28, 1956)

In the first paper of this series[1], the conditions for preparing 3-phenyl-4-bromosydnone (I) from 3-phenylsydnone (II) have been reported in detail, and it has been shown that an excellent result was obtained by treating an ether suspension of II with bromine in the presence of sodium bicarbonate, or by refluxing a chloroform solution of II with N-bromosuccinimide, but an attempt to prepare I by the method described by Baker et al.[2] was unsuccessful. The present investigation was undertaken to study the reactions of I, since previous communications[3] on sydnones have dealt almost exclusively with their unusual structure, and little attention has been paid to their reactions.

1) Part I, II. H. Kato, K. Nakahara and M. Ohta, *J. Chem. Soc. Japan (Pure Chem. Sect.)*, **77**, 1304 (1956).

2) W. Baker, W. D. Ollis and V. D. Poole, *J. Chem. Soc.*, **1949**, 307.

3) Works on this subject are reviewed by M. Ohta in *Chemistry and Chemical Industry Japan*, **9**, 311 (1956).

For instance, what are reported so far about I, are only its methods of preparation[1,2,4] and its decomposition reactions[4,5] by the action of acid or alkali.

When I was treated with sodium salt of *p*-thiocresol, it did not afford the expected 4-*p*-tolyl sulfide of II, but I was reduced to II and *p*-thiocresol was oxidized to form di-*p*-tolyl disulfide (III). The reaction of I with sodium hydrosulfide was then tried, and this procedure gave, quite unexpectedly, II and sulfur as reaction products. The same reaction products were obtained when I was treated with sodium sulfide. Considering the above reactions, it seems reasonable to conclude that I has a marked oxidative property. This consideration is further supported by the observation that iodine was liberated when an ethanolic solution of I and potassium iodide was kept standing at room temperature in the presence of diluted hydrogen chloride.

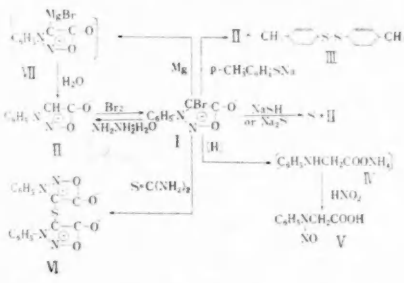

Fig. Reactions of 3-Phenyl-4-bromosydnone.

When warmed with an exess amount of hydrazine hydrate, I was reduced to II, but when an equimolecular amount of hydrazine hydrate in ethanol was used, I was recovered unchanged even after refluxing for prolonged hours. An attempt to remove the bromine atom by the action of diethylamine and Raney nickel was unsuccessful. When I was subjected to reduction with zinc dust in aqueous acetic acid, the bromine atom was removed but was accompanied by a reductive fission of the sydnone ring at the N–N bond, thus affording the ammonium salt of N-phenylglycine (IV), which was identified by conversion to N-nitroso-N-phenylglycine (V). It was not possible to determine which one of the two reactions, viz. the removal of the bromine atom or the cleavage of the sydnone ring, precedes the other. This mode of ring cleavage at the N–N bond is in accord with that reported by Earl[6] in the case of II. Considering this mode of ring cleavage, Earl concluded that, of the structures VIII and IX formerly proposed for the sydnones[7], structure VIII is more favoured. But the fact that

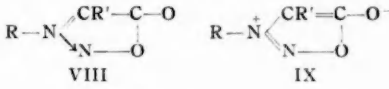

II is considerably soluble in highly polarized solvent e. g., chloroform, acetic acid or pyridine, and only sparingly soluble in carbon tetrachloride, benzine or ether favors rather the betaine type structure IX.

It seems inappropriate to conclude from these data alone reported by Earl, which structure of the two should be more favoured. Moreover, now that the structures of sydnones are best explained by molecular orbital theory[8], a trial to show their structures by conventional covalent formulae seems to have little significance.

When I was treated with thiourea, pale yellow needles (VI) melting at 164—165°C. were obtained. This substance was proved to contain sulfur, and had an empirical formula of $C_{16}H_{10}O_4N_4S$ and was insoluble in 10% sodium hydroxide solution and 10% hydrochloric acid. Woodbridge et al.[9] have reported that the reactions of 4-substituted-2-aminothiazoles with thiourea and iodine or bromine give di-5-thiazolyl sulfides. Considering the properties of VI and the above reactions on thiazoles it is evident that I reacted with thiourea to afford 4-bis (3-phenylsydnonyl) sulfide (VI) by an analogous reaction, though the mechanism of this is not known.

As for the reaction of I with magnesium metal, I did not react even at an elevated temperature when magnesium alone was used, but on adding methyl iodide I began to react smoothly with magnesium metal and went into solution. On decomposing the reaction product with water, II was obtained. From this fact, it is evident that in the presence of methyl iodide, I is capable of forming the corresponding Grignard reagent (VII).

4) J. Kenner and K. Mackay, *Nature*, **158**, 909 (1946).
5) R. A. Eade and J. C. Earl, *J. Chem. Soc.*, **1948**, 2307.
6) J. C. Earl, *Rec. trav. chim. Pay-Bas*, **75**, 346(1956).
7) J. C. Earl, *Chemistry and Industry*, **1953**, 746, W. Baker and W. D. Ollis, *Nature*, **158**, 703 (1936).
8) H. C. Longuet-Higgins, *J. chim. phys.*, **46**, 244 (1949); L. E. Orgel, T. L. Cottrel, W. Dick and L. E. Sutton, *Trans. Faraday Soc.*, **47**, 113 (1951).
9) R. G. Woodbridge and G. Dougherty, *J. Am. Chem. Soc.*, **71**, 1744 (1949).

No reaction occurred except a partial decomposition when I was treated with silver nitrate, sodium nitrite, sodium phenolate, acetyl nitrate, guanidine or sodium iodide.

In conclusion, the sydnone ring is highly aromatic in character, and I is inert to usual anionoid reagents. Most reactions reported here can be interpreted only when the oxidative effect of I is taken into consideration. Further studies on the reactions of I and VII are now under experiment.

Experimental

3-Phenyl-4-bromosydnone (I).—Into a suspension of 1g. of II and 2g. of sodium bicarbonate in 30 cc. of ether was added 1g. of bromine under stirring. After a few minutes, the reaction mixture was filtered and washed with water, and was recrystallized from ethanol giving 1.15 g. (yield 78%) of white needles, m. p. 141°C. (decomp.). Baker et al.[2] reports its m. p. 140°C. (decomp.). I turns to a red color on prolonged exposure to sunlight.

Reaction of I with *p*-Thiocresol.—To a solution of 0.5 g. of *p*-thiocresol in 20 cc. of anhydrous methanol containing 0.1 g. of metallic sodium was added 1g. of I under stirring at room temperature. After standing overnight, the solvent was evaporated under reduced pressure and the residue was first washed with water and then extracted with ether. The ether extract was evaporated to dryness and the residue was crystallized from methanol giving 0.4 g. of colorless leaflets, m. p. 47—48°C.. The melting point of this substance was not depressed by admixture with authentic di-*p*-tolyl disulfide. The residue (0.4 g.) left after the extraction with ether was recrystallized twice from ethanol giving 0.15 g. of white needles melting at 134—135°C. with slight decomposition, undepressed by admixture with authentic II.

Reaction of I with Sodium Hydrosulfide.—A solution of 0.09 g. of sodium hydroxide in 15cc. of methanol was saturated with dry hydrogen sulfide gas. To this solution were added 0.5 g. of I and a small amount of potassium iodide, both of which soon went into solution and pale yellow precipitate began to separate out. Stirring was continued for three hours at room temperature and then allowed to stand overnight. The pale yellow precipitate which separated out was filtered and was extracted with a small amount of carbon disulfide. On evaporating the carbon disulfide 0.1 g. of pale yellow amorphous powder (m. p. 120°C.) was obtained, which was identified as sulfur. The filtrate was evaporated under reduced pressure and the orange colored residue was washed with water and recrystallized from ethanol giving 0.23 g. of slightly brown colored long needles, m. p. 133—134°C. with slight decomposition, undepressed by admixture with authentic II.

Reaction of I with Sodium Sulfide.—To a methanol solution (15 cc.) of sodium hydrosulfide, prepared from 0.09 g. of sodium hydroxide by the same way as is described above, was added 0.09 g. of sodium hydroxide. One gram of I was added to this solution and was treated by essentially the same method as in the preceeding experiment. This also gave II and sulfur, both of which were identified by their melting points and mixed melting points with authentic samples.

Hydrogenolysis of I with Zinc Dust.—Into a solution of 0.5 g. of I in 20 cc. of 80% aqueous acetic acid was added portionwise 2 g. of zinc dust during two hours under stirring and cooling by water. Stirring was continued for six hours and allowed to stand overnight. This was filtered and the residue was washed with water. This filtrate was negative to Liebermann's nitroso test. A part (1/5) of this filtrate was made alkaline with sodium hydroxide, which evolved ammonia on heating. The residue was decomposed by hydrochloric acid and was added to the other part (4/5) of the filtrate. This solution was concentrated to 10 cc. under reduced pressure and the remaining acetic acid was extracted with ether. After evaporating the ether which was dissolved in water under reduced pressure, this solution was acidified with hydrogen chloride. To this solution was added dropwise a solution of 0.15 g. of sodium nitrite under stirring and ice cooling. The pale yellow precipitate (0.16 g.) which separated out was dissolved in 5% sodium bicarbonate solution, which on acidification with hydrogen chloride afforded pale yellow needles, m. p. 101—102°C. (decomp.). This substance was negative to Beilstein's halogen test and gave a strong Liebermann's nitroso test. A mixed m. p. with authentic N-nitroso-N-phenylglycine was 102—103°C. (decomp.).

Reaction of I with Thiourea.—To 20 cc. of ethanol were added 1 g. each of I and thiourea and was refluxed for six hours. After standing overnight, the pale yellow needles which separated out were collected by filtration (0.2 g. m. p. 157°C.), and recrystallized first from acetone and then from ethanol giving pale yellow needles, m. p. 164—165°C.. This substance was negative to Beilstein's halogen test, insoluble in 10% sodium hydroxide solution and in 10% hydrochloric acid, and gave a positive sulfur test.

Anal. Found: C, 54.47; H, 3.22; N, 15.83. Calcd. for $C_{16}H_{10}O_4N_4S$: C, 54.24; H, 2.85; N, 15.81%.

The same result was obtained when an equimolecular amount of thiourea was used, but the yield in this case was poorer and a considerable amount of I was recovered unchanged, accompanied by a small amount of sulfur.

Reaction of I with Magnesium Metal.—To a suspension of 0.5 g. of I and 0.22 g. of magnesium ribbons in 10 cc. of anhydrous ether, was added 1.0 g. of methyl iodide under stirring. After three hours the reaction was nearly completed. Water was added and was evaporated to dryness under reduced pressure, and the residue was extracted with ethanol. On evaporating the solvent under

reduced pressure, a small amount of oily substance was obtained, which became solidified on adding water; recrystallization of this substance (0.17 g.) from ethanol gave 0.1 g. of white needles, m. p. 134—135°C. with slight decomposition. The melting point of this substance was not depressed by admixture with authentic II. In the absence of methyl iodide, no reaction occurred even when *n*-butyl ether was used as the solvent and the reaction was conducted at 100°C..

Reaction of I with Hydrazine Hydrate.—To 1 cc. of 80% hydrazine hydrate were added 0.5 g. of I and a few drops of ethanol and this mixture was gently refluxed on a water bath for four hours, and was kept standing overnight. On adding water, 0.1 g. of pale brown needles melting at 132—135°C. were separated out, recrystallization of which from dilute ethanol gave pale yellow needles, m. p. 134°C. with slight decomposition. A mixed m. p. with authentic II was 135°C.. When I was refluxed in ethanol with equimolecular amount of hydrazine hydrate, no reaction occurred and I was recovered unchanged.

The authors are indebted to Mr. Asaji Kondo for carrying out the microanalyses.

Laboratory of Organic Chemistry
Tokyo Institute of Technology
Meguro, Tokyo

On the Distribution and Behavior of Water in Cation-Exchange Resin Membranes

By Yoshio ODA and Tadashi YAWATAYA

(Received October 9, 1956)

Introduction

In the preceding two papers[1,2], we reported on the electro-osmotic phenomena in cation-exchange resin membranes, and discussed to some extent on the distribution of water within the resin. Therein, the water in the resin phase was classified into two groups, i.e., "mobile- and fixed waters". The former was considered to consist of the hydration water of the exchangeable and non-exchangeable ions and the solvent water in the resin, whilst the latter to consist mainly of the hydration water of the structurally bound ions, e. g., sulfonate ions in the cation-exchange resin.

Hitherto several workers have studied the water in the ion-exchange resins basing their studies on different principles.

D. Reichenberg[3], discussing on the exchange rate of sodium- and hydrogen ions in cation-exchange resins of different cross-linkings, calculated the amount of water unavailable as a diffusion medium to find five molecules per equivalent of the resin, and assumed that the ions in the resin were hydrated to this extent.

G. E. Boyd and B. A. Soldano[4], from the study on the water adsorption isotherms for cation- and anion-exchange resins, ascribed one molecule of H_2O to the amount of water which is required by a structurally bond sulfonate ion.

E. Glueckauf[5] has recently determined the hydration number of sulfonate ions as 0.9 in cation exchanger of sulfonated polystyrene type. It was derived on the basis of the thermodynamical concept of electrolyte solution, modified so as to include the effect of co-volume.

According to G. H. Osborn[6], the recent work on the absorption of non-electrolyte by the hydrogen forms of the exchangers has confirmed that there are about four molecules of hydration water per equivalent of sulfonic group.

Referring to these published data, most of which are indicated with numbers of hydration water of total ionic species in the resin, including both fixed and mobile ions, our results[1], about ten molecules water for a sulfonate ion, seems far separated from them.

The difference may be explained that "the fixed water" which does not take part in electro-osmosis would involve not only the hydration water of the fixed ions but a part of water which is hindered to

1) Y. Oda and T. Yawataya, This Bulletin, **28**, 263 (1955).
2) Idem. ibid., **29**, 673 (1956).
3) D. Reichenberg, *J. Am. Chem. Soc.*, **75**, 589 (1953).
4) G. E. Boyd and B. A. Soldano, *Z. Elektrochem.*, **57**, 162 (1953).
5) E. Glueckauf, *Trans. Faraday Soc.*, **51**, 1235 (1955).
6) G. H. Osborn, "Synthetic Ion-Exchangers," Arrowsmith, London (1955), p. 7.

move due to the network structure of the resin. Thus, the determination of the number of fixed water molecules from the electro-osmotic measurements seems to deserve further discussion. The present paper deals with this problem.

Theoretical

In the first paper of this series[1], we assumed that the free water in the resin moves with mobility equal to that of the migrating ions.

It would be more reasonable, however, to suppose that in the electro-osmosing solution the mobility of ions differs from that of the solvent water, since the water moves with velocity depending on the balance between the driving force due to ionic migration and the retardation due to the network of resin.

Thus, it will be assumed in this paper that the electro-osmosing water within ion-exchange membrane consists of two sorts with different mobilities: (1) primary shell hydration water of the mobile ions with a mobility equal to that of the ions, and (2) solvent water with smaller mobility than (1). Naturally the transferring velocity of the solvent water would not be uniform over a whole resin pore section, but would have a distribution governed by the hydrodynamic principle. For simplicity, however, it is assumed to have a certain average mobility, u_s.

As was stated previously[2], the fixed ion concentration A_w based on the total water content in the resin is expressed as follows,

$$\frac{1}{A_w} = h_+ \cdot (1+s) + h_- \cdot s + f + \alpha \qquad (1)$$

where, from the definition of A_w, $1/A_w$ means the amount of total water per equivalent of fixed ion. h_+ and h_- are the amount of hydration of mobile cation and anion respectively. And s, f and α are respectively the amount of Donnan absorption, solvent water and fixed water, all these being indicated basing on an equivalent of fixed ion.

When an electric field is applied on a cation-exchange membrane interposed between two solutions of equal concentration, n_+' moles cations enter the cathode cell through the membrane and n_-' moles anions migrate out of the cathode cell into the anode cell for each faraday of electricity. Here, n_+' and n_-' denote* the ture transport numbers of the cation and the anion within the membrane. In this case, the water transference may be considered to take place as illustrated schematically in Fig. 1. The hydration water of cations

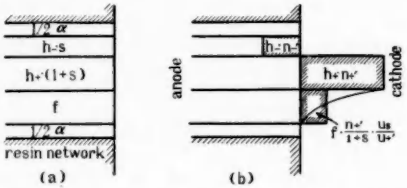

Fig. 1. (a) Distribution of water inside resin-pore
(b) Water transference for passage of one faraday (Shaded areas express the transfered water.)

or anions moves toward cathode or anode with the same mobilities as the respective ions. Whilst, the solvent water, whose amount is f moles per equivalent of fixed ion, or $f \cdot \frac{n_+'}{1+s}$ moles per n_+' moles of the migrating cation, transfers with a mobility u_s/u_+' times as small as that of the cation. Here, u_+' is the mobility of the cation in resin phase.

Therefore, the amount of electro-osmotic water transference, β_w, is correlated with the transport numbers of cation and anion as follows,

$$\begin{aligned}\beta_w \cdot F &= h_+ \cdot n_+' - h_- \cdot n_-' \\ &\quad + f \cdot \frac{n_+'}{1+s} \cdot \frac{u_s}{u_+'} \qquad (2) \\ &= \left(h_+ + f \cdot \frac{u_s}{u_+'}\right) \cdot n_+' \\ &\quad - \left(h_- + f \cdot \frac{u_s}{u_-'}\right) \cdot n_-'. \qquad (2')\end{aligned}$$

Cancelling f from (1) and (2), and noting the fact that $n_+' + n_-' = 1$,

$$\begin{aligned}\frac{1}{A_w} &= \alpha + \frac{\beta_w \cdot F}{u_s/u_+'} \cdot \frac{1+s}{n_+'} \\ &\quad + h_+ \cdot (1+s) \cdot \left(1 - \frac{1}{u_s/u_+'}\right) \\ &\quad + h_- \cdot s \cdot \left(1 + \frac{1}{u_s/u_+'}\right) \\ &= \alpha + \frac{\beta_w \cdot F}{u_s/u_+'} \cdot \frac{1+s}{n_+'} + h, \qquad (3)\end{aligned}$$

where

$$h = h_+ \cdot (1+s)\left(1 - \frac{1}{u_s/u_+'}\right)$$

* The mobility notation with or without a prime refers to the quantity relative to the solution or the resin.

$$+h_-\cdot s\cdot\left(1+\frac{1}{u_s/u'_-}\right).$$

On the other hand from equations (7), (9) and (12) in the preceding paper[2],

$$\frac{n'_+-n_+}{n_-+s}=\frac{k'-k}{k'}=\frac{u_s}{u'_+\cdot(1+s)+u'_-\cdot s}$$
$$=\frac{u_s}{u_+'}\cdot\frac{1}{1+s}\cdot\frac{u'_+\cdot(1+s)}{u'_+\cdot(1+s)+u'_-\cdot s}.$$

Then, considering the relations of equations (10) and (15) in the previous paper,

$$\frac{n'_+-n_+}{n_-+s}=\frac{u_s}{u_+'}\cdot\frac{n'_+}{1+s}=A'_w\cdot\beta_w\cdot F. \quad (4)$$

Therefore, the ratio of the mobility of solvent water to that of cation is,

$$\frac{u_s}{u'_+}=\frac{1+s}{n'_+}\cdot\frac{n'_+-n_+}{n_-+s}. \quad (5)$$

By the similar way,

$$\frac{u_s}{u'_-}=\frac{s}{n'_-}\cdot\frac{n'_--n_+}{n_-+s}. \quad (5')$$

Further, from equation (11) in the preceding of paper, the ratio anion's mobility to cation's within the moving solution is obtained as,

$$\frac{u_-}{u_+}=\frac{n_-}{n_+}\cdot\frac{1+s}{s}. \quad (6)$$

The concentration of fixed ion basing on "the mobile water", A'_w, is given, by use of the equation (4), as follows,

$$\frac{1}{A'_w}=\frac{\beta_w\cdot F}{u_s/u'_+}\cdot\frac{1+s}{n'_+}. \quad (7)$$

Hence,

$$\frac{1}{A'_w}=\frac{1}{A_w}-\alpha-h. \quad (8)$$

By means of equations (5) and (5') values of u_s/u'_+ and u_s/u'_- may be estimated for each membrane from the observed values of n'_-, n_+ and s. These values of u_s/u'_+ and u_s/u'_-, combined with the observed value of β_w, permit an estimation of α by use of equation (3).

Experimental

Membranes.—Two cation-exchange resin membranes were used in the present work. One is of sulfonated polystyrene type (CMA-24), and the other of sulfonated phenol resin type (P-13). The latter is one of the same series as those used previously[2]. Their exchange capacities and water contents are given in Table I.

Measurement.—Of the CMA-24 membrane, measurements were made for true transport numbers (n'_+, n'_-), Hittorf transport numbers (n_+, n_-), electro-osmotic water transference (β_w), Donnan absorption (s), and the fixed ions concentration (A_w) in the chloride solutions of 1:1 valency type such as LiCl, NaCl, NH_4Cl, KCl, CsCl, and HCl of varied concentration. Temperature was regulated at 25±0.2°C. The procedures of the measurements were quite the same as those described previously[2].

Of the P-13 membrane, such measurements were carried out solely in sodium chloride solution.

TABLE I

THE EXCHANGE CHARACTERISTICS OF SAMPLE MEMBRANES (Na-TYPE)

Sample No.	Thickness (mm.)	A°_w m.eq./g. H_2O	A_R m.eq./g.	Water content %
CMA-24	0.3	3.90	1.86	32.3
P-13	0.9	2.02	3.04	60.1

A°_w is the concentration of fixed ions basing on the total water content of the resin equilibrated with distilled water.
A_R is the exchange capacity per one gram of dry resin.

Results

The results are given for CMA-24 membrane unless specified.

The empirically determined true and Hittorf transport numbers of cation (n'_-, n_-) through the membrane are plotted in Fig. 2 over the concentration range of equilibrating solution from 0 to 4 N. The Hittorf transport number is highest in HCl-solution and decreases in the order, $H^+>Cs^+>K^+>NH_4^+>Na^+>Li^+$. The order is in good accord with that in free aqueous solutions. Such a situation cannot be seen so clearly regarding the true transport number curves, since in this case they

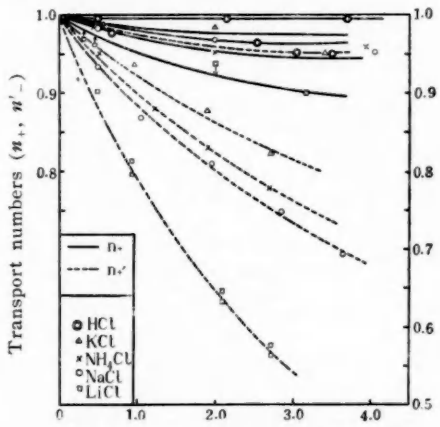

Fig. 2. Transport numbers in cation-exchange resin membrane (CMA-24).

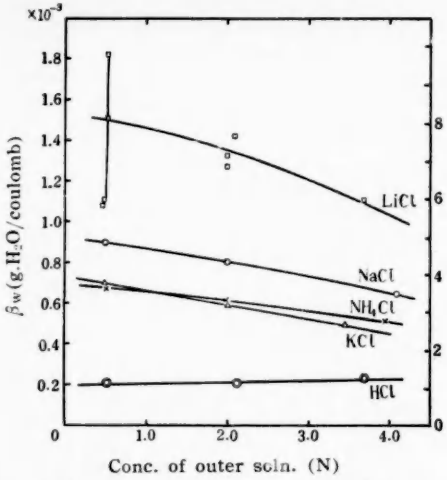

Fig. 3. Electro-osmotic water transference through cation-exchange resin membrane (CMA-24).

come together closely to approach the upper limit line: $n'_+ = 1$.

In Fig. 3 are plotted the electro-osmotic water transference, β_w, through the membrane against the concentration of outer solutions. It appears to become large as the hydration of the cation increases, except for the case of HCl-solution. The hydration numbers of the ions concerned are listed below in Table II according to E. Glueckauf. The β_w in HCl-solution is notably and small stays nearly constant over a wide concentration range.

With LiCl-solution the observed values of β_w, particularly in dilute solution region, showed remarkable large fluctuation, and appeared to rise gradually as the duration of electrolysis increased.

The Donnan absorptions are given in Fig. 4. They increase with the rise in the concentration of equilibrating solution, and little significant variation can be seen with the difference of cation species.

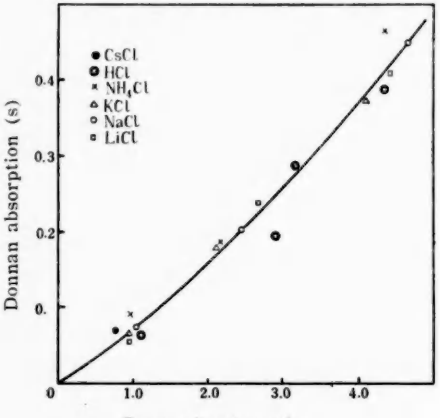

Fig. 4. Donnan absorption (CMA-24).

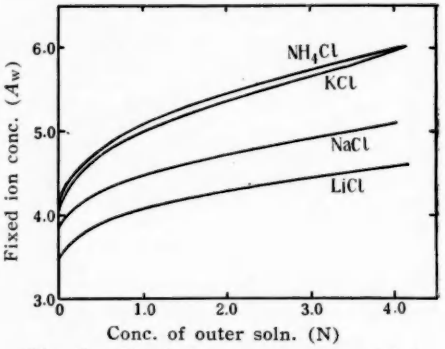

Fig. 5. Fixed ion concentration (A_w) (CMA-24).

Fig. 5 shows the curves of fixed ion concentrations, A_w, plotted against the concentration, of outer solution. As the outer solutions become concentrated, the shrinkage of the resin seems to cause the increase of A_w.

Discussion

The ratios of the mobility of solvent water to that of cation, u_s/u'_+, were cal-

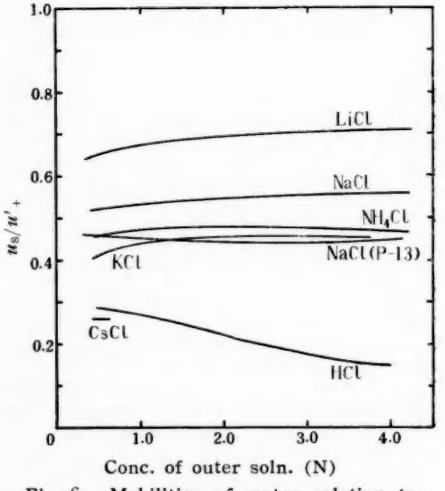

Fig. 6. Mobilities of water relative to cations.

culated by substituting the experimental data obtained above in equation (5). The results are plotted in Fig. 6 against the concentration of outer solution. In this calculation, accuracy decreases as the outer solutions become too diluted, because then the terms $(n'_+ - n_+)$ and $(n_- + s)$ in equation (5) approach zero.

It may be noted that the mobility ratio u_s/u'_+ appears to be almost constant over a wide concentration range of each solution, and that it becomes high to approach the limit line of $u_s/u' = 1$ as the hydration degree of the cation increases, the data for HCl-solution being one exception.

As was seen in Fig. 3, in HCl-solution the electro-osmotic water transference is merely about one mole H_2O per faraday through a membrane, being even smaller than the hydration number of hydrogen ion. These apparently anomalous results with HCl-solution are presumably attributable to the special conduction mechanism of hydrogen ion.

By the similar way, the ratios of anion's mobility to cation's, u_-/u_+, within the electro-osmosing solution were calculated using equation (6), and were shown in Fig. 7. For the sake of comparison, the ratios u_-/u_+ in aqueous solutions were plotted with broken lines in the same figure. It is seen that the u_-/u_+ ratios in electro-osmosing solution tend to approach those in free solutions as the concentration of equilibrating solution rises. This result seems reasonable, for the mobile cations and mobile anions are present in marked unbalance within the resin when the outer solution is dilute, and they tend to approach a balance, which is the case in free solution, as the outer solution, becomes concentrated.

Finally, the values of α, the amount of hydration of sulfonic group, were estimated using equation (3) and plotted in Fig. 8. In this calculation, Glueckauf's data of hydration number of ions were applied for h_+ and h_-. They are given in Table II.

From the result, we are tempted to reach a conclusion that the hydration of a sulfonic group decreases as the effective concentration rises in resin. But the derivation of the values of α is not so precise as to allow it. Though it has been assumed in the above calculation that the hydration degrees of mobile ions are constant irrespective of the concentration of solutions in resin, this seems oversimplified. Also, the determinations of α for the case of very dilute equilibrating solutions are

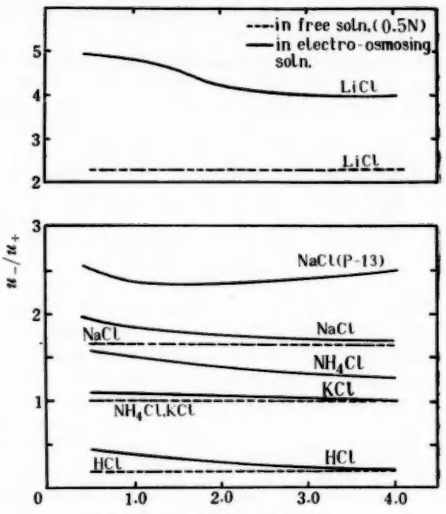

Fig. 7. Mobility ratio of anion's to cation's in electro-osmosing and free aqueous solutions.

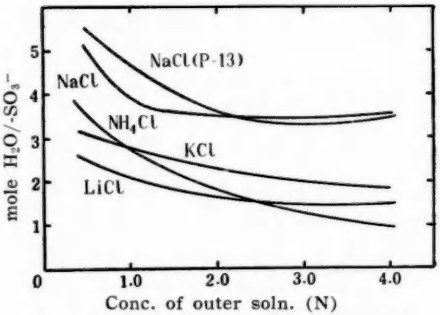

Fig. 8. Amount of hydration of sulfonic group.

TABLE II

	H^+	Li^+	Na^+	K^+	NH_4^+	Cl^-
Primary hydration number	4.0	3.4	2.0	0.6	0.2	0.9

not completely reliable, because as the solutions are diluted both the numerator $(n' - n_+)$ and the denominator $(n_- + s)$ in equation (4) approach zero, resulting in inaccurate values of u_s/u'_+.

Thus, if we take the data around 2N as the comparatively reliable values α may be estimated as 1.5 to 3.5 moles per equivalent. These values of α, though still slightly higher than those found in the literature of the subject, seem much more reasonable as the hydration number of the fixed

sulfonic group than that reported previously by us.

When the circuitous process of calculation and rather drastic assumptions basing on a simple model in our treatment are considered, the concordance appears comparatively good. But more precise experiments would be desirable for membranes of wide varieties in order to make more strict discussion.

Conclusion

It was assumed for a mechanism of electro-osmosis through ion-exchange resin membranes that (1) the primary shell hydration water of mobile ions transfers with the same mobility as the ions, and (2) the solvent water within the resin phase is dragged by the migrating cations or anions toward anode or cathode, the net result being observed as electro-osmosis. On this view, the mobilities of solvent water relative to those of cations were calculated from the measurements of electro-osmotic properties of cation exchange resin membranes equilibrated with varied concentration of LiCl, NaCl, KCl, NH_4Cl, CsCl and HCl solution. In addition, from these experimental data the amount of hydration of the fixed sulfonate ion was estimated as 1.5 to 3.5 moles per equivalent.

We are grateful to Dr. M. Sekino and other members in the Organic Laboratory, Asahi Glass Co. Ltd., for the kind supply of the sample membranes, and to Mr. H. Ukihashi for his valuable discussion.

Research Laboratory of Asahi Glass Co. Ltd. 2, Benten-cho Tsurumi-ku, Yokohama

Dipole Moments and Internal Rotation of Some Halogenated Hydrocarbons in the Vapor State

By Ichiro MIYAGAWA, Takehiko CHIBA, Shoichi IKEDA and Yonezo MORINO

(Received November 11, 1956)

In the previous papers[1,2] one of the present authors (I. M.) discussed the energy differences in the rotational isomers of some halogenated hydrocarbons. By use of the experimental data two relations were pointed out[1e]. The first one is that the energy difference in these molecules depends mainly upon the configuration of the halogen atoms: that is, 1,2-dichloro-compounds have the energy difference of about 1 kcal./mole, and 1,1,2-trichloro-compounds have very large ones (ca. 2 kcal./mole), while 1,1,2,2-tetrachloro-compounds have vanishingly small ones (<0.4 kcal./mole). (See Table II). This striking result was explained qualitatively by some empirical interatomic potentials[2c].

The second interesting relation was found in the change of energy difference in 1,2-dichloro-compounds by successive substitution of the hydrogen atoms by methyl groups. By assuming that the intramolecular potential is the sum of contributions of the potentials between non-bonded atoms or groups, the observed ΔE's of dichloro-compounds are successfully reproduced. In tri- and tetrachloro-compounds, however, ΔE cannot be reproduced so well as in the case of dichloro-compounds, and the qualitative explanation of these ΔE's are made in terms of the change in valence angles and of appropriate interatomic potentials. On the other hand it was inferred by Szasz[3] in his recent paper that the energy difference in *n*-propyl chlorides is very small. The second relation described above, gives 0.3 kcal./mole as the energy difference in this molecule. It is clear, therefore, that the second relation cannot be applied without any modification to such a molecule as *n*-propyl chloride. It is one of the purposes of this report to propose a possible explanation for this situation.

1) I. Miyagawa, (a) *J. Chem. Soc. Japan*, **75**, 970 (1954); (b) ibid., 1057; (c) ibid., 1061; (d) ibid., 1162; (e) ibid., 1165.

2) I. Miyagawa, (a) *J. Chem. Soc. Japan*, **75**, 1169 (1954); (b) ibid., 1173 (c) ibid., 1177.

3) G. I. Szasz, *J. Chem. Phys.*, **23**, 2449 (1955).

TABLE I

OBSERVED POLARIZATIONS, DIPOLE MOMENTS AND ΔE OF SOME HALOGENATED HYDROCARBONS*

Temp. °K	No. of obs.	Press. range mmHg	Molar polarizn. cc.	Mean deviatn. of polarizn. cc.	Dipole moment D.
1,2-Dichloro-2-methylpropane		$MR_D=30.5$ cc.	$P_E+P_A=32.0$ cc.		
339	6	68- 82	74.0	0.40	1.52_9
353	6	61- 84	73.0	0.35	1.54_1
384	7	82-144	72.2	0.45	1.63_1
411	6	78-138	71.1	0.41	1.62_4
467	8	106-205	66.6	0.80	1.62_3
	$(\mu_g)_{obs.}=2.5$ (assuming $\mu_t=0.49$)		$\Delta E=0.9$ kcal.		
	$(\mu_g)_{calcd.}=3.01$				
1,1,2,2-Tetrachloropropane		$MR_D=35.6$ cc.	$P_E+P_A=37.4$ cc.		
371.6	7	51- 77	75.7	0.50	1.52_8
412.7	6	71- 97	72.4	0.49	1.54_0
467	7	82-111	68.5	0.43	1.54_4
	$(\mu_g)_{obs.}=2.0$ (assuming $\mu_t=0.84$)		$\Delta E=0.3-0.4$ kcal.		
	$(\mu_g)_{calcd.}=2.24$				
1,2,2-Trichloropropane		$MR_D=30.8$ cc.	$P_E+P_A=32.3$ cc.		
353.5	8	61-101	76.4	0.52	1.59_9
383.2	8	74- 99	73.0	0.37	1.60_0
411.5	6	61-110	71.2	0.12	1.62_1
467.5	7	80-131	67.0	0.19	1.61_9
	$(\mu_g)_{obs.}=2.8$ (assuming $\mu_t=1.55$)		$E\geq 2.0$ kcal.		
	$(\mu_g)_{calcd.}=2.97$				
1,1,2-Trichloro-2-methylpropane		$MR_D=35.5$ cc.	$P_E+P_A=37.3$ cc.		
382.5	6	72- 88	90.6	0.41	1.82_9
413·2	8	76-103	87.5	0.52	1.84_5
429.6	7	69-102	84.3	0.43	1.82_0
467.4	7	78-110	80.7	0.59	1.82_5
	$(\mu_{asym.})_{obs.}=1.83$		$\Delta E\geq 1.5$ kcal. ($P_A\leq 2$ cc.)		
	$(\mu_{asym.})_{calcd.}=1.76$				
	$(\mu_{sym.})_{calcd.}=3.09$				
1,2-Dibromopropane		$MR_D=30.6$ cc.	$P_E+P_A=32.1$ cc.		
353.6	5	61- 82	54.2	0.12	1.13_2
371.1	6	65- 95	54.4_5	0.28	1.16_7
412.4	9	79-108	55.0	0.35	1.24_5
467.2	6	68-109	56.4	0.27	1.36_5
	$(\mu_g)_{obs.}=2.48$ (assuming $\mu_t=0$)		$\Delta E=1.25$ kcal.		
	$(\mu_g)_{calcd.}=2.41$				
1,2-Dibromo-2-methylpropane		$MR_D=35.2$ cc.	$P_E+P_A=37.0$ cc.		
353.6	6	47- 67	60.0	0.42	1.16_5
370.4	13	65- 98	61.0-61.8		1.21-1.23**
411.5	8	70- 91	60.2-62.6		1.25-1.31**

* $P_E+P_A=1.05\,MR_D$ is assumed throughout.

** Slight decomposition of the sample is noticed in these runs.

Experimental

All substances used were prepared by the methods described in Beilstein's Handbooks except those with special indication.

1,2-Dichloro-2-methylpropane and 1,1,2-trichloro-2-methylpropane.—Isobutyl alcohol saturated with hydrogen chloride on cooling, was heated to 120°C in a sealed tube for several hours. Isobutyl chloride thus obtained was chlorinated with chlorine gas in the presence of aluminum chloride. The product was fractionated into 1,2-dichloro-2-methylpropane (b. p. 107.0–108.0°C) and 1,1,2-trichloro-2-methylpropane (162.0–163.0°C).

1,2,2-Trichloropropane and 1,1,2,2-tetrachloropropane.—Monochloroacetone and dichloroacetone were prepared by the method described by S. Mizushima et al[4]. Monochloroacetone was added slowly to phosphorus pentachloride in a flask and the mixture was boiled for an hour. Then 1,2,2-trichloropropane was distilled: b. p. 121–123°C.

1,1,2,2-Tetrachloropropane was obtained by boiling a mixture of dichloroacetone and phosphorous pentachloride for fourteen hours: b. p. 153–154°C.

1,2-Dibromo-2-methylpropane.—A mixture of isobutyl alcohol, sulfuric acid in the weight ratio of 5 : 1, containing sea sand as a catalyser, was boiled and isobutylene thus produced was introduced into a vessel containing bromine: b. p. 148–149°/60 mmHg.

1,2-Dibromopropane.—A mixture of propyl alcohol, concentrated sulfuric acid, and sea sand was boiled. Propylene gas thus produced was introduced into a vessel containing bromine: b. p. 141–142°C.

The apparatus and the procedure for measuring the dielectric constant in the vapor state are described elsewhere[5].

Results

The results of the measurement of dipole moments in the gaseous state are given in Table I. In case when there exist two rigid rotational isomers, the *trans* and the *gauche* forms, the average moment μ at temperature T is given by

$$\mu^2 = \frac{\mu_g^2 s e^{-\Delta E/RT}}{1+s e^{-\Delta E/RT}} \qquad (1)$$

where μ_g denotes the moment of the *gauche* form and s the weight factor ratio of the *gauche* form to the *trans* one. When $\log \mu^2$ is plotted against $\log (1/T)$, the curve is parallel to that of $\log (se^{-x}/1+se^{-x})$ vs. $\log x$, since,

$$\log \mu^2 = \log \mu_g^2 + \log(se^{-x}/1+se^{-x}),$$

and

$$\log (1/T) = -\log(\Delta E/R) + \log x.$$

Hence the coordinate of the abscissa and that of the ordinate shifted in order to fit the experimental curve $\log \mu^2$ vs. $\log (1/T)$ to the curve $\log (se^{-x}/1+se^{-x})$ vs. $\log x$, must be equal to $\log \Delta E/R$ and $\log \mu_g^2$ respectively*.

Eq. (1) was derived from the assumption of the coexistence of the two separate isomers. Actually molecules are distributed among the whole range of internal rotational angle, depending on the shape of the potential curve, so that it may be more rigorous to take into account all positions of rotation. However, the above treatment assuming Eq. (1) is proved to be valid usually within the error in ΔE of 0.15 kcal./mole[1b].

In Table I are also given the values of ΔE and μ_g obtained from the experimental data by the above treatment. The values of μ_g are compared

TABLE II
ENERGY DIFFERENCE IN ROTATIONAL ISOMERS IN HALOGENATED HYDROCARBONS

Compound	Energy difference (kcal./mole) Observed	Calculated
$H_2ClC\text{-}CClH_2$	1.10[a]	1.2
$H_2ClC\text{-}CClHCH_3$*	1.0[b]	
g_1		0.9
g_2		1.2
$H_2ClC\text{-}CCl(CH_3)_2$	0.90[c]	0.9
$(CH_3)_2ClC\text{-}CCl(CH_3)_2$	1.30[d]	1.3
$HCl_2C\text{-}CClH_2$	≧2.4[e], 2.9[f]	
$CH_3Cl_2C\text{-}CClH_3)_2$	≧2.0[c]	
$HCl_2C\text{-}CCl(CH_3)_2$	≧1.5[c]	
$HCl_2C\text{-}CCl_2H$	0[e]	
$CH_3Cl_2C\text{-}CCl_2H$	0.4[c]	
$H_2BrC\text{-}CBrH_2$	1.54[a]	1.5
$H_2BrC\text{-}CBrHCH_3$*	1.25[c]	
g_1		1.2
g_2		1.5
$H_2BrC\text{-}CBr(CH_3)_2$	1.1[g]	1.2
$(CH_3)_2BrC\text{-}CBr(CH_3)_2$	1.6[d]	1.6
$HBr_2C\text{-}CBrH_2$	≧1.5[g]	
$HBr_2C\text{-}CBr_2H$	0, or $-\infty$[g]	
$H_2ClC\text{-}CCH_3H_2$	0[h]	0.3
$H_2BrC\text{-}CCH_3H_2$	0[h]	0.3

* This molecule has two *gauche* forms, g_1 and g_2.

a) K. Kuratani, T. Miyazawa and S. Mizushima, *J. Chem. Phys.*, **21**, 1411 (1953).
b) Y. Morino, I. Miyagawa and T. Haga, *ibid.*, **19**, 791 (1951).
c) Present results.
d) Y. Morino, I. Miyagawa, T. Haga and S. Mizushima, This Bulletin, **28**, 165 (1955).
e) J. R. Thomas and W. D. Gwinn, *J. Am. Chem. Soc.*, **71**, 2785 (1949).
f) K. Kuratani and S. Mizushima, *J. Chem. Phys.*, **22**, 1403 (1954).
g) I. Miyagawa, *J. Chem. Soc. Japan*, **75**, 1162 (1954).
h) Ref. (10).

* In case when the moment of trans (μ_t) has a non-zero value, the same relation can hold by taking $\mu^2-\mu_t^2$, and $\mu_g^2-\mu_t^2$ in place of μ^2 and μ_g^2. Therefore, assuming a finite μ_t, the same procedure can be applied. μ_t is always small and it produces no serious error.

4) S. Mizushima et al., *J. Chem. Phys.*, **21**, 815 (1953).
5) T. Chiba, This Bulletin, **28**, 19 (1955).

with those calculated by taking empirical induction moments[1c] into account. It is seen that the agreement between them is fairly good. A little discrepancy in a few cases may be due to the ambiguity of the *s*-values used. In fact, the change of the *s*-values exerts sensitive influence on μ_g but not on ΔE.

Discussion

In Table II are summarized the ΔE's obtained both by the present work and by the measurements[1d] made in solution for the compounds on which the measurement in the gaseous state is difficult owing to the small vapor pressure or thermal decomposition. It is proved that there is practically no difference between the energy difference found in the gaseous state and that in the heptane solution[1e], so that the energy difference obtained in heptane solution can be compared with those in the gaseous state without any precaution. Table II includes also the results of the related halogenated hydrocarbons which were measured by other authors.

From Table II it is easily seen that ΔE's are grouped into three classes depending on the configuration of chlorine atoms, just as Miyagawa pointed out[1e].

	configuration	ΔE
1	$\rangle ClC—CCl\langle$	ca. 1 kcal./mole
2	$—Cl_2C—CCl\langle$	ca. 2 kcal./mole
3	$—Cl_2C—CCl_2—$	ca. 0 kcal./mole

In dichloro-compounds small differences are found from one compound to another depending on the various types of methyl substitution. If the intramolecular potential is given by the sum of these potentials between non-bonded atoms or groups and, further, if it is assumed that the following relations hold between these potentials, the energy differences of many dichloro- and dibromo-compounds calculated are in excellent agreement with the observed:

$$(Cl\cdot Cl)-2(H\cdot Cl)+(H\cdot H)=1.2\text{kcal./mole} \quad (2)$$

$$(Cl\cdot CH_3)-(H\cdot Cl)-(H\cdot CH_3)+(H\cdot H)=0.3\text{ kcal./mole} \quad (3)$$

$$(CH_3\cdot CH_3)-2(H\cdot CH_3)+(H\cdot H)=0.7\text{ kcal./mole} \quad (4)$$

$$(Br\cdot Br)-2(H\cdot Br)+(H\cdot H)=1.5\text{ kcal./mole} \quad (5)$$

$$(Br\cdot CH_3)-(H\cdot Br)-(H\cdot CH_3)+(H\cdot H)=0.3\text{ kcal./mole} \quad (6)$$

where $(A\cdot B)$ denotes a potential difference due to the change of the relative position of the atom pair A and B from the *trans* to the *gauche*.

When the above relation is applied to the case of trichloro and tetrachloro-compounds, the discrepancy between the observed and the calculated becomes apparent. In fact, if the above relation holds, the energy differences of tri- and tetrachloroethane should be just as large as that of dichloroethane. A possible explanation of this discrepancy was presented qualitatively by Mizushima et al. for tetrachloroethane[6]. The two chlorine atoms attached to the same carbon atom have the $\angle ClCCl$ angle larger than the tetrahedral value and non-adjacent Cl···Cl atoms come closer in the *trans* form. It is expected, therefore, that the *trans* form becomes much less than that in the case when the tetrahedral angle is maintained. If it is assumed that the angle of $\angle ClCCl$ is reduced to the tetrahedral one by the substitution of a methyl group in place of a hydrogen atom of $CHCl_2—$ group then the energy difference will be expected to be between those of dichloro- and tetrachloro-ethane. This is what is found in the experiment. The observed valence angles, 111° for $\angle ClCCl$ in methylene chloride[7], 111.5° for $\angle CCC$ in propane[8], and 109.5° for $\angle ClCCl$ and 109.2° for $\angle CCCl$ in 2,2-dichloropropane[9] from the electron diffraction investigation, seem to support the above hypothesis.

Eqs. (3), (6), and (4) correspond respectively to the ΔE's of chloropropane, bromopropane, and *n*-butane. The energy difference in chloropropane obtained by spectroscopy[10] is nearly equal to zero, which was confirmed recently by electron diffraction investigation[11]. Therefore, the energy relation assumed by these equations cannot be applied accurately to *n*-propyl halide molecules. Recently Szasz[3] proposed an interesting assumption that between a halogen atom and a methyl group there must be some attractive force, large enough to cancel the so-called steric repulsion. This assumption can explain the

6) S. Mizushima, Y. Morino and K. Kozima, *Sci. Papers Inst. Phys. Chem. Research* (Tokyo), **29**, 111 (1936).
7) L. E. Sutton and L. O. Brockway, *J. Am. Chem. Soc.*, **57**, 473 (1935).
8) L. Pauling and L. O. Brockway, ibid., **59**, 1223 (1937).
9) J. W. Coutts and R. L. Livingston, ibid., **75**, 1542 (1953).
10) C. Komaki et al., This Bulletin, **28**, 330 (1955).
11) Y. Morino and K. Kuchitsu, to be published in *J. Chem. Phys.*

extremely small energy difference in *n*-propyl chloride and the related hydrocarbons but it conflicts with the energy relation found in dichloro-isobutane; that is, the observed energy difference in this molecule is considerably lower than that in 1,2-dichloroethane, contrary to what is expected from Szasz's hypothesis. It should be assumed, therefore, that the methyl groups in *n*-propyl halides are quite different from the CH_3 groups in 1,2-dichloro-compounds. It may be probable to assume that the methyl group in *n*-propyl chloride rotates slightly about its symmetry axis to minimize the repulsion between the halogen atom and the methyl group and to make the energy difference small.

According to this assumption the two methyl groups in isobutyl chloride rotate around their axis, keeping some liaison to each other like gears, and this fact also makes the energy difference small. In dichloro-isobutane, on the contrary, the rotation of a methyl group is hindered, probably to a considerable extent, by the chlorine atom attached to the carbon atom. Therefore, the energy difference due to this effect will make the *trans* forms unstable, and, accordingly, decrease the net energy difference from that in 1,2-dichloroethane.

The situation may be the same for the methyl-methyl interaction when a halogen atom is attached to the carbon atom to which one of the methyl groups is attached. The degrees of rigidness of methyl groups in dichloropropane, dichloro-isobutane and 2,3-dichloro-2,3-dimethylbutane may not be perfectly equal to each other. The difference of this effect in the above three molecules, however, is supposed to be small, though it may be one of the origins of a small disagreement between the observed energy difference and the calculated one given in Table II. The energy difference 0.77 kcal./mole of *n*-butane may be a result of the fact that methyl-methyl repulsion cannot be cancelled out perpectly by such a rotation of the methyl group, because van der Waals' distance between the methyl groups, 4.33 Å, is larger than the distance of the methyl groups at the *gauche* position, 3.02 Å.

The authors are grateful for aid from the Scientific Research Grant given by the Department of Education of Japan in support of this research.

Department of Chemistry
Faculty of Science
The University of Tokyo
Hongo, Tokyo

12) G. J. Szasz, N. Sheppard, and D. H. Rank, *J. Chem. Phys.*, **16**, 704 (1948).

Dipole Moment and Internal Rotation of 1,4-Dichloro-2-butyne in the gaseous State

By Yonezo MORINO, Ichiro MIYAGAWA, Takehiko CHIBA and Takashi SHIMOZAWA

(Received November 24, 1956)

The dipole moment of 1,4-dichloro-2-butyne in carbon tetrachloride and benzene solutions was previously reported by us[1], and the report showed a slight increase with temperature, causing the hindering potential of 700 cal./mole. Since the solvent exerts considerable influence upon the hindering potential of the internal rotation[2], it is desirable to measure the dipole moment in the vapor state to evaluate the hindering potential of the free molecule. The sample was prepared from 2-butyne-1,4-diol according to the method of Johnson[3], b. p., 66–68°C/17 mmHg. The apparatus used is the one described already[4]. The result of the measurement is given in Table I. The moment is found to be constant through the whole range of temperature of the measurement, contrary to the

1) Y. Morino, I. Miyagawa and A. Wada, *J. Chem. Phys.*, **20**, 1976 (1952).
2) S. Mizushima, Y. Morino and K. Higasi, *Sci. Pap. Inst. Phys. Chem. Res. Tokyo*, **25**, 159 (1934).
3) A. W. Johnson, *J. Chem. Soc.*, **1946**, 1009.
4) T. Chiba, This Bulletin, **28**, 19 (1955).

TABLE I

THE OBSERVED POLARIZATIONS AND DIPOLE MOMENT OF 1,4-DICHLORO-2-BUTYNE

$P_E + P_A = 1.05\,MR_D$ (assumed) = 29.8 cc.

Temperature °K	No. of observations	Pressure range mmHg	Polarization cc.	Mean deviation of polarization	Dipole moment *D*.
364.8	9	34- 56	102.9	0.9 cc.	2.09_1
372.3	14	32- 73	100.5	2.1	2.07_9
392.3	10	43- 92	97.9	0.9	2.09_3
414.1	10	45- 81	93.7	1.0	2.08_2
433.3	9	51-161	90.8	1.2	2.08_1

previous results in solutions. If we assume the hindering potential of the form of $V=(V_0/2)(1-\cos\theta)$, V_0 is found to be less than 0.1 kcal./mole. This result confirms the results of the electron diffraction investigation on this molecule recently made by Morino and Kuchitsu[5] that in the gaseous state this molecule has no preferred position for the internal rotation.

It should be noted that the component of the CH_2Cl group moment perpendicular to the C—C≡C—C axis is found to be 1.47 *D*. If we assume the C—C—Cl angle of 111°[5], this corresponds to the C-Cl moment of 1.57 *D*, which is appreciably smaller than the normal C—Cl moment, 1.86 *D*. Pauling, Gordy and Saylor[6] suggested that propargyl chloride $CH{\equiv}C-CH_2Cl$ resonates between the two formulas $CH{\equiv}C-CH_2Cl$ and $C^+H=C=CH_2\ Cl^-$, and this resonance brings about the elongation of the C—Cl bond and the contraction of the adjacent C—C bond. If the resonance of this type takes place also in dichlorobutyne, it would produce an increase of the dipole moment of the CH_2Cl group, but not its decrease. Therefore, the observed decrease of the said group moment denies Pauling's resonance scheme, or at least, it indicates that the predominant form is not Pauling's one.

Department of Chemistry
Faculty of Science
The University of Tokyo
Hongo, Tokyo

5) Y. Morino and K. Kuchitsu. This Bulletin, (to be published).
6) L. Pauling, W. Gordy and J. H. Saylor, *J. Am. Chem. Soc.* **64**, 1753 (1942).

Dipole Moment and Bond Character of Propargyl Halides and Mono- and Di-chlorobutynes

By Takehiko CHIBA, Takashi SHIMOZAWA, Ichiro MIYAGAWA and Yonezo MORINO

(Received November 24, 1956)

In the preceding paper[1] it was shown that the C—Cl bond moment of 1,4-dichlorobutyne was abnormally small. This is an unexpected result from the current resonance theory. In order to elucidate this circumstance, a measurement was made on the dipole moments of propargyl chloride and bromide, and monochlorobutyne in the gaseous state. Quite recently Rogers and Panish[2] made a study on the dipole moments of similar compounds including propargyl bromide and iodide. Although their measurement was made in solution, the results agreed substantially with the present one.

Experimental

Propargyl chloride was prepared by the chlorination[3] of propargyl alcohol with phosphorus trichloride in the presence of pyridine at about 0°C. The raw product was washed with ice-

1) Y. Morino et al., This Bulletin, **30**, 222 (1957).
2) M. T. Rogers and M. B. Panish, *J. Am. Chem. Soc.*, **77**, 3684 (1955).
3) L. F. Hatch and V. Chiola, ibid., **73**, 360 (1951).

water and fractionated: b. p. 56-57°C.

Propargyl bromide was fractionated from a commercial product of General Anilin and Film Corps.: b. p. 83-84°C.

1-Chloro-2-butyne was prepared from an isomeride of 1,3-dichloro-2-butene (b. p. 66-67°C/95 mmHg) by the following procedure[4]: first dichlorobutene was hydrated to 1-chloro-2-butene-3-ol (b. p. 93-94°C/50 mmHg) by boiling with sodium carbonate solution. This alcohol was dehydrochlorinated to 2-butene-1-ol (b. p. 90-96°C/95 mmHg) by boiling with a concentrated solution of potassium hydroxide. 2-Butyne-1-ol was chlorinated to 1-chloro-2-butyne by the method used for propargyl chloride. The fractionated product had the boiling point of 104-107°C.

The apparatus and the procedure of the measurement of the dipole moments is described elsewhere[5].

Results and Discussions

The results of the measurement of the dipole moments are given in Table I.

As regards propargyl chloride, Pauling et al.[6] proposed the following resonance structure for the explanation of the longer C—Cl distance;

(A) $HC{\equiv}C{-}CH_2Cl$

and (B) $H{-}C^{+}{=}C{=}CH_2\ Cl^{-}$.

If it is true, the dipole moment of propargyl chloride will be large, because the form (B) has a large moment (ca. 18 *D*) due to the positive charge at the carbon atom and the negative charge at the chlorine atom. The observed values 1.65 *D* of chloride and 1.52 *D* of bromide do not show any trace of this tendency. Therefore, it is impossible to take this resonance formula for the main structure of propargyl chloride.

This anomalous feature is more distinct when propargyl halides are compared with the corresponding compounds having a double bond. The moment of allyl chloride, 1.98 *D*[7], is somewhat less than that of propyl chloride, 2.10 *D*[8]. As Smyth has pointed out[7], the difference between them can be explained by taking into account a hyperconjugation of

(C) $C^1H_2{=}C^2H{-}C^3H_2Cl$

and (D) $H_2C^{-}{-}CH{=}CHCl\ H^{+}$.

According to this opinion, the observed moment 0.35 *D* of propylene molecule itself may be ascribed to this hyperconjugation, and, if this hyperconjugation is not disturbed by the substitution of a chlorine atom, the moment of allyl chloride will be calculated by taking a resultant of the two dipoles, one in the C-Cl bond direction,

TABLE I

RESULTS OF THE MEASUREMENT OF THE DIPOLE MOMENT IN THE GASEOUS STATE

Temp. K	No. of obs.	Press. range mmHg	Molar polarizn. cc.	Mean deviatn. of polarizn. cc.	Dipole moment *D*
Propargyl chloride					
MR_D=18.8 cc.[a]		P_E+P_A=19.7 cc.			
294.3	7	26-56	76.2	0.1	1.65_2
326.3	9	54-79	70.8	0.4	1.65_3
					av. 1.65_3
Propargyl bromide					
MR_D=22.1 cc[b]		P_E+_A=23.2 cc.			
306.3	8	45-77	69.2	0.3	1.52_1
349.8	9	54-93	63.6	0.7	1.52_3
373.3	8	67-95	60.6	0.3	1.51_4
					av. 1.51_9
1-Chloro-2-butyne					
MR_D=23.7 cc.[a]		P_E+P_A=24.9 cc.			
328.4	8	51-59	113.1	0.6	2.18_0
354.4	10	57-85	105.5	1.0	2.16_5
385.6	9	61-91	99.6	0.8	2.17_4
					av. 2.17_3

a) Ref. (3)

b) Ref. (2)

$P_E+P_A=1.05\ MR_D$ is assumed throughout.

4) M. S. Schechter et al., idid., **74**, 4903 (1952).

5) T. Chiba, This Bulletin, **28**, 19 (1955), refer also to the forthcoming paper on the dipole moment of cyclohexadione.

6) L. Pauling, W. Gordy and J. H. Saylor, *J. Am. Chem. Soc.*, **64**, 1753 (1942).

7) N. B. Hanney and C. P. Smyth, ibid., **68**, 1005 (1946).

8) Groves and Sugden, *J. Chem. Soc.*, **1937**, 158.

and the other, that of the propylene skeleton, in the direction of the C^2—C^3 bond*. Thus, by substrating 0.35 *D* vectorially from the observed moment of allyl chloride, 1.98 *D*, the apparent C—Cl moment is calculated to be 2.08 *D*, which can be compared with the moment of the propyl chloride, 2.10 D. It will be permissible to consider that this is the moment which the form (C) has when the effect of the form (D) is eliminated.

Now, in case of propargyl halides, in order to obtain the apparent C—Cl moment eliminating the contribution from the C≡C—C skeleton, the same kind of correction should be made by taking the moment of methyl acetylene, 0.75 *D*, as the moment of the C≡C—C skeleton on the molecular axis. The observed moments of propargyl chloride, 1.65 *D*, and bromide, 1.52 *D*, yield 1.76 *D* and 1.62 *D*, which are less than those of the corresponding saturated chloride and bromide by 0.28 *D* and 0.40 *D* respectively. According to Rogers[2], this tendency is much more prominent in the case of propargyl iodide, the difference being −0.60 *D***. Thus we have no evidence for the increase of the moments of propargyl halides, so that it is difficult to regard Pauling's resonance structure as a significant contribution to these compounds.

As described in the preceding paper, the component of the CH_2Cl-group moment perpendicular to the C—C axis in dichlorobutyne was found to be 1.47 *D*, assuming free internal rotation, which is definitely smaller than the value 1.74 *D* calculated on the basis of the usual C-Cl bond moment, 1.86 *D*, and of the C—C—Cl angle of 111°[9]. This cannot be accounted for by the mutual induction of the two C—Cl bonds as found in case of 1,2-dichloroethane, since the C—Cl dipoles are far apart in this compound (ca. 5A). Now, if the resonance scheme proposed by Pauling takes place in this molecule too, the following structures are to be taken into account, both of which would bring about the increase of the perpendicular component of the C—C bond moment:

(E) $Cl—CH_2—C^+=C=CH_2Cl^-$

and (F) $Cl^-H_2C=C=C^+—CH_2Cl$.

* Strictly speaking, the moment induced by the hyperconjugation is not in the direction of C^2-C^3 bond, but, considering the possible positions of the C^1-H_2-group, the above assumption on the direction of this moment may be justified.

** Rogers took 0.80 *D* for methyl acetylene moment.

9) Y. Morino and K. Kuchitsu, This Bulletin, (to be published).

Hence there is another evidence against Pauling's resonance structure.

For monochlorobutyne the measurement of the dipole moment is promising because this molecule has a symmetrical structure of carbon skeleton with no dipole moment, so that it will provide a direct estimation of the C—Cl bond moment in these molecules. The observed moment, 2.17 *D*, is unexpectedly large and really almost equal to that of the corresponding saturated compound***. Rogers attributed the small dipole moments and the long C—X bond distances of propargyl halides to the contribution of the following resonance formulas:

(G) $H—C≡C—CH_2^-\ X^+$

and (H) $H—C^-=C=CH_2\ X^+$

The dipole moments of propargyl halides are explained by this resonance, but the C—I bond should have larger increase than does the C—Cl bond, because the moment decrease was found to be pronounced in propargyl iodide compared with the chloride. The C—Br and C—I distances observed by Pauling et al.[6] seem to be practically normal. In addition,the large moment of monochlorobutyne described above cannot be explained by this resonance scheme alone.

If the valence angles and bond moments are assumed to be the same in the three compounds: propargyl chloride, mono- and di-chlorobutynes, the most plausible way to make all moments of these compounds consistent is to take the group moments and their directions as follows:

1. The C—Cl bond moment is 1.58 *D* along the bond direction.
2. The methyl acetylene skeleton of propargyl chloride has a moment 0.75 *D* along the axis of C≡C—C.
3. A moment of 0.93 *D* is induced in the direction of the C≡C—C bond in propargyl chloride, and a moment of 1.04 *D* is induced in monochlorobutyne.

The moment of C—Cl bond, 1.58 *D*, is obtained by use of the perpendicular component of dichlorobutyne, 1.47 *D*, and of the C—C—Cl angle of 111° (see Fig. 1(a)). If this value is kept in the molecule of monochlorobutyne and of propargyl chloride, the vector addition will not hold unless an induced moment is taken into

*** If the sample we prepared were 3-chloro-1-butyne, it could be expected to give a dipole moment as high as 2 *D*. However, the boiling point and the refractive index of our sample agreed with those in the literature, and the configuration 1-chloro-2-butyne was already verified in organic chemical process (Ref. 3. p. 362).

consideration. If we assume that this induced moment is along the direction of the molecular axis, the value of 1.04 D will be obtained for monochlorobutyne (see Fig. 1(b)). Similar consideration gives

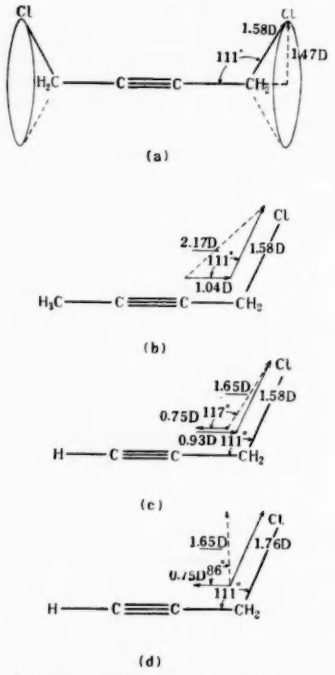

Fig. 1. Dipole moment components and their directions in mono- and di-chlorobutyne and propargyl chloride.

the value of 0.93 D for the induced moment in propargyl chloride in the direction of the molecular axis, using 0.75 D as the moment of the skeleton of C≡C—C (see Fig. 1(c)). Thus it must be concluded that the moment of the C—Cl bond attached to the α position of a C≡C bond is 0.3 D smaller than the usual value and is accompanied with a fairly large moment lying on the axial direction.

Of course this is a tentative conclusion, ignoring a possible difference of the bond moments from one compound to another, as well as the difference in the direction of the induced moments. At first sight, this result may look untrustworthy and peculiar, but a similar phenomenon was found recently by microwave spectroscopy in case of propiolic aldehyde H—C≡C—CHO[10]. It was concluded that the total moment of 2.46 D does not lie along the direction of the C=O bond, but in the direction close to the C≡C—C axis, making an angle of 25–30° with the carbonyl bond direction. This situation is just similar to the case of the chlorine compounds described above.

If the above argument is the case, the resultant moment of propargyl chloride lies along the direction making an angle of 117° with the molecular axis (Fig. 1(c)). On the contrary, if the moment of this compound is composed only of a moment of the C—Cl bond and of methyl acetylene skeleton, as shown in the Fig. 1(d), the resultant should lie in the direction of 86° with the axis. Therefore, it is desirable to determine the direction of the total moment of propargyl chloride by means of microwave spectroscopy, which will make a choice between the alternatives stated above.

Recently Mr. I'Haya calculated the dipole moment of propargyl chloride by the method of MO theory[11]. His result is in excellent agreement with the observed value reported here. The same calculation, however, cannot be applied to dichlorobutyne, because it does not give the dipole moment found by the measurement.

I'Haya suggested us that the induction moment along the C≡C—C axis given in Fig. 1(b) and (c) can reasonably be made smaller from the following reason. The hyperconjugation which takes place in methyl acetylene is twice as large as that in propargyl halide, since the $-CH_3$ group forms two mutually perpendicular "π-type orbitals", each of which is equivalent to that formed by $-CH_2$ group. Therefore, if the moment of methyl acetylene is entirely due to hyperconjugation, 0.38 D must be assumed for the moment of the C≡C—C skeleton in propargyl chloride instead of 0.75 D. This enables one to reduce the inductive moment in propargyl chloride to a more reasonable value 0.56 D. Similarly, in monochlorobutyne one can expect that skeletal moment does not vanish but has a value 0.38 D. This reduces an induction moment to 0.67 D in this compound.

Summary

The dipole moments of propargyl chloride, bromide and monochlorobutyne in the gaseous state are measured to be 1.65 D,

10) J. A. Howe and J. H. Goldstein, *J. Chem. Phys.*, **23**, 1223 (1955).

11) I'Haya, presented at the Discussion Meeting of Structural Chemistry held in Tokyo by the Chemical Society of Japan on October, 1955.

1.52 *D* and 2.17 *D* respectively. The moment of propargyl chloride and bromide are considerably smaller than the saturated one even though the correction of C≡C—C skeletal moment is taken into account. This is consistent with the $-CH_2Cl$ group moment of dichlorobutyne obtained in the preceding work. These results are inconsistent with the resonance scheme presented by Pauling et al. for propargyl halide. The anomaly is considered as a characteristic feature of the molecules having triple bonds of this kind. By taking all of the moments of dichloro- and monochlorobutynes and propargyl chloride into account, the bond moments, the induction moments and the direction of the resultants are predicted as shown in Fig. 1.

The authors wish to express their sincere gratitude to Mr. Y. I'Haya for his valuable suggestion concerning hyperconjugation. They are also indebted to the Ministry of Education of Japan for the research grant.

Department of Chemistry
Faculty of Science
The University of Tokyo
Hongo, Tokyo

Magnetochemical Study of Sydnones

By Yoshio MATSUNAGA

(Received November 26, 1956)

Introduction

The problem of providing an adequate structural formula for sydnones has engaged the minds of chemists, since Earl and Mackney[1] obtained N-phenylsydnone by dehydration of N-nitroso-N-phenylglycine about twenty years ago. The bicylic structure proposed by the discoverers was considered to be unacceptable, and the hybrid structure derived from a number of contributing ionic forms suggested by Baker[2] seems to be consistent with the known properties of the compounds, i. e. general stability of aromatic type, dipole moment [3,4] and ultra-violet absorption spectra[2,5]. The non-localized electrons in the sydnone ring will bring about the large diamagnetic contribution, so that the exaltation of molar susceptibility may be expected against the calculated values for any of the contributing ionic forms, and its magnitude may be considered as a measure of its aromatic character. With the intention of ascertaining the aromatic character of sydnone ring, we examined the diamagnetic susceptibilities of some derivatives of sydnone.

1) J. C. Earl and A. W. Mackney, *J. Chem. Soc.*, **1935**, 899.
2) W. Baker, W. D. Ollis and V. D. Poole, ibid., **1949**, 307.
3) J. C. Earl, E. M. W. Leake and R. J. W. Le Fèvre ibid., **1948**, 2269.
4) R. A. W. Hill and L. E. Sutton, ibid., **1949**, 746; **1953**, 1482.
5) J. C. Earl,R. J. W. Le Fèvre and I. R. Wilson, ibid., **1949**, S. 103.

Experimental

Materials.— They were prepared by the methods described in the references cited. N-phenylsydnone[1], recrystallized from boiling water and sublimed in vacuum. m. p. 132-3°C. (all of m. p. are not corrected.) N-*p*-tolylsydnone[2], sublimed in vacuum. m. p. 140-1°C. N-*p*-methoxyphenylsydnone[6], sublimed in vacuum. m. p. 123-4°C. N-*p*-chlorophenylsydnone[2], recrystallized from the mixture of benzene and light petroleum. m. p. 113°C. N-*m*-nitrophenylsydnone. The mixture of nitrosoglycine and acetic anhydride was warmed on a steam bath for six hours and concentrated under reduced pressure. The precipitated crystals were washed and recrystallized from ethanol. m. p. 137-8°C. Eade and Earl[6] obtained the same material by the reaction at room temperature for two months; the above procedure was in imitation of that for *p*-analogue given by Baker. N-*p*-nitrophenylsydnone[2], recrystallized from the mixture of benzene and light petroleum. m. p. 180-2°C. N-β-naphthylsydnone[6], recrystallized from ethanol and sublimed in vacuum. m. p. 157°C. N-benzylsydnone[2], recrystallized from the mixture of benzene and light petroleum. m. p. 67-9°C. N-phenyl-C-bromosydnone[2], recrystallized from ethanol repeatedly. m. p. 133-4°C. N-phenyl-C-iodosydnone[7], recrystallized from methanol. m. p. 157-8°C. N-phenyl-C-chloromercurysydnone[7], recrystallized from methanol. m. p. 196-8°C. bis(N-phenylsyd-

6) R. A. Eade and J. C. Earl, ibid., **1946**, 591.
7) K. Nakahara and M. Ohta, *J. Chem. Soc. Japan (Pure Chem. Sect.)*, **77**, 1306 (1956).

nonyl-C-)mercury[7], precipitated crystals were washed with methanol and used without further purification.

Magnetic Measurement. — The susceptibility was measured using a Gouy balance as previously described[8].

Results and Discussion

The results are shown in Table I[9] for N-arylsydnones which have no substituent in the sydnone ring. If we assume that the effect of conjugation between aryl and sydnonyl groups on the molar susceptibility is small, we may approximate their susceptibilities by the sum of those of constitutional fragments of the molecule, namely aryl and sydnonyl groups. For example, from the molar susceptibility of N-phenylsydnone the value of benzene is subtracted and twice the amount of Pascal's constant for hydrogen is added; the remainder may be considered as the molar susceptibility of the unsubstituted sydnone $C_2H_2N_2O_2$. The evaluated values by the similar method from the data of the other seven compounds are also given in column four of Table I. The following values were used for the calculations, benzene 55.2[10], toluene 65.8[11], anisol 72.6[12], chlorobenzene 70.0[13], nitrobenzene 61.8[11] and naphthalene 92.2[14]. Including the value derived from the molar susceptibility of N-benzylsydnone in which the conjugation between two constitutional fragments does not exist, their agreements are satisfactorily good, and the assumption made in the above evaluations is supported by this fact. The mean value 38.7 will be used in the discussion hereafter.

TABLE I

MOLAR SUSCEPTIBILITIES OF N-ARYLSYDNONES

Substance	Suscept. (χ)	Molar Suscept. (χ_M) ArSy.*	HSy.*
N-Phenylsydnone	0.540	87.6	38.3
N-*p*-Tolylsydnone	0.556	98.0	38.1
N-*p*-Methoxy-phenylsydnone	0.542	104.2	38.0
N-*p*-Chloro-phenylsydnone	0.518	101.8	37.7
N-*m*-Nitro-phenylsydnone	0.458	94.9	39.0
N-*p*-Nitro-phenylsydnone	0.458	94.9	39.0
N-β-Naphthyl-sydnone	0.593	125.8	39.5
N-Benzylsydnone	0.568	100.1	40.2

* Sy is the abbreviation of sydnonyl group.

Generally the diamagnetic anisotropy of a molecule is expressed as

$$\Delta K = 3(\chi_M - K_i)$$

where χ_M and K_i are the observed molar susceptibility for powdered specimen and its isotropic part respectively. The isotropic part of an ordinary aromatic compound is usually assumed to be equal to the principal molar susceptibility in the plane of a molecule, and approximated by the calculated value for its Kekulé form[15]. It seems to be acceptable that the isotropic part of molar susceptibility of meso-ionic compound can be approximated by the calculated value for the contributing ionic form; and the anisotropic part corresponds to the diamagnetic contribution of non-localized electrons in the meso-ionic ring. Although a regular pentagon was assigned by many chemists for the simplest model of sydnone ring, it must be noted that the application of the above formula is not restricted by the non-coplanarity of the ring[16]. In the case of aromatic compounds, the magnitude of the isotropic part does not depend on the forms in so far as we choose the Kekulé form for the purpose of evaluating it. But in the present case, the calculated values for the contributing ionic forms are not necessarily equal to each other, and it is incorrect to pick out one of them as the representative for which the isotropic part must be calculated. The following five forms (I—V) were considered by Baker[2] to make important contributions to the hybrid, and Hill and Sutton[1] suggested that there is a major contribution from form (I) and a lesser from (II) and (IV).

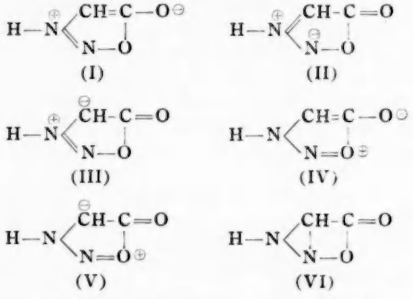

8) H. Akamatu and Y. Matsunaga, This Bulletin, **26**, 364 (1953).
9) All susceptibility values in this paper are recorded in 10^{-6} c. g. s. units and the negative signs are omitted.
10) B. C. Eggleston et al., *J. Chem. Soc.*, **1954**, 941.
11) F. G. Baddar and S. Sugden, ibid., **1950**, 308.
12) P. Rumpf snd M. Séguin, *Bull. soc. chim. France*, **1949**, D 366.
13) C. M. French and V. C. G. Trew, *Trans. Faraday Soc.*, **41**, 439 (1945).
14) H. Akamatu and Y. Matsunaga, This Bulletin, **29**, 800 (1956).
15) H. Shiba and G. Hazato, ibid., **22**, 92 (1949).
16) A. Pacault, *Bull. soc. chim. France*, **1949**, D 371.

Therefore, by means of Gray-Cruickshank's system[17] we calculated the values for these forms as the isotropic part of molar susceptibility of unsubstituted sydnone. For example, the value for form (I) was calculated based on the model shown in Fig. 1 using the constants presented in Table II.

TABLE II

CALCULATION OF MOLAR SUSCEPTIBILITY OF IONIC FORM (I) OF SYDNONE

Atom	(Charge)	Ionic Diamagnetism	Bond	Bond Depression
H	(+0.04)	2.28	C—H	0.53
H	(+0.29)	1.68	C=C	9.50
C	(−0.02)	9.89	C—N	1.78
C	(−0.26)	9.10	C—O	1.92
N	(−0.08)	8.09	C—O	1.92
N	(−0.65)	6.74	N—H	0.57
O	(−0.21)	7.58	N=N	13.3*
O	(−1.13)	9.82	N—O	2.06
Total Diamagnetism		55.18		31.58
Total Bond Depression		31.58		
Resultant Molar Suscept.		23.60		

* Estimated from the constant for azo group determined previously[15].

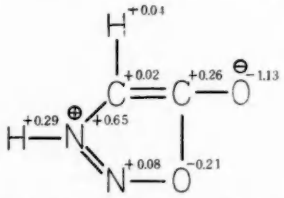

Fig. 1. Model of ionic form (I) of sydnone.

Table III illustrates the calculated values for the five forms, including also the value for bicyclic structure (VI) calculated using Pascal's constants, and the latter which must be compared directly with the experimental value appears to be unacceptable again from this standpoint. Fortunately the calculated values for (I—V) are so close to each other that we estimate the isotropic part of molar susceptibility of sydnone at the mean value 24.57. By the comparison between the value derived from the experimental data shown in Table I and the estimated one, we obtain 14.1 as the exaltation of molar susceptibility i. e. $\Delta K/3$ which must be due to the contribution of non-localized electrons in the sydnone ring. The estimated exaltation is nearly equal to those of furan 13.4 and pyrrole 14.4 and slightly less than that of thiophene 17.9 given by Pacault[19]. According to Dewar[20], an aromatic compound is defined as a cyclic compound with a large resonance energy. The relation between resonance energy and diamagnetic anisotropy is uncertain and not simple. It is not correct to affirm that the molecule which shows the larger diamagnetic anisotropy has always the larger resonance energy. As an example of the extremely conflicting cases, perylene shows the diamagnetic anisotropy less than twice as large as that of naphthalene, but its resonance energy is larger than twice the latter's[21]. As to sydnone, however, the

TABLE III

CALCULATED MOLAR SUSCEPTIBILITIES OF IONIC AND BICYCLIC FORMS OF SYDNONE

Form	Molar Suscept. (χ_M or K_i)
Ionic (I)	23.60
Ionic (II)	24.69
Ionic (III)	24.74
Ionic (IV)	24.08
Ionic (V)	25.22
Bicyclic (VI)	25.46

nearly isoelectronic structure with furan and pyrrole results from a large fractional negative charge borne by the oxygen atom in carbonyl group, so it seems to be probable that sydnone ring has the aromatic character in the same order with furan and pyrrole rings.

Next we examined the molar susceptibilities of four derivatives of N-phenylsydnone in which the substituent is linked to the carbon atom of the sydnone ring, and compared them with the calculated values based on the constant for sydnone 38.7 derived from eight N-arylsydnone by the aid of the additivity rule. The results are presented in Table IV. Kadomtzeff[22] showed that the magnetic contribution of mercury depends markedly on the nature of the rest of the molecule and gave the values from 23.8 to 43.0 for the mercury in RHgX, and from 28.5 to 46.0 for the same atom in R_2Hg. We used in our cal-

17) F. W. Gray and J. H. Cruickshank, *Trans. Faraday Soc.*, **31**, 1491 (1935).
18) Y. Matsunaga, This Bulletin, **29**, 308 (1956).
19) A. Pacault, *Rev. sci.*, **86**, 38 (1948).
20) M. J. S. Dewar, "The Electronic Theory of Organic Chemistry", Oxford Univ. Press, Oxford, (1949) p. 160.
21) F. Klages, *Ber.*, **82**, 358 (1949).
22) I. Kadomtzeff, *Bull. soc. chim. France*, **1949**, D 394.

culations the constants of mercury in the most similar compounds which have ever been measured, namely the derivatives of thiophene.

TABLE IV

MOLAR SUSCEPTIBILITIES OF DERIVATIVES OF N-PHENYLSYDNONE

Substance	Suscept. (χ)	Molar Suscept. (χ_M) Obs.	Calcd.	Diff. (%)
N-Phenyl-C-bromosydnone	0.461	111.1	111.5	−0.3
N-Phenyl-C-iodosydnone	0.429	123.6	125.5	−1.4
N-Phenyl-C-chloromercury-sydnone	0.378	150.1	144.0*	+4.3
Bis (N-phenyl-sydnonyl-C-) mercury	0.383	200.3	198.5**	+1.0

* The constant of mercury 38.9 was used.
** The constant of mercury 28.5 was used.

The calculated molar susceptibilities agree well with the observed ones, except the case of N-phenyl-C-chloromercury-sydnone. At the present, we cannot decide conclusively between the incorrect estimation of the constant of mercury used in the calculation and the remarkable change of the contribution of non-localized electrons in a sydnone ring as the cause of this disagreement. The latter case was found by Hazato[23] in the derivatives of tropolone which some investigators regard as one type of meso-ionic compounds. However, the author is inclined to the former cause, as such a large influence of substituent on diamagnetism is not common in a number of aromatic compounds, besides such a disagreement is not found in the other three cases presented here.

23) G. Hazato et al, *Sci. Repts. Research Insts. Tohoku Univ., Ser.* A, **5**, 278 (1953); **6**, 193 (1954).

Summary

The molar susceptibilities of eight N-arylsydnones were measured by the Gouy method. Assuming that the influence of the conjugation between aryl and sydnonyl groups on diamagnetism is practically negligible, the molar susceptibility of unsubstituted sydnone was estimated as 38.7. Its isotropic part 24.57 was evaluated from the values for five of the contributing ionic forms calculated by the Gray-Cruickshank's method. From the magnitude of the exaltation of molar susceptibility which is equal to one third of an anisotropic part, the author suggested that the aromatic character of a sydnone ring is in the same order with those of furan and pyrrole rings. Four derivatives of N-phenylsydnone which have a substituent in meso-ionic ring were also measured, and the agreements between the observed and the calculated molar susceptibilities were found to be good within the limit of the latter's estimation.

The author wishes to express his hearty thanks to Prof. H. Akamatu for his kind direction. The cost of this study has been defrayed by the Grant in Aid for Fundamental Scientific Research from the Ministry of Education, to which the author's thanks are also due.

Department of Chemistry
Faculty of Science
The University of Tokyo
Hongo, Tokyo

The Molecular Structure of 1,2-Difluoro-1,1,2,2-tetrachloroethane

By Machio IWASAKI, Shunji NAGASE and Rimpei KOJIMA

(Received October 8, 1956)

Introduction

The molecular structure of 1,2-difluorotetrachloroethane offers two interesting problems. One is concerned with rotational isomerism while the other with the effect of the neighbouring halogen atoms on the C—F and C—Cl bond distances.

The phenomenon of the rotational isomerism in halogenated ethanes has been the subject of a great number of investigations during the past two decades. However, most of these works have been carried out by measuring the change of dipole moments or infrared absorptions with temperature compared with the

results of which measurements by electron diffraction are meagre. Furthermore, the general applicability and the merits of various potential functions[1,2] that have recently been proposed cannot be criticized until comprehensive data on the structure of related molecules are available. Therefore it is desirable to carry out a study by electron diffraction side by side with studies by spectroscopy and dipole moment measurement.

Having such points in mind, the present writers have undertaken the herein described work in order to determine the molecular structure and the energy difference between two isomers by means of electron diffraction.

Experimental

Sample

The sample was prepared by the fluorination of hexachloroethane with SbF_3 in the presence of $SbCl_5$ as a catalyst. The product distilled at 92.5°C. The purity of this sample was tested with an infrared absorption spectrum. It was confirmed that the amount of CCl_3—CF_2Cl, which could not be removed by fractionation, was less than about one per cent. Hence the amount was not great enough to affect the electron diffraction pattern.

Procedure

The diffraction patterns of 40 KV. electrons were obtained at a temperature of about 15°C using a rotating sector apparatus, which will be described in detail elsewhere. Two camera distances of 28 cm. and 12 cm. were used with an s^2 sector. The photographic density was measured up to $q=90$ by a recording microphotometer. In this measurment, the photographic plate was rotated rapidly about the center of the diffraction pattern in order to smooth out the inevitable irregularities. The traces thus obtained were measured by a coordinate comparator as a function of q. A procedure[3] similar to that employed by J. Karle was used for deriving an experimental intensity curve from the microphotometer record.

The experimental intensity curve, I_m, was obtained from the curve of the total scattered intensity, I_t, by drawing a smooth background, I_b, then

$$I_m=(I_t/I_b)-1. \tag{1}$$

The curve A shown in Fig. 4 is I_m multiplied by q, where the dotted portion is drawn by use of a theoretical intensity curve described below.

1) W. D. Gwinn and K. S. Pitzer, *J. Chem. Phys.*, **16**, 303 (1948).
2) H. J. Bernstein, ibid., **17**, 262 (1949).
3) I. L. Karle and J. Karle, ibid., **17**, 1052 (1949); **18**, 957 (1950).

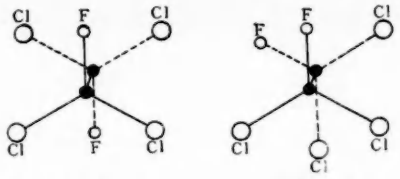

trans form *gauche* form

Fig. 1. Stable configurations of $CFCl_2$-$CFCl_2$.

Analysis

The radial distribution curve shown in Fig. 2 was calculated by the following equation:

$$f(r)=\sum_{q=0}^{q_{max}} qI_m \exp(-aq^2)\sin(\pi qr/10), \tag{2}$$

where $a=0.00288$.

The curve has maxima at 1.38, 1.76, 2.5—3.3, 3.92 and 4.33 Å. The first two peaks at 1.38 and 1.76 Å correspond to C—F and C—Cl bond distances, respectively. The peak at 2.5—3.3 Å is due to various non-bonded distances, while that at 4.33 Å to the *trans* Cl···Cl distance. The peak at 3.92 Å corresponds to the *trans* F···Cl distance, which is characteristic of *gauche* configuration (see Fig. 1). This peak evidently shows the existence of the *gauche* form. If only the *gauche* form exists, the ratio of the area of the peak at 4.33 Å to that at 3.92 Å must have the value of 0.86. The fact that the observed ratio has the value of 2.43, indicates that the *trans* form, having no *trans* F···Cl distance, coexists with the *gauche* form (see Fig. 1). The ratio of the two forms, N_t/N_g, can be calculated from the areas of the two peaks noted above by means of the following formula:

$$\frac{N_t}{N_g}=\frac{Z_F r_{Cl\cdots Cl}A_{Cl\cdots Cl}}{Z_{Cl}r_{F\cdots Cl}A_{F\cdots Cl}}-\frac{1}{2}, \tag{3}$$

where $A_{Cl\cdots Cl}$ and $A_{F\cdots Cl}$ are the areas of the peaks and $r_{Cl\cdots Cl}$ and $r_{F\cdots Cl}$ are the equilibrium distances for the *trans* Cl···Cl and *trans* F···Cl, respectively. The application of this formula leads to a value of 52 per cent. for the amount of the *gauche* form.

In the calculation of the radial distribution curve, in place of the intensity curve below $q=17$ the theoretical intensity was substituted. The ratio of the areas was affected by the value of the abundance ratio of the two isomers assumed in the calculation of the theoretical part of the intensity. Therefore, the method of successive approximation was taken. If the theoretical part is calculated for 100 per cent. *gauche* form, formula 3 above leads to a value of 78 per cent. for the amount of the *gauche* form. Next, assuming the amount of the *gauche* form to be equal to 78 per cent. a value of 71 per cent. was obtained. The successive approximation being carried out as given above, a self-consistent value of 52 per cent. was obtained. This value was scarcely affected by the values of molecular parameters assumed in the calculation. The radial distribution curve shown in Fig. 2 was

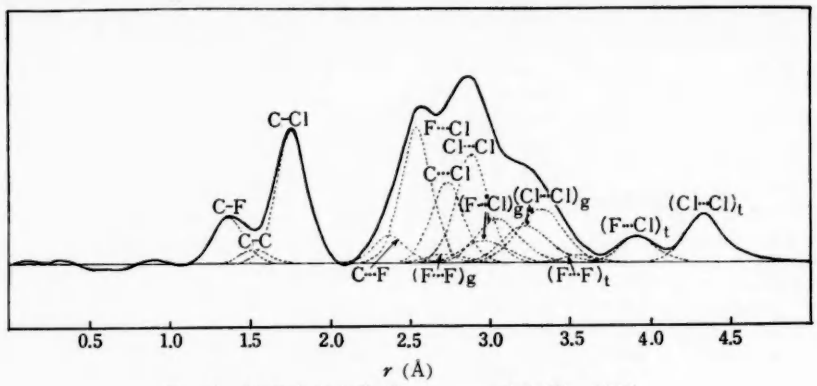

Fig. 2. Radial distribution curve of $CFCl_2$—$CFCl_2$.

obtained by the procedure described above using the values of molecular parameters listed in Table III.

The part from 2.5 to 3.3 Å of the radial distribution curve corresponds to the superposition of the contributions of 10 interatomic distances in the *trans* as well as in the *gauche* form. This part of the radial distribution curve calculated as the sum of Gaussian curves, each corresponding to the contribution of an interatomic distance, was in good agreement with the experimental curve, when the amount of the *gauche* form was assumed to be about 50 per cent. The assumed values of the mean amplitudes used in this calculation are listed in Table I. The dotted curves shown in Fig. 2 depict the contributions of various interatomic distances. Although the assumed values were used for the mean amplitudes, the result from this part of the radial distribution curve serves to confirm the percentage of the *gauche* form derived from the ratio of the peak areas at 4.33 and 3.92 Å.

The shelf at 3.2 Å corresponds to the *gauche* Cl···Cl distance in the *gauche* form*. Therefore, from this portion of the radial distribution curve, the value of 55—63° was obtained for the azimuthal angle of F—C—C—F of the *gauche* form.

The analysis of the over-all feature of the radial distribution curve gave the values listed in Table III for the interatomic distances and the valency angles. Other items of information obtained from the radial distribution curve are the values of the mean amplitudes of the bonded C—F, bonded C—Cl, *trans* F···Cl, and *trans* Cl···Cl distances. The mean amplitudes of other distances could not be determined because of the superposition of many interatomic distances in the radial distribution curve. If the observed peaks are made to fit Gaussian curves, the values listed in Table I are obtained for the mean amplitudes of these distances, which agree with the values calculated by Morino et al.[4]

TABLE I

OBSERVED AND ASSUMED MEAN AMPLITUDES IN Å

Distance	Obs.	Calcd.	Distance	Obs.	Calcd.
C—F	0.064	0.045	$(F\cdots F)_g$		0.114
C—C		0.050	$(F\cdots Cl)_g$		0.120
C—Cl	0.062	0.050	$(Cl\cdots Cl)_g$		0.125
C···F		0.059	$(F\cdots F)_t$		0.061
F···Cl		0.065	$(F\cdots Cl)_t$	0.070	0.070
C···Cl		0.073	$(Cl\cdots Cl)_t$	0.081	0.074
Cl···Cl		0.070			

* The *gauche* Cl·····Cl distance of the *trans* form is somewhat smaller than this value.

The theoretical intensity curves were calculated by use of the following equation:

$$qI(q) = \sum_{i>j}\sum \frac{Z_i Z_j}{r_{ij}} \exp(-b_{ij}q^2)\sin(\pi q r_{ij}/10) \quad .(4)$$

In this equation, notations have their usual significances. The constant b_{ij} was calculated from the mean amplitudes listed in Table I. Though the majority of these values are calculated by Morino et al.[4] from spectroscopic data, the values for the non-bonded F···Cl and the *trans* F···Cl distances were assumed appropriately from other data. The values for the *gauche* F···F and the *gauche* Cl···Cl distances were taken from Karle's experimental data on C_2Cl_6[5] and C_2F_6[6] by ascribing the contribution of the torsional oscillation to the over-all vibration. For the *gauche* F···Cl distance, use was also made of Karle's data.

The curve A in Fig. 3 is of 100 per cent. *trans* form and the curve E of 100 per cent. *gauche* form for the model obtained from the radial distribution curve on the assumption that the structural frame of the molecule does not change with rotation. The curves B, C and D are of the isomeric mixture, in which the amount of the *gauche* form is 30, 50 and 70 per cent. respectively. The curve for the *trans* form as well as the *gauche* does not agree with the experi-

4) Y. Morino, K. Kuchitsu, A. Takahashi and K. Maeda, *J. Chem. Phys.*, **21**, 1927 (1953).
5) D. A. Swick, I. L. Karle and J. Karle, ibid., **22**, 1242 (1954).
6) D. A. Swick and I. L. Karle, ibid., **23**, 1499 (1955).

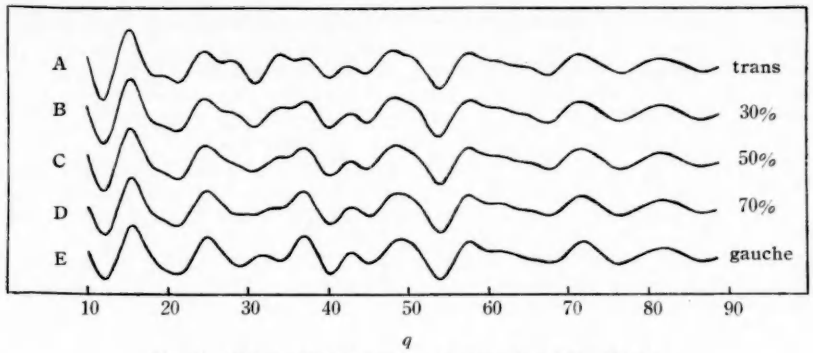

Fig. 3. Theoretical intensity curves of $CFCl_2$—$CFCl_2$.

TABLE II
MOLECULAR PARAMETERS FOR $CFCl_2$—$CFCl_2$

Model	C—F	C—C	C—Cl	∠CCCl	∠ClCCl	∠FCCl
B	1.38 Å	1.54 Å	1.76 Å	112°	110°30′	107°30′
C	〃	〃	〃	110°	〃	107°
D	〃	〃	〃	114°	〃	〃
E	〃	〃	〃	112°	109°30′	〃
F	〃	〃	〃	〃	110°30′	〃
G	〃	〃	〃	〃	111°30′	〃
H	〃	〃	〃	〃	110°30′	106°
I	〃	〃	〃	〃	〃	108°
J	〃	〃	1.73	〃	〃	107°
K	〃	〃	1.79	〃	〃	〃
L	1.34	〃	1.76	〃	〃	〃
M	1.42	〃	〃	〃	〃	〃
N	1.38	1.48	〃	〃	〃	〃
O	〃	1.60	〃	〃	〃	〃
P	〃	1.54	〃	〃	〃	〃
Q	〃	〃	〃	〃	〃	〃
R	〃	〃	〃	〃	〃	〃

ment. The curve for the mixture is in satisfactory agreement with the experiment, if the *gauche* form is present in an amount nearly equal to 50 per cent. The result confirms definitely the amount of the *gauche* form already derived from the radial distribution curve.

Moreover, the limits of errors in the percentage of the *gauche* form as well as the values of the interatomic distances, the valency angles, and the azimuthal angle of the *gauche* form were determined by the analysis of 100 theroretical intensity curves for models having a C—F distance ranging from 1.30 to 1.42 Å, a C—Cl distance from 1.73 to 1.79 Å, a C—C distance from 1.45 to 1.60 Å, ∠CCCl from 109°28′ to 115°, ∠ClCCl from 109°28′ to 111°30′ and ∠FCCl from 109°28′ to 105°30′. Some of them are shown in Fig. 3 in order to illustrate the dependence of the relative positions and intensities of maxima and minima upon the parameters. The values of the parameters used are listed in Table II. Curve B in Fig. 4 gives the best model. It reproduces the feature of the experimental curve in a satisfactory manner. The mean value of q/q_0 for the maximum and minimum positions is 1.000 with an average deviation of 0.002.

The variation in the parameter ∠CCCl causes changes mainly in the regions $18<q<23$ and $30<q<40$, that of ∠ClCCl mainly in the region $39<q<47$, that of ∠FCCl mainly in the region $47<q<52$, that of C—Cl mainly in the positions of the maxima and minima, and those of C—F and C—C mainly in the regions $30<q<40$ and $47<q<52$ as shown in curves C, F and D, curves E, F and G, curves H, F and I, curves J, F and K, curves L, F and M, and curves N, F and O, respectively. It was assumed for the sake of comparison that the three *gauche* Cl···Cl distances in the *gauche* form were equal and the amount of the *gauche* form was 50 per cent. in all of the models described above, although the change in the azimuthal angle or the amount of the *gauche* form may improve the agreement with the experimental curve. The changes due to the variation of these two parameters are illustrated in curves P, Q and R of Fig. 4 and curves B, C and D of Fig. 3. The curves P, Q and R depict the theoretical intensity for the models of the azimuthal

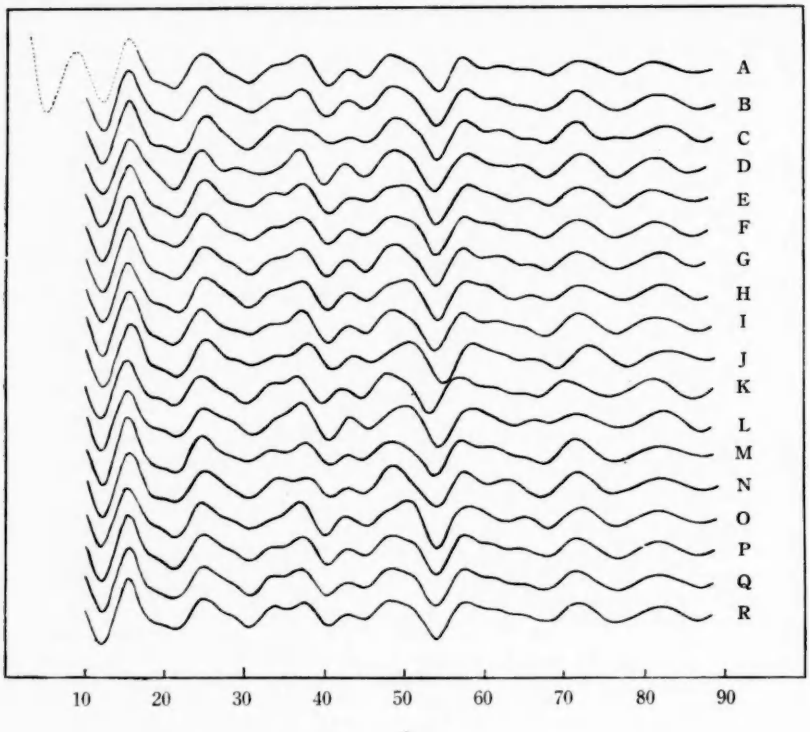

Fig. 4. Theoretical intensity curves of $CFCl_2$—$CFCl_2$

angles of 60°00′, 57°36′ and 55°12′, respectively.

As the parameter C—Cl gave large shifts for the positions of maxima and minima, the value of 1.76±0.01 Å was determined for the C—Cl distance. The relation between the depths of minima at q=40.3 and q=45.0 is very sensitive to the parameter ∠ClCCl. The feature of this region leads to the value of 110°30′±1° for the ∠ClCCl. The feature of the region $30<q<40$ is sensitive to the parameter ∠CCCl, C—F and C—C, while the feature of the region $47<q<52$ is sensitive to the parameter ∠FCCl, C—F and C—C. As the effects of these parameters appear in the same region, the limits of errors become somewhat larger for these parameters, especially for C—C. The values of C—F, C—C, ∠CCCl and ∠FCCl were determined as 1.38±0.02 Å, 1.54±0.06 Å, 112°±2° and 107°30′±1°30′, respectively. And the azimuthal angle and the amount of the *gauche* form were determined as 59°±4° and 55±10 per cent., respectively.

TABLE III

RESULTS OF ANALYSIS OF RADIAL DISTRIBUTION CURVE AND FINAL RESULTS FROM ADDITIONAL STUDY OF THEORETICAL INTENSITY CURVES

	From radial distribution curve	Final results
Bond distance in Å		
C—F	1.37	1.38±0.02
C—C	1.54	1.54±0.06
C—Cl	1.76	1.76±0.01
Valency angle		
∠CCCl	112°	112°±2°
∠ClCCl	110°30′	110°30′±1°
∠FCCl	107°	107°30′±1°30′
Azimuthal angle of *gauche* form	55—63°	59°±4°
Amount of *gauche* form	52% at 15°C	55±10% at 15°C

Discussion of Results

Using infrared and Raman spectra, Kagarise and Daasch[7] investigated the energy difference between the isomers of the molecule under investigation. On the basis of the invariance of the spectrum with respect to temperature, they proposed two possible explanations of the spectroscopic data, neither of which is completely satisfactory. One is based on the assumption of a single molecular species corresponding to a largey energ difference, while

7) R. E. Kagarise and L. W. Daasch, *J. Chem. Phys.*, **23**, 113 (1955).

the other is based on the presence of two forms having an almost equal energy (ΔE <300 cal./mol.). Although a definite conclusion could not be obtained from the spectroscopic data, the existence of two isomeric forms was concluded from the result of the electron diffraction. The energy difference of the two isomers was calculated approximately from the obtained diffraction data by use of the following formula:

$$N_g/N_t = 2\exp(-\Delta E/RT). \quad (5)$$

The application of this formula leads to a value of 0—500 cal./mol. for the energy difference of the two isomers, the *trans* form being somewhat more stable than the *gauche* form. The result of the use of the electron diffraction method favors the second explanation proposed by Kagarise and Daasch.

A number of investigations on the molecular structures of organic fluorides indicated that the C—F and C—Cl bond lengths decrease with the number of fluorine atoms bonded with a carbon atom. The data on the molecular structures of some related compounds are listed in Table IV. Although $CFCl_2$—$CFCl_2$ is a difluoride, there is only one fluorine atom bonded with a carbon atom, and therefore C—F bond distance has almost the same value as that of a monofluoride. This fact indicates that the effect of substitution by fluorine atoms on the adjacent carbon atom is very small. The C—Cl bond distance in this molecule is affected scarcely at all by the fluorine atom, but it seems to be slightly shorter than the C—Cl bond in CH_2Cl_2 or $CHCl_3$, although this fact can not definitely be confirmed because of the uncertainty in the value of this distance.

TABLE IV

MOLECULAR STRUCTURES OF SOME RELATED COMPOUNDS

Compound	C—F (Å)	C—Cl(Å)	Method
CH_3F[a]	1.385		M. W.*
CH_2ClF[b]	1.378±0.006	1.759±0.003	〃
$CHCl_2F$[c]	1.41 ±0.03	1.73 ±0.04	V. E. D.**
CCl_3F[c]	1.40 ±0.04	1.76 ±0.02	〃
$C(CH_3)_3F$[d]	1.38 ±0.02		V. E. D. & M. W.
CH_3CH_2F[e]	1.375±0.02		M. W.
CCl_2F—CCl_2F[f]	1.38 ±0.02	1.76 ±0.01	S. E. D.***
CH_2F_2[g]	1.358		M. W.
$CHClF_2$[c]	1.36 ±0.03	1.73 ±0.03	V. E. D.
CCl_2F_2[c]	1.35 ±0.03	1.74 ±0.03	〃
CHF_3[h]	1.332±0.008		M. W.
$CClF_3$[i]	1.328±0.002	1.751±0.004	S. E. D.
CF_4[j]	1.323±0.005		S. E. D.
C_2F_6[k]	1.32 ±0.01		〃
CH_3Cl[l]		1.783 ±0.003	S. E. D.
$C(CH_3)_3Cl$[l]		1.80 ±0.01	〃
CH_2Cl_2[m]		1.7724±0.0005	M. W.
$CHCl_3$[h]		1.767	〃

* Microwave ** Visual electron diffraction *** Sector electron diffraction.

a) O. R. Gillam, H. D. Edwards and W. Gordy, *Phys. Rev.*, **75**, 1014 (1949).
b) N. Muller, *J. Am. Chem. Soc.*, **75**, 860 (1953).
c) L. O. Brockway, *J. Phys. Chem.*, **40**, 747 (1936).
d) F. Andersen, J. R. Andersen, B. Bak, O. Bastiansen, E. Risberg and L. Smedvik, *J. Chem. Phys.*, **21**, 373 (1953).
e) J. Kraitchman and B. P. Dailey, ibid., **23**, 184 (1955).
f) The present work.
g) D. R. Lide, *J. Am. Chem. Soc.*, **74**, 3548 (1952).
h) S. N. Ghosh, R. Trambarulo and W. Gordy, *J. Chem. Phys.*, **20**, 605 (1952).
i) L. S. Bartell and L. O. Brockway, ibid., **23**, 1860 (1955).
j) L. O. Brockway, C. G. Thornton and L. S. Bartell, *Am. Chem. Soc.*, Meeting, Los Angeles, California, March 1953.
k) See ref. 6.
l) O. Bastiansen and L. Smedvik, *Acta. Chem. Scand.*, **7**, 652 (1953).
m) R. J. Myers and W. D. Gwinn, *J. Chem. Phys.*, **20**, 1420 (1952).

Summary

The molecular structure of 1,2-difluorotetrachloroethane was studied by the electron diffraction method. The existence of the two isomeric forms, *trans* and *gauche*, was ascertained and the amount of the *gauche* form was found to be 55±10 per cent. This corresponds to the energy difference of 0—500 cal./mol. the *trans* form being more stable. The interatomic distances and the valency angles were determind as follows:

C—F=1.38±0.02 Å, C—Cl=1.76±0.01 Å, C—C=1.54±0.06 Å, ∠CCCl=112°±2°, ∠ClCCl=110°30′±1°, ∠FCCl=107°30′±1°30′, and the azimuthal angle of the *gauche* form=59°±4°.

The C—F bond distance in this molecule is greater than those distances of compounds having more than one fluorine atom bonded with a carbon atom. On the other hand, the C—Cl bond distance seems to be slightly shorter than those of chloroalkanes having no substituted fluorine atom.

The diffraction patterns and the microphotometer records were taken by using an apparatus in Nagoya University. The writers wish to express sincere gratitude to Professor M. Kubo, Professor R. Uyeda and Dr. M. Kimura for giving permission to use the apparatus and for their valuable advice. Thanks are also due to Mr. S. Shibata, Mr. H. Morimoto and Mr. K. Kimura of Nagoya University for their friendly assistance and to Mr. K. Kuchitsu and Mr. E. Hirota of Tokyo University for their help concerning a part of the calculations of the theoretical intensity by means of a punched card machine in the Division of Health and Welfare Statistics, Welfare Minister's Secretariat.

The writers are further greatly indebted to Professor Y. Morino of Tokyo University for his helpful criticisms on this investigation.

Government Industrial Research Institute, Chigusa-ku, Nagoya

The Adsorption of Non-Polar Gases on Alkali Halide Crystals. II[1]*. Calculations of The Adsorption Behaviour of Non-Polar Gases on Cubic Sodium Chloride**

By Teruo HAYAKAWA

(Received September 15, 1956)

Introduction

The refined calculations of the adsorption energy of an isolated argon atom on cubic (100) potassium chloride crystal were carried out by Orr[2]. There is some discordance, however, between theory and experiment which may be attributed to the fact that the repulsive constant of Herzfeld for argon has been used in his theoretical calculations. The theoretical treatment of the quadrupole interaction of an isolated nitrogen molecule with cubic (100) potassium chloride crystal has recently been carried out by Drain[3]. His treatment, however, contains some incorrectness due to careless mistake. Moreover, his results on the total adsorption potential of an isolated nitrogen molecule on cubic (100) potassium chloride also contain considerable uncertainty.

The approximate calculation of the heat curve for argon on cubic (100) potassium chloride was carried out by Orr[2] and also by Young[4]. However, the discrepancy between the experimental and calculated heat curves is fairly remakable. It was, therefore, of interest in the present work to obtain the theoretical values for the heats of adsorption of non-polar gases

1) Part I of this series, T. Hayakawa, This Bulletin, **30**, 124 (1957).

* Part of this paper was read before the 8 th Annual Meeting of the Chemical Society of Japan held in Tokyo, April, 1955. Other part of this paper was also read before the symposium on the surface heterogeneity of catalysis held in Kyoto, March, 1956.

2) W. J. C. Orr, *Trans. Faraday Soc.*, **35**, 1247 (1939).

3) L. E. Drain, ibid., **49**, 650 (1953).

4) D. M. Young, ibid., **48**, 548 (1952).

(argon, nitrogen and carbon dioxide) on the (100) plane of sodium chloride crystal and to compare these values with the experimental results given in the preceding paper.

In the present work, the total repulsive potential between an isolated atom or molecule and the lattice ions was calculated using the repulsive constants of the modified Buckingham-Corner (6-exp) potential for these non-polar gases. In the case of nitrogen or carbon dioxide, the total quadrupole potential was calculated, using a method similar to that adopted by Drain and the correction due to the potential barrier hindering the turning over of the molecular axis was made.

Outline of Calculation

Theoretical Calculation of the Adsorption Potential of an Isolated Atom or Molecule on the (100) Face of an Alkali Halide Crystal.—The calculation of the adsorption potential may be divided into four sections,

(A) the Van der Waals' (dispersion) potential, (B) the electrostatic potential, (C) the repulsive potential, (D) the quadrupole potential and the correction due to the potential barrier hindering the turning over of the molecular axis.

Calculations were made of these quantities for the following representative positions on the (100) plane of an alkali halide crystal: (i) above the centre of a lattice cell (sites type A), (ii) above the mid-point of a lattice edge (sites type B), (iii) above an alkali ion (sites type C) and (iv) above a halogen ion (sites type D).

A. The Van der Waals' (Dispersion) Potential.—The total Van der Waals' potential between an adsorbate atom or molecule and a crystal is given by the Kirkwood-Müller formula[5] as

$$\left.\begin{aligned}\Phi_D = \frac{6m_e c^2}{a^6}\Bigg[&\frac{\alpha_0\alpha_+}{\alpha_0/\chi_0+\alpha_+/\chi_+}S_+(\rho)\\ &+\frac{\alpha_0\alpha_-}{\alpha_0/\chi_0+\alpha_-/\chi_-}S_-(\rho)\Bigg]\\ \rho = z/a\end{aligned}\right\} \quad (1)$$

where $S_+(\rho)$ and $S_-(\rho)$ are summations involving inverse sixth powers of ρ, z the perpendicular distance from the centre of gravity of the adsorbate atom or molecule to the (100) plane, a the lattice parameter of the crystal, m_e the mass of the electron, C the velocity of light, α the polarizability, χ the magnetic susceptibility. The subscripts o, $+$ and $-$ refer to the adsorbate, alkali ions and halogen ions respectively. For the present systems the required values of α for the crystal ions have been derived by Mayer[6], and of χ by Brindley and Hoare[7]. The values of the ionic radii of alkali halide crystals have been given by Goldschmidt[8]. The values of α for these adsorbates* have been given by Landolt-Börnstein[9], and of χ by Mann[10], Havens[11] and Stoner[12].

The quantities of $S_+(\rho)$ and $S_-(\rho)$ as a function of ρ for four representative positions mentioned above were evaluated by summation over the nearest 280 ions using expressions derived by Orr, and the remaining contributions were found by integration. The results are in good agreement with those obtained by Orr[2].

B. The Electrostatic Potential.—The resultant electrostatic potential in any given position of a non-polar molecule is given by

$$\Phi_E = -\frac{1}{2}\alpha_0 F_z^2 \quad (2)$$

where α_0 is the polarizability of a non-polar molecule, F_z the resultant electrostatic field along a line perpendicular to the surface.

The calculation of the resultant electrostatic field, F_z, as a function of ρ was carried out following closely the method used by Lennard-Jones and Dent[13] for the (100) plane of alkali halide crystals. It is easily shown that the resultant electrostatic field is zero along a line perpendicular to the centre of a lattice cell and also along lines perpendicular to the midpoint of a lattice edge. The resultant electrostatic field, as functions of ρ, above an alkali ion in the lattice plane was evaluated by summation over the nearest 40 ions. The present results are in good agreement with those obtained by Lennard-Jones and Dent[13].

C. The Repulsive Potential.—The theoretical calculations of the total repulsive

5) A. Müller, *Proc. Roy. Soc. London*, **A 154**, 624 (1936).

6) J. E. Mayer, *J. Chem. Phys.*, **1**, 270 (1933).

7) G. W. Brindley and F. E. Hoare, *Proc. Roy. Soc. London*, **A 152**, 342 (1935).

8) V. M. Goldschmidt, *Trans. Faraday Soc.*, **25**, 253 (1929).

9) Landolt-Börnstein. "Zahlenwerte und Funktionen", Band 1, Part 3, Springer (1951), p. 510.

* In the case of the nitrogen or carbon dioxide molecule, the average value of α in the three directions was adopted.

10) K. E. Mann, *Z. Physik*, **98**, 548 (1936).

11) G. G. Havens, *Phys. Rev.*, **43**, 992 (1932).

12) E. C. Stoner, "Magnetism and Matter", Methuen and Co. Ltd., London (1934), p. 460.

13) J. E. Lennard-Jones and B. M. Dent, *Trans. Faraday Soc.*, **24**, 92 (1928); **28**, 333 (1932).

potential between an isolated argon atom and the lattice ions of potassium chloride crystal were carried out by Orr[2] and Young[4]. Their results, however, seem to be insufficiently accurate because the repulsive constant of Herzfeld for argon has been used.

In the present work, therefore, the total repulsive potential was calculated using an exponential expression derived from the Born-Mayer repulsive potential formula[14] for the lattice ions and the modified Buckingham-Corner repulsive potential formula for these non-polar molecules. The modified Buckingham-Corner (6-exp) intermolecular potential[15] is given by

$$\begin{aligned}\phi(r) &= \frac{\varepsilon}{1-6/\alpha}\left\{6/\alpha \exp(\alpha-\alpha r/r_m) - (r_m/r)^6\right\} = -Ar^{-6} \\ &\quad + B\exp(-\alpha r/r_m) \qquad (3)\\ A &= \left(\frac{\varepsilon}{1-6/\alpha}\right) r_m^6, \\ B &= b_0^2 = \left(\frac{6\varepsilon}{\alpha-6}\right)\exp(\alpha)\end{aligned}$$

where ε is the maximum energy of attraction, r the intermolecular separation, r_m the separation at the minimum potential, α the parameter measuring the steepness of the repulsive potential, b_0 the repulsive constant of a molecule.

The values of the force constants are summarized in Table I. In this table the force constants for argon and nitrogen were evaluated by Mason and Rice[16] and those for oxygen and carbon dioxide were evaluated by the present author.

TABLE I

FORCE CONSTANTS OF THE MODIFIED BUCKINGHAM-CORNER INTERMOLECULAR POTENTIAL

Molecule	α	ε/k (°K)	r_m(Å)	b_0 ($.10^{-6}$ erg$^{1/2}$)
Argon	14.0	123.2	3.86_6	123.6
Oxygen	15.2	120.1	3.79_5	207.5
Nitrogen	16.2	113.5	4.04_0	315.6
Carbon dioxide	15.1	266.1	4.11_3	287.5

In the present calculations the repulsive constants of Huggins and Mayer[17] for the crystal ions were used. For four representative positions considered, the total repulsive potential was calculated, for various values of ρ, by direct summation over the 14 to 20 nearest ions. Contributions from the remaining ions are entirely negligible.

Since these results are not of general applicability, no further details need be given.

D. The Quadrupole Potential.—Although, in general, permanent electric quadrupoles are of minor importance in the intermolecular potential between gas molecules[18], the situation is quite different when considering the adsorption potential of a molecule in the large electric fields near the surface of an ionic crystal. The permanent quadrupole moments of several molecules have been measured by Smith and Howard[19] and Hill and Smith[20] from line broadening of microwave spectra. Molecular orbital calculations of the permanent quadrupole moments of nitrogen and oxygen have been made by Greenhow and Smith[21]. Although many of these microwave values are somewhat uncertain, the order of magnitude is probably correct.

The total interaction potential of a linear quadrupole, Q, with an inhomogeneous electric field whose potential is ϕ is given by

$$\Phi_Q = \frac{1}{2} Q \cdot \partial^2\phi/\partial t^2 \qquad (4)$$

where the axis t is taken along the axis of symmetry of the quadrupole. The expression for the resultant Coulomb potential at any position near the surface of an alkali halide crystal has been derived by Lennard-Jones and Dent[13]. The non-zero second derivatives of the resultant Coulomb potential for three representative positions on the (100) plane of potassium chloride were evaluated by Drain[3]. However, since his results contain some uncertainties due to a careless mistake, the evaluation of the electric field gradient near the surface was carried out by the present author.

The maximum quadrupole interaction of the nitrogen or carbon dioxide molecule for four representative positions on the (100) plane of an alkali halide crystal are obtained from the following orientations:

(i) above the centre of a lattice cell (sites type A),

$$\partial^2\phi/\partial x\partial y = e/a^3 \cdot \sigma_A;$$

14) M. Born and J. E. Mayer, *Z. Physik*, **75**, 1 (1932).
15) W. E. Rice and J. O. Hirschfelder, *J. Chem. Phys.*, **22**, 187 (1954).
16) E. A. Mason and W. E. Rice, *J. Chem. Phys.*, **22**, 522 (1954).
17) M. L. Huggins and J. E. Mayer, ibid., **1**, 643 (1933).
18) H. Margenau, *Rev. Modern Phys.*, **11**, 1 (1939).
19) W. V. Smith and R. Howard, *Phys. Rev.*, **79**, 132 (1950).
20) R. M. Hill and W. V. Smith, ibid., **82**, 451 (1951).
21) C. Greenhow and W. V. Smith, *J. Chem. Phys.*, **19**, 1298 (1951).

(ii) above the mid-point of a lattice edge (sites type B),

$$\partial^2\phi/\partial x\partial z=\partial^2\phi/\partial y\partial z=e/a^3\cdot\sigma_B;$$

(iii) above an alkali ion (sites type C),

$$\partial^2\phi/\partial z^2=-2\partial^2\phi/\partial x^2=-2\partial^2\phi/\partial y^2=e/a^3\cdot\sigma_C;$$

(iv) above a halogen ion (sites type D),

$$\partial^2\phi/\partial x^2=\partial^2\phi/\partial y^2=e/a^3\cdot\sigma_D.$$

The cartecian axes x, y, z are along the sides of a unit cell, z is normal to the surface and a is the lattice parameter and e the electronic charge. The quantities σ which represent summations over the lattice ions depend on the distance $a\rho$ of the point under consideration from the surface. The present results on the evaluations of these quantities σ are summarized in Table II.

TABLE II

VALUES OF σ, ON THE (100) PLANE OF AN ALKALI HALIDE CRYSTAL

ρ	σ_A	σ_B	σ_C	σ_D
0.8	1.5310	2.1739	3.3463	1.6732
0.9	0.9942	1.4102	2.0933	1.0467
1.0	0.6424	0.9105	1.3238	0.6619
1.1	0.4142	0.5865	0.8426	0.4213
1.2	0.2662	0.3768	0.5377	0.2688
1.3	0.1711	0.2420	0.3439	0.1719
1.4	0.1098	0.1553	0.2203	0.1101
1.5	0.0704	0.0996	0.1411	0.0705
1.6	0.0452	0.0639	0.0905	0.0452
2.0	0.0076	0.0108	0.0153	0.0076

As is easily seen in these relations, at the positon of sites type A (above the centre of a lattice cell) or sites type D (above a halogen ion), the orientation for maximum quadrupole interaction is with the molecular axis parallel to the surface. Consequently, no correction due to the potential barrier hindering the turning over of the molecule is required in these positions. On the other hand, at the positions of sites type B (above the mid-point of a lattice edge) and sites type C (above an alkali ion), the maximum quadrupole energies are obtained from the orientations in which the molecular axis makes an angle of $\pi/4$ and $\pi/2$ with the surface respectively. In these positions, then the corrections due to the potential barrier hindering the rotation must be made.

In the present calculations, the approximate estimation of this potential barrier was carried out following closely the method used by Hill[22]. Although this method seems rather inadequate for the present calculations*, unfortunately, no other reliable method has been found.

The Total Adsorption Potential.—The total adsorption potential is then given by

$$\Phi=\Phi_D+\Phi_E+\Phi_Q+\Phi_R-\Phi_{H.R.} \qquad (5)$$

where Φ_R is the total repulsive potential,

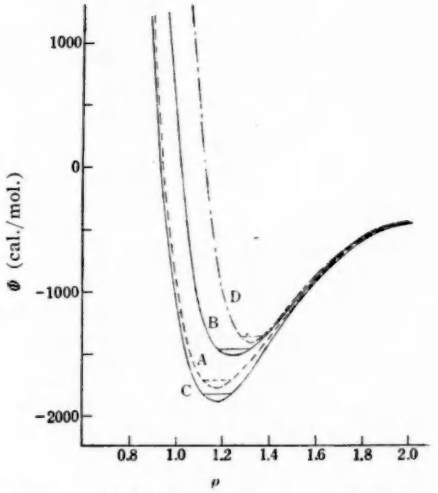

Fig. 1. Potential energy curves of argon on cubic (100) NaCl. Each symbol denotes the type of sites.

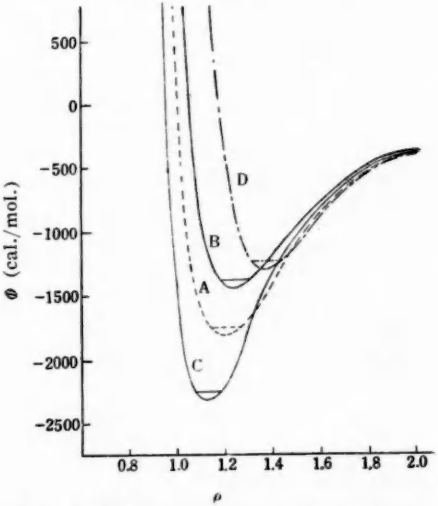

Fig. 2. Potential energy curves of nitrogen on cubic (100) NaCl. Each symbol denotes the type of sites.

22) T. L. Hill, *J. Chem. Phys.*, **17**, 762 (1949).

* In the estimations made by Hill, the adsorption potential was given by the Lennard-Jones (6-12) potential formula.

and $\Phi_{H.R.}$ the potential barrier hindering the turning over of the molecular axis. In the case of argon, both values of Φ_Q and $\Phi_{H.R.}$ are surely zero.

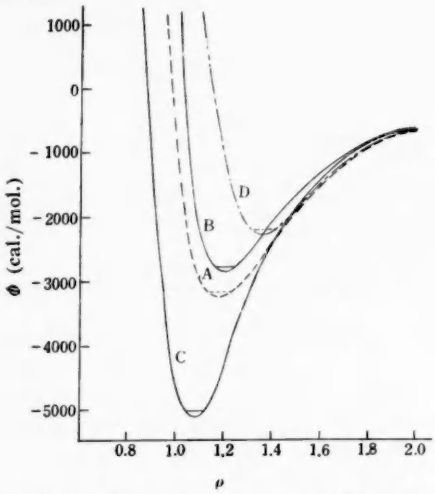

Fig. 3. Potential energy curves of carbon dioxide on cubic (100) NaCl. Each symbol denotes the type of sites.

The calculated potential energy curves for the four types of sites considered are shown in Figs. 1, 2 and 3. By plotting the region around the minimum potential on a large scale, the restoring force per unit displacement, f', of the molecule (i. e. the centre of gravity) normal to the surface in this region was calculated from the following equation**

$$(\Phi - \Phi_m) = \frac{1}{2} f' (z - z_e)^2 \tag{6}$$

where Φ_m is the minimum potential, z the perpendicular distance from the surface, z_e the equilibrium distance given by the position of the minimum potential.

The vibrational frequency normal to the surface, ν_z (sec.$^{-1}$), was then calculated from the relation

$$\nu_z = \frac{1}{2\pi} \sqrt{f' N / M} \tag{7}$$

where M is the molecular (or atomic) weight, N the Avogadro's constant.

Then, the zero-point energy, ε_0 (cal./mol.), was calculated from the relation

$$\varepsilon_0 = Nh\nu_z \times 10^{-7} / 2 \times 4.186 \tag{8}$$

TABLE III

RESULTS OBTAINED FROM THE POTENTIAL ENERGY CURVE, ARGON ON CUBIC (100) NaCl

Sites type	Z_e (Å)	r_{eff} (Å)	$-\Phi_m$ (cal./mol.)	$\nu_z \times 10^{-12}$ (sec.$^{-1}$.)	ε_0 (cal./mol.)	$-\Delta H_0$ at 76°K (ca./mol.)
A, above the centre of a lattice cell	3.30	2.04	1768	0.95	44.8	1875
B, above the mid-point of a lattice edge	3.47	1.94	1514	0.88	41.5	1624
C, above an Na^+	3.29	2.31	1876	1.05	49.7	1978
D, above a Cl^-	3.72	1.91	1401	0.92	43.4	1510

TABLE IV

RESULTS OBTAINED FROM THE POTENTIAL ENERGY CURVE, NITROGEN ON CUBIC (100) NaCl

Sites type	Z_e (Å)	$-\Phi_m$ (cal./mol.)	$-\Phi_Q$ at Z_e (cal./mol.)	$\nu_z \times 10^{-12}$ (sec.$^{-1}$)	ε_0 (cal./mol.)	$-\Delta H_0$ at 76°K (cal./mol.)
A, above the centre of a lattice cell	3.38	1807	550	1.23	58.1	1901
B, above the mid-point of a lattice edge	3.42	1432	774	1.10	51.9	1532
C, above an Na^+	3.12	2308	1738	1.32	62.3	2398
D, above a Cl^-	3.84	1277	232	1.12	52.9	1376

TABLE V

RESULTS OBTAINED FROM THE POTENTIAL ENERGY CURVE, CARBON DIOXIDE ON CUBIC (100) NaCl

Sites type	Z_e (Å)	$-\Phi_m$ (cal./mol.)	$-\Phi_Q$ at Z_e (cal./mol.)	$\nu_z \times 10^{-12}$ (sec.$^{-1}$)	ε_0 (cal./mol.)	$-\Delta H_0$ at 190°K (cal./mol.)
A, above the centre of a lattice cell	3.28	3245	1328	1.12	52.9	3572
B, above the mid-point of an lattice edge	3.36	2852	1869	1.07	50.6	3181
C, above an Na^+	3.03	5102	4184	1.33	62.7	5419
D, above a Cl^-	3.77	2237	554	1.06	50.2	2567

** In Equ. (6), Φ and Φ_m must be expressed in erg/molecule.

where h is the Planck's constant.

Consequently, the initial heat of adsorption (i.e. the isosteric heat of adsorption at zero coverage), $-\Delta H_0$ (cal./mol.), is given by the expression

$$-\Delta H_0 = (-\Phi_m - \varepsilon_0) + RT = -U_0 + RT \quad (9)$$

where U_0 is the potential energy of the lowest vibrational state of the molecule on the bare surface.

The calculated values of these quantities for these non-polar gases are summarized in Table III, IV and V. The values of the effective radius of argon, $r_{eff.}$, were calculated from the equilibrium distances, and the results are given in column 3 of Table III.

Approximate Calculation of the Heat Curve for Argon on the (100) Plane of Cubic Sodium Chloride.—The approximate calculation of the heat curve for argon was carried out following similar method used by Young[4] for the (100) plane of cubic potassium chloride. In the present calculations, as well as in those made by Young, the following assumptions were made:

(1) In the formation of a primary monolayer, argon atoms are exclusively adsorbed from $\theta=0$ to about 0.4* above sodium ions (c.f. Table III), but as θ tends to unity there will be a phase transition from localized square arrays to a hexagonally closed-packed layer.
(2) The non-uniformity of the surface is negligible.
(3) The heat of adsorption of the second-layer atoms is close to the heat of sublimation of argon (i.e. 1860 cal./mol. at 76°K).
(4) In the range restricted to θ values near unity, the adsorption in the third and higher layers is negligible.

The variation of the heats of adsorption in the primary monolayer with coverage, due to Van der Waals' mutual interaction between the adsorbed atoms, was calculated using the equation statistically derived by Wang[23]. The intermolecular potential energy of a pair of argon atoms was calculated using the modified Buckingham-Corner (6-exp) potential formula, and the effect of the electrostatic repulsion between the adsorbed atoms was taken into consideration.

The effect of the second-layer formation was evaluated using the equations developed by Tompkins and Young[24].

The calculated heat curve is shown in Fig. 4, together with the experimental values reported in the preceding paper.

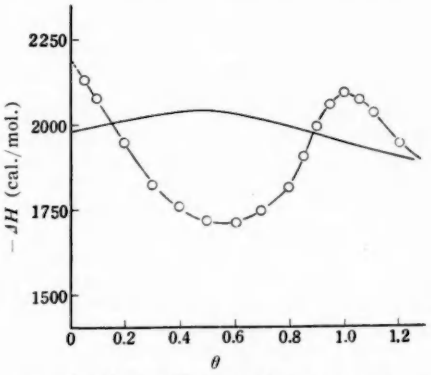

Fig. 4. Heats of adsorption of argon on cubic (100) NaCl.
——, approximately calculated curve;
-○-○-, observed curve.

Discussion

The Initial Heat of Adsorption.—As seen in Table III, IV and V, the most energetic positions for these non-polar gases (argon, nitrogen and carbon dioxide) on the (100) plane of cubic sodium chloride are all sites type C (above an Na^+ in the lattice plane). These results are peculiar to the (100) plane of cubic sodium chloride. As will be shown in the succeeding paper, the most energetic positions for argon and nitrogen on cubic (100) KCl and cubic (100) KBr are sites type A* (above the centre of a lattice cell). This particular nature of the (100) plane of sodium chloride crystal may be attributed to the fact that the ionic radius and the repulsive constant of Na^+ are both considerably smaller than those of K^+.

The values of the initial heats of adsorption obtained from the present theoretical calculations are listed in Table VI, together with the experimental values reported in the preceding paper.

As seen in Table VI, the calculated values for these non-polar gases are in rather good agreement with the experimental values. It is quite reasonable,

* The diameter of an argon atom derived from the liquid density was taken at 4.05 Å.

23) J. S. Wang, *Proc. Roy. Soc. London*, **A 161**, 127 (1937).

24) F. C. Tompkins and D. M. Young, *Trans. Faraday Soc.*, **47**, 77 (1951).

* According to the theoretical calculations made by Orr[2], the most energetic position for argon on cubic (100) KCl is also sites type A.

TABLE VI

INITIAL HEATS OF ADSORPTION ON CUBIC (100) NaCl

Adsorbate	$(-\Delta H_0)_{\text{expt.}}$ (cal./mol.)	$(-\Delta H_0)_{\text{calc.}}$ (cal./mol.)	$(-\Delta H_0)_{\text{expt.}} - (-\Delta H_0)_{\text{calc.}}$ (cal./mol.)
Argon	2190	1980	210
Nitrogen	2670	2400	270
Carbon dioxide	6070	5420	650

therefore, to consider that the high initial heats of adsorption experimentally found for nitrogen and carbon dioxide are mainly attributed to the quadrupole interactions of these molecules with the surface of cubic sodium chloride.

The Non-Uniformity of the Adsorbent Surface.—Table III indicates that the maximum difference of the initial heat of adsorption for argon between these sites grouped in patches amounts to about 500 cal./mol. The corresponding values for nitrogen and carbon dioxide amount, as seen in Table IV and V, to about 1000 cal./mol. and about 2850 cal./mol. respectively. Since the mutual interaction between the adsorbed atoms or molecules in the low coverage region is slightly attractive and gives no marked influence upon the heats of adsorption, the surface heterogeneity of this type may be maintained, especially in the non-localized adsorption, in this low coverage region.

The difference between the experimental and theoretical values of the initial heat of adsorption shown in Table VI gives a crude measure of the surface heterogeneity of the other type due to the lattice imperfection or the defects of the crystals. An argon atom has no permanent quadrupole moment; then the value of 210 cal./mol. shown in Table VI may be attributed to the surface heterogeneity of this type. On the other hand, the theoretical values of the initial heats of adsorption for nitrogen and carbon dioxide are somewhat inaccurate, and this uncertainty is attributed to two causes:

(a) The values of the quadrupole moment of these molecules cannot yet be considered as definitely proved.

(b) The estimation of the potential barrier hindering the turning over of the molecule was carried out following the method used by Hill, but this method is rather inadequate for the present calculations.

Nevertheless, Table VI shows that the difference between the experimental and theoretical values of the initial heat of adsorption for each adsorbate is of the right magnitude to explain the difference of the intermolecular potential energy betwen these non-polar gases.

For the reasons discussed above, it is reasonable to consider that the surface heterogeneity due to the distribution of sites grouped in patches is more distinguished than that due to the lattice imperfection or crystal defects. Both types of the surface heterogeneity discussed above give rise to the decrease of the heat of adsorption as more molecules are adsorbed in the low coverage region. This is qualitatively in good agreement with the experimental heat curves.

Surface Migration of the Adsorbed Atoms or Molecules.—In order to enable the adsorbed atom or molecule to move along the surface from one site to the next site, where it is bounded in exactly the same manner as in the first one, this atom or molecule must pick up such an amount of energy that it may overcome the potential energy barrier separating the atoms and molecules. Owing to the high symmetry of the (100) plane of an alkali halide crystal and the small distance from one site to the adjacent site of another type, it is not unreasonable to consider that the height of this potential energy barrier is roughly equal to the difference of the heat of adsorption between them[25]. Since the mutual interaction between the adsorbed atoms or molecules in the low coverage region gives no marked influence, the heat of adsorption at each site in the low coverage region may be replaced by the initial heat of adsorption in the present discussion.

As seen in Table III, the difference of the initial heat of adsorption between two adjacent sites (i.e. the height of the potential energy barrier mentioned above) for argon amounts to about $0.7 \sim 2RT$. In the case of nitrogen, as seen in Table IV, the height of this potential energy barrier roughly amounts to about $1 \sim 3\ RT$ (excepting the value corresponding to the difference between site B and C). Since the mean kinetic energy of thermal movement of the adsorbed atom or molecule is RT per mole, it is reasonable to consider that the adsorbed argon atom or nitrogen molecule easily picks up the energy corresponding to each potential energy barrier from the thermal energy fluctuations. The present results on the surface migration of the adsorbed argon atom or nitrogen molecule

25) J. H. de Boer, "The Dynamical Character of Adsorption", Clarendon Press, Oxford (1953), p. 96.

in the low coverage region are qualitatively in good agreement with the nature of the experimental entropy curves for argon and nitrogen already reported in the preceding paper.

The Heat Curve for Argon.—As seen in Fig. 4, the discrepancy between the experimental and approximately calculated heat curves in the region of $\theta=0.2\sim0.8$ is considerably remakable. This is mainly attributed to the fact that in the present approximate calculations, as well as in those made by Orr and Young, the uniform surface and the localized model have been assumed. These two assumptions are inconsistent not only with the results of the present theoretical calculations but with the experimental results reported in the preceding paper.

Summary

The potential energy of each isolated atom or non-polar molecule (argon, nitrogen, or carbon dioxide) adsorbed on the (100) plane of cubic sodium chloride has been theoretically calculated at four different positions on the crystal surface. In the present calculations, the repulsive constants of the modified Buckingham-Corner (6-exp) intermolecular potential for these non-polar gases have been used. The quadrupole interaction of the nitrogen or carbon dioxide molecule with a crystal has been taken into consideration. The good agreement between the theoretical and experimental values of the initial heat of adsorption for each adsorbate has been obtained.

The present theoretical calculations suggest that the surface heterogeneity caused by the lattice imperfection or crystal defects is of minor importance compared with other types of surface heterogeneity due to the distribution of sites grouped in patches. The present results also suggest that the adsorbed argon atoms or nitrogen molecules easily migrate two-dimensionally along the surface in the low coverage region. These results on the surface migration are in good agreement with the entropy curves of adsorbed argon and nitrogen experimentally determined.

The approximate calculation of the heat curve for argon on the (100) plane of cubic sodium chloride has been carried out following a similar method used by Young. The discordance between the experimental and approximately calculated heat curves is considerable, and this is attributed to the fact that the unreliable model (i.e. the uniform surface and the localized adsorption) has been assumed in these approximate calculations.

The author wishes to express his grateful thanks to Dr. S. Horiba and Professor O. Toyama of Osaka Prefectural University for their kind encouragement and discussion. The author's sincere thanks are also due to Professor R. Kiyama of Kyoto University for his kind discussion.

Department of Chemistry, Faculty of Education, Osaka Prefectural University, Sakai

*The Adsorption of Non-Polar Gases on Alkali Halide Crystals. III. The Low-Temperature Adsorption of Non-Polar Gases on Cubic Potassium Chloride**

By Teruo HAYAKAWA

(Received November 2, 1956)

Introduction

In the former papers of this series[1,2] the author studied the adsorptive properties of non-polar gases (argon, oxygen, nitrogen and carbon dioxide) on cubic

* Part of this paper was read before the 6 th Annual Meeting of the Chemical Society of Japan held in Kyoto, April, 1953. Another part of this paper was also read before the symposium on the surface heterogeneity of catalysis held in Kyoto, March, 1956.

1) Part I of this series, T. Hayakawa, This Bulletin, **30**, 124 (1957).
2) Part II of this series, T. Hayakawa, This Bulletin, **30**, 236 (1957).

sodium chloride. Considerably good agreement between the theoretical and experimental values of the initial heat of adsorption for argon, nitrogen, or carbon dioxide was obtained. The experimental results also indicated that the adsorbed molecules of argon, oxygen, or nitrogen on cubic sodium chloride have the nature of two-dimensional gas at least in the range of $\theta=0.3\sim0.9$. The measurements of the low-temperature adsorption of non-polar gases (argon, oxygen and nitrogen) on cubic potassium chloride were already reported by Orr[3]. However, since his results were limited to the variation in the isosteric heats of adsorption with coverage, no definite information on the non-uniformity of the surface and on the freedom of the adsorbed molecules was obtained. Moreover, no reasonable explanation was given for the differences in the values of the initial heat of adsorption with molecular species of adsorbates.

It was therefore of interest in the present work to re-examine the adsorptive properties of non-polar gases on cubic potassium chloride and to compare the results with those obtained for cubic sodium chloride.

Experimental

Materials.—*Potassium chloride* was recrystallized by rapidly cooling an aqueous solution of potassium chloride (Merck reagent) saturated at 100°C. The crystals were collected on a sintered glass filter funnel, washed with successive portions of 70% ethyl alcohol, absolute alcohol, and dry ether, and stored in vacuum desiccator over phosphorous anhydride during about two weeks. Microscopic examination of this sample revealed a large number of small cubes plus a few cubes in which the defects in the corners or edges were somewhat perceptible. The examination of this sample by an electron diffraction apparatus also revealed the regular pattern of (100) faces. 24.9 g. of this sample which passed through a 45-mesh sieve was used in the subsequent experiments. *Helium* was supplied by the Teikoku Oxygen Co. as spectroscopically pure and was not further purified. The method of preparation of argon, oxygen, nitrogen and carbon dioxide has already been described[1].

Apparatus and Procedure.—The apparatus and the procedure were already described in a previous communication[1]. The salt was outgassed by heating in vacuo at 300°C for a minimum period of 6 hr. prior to each experiment.

Results

The isotherms obtained for the four gases on cubic potassium chloride are summarized in Fig.

3) W. J. C. Orr, *Proc. Roy. Soc.*, **A173**, 349 (1939).

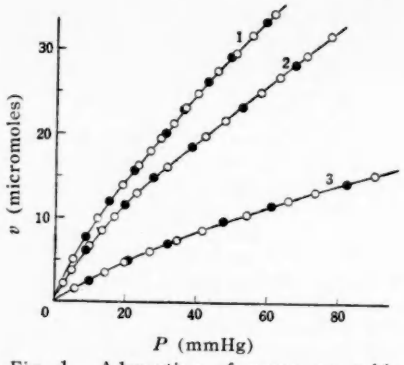

Fig. 1. Adsorption of argon on cubic potassium chloride.
curve 1……75.29°K, curve 2……77.32°K, curve 3……85.42°K; ○……adsorption, ●……desorption.

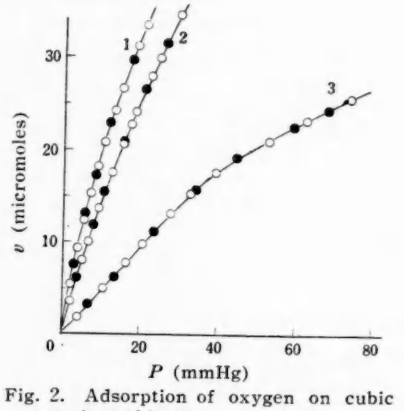

Fig. 2. Adsorption of oxygen on cubic potassium chloride.
curve 1……75.29°K, curve 2……77.32°K, curve 3……85.42°K; ○……adsorption, ●……desorption.

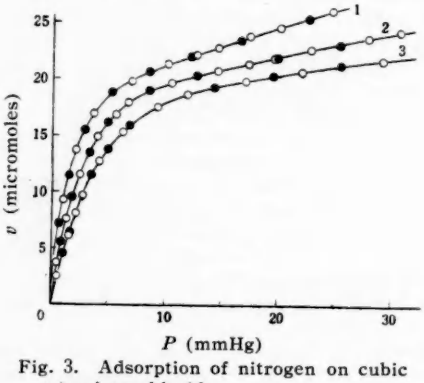

Fig. 3. Adsorption of nitrogen on cubic potassium chloride.
curve 1……73.74°K, curve 2……75.69°K, curve 3……77.32°K; ○……adsorption, ●……desorption.

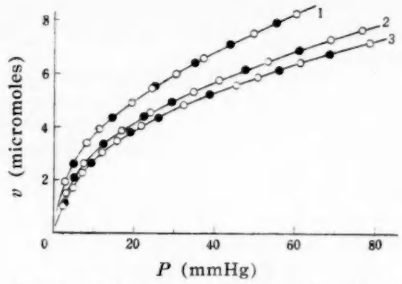

Fig. 4. Adsorption of carbon dioxide on cubic potassium chloride.
curve 1……187.66°K, curve 2……192.63°K, curve 3……194.64°K; ○……adsorption, ●……desorption.

1, 2, 3 and 4. The adsorption was found to be reversible in this temperature range. The isosteric heats of adsorption were calculated from these isotherms using the Clausius-Clapeyron equation, and these showed no definite trend with temperature within the experimental error. For the calculations of the entropy decrease due to the adsorption, the choice of the standard states of the gas phase was such that the pressure is 760 mmHg and the temperature coincides with that of each isotherm.

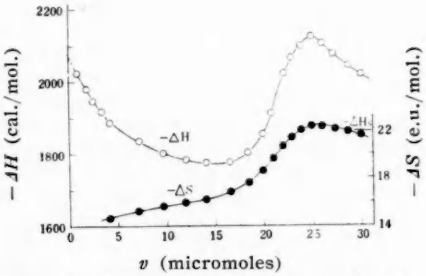

Fig. 5. Isosteric heats and entropies of adsorption for argon on cubic potassium chloride.
$-\Delta H_s$……heat of sublimation.

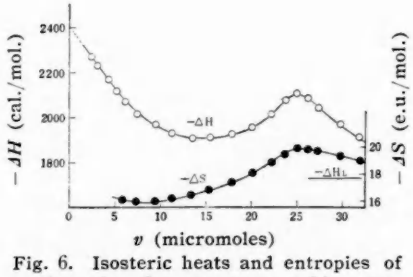

Fig. 6. Isosteric heats and entropies of adsorption for oxygen on cubic potassium chloride.
$-\Delta H_L$……heat of vaporization.

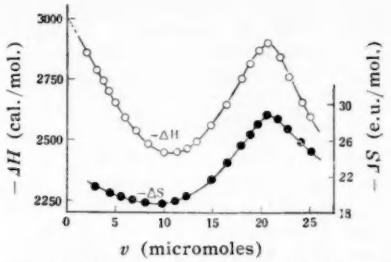

Fig. 7. Isosteric heats and entropies of adsorption for nitrogen on cubic potassium chloride.

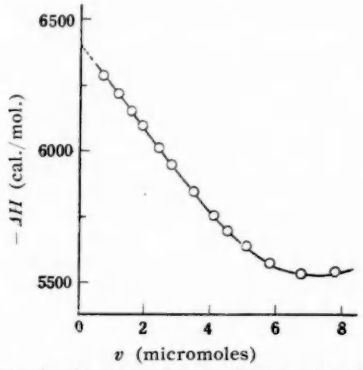

Fig. 8. Isosteric heats of adsorption for carbon dioxide on cubic potassium chloride.

The present results on the isosteric heats of adsorption and the entropy decrease due to the adsorption are shown in Fig. 5, 6, 7 and 8. The measurements were not extended to the high coverage region for carbon dioxide, since the amount adsorbed was fairly small in this temperature range.

Discussion

The Isosteric Heats of Adsorption.— The magnitudes of the isosteric heats of adsorption and the variation of these with coverage for the three gases (argon, oxygen and nitrogen) are in fairly good agreement with the experimental values of Orr[3]. The experimental values of the initial heat of adsorption (i.e. the isosteric heat of adsorption extrapolated to zero coverage) obtained for the four gases are summarized in Table I, together with the experimental values of Orr[3] and Lenel[4] and the theoretical values of the present author.

4) F. V. Lenel, *Z. physik. Chem.*, **B23**, 379 (1933).

TABLE I

INITIAL HEAT OF ADSORPTION, $-\Delta H_0$, ON CUBIC POTASSIUM CHLORIDE

Adsorbate	$(-H_0)$expt. (cal./mol.) Present author	(Literature)	$(-\Delta H_0)$calc. (cal./mol.)
Argon	2080	(2140*)	1900
Oxygen	2410	(2350*)	—
Nitrogen	3010	(3200*)	2120
Carbon dioxide	6400	(6500**)	4970

* Obtained by Orr.
** Obtained by Lenel.

In the theoretical calculations, as will be reported in the succeeding paper, the crystal lattice was assumed to be an ideal (i. e. the surface heterogeneity due to the defects or the lattice imperfection was ignored) and the quadrupole interaction of the molecule (nitrogen or carbon dioxide) with the surface was taken into consideration. Table I indicates that the present experimental values of the initial heat of adsorption are in good agreement with those of other investigators. Although the discrepancies between the experimental and theoretical values for nitrogen and carbon dioxide are quite remarkable, as seen in Table I, the order of magnitude of the experimental values for these non-polar gases is similar to that of the theoretical values. Considering the matter from this fact, it seems reasonable to consider that the high initial heats of adsorption experimentally found for nitrogen and carbon dioxide are mainly attributed to the quadrupole interactions of these molecules with the surface of cubic potassium chloride.

The initial decrease in each heat curve is attributed to the non-uniformity of the surface, since mutual interaction forces of adsorbed molecules, being attactive, would result in an increase in the heat. The difference between the experimental and theoretical values of the initial heat of adsorption shown in Table I gives a crude measure of the surface heterogeneity due to the lattice imperfection or the defects of the crystals. Then, the value of 180 cal./mol. for argon (i. e. the difference between the experimental and theoretical values of the initial heat of adsorption) may be attributed to the surface hetrogeneity of this type, while Fig. 5 indicates that the initial decrease in the heat curve for argon roughly amounts to about 300 cal./mol.* Consequently, it is reasonable to consider that the surface may be influenced by the non-uniformity of the other type.

In the case of nitrogen or carbon dioxide, however, the situation seems quite different, since the difference between the experimental and theoretical values of the initial heat of adsorption is considerably greater than the initial decrease in the heat curve shown in Figs. 7 or Fig. 8. Although these results obtained for nitrogen and carbon dioxide are inconsistent with those for argon, it may be pointed out that the theoretical calculations of the initial heat of adsorption for nitrogen and carbon dioxide are less correct than those for argon. This incorrectness in the theoretical calculations is mainly attributed to the fact that the values of the quadrupole moment of these molecules (nitrogen and carbon dioxide) cannot yet be considered as definitely proved.

The Monolayer Capacities and the Surface Areas.—Since the heat curves (Figs. 5, 6 and 7) indicate that the non-uniformity of the surface considerably predominates in the low coverage region and that the mutual interaction between the adsorbed molecules in the succeeding region is sharply increased with the increase of the amount adsorbed, it is quite unreasonable to apply the B. E. T. theory to the present systems. As seen in Figs. 5, 6 and 7, there are fairly sharp maxima in the isosteric heat and the entropy decrease curves for all these gases. The gradual decrease in each heat or entropy decrease curve beyond the maximum may be attributed to the formation of multilayers. Considering these facts, it seems reasonable to assign the value corresponding to the maximum in the heat or entropy decrease curve as the monolayer capacity.

The present results on the monolayer capacities and the surface areas are summarized in Table II. Each value of the cross-sectional area in this table was determined from the results on the entropies of the adsorbed molecules.

TABLE II

MONOLAYER CAPACITIES (v_m) AND SURFACE AREAS (A), CUBIC POTASSIUM CHLORIDE (24.9 g.)

Adsorbate	Cross-sectional area a_0(Å^2)	v_m (micromoles) from $(-\Delta H)$	(B.E.T.)	A (m^2) from $(-\Delta H)$	(B.E.T.)
Argon	12.8	25.1	(24.0)	1.93	(1.85)
Oxygen	14.1	25.0	(23.6)	2.12	(2.00)
Nitrogen	13.8	20.7	(23.2)	1.73	(1.93)

* Since the value of 300 cal./mol. includes the effect of the intermolecular attraction between adsorbed atoms, the true effect of the surface heterogeneity may amount to a considerably greater value than 300 cal./mol.

The Entropies of Adsorption.—As seen in Figs. 5, 6 and 7, the entropy decrease curve for each non-polar gas in the comparatively high coverage region has a tendency similar to the respective heat curve. The present results on the entropy of adsorption for the three gases are listed in Table III.

TABLE III
ENTROPY OF ADSORPTION, $-\Delta S$, ON CUBIC POTASSIUM CHLORIDE

Adsorbate	Temperature (°K)	$-\Delta S$ (e. u./mol.) $\theta=0.5$	$\theta=1.0$
Argon	76.3	15.9	22.2
Oxygen	76.3	16.9	19.8
Nitrogen	76.5	19.0	28.7

As seen in Table III, Figs. 5, 6 and 7, the magnitudes of the entropies of adsorption and the variation of these with coverage for argon and oxygen resemble each other, while nitrogen shows a considerably different feature from other gases in the region of $\theta=0.5\sim1$. In order to obtain more information about the freedom of the adsorbed molecules, the entropies of the adsorbed molecules obtained from the present experiments were compared with those statistically calculated. The methods of the statistical calculations of the entropy for each gas under the standard states and of the entropy of each adsorbed phase were already given in the preceding paper[1].

The entropy curves of the adsorbed molecules obtained from the present experiments are summarized in Figs. 9, 10 and 11, together with the calculated curves. For the sake of comparison, Kemball's values[5] obtained from Orr's results[3] are also shown in Fig. 9. The experimentally determined values in these figures are the partial molar total entropies and hence contain the entropy changes of the adsorbent[6], while the calculated values are all the integral entropies and are usually somewhat greater than the values of the partial molar total entropies. Considering this fact, the experimental values (S_S) for adsorbed argon and nitrogen are in fairly good agreement with the calculated values of the two-dimensional gas (S_T) in the range of $\theta=0.3\sim0.9$. Since the entropy for oxygen associated with the vibrational

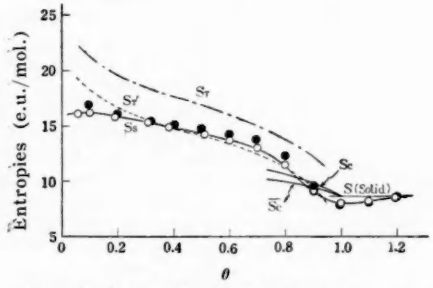

Fig. 9. Entropies of adsorbed argon on cubic potassium chloride at 76.3°K.
S_S……Experimental values;
○……Present values,
●……Kemball's values (79°K).
S_T……Entropies of the two-dimensional gas.
$S_{T'}$……Translational entropies of the two-dimensional gas.
S_C……Configurational entropies.
$\bar{S}_C$……Differential configurational entropies.

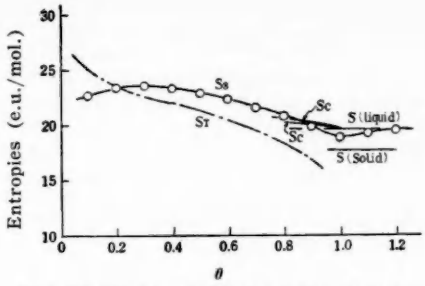

Fig. 10. Entropies of adsorbed oxygen on cubic potassium chloride at 76.3°K.
S_S……Experimental values.
S_T……Entropies of the two-dimensional gas.
S_C……Configurational entropies.
$\bar{S}_C$……Differential configurational entropies.

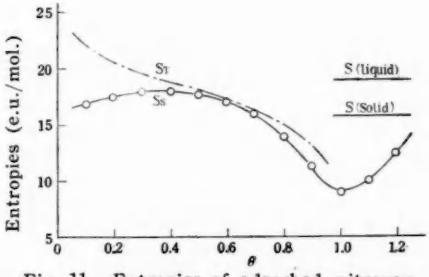

Fig. 11. Entropies of adsorbed nitrogen on cubic potassium chloride at 76.5°K.
S_S……Experimental values.
S_T……Entropies of the two-dimentional gas.

5) C. Kemball, "Advances in Catalysis", Vol. II, Academic Press Inc., New York (1950), p. 233.
6) T. L. Hill, *J. Chem. Phys.*, **17**, 520 (1949).

motion normal to the surface was calculated from assuming that the vibrational frequency of oxygen is identical with that of argon, the present calculations of the two-dimensional gas for oxygen (S_T in Fig. 10) probably resulted in smaller values. Therefore, the agreement of the experimental curve (S_S) for oxygen with the calculated curve (S_T) of the two-dimensional gas in the region of $\theta=0.2\sim0.9$ is satisfied to a great extent.

The discrepancy between the experimental and calculated values at lower coverage ($\theta<0.2$) in each entropy curve would imply the entropy changes of the adsorbent. When θ approaches to unity, as seen in these figures, the restriction on the freedom of the adsorbed molecules is further increased and each entropy curve (S_S) falls below the calculated curve of the two-dimensional gas (S_T). In the range of $\theta>1$, the entropy of adsorbed argon remains close to the entropy of solid argon*, while the entropy of adsorbed oxygen closely approaches to the entropy of liquid oxygen**. This is in accord with the fact that the heat of sublimation of argon is similar to that of vaporization of oxygen. On the other hand, the entropy of adsorbed nitrogen in this same range is considerably smaller than that of solid nitrogen***.

According to the suggestion given by Kemball[5], the phase change of argon on cubic potassium chloride occurred at about $\theta=0.8$, since the experimental values shifted from the entropy curve of the two-dimensional gas to the entropy curve of the localized adsorption obtained by adding the configurational entropy on the Langmuir model to the entropy of solid argon. This explanation, however, contains considerable uncertainties, since it is unreasonable to adopt the Langmuir model for the systems in which the non-uniformity of the surface in the low coverage region and the mutual interaction in the succeeding region are both predominant. In the present work, the configurational entropy for the localized adsorption was calculated from the expression given by Drain and Morrison[7]. The results shown in Fig. 9 or Fig. 10 indicate that the phase change of argon or oxygen from a gaseous film to a condensed film occurs at about $\theta=0.9$. However, since the mutual interaction between the adsorbed molecules was ignored in the present calculations of the configurational entropy, the present results on the phase change are also somewhat inaccurate.

* The entropy of solid argon was calculated from the heat of sublimation and the value of the saturation pressure at 76.3° K.

** The entropy of liquid oxygen was calculated from the work of Giauque and Johnston(*J. Am. Chem. Soc.*, **51**, 2300 (1929)).

*** The entropy of solid nitrogen was calculated from the work of Kingston, et al (*J. Am. Chem. Soc.*, **72**, 1780 (1950)).

Summary

The low-temperature adsorption of non-polar gases (argon, oxygen, nitrogen and carbon dioxide) on cubic potassium chloride was investigated. The present results on the isosteric heats of adsorption for these four gases indicate that the non-uniformity of the surface considerably predominates in the low coverage region and this is partly attributed to the lattice imperfection or the defects of the crystals.

The entropies of the adsorbed molecules were experimentally determined and compared with the calculated values of the perfect two-dimensional gas. These results show that the adsorbed molecules of argon, oxygen and nitrogen have the nature of the two-dimensional gas at least in the range of $\theta=0.3\sim0.9$. The present results also suggest that the phase change of adsorbed argon or oxygen from a gaseous film to a condensed film may occur at about $\theta=0.9$. These results on the freedom of the adsorbed molecules are similar with those on cubic sodium chloride previously reported.

The author wishes to express his grateful thanks to Dr. S. Horiba and Professor O. Toyama of Osaka Prefectural University for their kind encouragements and discussions. The author's sincere thanks are also due to Professor R. Kiyama of Kyoto University for his kindly discussing the problems.

Department of Chemistly, Faculty of Education Osaka Prefectural University, Sakai

7) J. M. Drain and J. O. Morrison, *Trans. Faraday Soc.*, **48**, 316 (1952).

Irreversible Photobleaching of the Solutions of Fluorescent Dyes. IV. Photoreactions in Methanol, Isopropanol and Ketones, and the General Conclusion for the Photobleaching of Eosine

By Masashi IMAMURA

(Received November 19, 1956)

Introduction

The present author and Koizumi have reported some investigations concerning the photoreaction of eosine in water, ethanol and water-ethanol in vacuo and in the presence of oxygen (air)[1-4]. In vacuo, no reaction occurs in water but in alcohol and in water-alcohol mixtures eosine is decolorized irreversively. In the presence of oxygen, eosine in alcohol acts as a sensitizer for the photoöxidation of alcohol, while in the aqueous solution the dye photobleaches irreversively. Our first plan was to gain some definite information on the primary processes of the photobleaching of eosine in water in the presence of oxygen, and the problem has already been partly cleared up; two possible mechanisms of the primary processes have been proposed in Part I[1] and a further discussion has been given in Part III[4].

In this paper, some results obtained in methanol, isopropanol, *n*-butanol, acetone and methyl ethyl ketone, and in their mixtures with water will be reported, and a conclusive discussion will be given of the photochemical primary process of eosine in the aqueous solution.

Experimental

Materials. — Merck Co. and Grübler's Eosin Yellow were used. These two species showed almost the same absorption spectra and similar photochemical behavior. Solvents were commercial products purified by the usual methods[5]. Apparatus and procedures were exactly as described in the previous papers[1-4].

1. Retarding Effects of Alcohols upon the Aerobic Photobleaching of the Aqueous Solution. — As already reported[1,2], ethanol shows a very marked retardation in the aerobic photobleaching of the aqueous solution of eosine and the quantum yield, k, is expressed, in the low concentration region of ethanol, by the equation:

$$\frac{1}{k}=\frac{1}{k^0}+K\frac{[\mathrm{EtOH}]}{[\mathrm{H_2O}]}, \qquad (1)$$

where k^0 is the quantum yield in the pure aqueous solution, [EtOH] and [H_2O] are molar concentrations, and K is a constant which gives a measure of the retarding effect of ethanol[1].

Now, it was established that other alcohols show similar behavior as ethanol[6] in the low concentration region, the rate of photobleaching

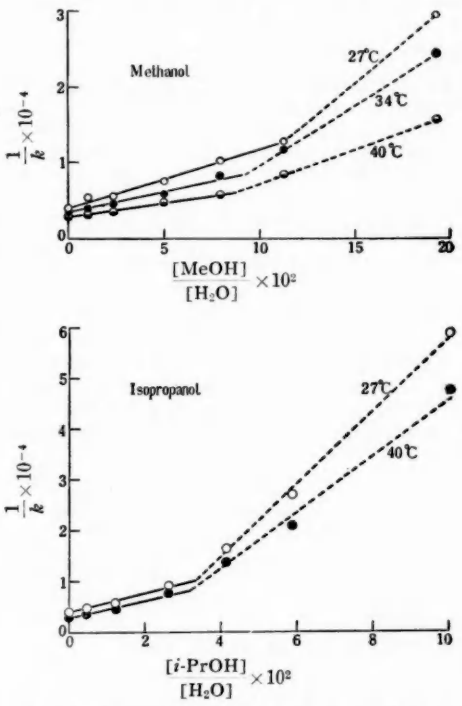

Fig. 1. Variation of the quantum yield with the mole ratio of alcohol to water. (Eq. (1))

1) M. Imamura and M. Koizumi, This Bulletin, **28**, 117 (1955).
2) M. Imamura, *J. Inst. Polytech. Osaka City Univ.*, **6**, No. 1, c, 85 (1956).
3) M. Imamura and M. Koizumi, This Bulletin, **29**, 899 (1956).
4) M. Imamura and M. Koizumi, ibid., **29**, 913 (1956).
5) A. Weissberger and E. S. Proskauer, "Organic Solvents", (Revised by J. A. Riddick and E. E. Toops, Jr.), Interscience, New York (1955).

6) Owing to the restriction of the solubility of *n*-butanol in water, experiment in a concentration higher than 8 vol. percent was impossible for it.

being expressed (Fig. 1) also by eq. (1). Values of K for these alcohols are listed with those for ethanol in the third column of Table I.

TABLE I

RH	Temp. °C	$K\times10^{-5}$	$k^0\times10^4$	k^0K	k^s_2/k^s_1
MeOH	27	0.77	2.5	19	—
	34	.58	2.9	17	9
	40	.37	3.6	13	—
EtOH	20	1.73	1.9	33	—
	27	1.62	2.5	41	19
	34	1.45	2.9	42	—
	40	1.33	3.6	48	—
i-PrOH	27	1.94	2.5	49	17
	40	1.83	2.9	53	—
n-BuOH	20	5.18	1.9	98	—
	27	3.41	2.5	85	—
Acetone	27	2.3	2.5	58	—
Methyl ethyl ketone	27	4.6	2.5	115	—

It is evident that K increases at constant temperature in the order, MeOH, EtOH, *i*-PrOH, *n*-BuOH, and the temperature coefficient is negative. As seen from Fig. 1, discontinuity appearing on each line is displaced towards the lower value of $[RH]/[H_2O]$ in the same order as above and with rising temperature.

2. Photoreactions of Eosine in Methanol- and Isopropanol-Water Mixtures.— As already described[4], eosine in ethanol-water mixture is converted more or less to uranine by irradiation in vacuo; the initial rate of the reaction increases with the rising concentration of ethanol and reaches a limiting value in the neighborhood of ethanol concentration of 20 vol. percent.

In expectation of similar phenomena, the experiments were made on the methanol- and isopropanol-water solutions. Experimental procedures and the calculation of the quantum yields were exactly the same as before[4].

The result with methanol at 34°C is shown in Fig. 2. Uranine production was also observed in this case but was less than with ethanol. Quantum yield reaches a limiting value in the neighborhood of concentration of 30 vol. percent methanol (in contrast to 20 vol. percent with ethanol). It is evident, from Fig. 2, that the participation of water in the primary process of the reaction can be neglected at a concentration of 30 vol. percent in vacuo, while, in the presence of oxygen (air), measurable amount of photobleaching is seen at this concentration (dotted line). The behavior is similar to that observed in the case of ethanol and this is another support in favor of the conclusion given in Part III[4] that the primary process of the photobleaching of eosine is the attack of oxygen on D^t.

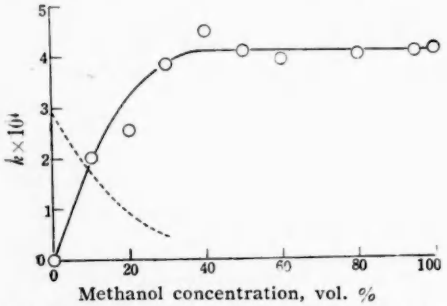

Fig. 2. Dependence of the quantum yield on methanol concentration. 34°C. Full line : in vacuo; Dotted line : aerobic.

On the other hand, quite a different result was obtained with isopropanol. In this case, uranine production was as much as with ethanol, and the difference between the quantum yields in the two pure alcohols in vacuo was not large. Nevertheless, as illustrated in Fig. 3, a prominent maximum in quantum yield was observed at a concentration of about 50 vol. percent isopropanol.

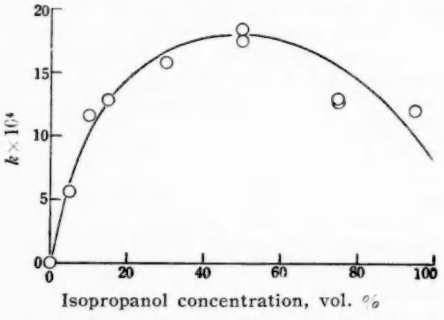

Fig. 3. Dependence of the quantum yield of the vacuum photobleaching on isopropanol concentration. 27°C.

3. Photobleaching in Acetone and Methyl Ethyl Ketone.— As organic solvents other than alcohols, it was attempted to use acetone and methyl ethyl ketone. Solubilities of eosine in such ketones are fairly low compared with those in alcohols. There were, in carrying out experiments with those ketones, some other difficulties since the absorption maximum gradually changes during storage in the dark. For instance, the peak at 534—536 mμ of acetone solution (10^{-5} mol./l. eosine) gradually shifts to the wavelength region of 540—542 mμ and the maximum optical density increases by a small percent after several days in the dark. Though the cause for the phenomenon is not clear, it may be attributed, partially at least, to the presence of oxygen, since the evacuated solution did not show any such displacements, but its absorption maximum was fixed at 540—542 mμ.

In view of the above fact, experiments were done with the solution which was maintained in the dark for a long time to attain the equilibrium condition. Rates of aerobic photobleaching of eosine both in acetone- and in methyl ethyl ketone-water mixtures were expressed well by the simple rate equation[3]:

$$-\frac{dc}{dt}=1000\,k\frac{I_0}{d}(1-e^{-acd}). \qquad (2)$$

Quantum yield, k, decreases markedly with increasing concentration of acetone in the low concentration region as seen for alcohols. In the higher concentration region, however, k increases rapidly and reaches a high value, nearly five times that in the pure aqueous solution. This behavior is in sharp contrast with that of alcoholic solutions, in which such an increase in k was not observed but k was zero at 100 percent alcohols.

In methyl-ethyl-ketone, though the experiments between 20 and 95 vol. percent could not be done because of the restriction of its solubility in water, an analogous result was obtained. Though the rate at 100 percent methyl ethyl ketone does not obey eq. (2), the rate appears to be considerably large (Fig. 4).

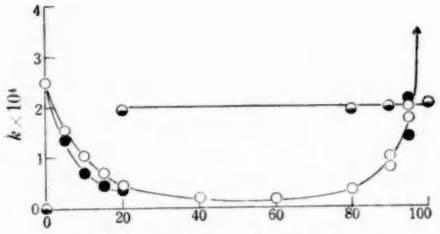

Fig. 4. Dependence of the quantum yield on the ketone concentration. 27°C.
○: acetone, aerobic
●: methyl ethyl ketone, aerobic
◒: acetone, in vacuo

Retarding effects of acetone and methyl ethyl ketone in the low concentration region can be expressed by eq. (1), values of K being listed in Table I.

In the vacuum photobleaching of acetone-water solution, no such spectral displacement as in alcohol-water mixtures[4] was observed and, therefore, uranine production was not realized.

At a concentration of acetone above 20 vol. percent the rate of photobleaching is expressed by eq. (2), while below this concentration deviation from eq. (2) is remarkable. Limiting quantum yield is 2×10^{-4} as illustrated in Fig. 4.

General Discussion

From the results so far obtained, some quantitative discussions will be given of the reaction scheme for the photobleaching of eosine in various conditions. For this purpose, the rate equation for the various cases must be given. It is to be noted that the rate equations proposed in Part I must be corrected in some respects.

1. Rate Equations.—In Part I the following two plausible schemes were proposed for the primary processes in the aerobic photobleaching of eosine in the water-alcohol solution.

(I) First attack of oxygen on the triplet state of dye:

$$D^t+O_2\rightarrow D\cdots O_2,\quad D\cdots O_2+H_2O\cdots\rightarrow\text{products}.$$

(II) First attack of water on the triplet state of dye:

$$D^t+H_2O\rightarrow D\cdots H_2O,$$
$$D\cdots H_2O+O_2\cdots\rightarrow\text{products}.$$

The rate equations given for these two cases were, for (I)

$$k=\varphi_{S\rightarrow T}\cdot\frac{k_{O_2}}{k_{qi}+k_1[H_2O]+k_2[RH]+k_{O_2}}\times\frac{k_1'[H_2O]}{k'_{-1}+k_1'[H_2O]+k_2'[RH]} \qquad (3)$$

and for (II)

$$k=\varphi_{S\rightarrow T}\cdot\frac{k_1[H_2O]}{k_{qi}+k_1[H_2O]+k_2[RH]}\times\frac{k'_{O_2}}{k'_{-2}+k_1'[H_2O]+k_2'[RH]+k'_{O_2}} \qquad (4)$$

Both equations can be simplified into eqs. (9) and (10) to fit the experimental results, if $\varphi_{S\rightarrow T}$ is practically constant in various solvents and the following conditions are fulfilled:

$$\text{for (I)}\quad k_{O_2}\gg k_{qi}+k_1[H_2O]+k_2[RH] \qquad (5)$$
$$k'_{-1}\approx 0 \qquad (6)$$
$$\text{for (II)}\quad k'_{O_2}\gg k'_{-2}+k_1'[H_2O]+k_2'[RH] \qquad (7)$$
$$k_{qi}\approx 0 \qquad (8)$$

The conditions (5) and (7) actually hold in view of the experimental fact that the rate does not depend upon the pressure of oxygen under ordinary conditions.

Then from eq. (3)

$$k=\varphi_{S\rightarrow T}\frac{k_1'[H_2O]}{k_1'[H_2O]+k_2'[RH]} \qquad (9)$$

and from eq. (4)

$$k=\varphi_{S\rightarrow T}\frac{k_1[H_2O]}{k_1[H_2O]+k_2[RH]} \qquad (10)$$

If eqs. (9) and (10) were correct, the values of k in the pure aqueous solution should be $\varphi_{S\rightarrow T}$ in both cases. The value of $\varphi_{S\rightarrow T}$ is ca. 0.1 according to Oster and Adelman[7], while k is found to be of the order of 10^{-4}. This discrepancy has arisen from the neglect of the following processes. Taking eq. (3) for example, it was assumed in Part I that the attack of oxygen on the

7) G. Oster and A. H. Adelman, *J. Am. Chem. Soc.*, **78**, 913 (1956).

triplet state leads solely to the reaction intermediate D···O_2, which only gives reaction products by the attack of water. But, in reality, it is very plausible that oxygen may partially deactivate D^t without formation of D···O_2 and the similar situation can exist in the attack of water on D···O_2.

If one takes these deactivation processes into account, eq. (3) must be rewritten as

$$k=\varphi_{S\to T}\frac{k_{O_2}[O_2]}{k^s_{O_2}[O_2]}\cdot\frac{k_1'[H_2O]}{k_1'^s[H_2O]+k_2'^s[RH]} \tag{11}$$

where the superscript s represents the summation of the mere deactivation and the effective process leading to the bleaching reaction.

From the similar reasoning, eq. (4) must be corrected as

$$k=\varphi_{S\to T}\frac{k_1[H_2O]}{k_1^s[H_2O]+k_2^s[RH]}\cdot\frac{k'_{O_2}[O_2]}{k'^s_{O_2}[O_2]} \tag{12}$$

For the vacuum photobleaching in the aqueous alcoholic solution, the primary process is

$$D^t+RH\rightarrow DH\cdot+R\cdot$$

and the specific rate of this reaction gives certainly the rate constant of the overall bleaching reaction.

$$k=\varphi_{S\to T}\frac{k_2[RH]}{k_1^s[H_2O]+k_2^s[RH]} \tag{13}$$

2. Further Confirmation of the Primary Processes in the Aerobic Photobleaching of the Aqueous Eosine Solution.— Though some evidences have already been presented in favor of the scheme I[1], more definite discussions will be given here analyzing the experimental data on the basis of the rate equations (11), (12) and (13).

Now all the experimental results so far obtained for the aerobic photobleaching are expressed by eq. (1) which holds in the low concentration region of alcohols or ketones. Eqs. (11) and (12) can be written in the form of eq. (1). From eq. (11),

$$\frac{1}{k}=\frac{1}{\varphi_{S\to T}}\frac{k'^s_{O_2}}{k'_{O_2}}\frac{k_1'^s}{k_1'}\left(1+\frac{k_2'^s[RH]}{k_1'^s[H_2O]}\right), \tag{14}$$

$$k^0=\varphi_{S\to T}\frac{k_{O_2}}{k^s_{O_2}}\frac{k_1'}{k_1'^s}$$

$$K=\frac{k_2'^s}{k_1'^s}\frac{1}{k^0}\quad\text{or}\quad\frac{k_2'^s}{k_1'^s}=k^0K \tag{15}$$

From eq. (12),

$$\frac{1}{k}=\frac{1}{\varphi_{S\to T}}\frac{k'_{O_2}}{k'^s_{O_2}}\frac{k_1^s}{k_1}\left(1+\frac{k_2^s[RH]}{k_1^s[H_2O]}\right) \tag{16}$$

$$k^0=\varphi_{S\to T}\frac{k'^s_{O_2}}{k'_{O_2}}\frac{k_1}{k_1^s}$$

$$\frac{k_2^s}{k_1^s}=k^0K \tag{17}$$

While for the vacuum photobleaching, from eq. (13).

$$\frac{1}{k}=\frac{1}{\varphi_{S\to T}}\frac{k_2^s}{k_2}+\frac{1}{\varphi_{S\to T}}\frac{k_1^s[H_2O]}{k_2[RH]}$$

or $$\frac{1}{k}\frac{[RH]}{[H_2O]}=\frac{1}{\varphi_{S\to T}}\frac{k_1^s}{k_2}+\frac{1}{\varphi_{S\to T}}\frac{k_2^s[RH]}{k_2[H_2O]} \tag{18}$$

According to eq. (18), a plot of $[RH]/k[H_2O]$ against $[RH]/[H_2O]$ should give a straight line of slope $k_2^s/\varphi_{S\to T}k_2$ and intercept $k_1^s/\varphi_{S\to T}k_2$; from these two values k_2^s/k_1^s can be evaluated. An example of such plots is shown in Fig. 5, which is satisfactory at least in the low concentration region of alcohol. In the higher

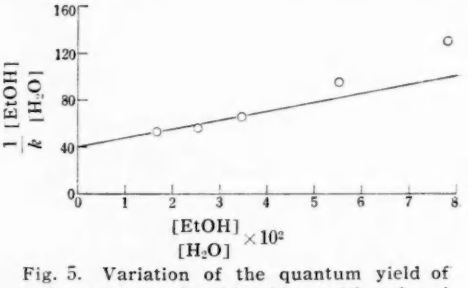

Fig. 5. Variation of the quantum yield of the vacuum photobleaching with ethanol concentration. 27°C. (Eq. (18))

region of the concentration, the deviation from the linearity becomes appreciable, and this deviation will be due to the similar situations for the aerobic photobleaching. Values of k_2^s/k_1^s thus obtained for methanol, ethanol and isopropanol are summarized in the sixth column of Table I.

Now if the scheme (II) be a real one, values of k^0K obtained from the aerobic photobleaching ought to be the same as those of k_2^s/k_1^s obtained from the vacuum photobleaching, while this does not hold for the scheme (I) (see eqs. (15) and (17)). Values of k^0K calculated from the data are listed in the fifth column of Table I.

Comparing k^0K with k_2^s/k_1^s, it is clear that there is a large difference between them, which definitely exceeds the experimental errors. Thus it can be concluded that the primary processes of the photobleaching of eosine in the aerobic aqueous

solution proceed via the mechanism (I). The values of k^0K in Table I are therefore interpreted as those of $k_2'^s/k_1'^s$ for the process (I).

Having established the reaction scheme, the values of $\varphi_{S\to T}\frac{k_2}{k_2^s}$ and $\varphi_{S\to T}\frac{k_2}{k_1^s}$ determined experimentally are tabulated in Table II.

TABLE II

RH	Temp. °C	$\varphi_{S\to T}\frac{k_2}{k_2^s}$	$\varphi_{S\to T}\frac{k_2}{k_1^s}$
MeOH	34	6.3×10^{-4}	5.6×10^{-3}
EtOH	27	13×10^{-4}	25×10^{-3}
i-PrOH	27	30×10^{-4}	53×10^{-3}

3. Reactivities of D^t and DH· with Oxygen.— In Part I the effect of oxygen pressure on the rate of photobleaching of eosine in the aqueous solution was examined, and it was found that the rate begins to decrease below ca. 10^{-5} mol./l. oxygen. Though the results are not very accurate, it is possible from the data to make a rough estimation about the reactivity of D^t towards oxygen and water. Since alcohol is absent in this case, the rate equation can be written as

$$k=\varphi_{S\to T}\frac{k_{O_2}[O_2]}{k^s_{O_2}[O_2]+k_1^s[H_2O]}\cdot\frac{k_1'[H_2O]}{k_1'^s[H_2O]} \tag{19}$$

From eq. (19),

$$\frac{1}{k}\frac{[O_2]}{[H_2O]}=\frac{1}{k^0}\frac{[O_2]}{[H_2O]}+\frac{1}{k^0}\frac{k_1^s}{k^s_{O_2}}, \tag{20}$$

where $k^0=\varphi_{S\to T}\frac{k_{O_2}}{k^s_{O_2}}\frac{k_1'}{k_1'^s}$ is the specific rate when enough oxygen is present. A plot of $[O_2]/k[H_2O]$ against $[O_2]/[H_2O]$ gives a straight line as illustrated in Fig. 6. The values of $\varphi_{S\to T}\frac{k_{O_2}}{k^s_{O_2}}\frac{k_1'}{k_1'^s}$ and $\frac{k_1^s}{k^s_{O_2}}$ at 15, 30 and 40°C are summarized in Table III.

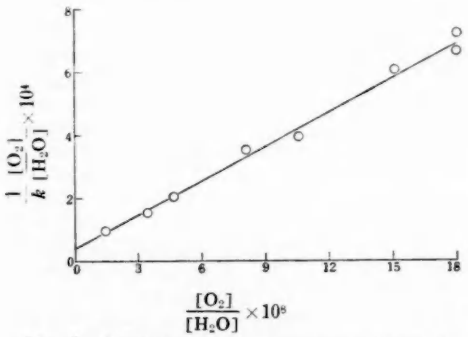

Fig. 6. Variation of the quantum yield with oxygen concentration in aqueous solution. 30°C. (Eq. (20))

TABLE III

Temp. °C	$\varphi_{S\to T}\frac{k_{O_2}}{k^s_{O_2}}\frac{k_1'}{k_1'^s}$	$\frac{k_1^s}{k^s_{O_2}}$
15	1.5×10^{-4}	2.1×10^{-5}
30	2.8×10^{-4}	1.3×10^{-5}
40	3.8×10^{-4}	3.4×10^{-5}

From the above results the ratio of the reactivity of D^t with oxygen to that with ethanol can be estimated as follows. Tentatively using the values of k^s_2/k^s_1 at 27°C for ethanol, it may be estimated that

$$\frac{k_2^s}{k^s_{O_2}}\approx40\times10^{-5}$$

Hence, it is expected that the quantity of oxygen required for the reaction between D^t and oxygen to overwhelm that between D^t and alcohol, is larger than 10^{-5} mol./l., above which quantity the reaction between D^t and water can be neglected against the reaction between D^t and oxygen. In contrast to this expectation, the experimental result that 10^{-6} mol./l. or less oxygen is enough to inhibit the vacuum photobleaching in pure ethanol[1]. This is certainly a strong evidence that oxygen in this system acts not on D^t but on DH·. The same conclusion has already been presented on the basis of different arguments in Part II.

4. The Deviation from the Linearity between $1/k$ and $[RH]/[H_2O]$ in the Higher Region of Alcohol Concentration. — In Part I this deviation was attributed to the change of environment around the dye ion. There is another thing, however, to be taken into account. When the concentration of alcohol is high, the term $k^s_2[RH]$ cannot be neglected against $k^s_{O_2}[O_2]$. The specific rate under this condition must be written as

$$k=\varphi_{S\to T}\frac{k_{O_2}[O_2]}{k^s_{O_2}[O_2]+k_2^s[RH]}\times\frac{k_1'[H_2O]}{k_1'^s[H_2O]+k_2'^s[RH]}$$

and eq. (14) must be replaced by

$$\frac{1}{k}=\frac{1}{\varphi_{S\to T}}\frac{k^s_{O_2}}{k_{O_2}}\frac{k_1'^s}{k_1'}\left(1+\frac{k_2'^s[RH]}{k_1'^s[H_2O]}\right)\times\left(1+\frac{k_2^s[RH]}{k^s_{O_2}[O_2]}\right) \tag{21}$$

Though eq. (21) can qualitatively explain the above deviation, it cannot be decided at the present stage what is the principal cause for the deviation.

5. Abnormalities Observed in Acetone and Isopropanol.— The experimental results obtained for the aerobic photobleaching of eosine in the acetone-rich aqueous solution and those for the vacuum photobleaching in isopropanol-water mixture are somewhat anomalous as compared with the results obtained with methanol and ethanol. Generally speaking, however, there is no reason why organic substances in the aqueous solution should behave in the same way irrespective of their concentration. From the experimental results that neither aldehyde nor acid was detected in the aerobic photobleaching of eosine in the aqueous solution containing a small amount of acetone, the retarding effect of acetone might be the mere deactivation of $D\cdots O_2$ in this concentration region, while in the higher region the fate of $D\cdots O_2$ would be quite different. The result that the vacuum photobleaching of eosine in isopropanol-water mixture has its maximum rate at a concentration of about 50 vol. percent alcohol would perhaps be ascribed to the similar change of environment around the dye ion. The elucidation of these phenomena must await further studies.

Summary

Studies on the photoreaction of eosine in the water-alcohols and -ketones have been made both in the presence and in the absence of oxygen. The corrected rate equations, giving the satisfactory explanation for the data obtained, have been presented. Analysis of the experimental results so far obtained, on the basis of these rate equations, has led to the conclusion unambigously that the primary process of the aerobic photobleaching of eosine in the aqueous solution is the attack of oxygen on the triplet state of dye.

The author indebted to Prof. M. Koizumi for many helpful discussions with respect to this research problem and to Mr. S. Ooi for carrying out a part of the experiments. The cost of this research has been partly defrayed by the Scientific Research Grant from the Ministry of Education, to which the author wishes to express his gratitude.

Institute of Polytechnics
Osaka City University
Kita-ku, Osaka

*Relative Volatility of H_2O^{16}/H_2O^{18} and Equilibration Time for Fractional Distillation of Water**

By Sadahiro SAKATA and Noriyoshi MORITA

(Received November 21, 1956)

Introduction

In a previous experiment[1], fractional distillation of water was accomplished with a packed column under total reflux by continuously supplying at the top of the column the same volume of fresh normal water as that of the distillate, and the relative volatility of light- to heavy-oxygen water was calculated from the concentration of heavy oxygen in the still water by assuming the same number of theoretical plates as that determined from concentration of heavy hydrogen and by using 1.026 for the relative volatility of H_2O/HDO. In the kind of fractionation applied there, the equilibration time for hydrogen isotopes was about twice that for oxygen isotopes and, therefore, the apparent value of the relative volatility of light- to heavy-oxygen water diminished gradually as the fractionation proceeded toward equilibrium. Extrapolating our experimental results, we concluded that the correct value lies between 1.0043 and 1.0040.

For further confirmation of the result,

* The main part of this paper was presented at the Local Meeting of the Society of Chemical Engineers, Japan, on October 29, 1956, at Yokkaichi.

1) S. Sakata and N. Morita, This Bulletin, **29**, 284 (1956).

another kind of experiment was made with a packed column where equilibrium of fractional distillation between waters in the still and in the condenser was obtained. The effect of the concentration of H_2O^{17} upon the concentration of H_2O^{18} was taken into consideration. The mean value of the relative volatility of H_2O^{16}/H_2O^{18} was proved to be 1.0039 with a possible error of ± 0.0002.

Experimental Procedure and Results

Distillation apparatus is shown diagramatically in Fig. 1. The column, 250 cm. in height, was

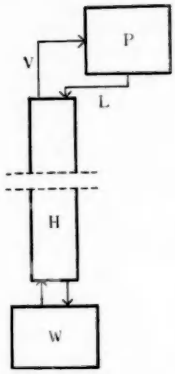

Fig. 1. Fractionation Apparatus.

made of 50 mm. copper tube with 1 mm. wall thickness. It was packed with heli-pack type packings, size $5\times5\times3$ mm., made from 0.3 mm. copper wire. The volume of the still was 2.0 l. and that of condenser was 5.0 l.

At the beginning of each series of experiments, 1.5 l. of normal water was poured into the still and 5.0 l. into the condenser. The still was heated externally with an electric furnace, and the column hold-up of water after boiling-up was judged to be about 100 cc. from the decrease of water in the still. The uncertainty of the hold-up does not seriously alter the conclusions given later. The through-put was determined from the quantity of condensate obtained during a short given interval and was calculated to be 3.3 cc./min. or 200 cc./hr.

Two series of experiments were done, the results of which are tabulated in Tables I and II. During each series of experiments, samples of about 15 cc. were taken from the still at intervals of several days and their total excess densities due to both heavy oxygen and heavy hydrogen were measured as compared with normal water. After equilibrium of fractionation was reached, two samples of water, one from the still and the other from the condenser, were taken. The total excess densities of these samples were measured first and then the heavy oxygen content of each

Table I
Results, series-1

Duration days	Excess in Density Still γ	Condenser γ
0.0	0.0	—
5.0	15.9	—
10.0	19.5	—
17.0	19.4	—
33.0	20.7	−6.0
D	7.1	−1.8
	$n-1=19.4_1$	
O^{18}	13.0	−4.0
(O^{17}	0.6	−0.2)
	$\alpha=1.0038_3$	
51.0	21.9	−5.0
D	7.3	−1.5
	$n-1=18.9_2$	
O^{18}	13.9	−3.3
(O^{17}	0.7	−0.2)
	$\alpha=1.0039_7$	

Table II
Results, series-2

Duration days	Excess in Density Still γ	Condenser γ
0.00	0.0	—
1.00	5.2	—
2.00	9.0	—
3.10	12.7	—
4.23	14.8	—
5.90	16.9	—
8.00	19.9	—
11.00	21.5	—
15.00	23.6	—
18.00	24.1	—
23.14	23.8	−7.5
D	7.8	−2.6
	$n-1=22.9_2$	
O^{18}	15.3	−4.6,
	$\alpha=1.0038_0$	
27.00	24.2	−7.1
D	7.3	−2.6
	$n-1=22.0_8$	
O^{18}	16.1	−4.3$_0$
	$\alpha=1.0040_2$	

of these samples was determined by electrolyzing the sample and combining the evolved oxygen with standard hydrogen[2]. As will be seen from the experimental procedure, the excess density of water taken from the condenser is negative. The density due to H_2O^{17} was separated from the density due to total heavy oxygen water by calculation on the assumptions that the relative volatility of H_2O^{16}/H_2O^{18} was 1.0039 and of H_2O^{16}/H_2O^{17} was $\sqrt{1.0039}$, and that the concentrations

2) N. Morita and T. Titani, This Bulletin, **11**, 414 (1936).

of H_2O^{18} and H_2O^{17} in normal water were respectively 224.7 and 21.9 in γ unit[3,4]. The number of theoretical plates $n+1$ was calculated from the excess densities due to heavy hydrogen of the samples as determined by subtracting the densities due to heavy oxygen from the total excess densities and by using $\sqrt{1.052}$ as the relative volatility of H_2O/HDO and 0.000147 (15.8γ) as the atomic fraction of deuterium in normal water. Using this number of theoretical plates, the relative volatility α of H_2O^{16}/H_2O^{18} was calculated from the excess densities due to H_2O^{18} of the two samples, Δs_w for the water from the still and Δs_p for the water from the condenser, by the equation

$$(224.7+\Delta s_w)/(224.7+\Delta s_p)=\alpha^{n+1} \qquad (1)$$

Two sets of measurements were made for each series of experiments. Four values of α in Table I and II give a mean value $\alpha=1.0039_1$. If we assume an error of $\pm 0.1\gamma$ for each value of measured excess densities due to deuterium and that due to O^{18}, the largest possible error in α is ± 0.00014. Although the error of each value of excess densities may be larger than $\pm 0.1\gamma$, the deviation of each calculated value of α from the mean value was rather small, and we concluded ± 0.0002 to be the possible error of the mean value.

Relation of Simultaneous Concentration of Heavy Oxygen and Heavy Hydrogen

Harbert[5] assumed Fenske's relation for each pair of components of a multicomponent system at equilibrium under total reflux. Normal water consists of nine components, as is shown in Table III. Mole fraction of each component in Table III was calculated by using values[3,4] of

TABLE III

COMPOSITION OF NORMAL WATER

No.	Formula	Mole fraction
1	HHO^{16}	$99.73467\cdot10^{-2}$
2	HHO^{18}	$19.80418\cdot10^{-4}$
3	HHO^{17}	$3.78889\cdot10^{-4}$
4	HDO^{16}	$29.32616\cdot10^{-5}$
5	HDO^{18}	$5.82326\cdot10^{-7}$
6	HDO^{17}	$1.11409\cdot10^{-7}$
7	DDO^{16}	$22.28229\cdot10^{-9}$
8	DDO^{18}	$4.42456\cdot10^{-11}$
9	DDO^{17}	$0.84650\cdot10^{-11}$

atomic fraction of isotopes, i.e. H=0.999853, D=0.000147, O^{16}=0.997640, O^{18}=0.001981 and O^{17}=0.000379, as well as by using the equilibrium constant for hydrogen isotopes

3) H. E. Watson, *J. appl. Chem.*, **3**, 556 (1953).
4) I. Kirshenbaum, "Physical Properties and Analysis of Heavy Water", McGraw-Hill Book Co., N. Y. (1951).
5) W. D. Harbert, *Ind. Eng. Chem.*, **37**, 1162 (1945).

$[HOD]^2/[HOH][DOD]=3.87$ and by assuming no isotopic effect for oxygen isotopes. As we can consider that these components in water constitute an ideal solution, we can apply Harbert's equation for equilibrium

$$x_{jw}=\alpha_{1j}^{n+1}x_{jp}/\sum_{i=1}^{9}\alpha_{1i}^{n+1}x_{ip} \qquad (2)$$

where x is concentration in mole fraction, suffix i or j indicates any one component in these nine components, suffix w indicates water in still, suffix p indicates water in condenser, and α_{1j} is the relative volatility of the most volatile component H_2O^{16} to j's component. As will be seen from Eq. (2), any two components show Fenske's relation because the denominator of the equation is common for all components and because for a pair of components j and j' there exists a relation $\alpha_{1j'}/\alpha_{1j}=\alpha_{jj'}$.

In addition to the fractionation by distillation, we must consider the following exchange reaction of hydrogen isotopes as a possible cause of change in concentration of components

$$\underset{k}{HOH}+\underset{l}{DOD}=2\underset{m}{HOD} \qquad (3)$$

From Harbert's equation we can write

$$x_{mw}/x_{kw}=\alpha_{km}^{n+1}(x_{mp}/x_{kp})$$
$$x_{mw}/x_{lw}=\alpha_{lm}^{n+1}\quad(x_{mp}/x_{lp})$$

where suffixes k, l and m indicate components as shown under Eq. (3). Then

$$x_{mw}^2/x_{kw}\cdot x_{lw}=(\alpha_{km}\cdot\alpha_{lm})^{n+1}(x_{mp}^2/x_{kp}\cdot x_{lp})$$

When vapor pressures of pure components are written as P_k, P_l and P_m we have the relation

$$\alpha_{km}\cdot\alpha_{lm}=P_k\cdot P_l/P_m^2$$

Therefore when P_m is geometrical mean of P_k and P_l, $\alpha_{km}\cdot\alpha_{lm}$ becomes unity, and we have the relation

$$x_{mw}^2/x_{kw}\cdot x_{lw}=x_{mp}^2/x_{kp}\cdot x_{lp}$$

Thus we can conclude that when either the water in the still or in the condenser is in isotopic equilibrium, the other is also in isotopic equilibrium and the exchange reaction shown in Eq. (3) has no effect on change in concentration of components of water under fractional distillation.

Fig. 2 shows the calculated values of fractional concentration of each component of water which is in equilibrium with normal water versus the number of theoretical plates of a fractionation column. In this calculation we assumed the relative volatility of H_2O^{16} to each component to

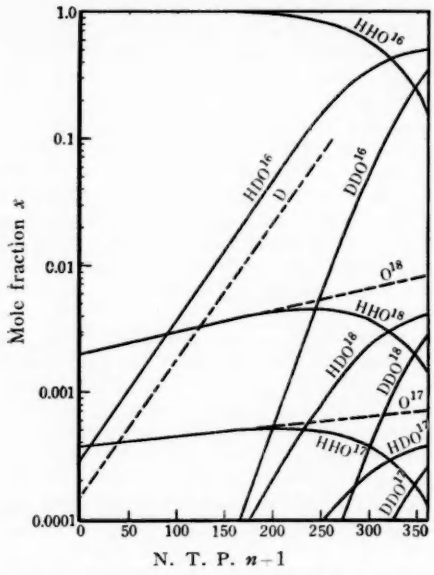

Fig. 2. Change of concentration with N. T. P.

TABLE IV

RELATIVE VOLATILITY

HHO^{16}	HDO^{16}	DDO^{16}
1.0000	$\sqrt{1.052}$	1.052
HHO^{17}	HDO^{17}	DDO^{17}
$\sqrt{1.0039}$	$\sqrt{1.0039 \cdot 1.052}$	$1.052\sqrt{1.0039}$
HHO^{18}	HDO^{18}	DDO^{18}
1.0039	$1.0039\sqrt{1.052}$	$1.0039 \cdot 1.052$

be as shown in Table IV. As are shown by dotted lines in the Fig. 2, the logarism of atomic fraction of D, O^{18}, and O^{17} in the range as shown in the Figure each shows a linear relation with $n+1$.

Equilibration Time

Urey and others[6,7] showed that the velocity of enrichment of a less-volatile component in a column is the greater, the nearer the plate is to the still, so that a stationary state sets in first at the lower part of the column. They, therefore, assumed that at a given moment shorter than equilibration time, the lower part of the column reaches the stationary state determined by Fenske's equation, while the upper part has the composition of the initial mixture. By applying the assumption to our experiment and assuming the upper part of the column to have the composition of the water in the condenser, the mean concentration $\bar{\eta}$ of a less-volatile component in the column is shown by

$$\bar{\eta}=\{x_w+\alpha x_p(\ln[x_w]/x_w-1)\}/n\alpha \ln \alpha \qquad (4)$$

where x_w is the concentration of a less-volatile component in the still at a given moment, x_p is that in the condenser, and x with square brackets shows a value at equilibrium.

Additionally we assume, as was done by Urey and others, that the vapor which enters into the condenser is in one-plate equilibrium with the refluxing water, and then we have the following relation by a material balance in a short interval dt

$$x_pLdt-(x_p/\alpha)Vdt=Wdx_w+Hd\bar{\eta} \qquad (5)$$

where V is the molar vapor velocity, L is the reflux velocity, W is the still hold-up, and H is the column hold-up. Under total reflux $L=V$, and at any moment from material balance we have $Wx_w+Px_p=(W+P)x_0$, where P is the condenser hold-up and x_0 is the fractional concentration of the less-volatile component in normal water. By setting $W/P=a$, $W/L=b$, and $H/L=c$, and substituting Eq. (4) into Eq. (5), we have

$$\begin{aligned} dt=&\binom{\alpha}{\alpha-1}\left[b+\frac{c\{1+\alpha a(1-\ln[x_w])\}}{n\alpha \ln \alpha}\right] \\ &\times\frac{dx_w}{\{(1+a)x_0-ax_w\}} \\ &+\binom{\alpha}{\alpha-1}\frac{ca \ln x_w dx_w}{\{(1+a)x_0-ax_w\}n \ln \alpha} \\ &-\binom{\alpha}{\alpha-1}\frac{cdx_w}{(n \ln \alpha)x_w} \end{aligned} \qquad (6)$$

Integration of Eq. (6) with a constriction that $x_w=x_0$ at $t=0$ and with the relation $(1+a)x_0-ax_w=x_p$ gives

$$\begin{aligned} t=&\binom{\alpha}{\alpha-1}\left[b+\frac{c\{1+\alpha a(1-\ln[x_w])\}}{n\alpha \ln \alpha}\right]\frac{1}{a}\ln\frac{x_0}{x_p} \\ &+\binom{\alpha}{\alpha-1}\binom{c}{n \ln \alpha}\left[-\ln\frac{x_p}{a}\ln x_w+\ln\frac{x_0}{a}\ln x_0\right. \\ &+\ln\binom{1+a}{a}x_0\ln\frac{x_w}{x_0}+\binom{a}{1+a}\left(1-\frac{x_w}{x_0}\right) \\ &\left.+\frac{1}{2^2}\binom{a}{1+a}^2\left(1-\frac{x_w^2}{x_0^2}\right)+\cdots\cdots\right] \\ &+\binom{\alpha}{\alpha-1}\binom{c}{n \ln \alpha}\ln\frac{x_0}{x_w}. \end{aligned} \qquad (7)$$

6) H. C. Urey, J. R. Huffman, H. C. Thode and M. Fox, *J. Chem. Phys.*, **5**, 856 (1937).
7) A. E. Brodsky and O. Ch. Scarre, *Acta Phys. Chim. U. R. S. S.*, **10**, 729 (1939).

Introducing in Eq. (7) the values applied in the experiments, i.e. $a=W/P=(1.5-0.1)/5.0=0.28$, $b=W/L=(1.5-0.1)/0.2=7$ hrs., and $c=H/L=0.1/0.2=0.5$ hr., and setting $n+1=20$, we obtain equilibration time 144 hrs. (6.0 days) for HDO and 147 hrs. (6.1 days) for H_2O^{18}. The values of x_w and x_p at equilibrium are calculated from the material balance relation, $Wx_w+Px_p=(W+P)x_0$, and from Fenske's equation for low concentration, $x_w/x_p=\alpha$[20]. The time necessary for equilibration for HDO is almost equal to that for H_2O^{18}, which is in marked contrast to the previous experiment[1].

If we neglect the column hold-up, c in Eq. (7) vanishes, and the relation reduces to a simple equation

$$t=\{\alpha/(\alpha-1)\}(b/a)\ln(x_0/x_p) \qquad (8)$$

Eq. (8) gives equilibration time 135 hrs. for HDO and 113 hrs. for H_2O^{18}. In this case the latter is a little shorter than the former. They are not, however, so far different from those obtained above from Eq. (7).

The assumption made in Eq. (5) becomes incorrect as the fractionation approachs equilibrium. In this respect Jackson and Pigford mentioned in their recent paper[8] that at a range of very small concentration of a less-volatile component, such as we have treated, the time necessary to reach 90% of equilibrium from initial concentration is about twice the value of equilibration time as calculated by such an equation submitted by Urey and others. Taking this fact into consideration calculated values are nearly coincident with our experimental values.

Discussion

As has already been mentioned, an error $\pm0.1\gamma$ each in excess densities due to deuterium in still and that in condenser combined gives, for our experimental conditions a maximum deviation of ±0.45 in $n+1$, and this error combined with an error of $\pm0.1\gamma$ each in excess densities due to O^{18} in still and that in condenser makes an error of ±0.00014 in the relative volatility α of H_2O^{16}/H_2O^{18}. In addition to this, an error of 0.001 in the relative volatility A of H_2O/HDO gives an error of $(\Delta n/n)=0.038$, and this error results in an error of 0.00015 in α (increases when A increases). For example, if we apply Schutz and Zmachinsky's value[9,10] $A=1.0295$ in place of $\sqrt{1.052}$, α becomes 1.0044$_8$.

As concerns the relative volatility of light- to heavy-oxygen water at 100°C., Watson gave a short summary in his recent paper[3]. In his paper he introduced data from Lewis and Cornish[10], Wahl and Urey[11], and Riesenfeld and Chang[12], giving values of 1.0056–1.0060, 1.003 and 1.0046, respectively, as the relative volatility. Watson also introduced the studies of Brodsky and Scarre[7] and Hayter[13] which gave 1.0055 and 1.0056, and he himself concluded 1.0056 as the most probable value.

Although the value 1.003 of Wahl and Urey was long accepted, it was not exact enough because it was a value which was extrapolated far from the measured values between 11.25 and 46.35°C., and this value seems much too low. Calculated values of 1.0056–1.0060 from Lewis and Cornish's data also seem inexact because their data were based on an uncertain number of the theoretical plates of their fractionation column. Increase in the assumed number of theoretical plates decreases the value of the relative volatility, and if we use a number around 50 instead of the 40 which they assumed, the value of the relative volatility of H_2O^{16}/H_2O^{18} becomes 1.004. Moreover, it is uncertain whether a true equilibrium of fractionation had been reached or not within such a short time as they applied to their experiments.

Brodsky and Scarre measured ratios of concentration of heavy hydrogen and heavy oxygen of water in a still to those of normal water by using a rotating column under total reflux by continuously supplying fresh normal water at the top of the column, as was done in our previous experiment[1]. In their calculation, howerer, they used a value of 17.9γ as the concentration of heavy hydrogen in normal water and a value of 171γ as that of heavy oxygen. The resultant values of the ratio under atmospheric pressure were 2.74 for hydrogen and 1.26 for oxygen. In place of the above values for natural abundance we use 15.8γ for heavy hydrogen and 224.7γ for O^{18}. Then the ratios reduce to 2.97 and 1.20, respectively. The

8) R. F. Jackson and R. L. Pigford, *Ind. Eng. Chem.*, **48**, 1020 (1956), Fig. 4.

9) P. W. Schutz, SAM Report A-595, Apr. 12, 1943.

10) G. N. Lewis and R. E. Cornish, *J. Am. Chem. Soc.*, **55**, 2616 (1933).

11) M. H. Wahl and H. C. Urey, *J. Chem. Phys.*, **3**, 411 (1935).

12) E. H. Riesenfeld and T. L. Chang, *Z. physik. Chem.*, **B33**, 127 (1936).

13) A. J. Hayter, Ph. D. Thesis, London Univ., 1950.

ratio for heavy hydrogen, combined with $\sqrt{1.052}$ for the relative volatility of H_2O/HDO, gives $n+1=43.0$, and this value, combined with the ratio for heavy oxygen, gives 1.0042 for the relatives volatility of light- to heavy-oxygen water. If the density due to O^{17} be excluded, the value of the relative volatility will reduce to about 1.0040.

Hayter's experiment, on which Watson's conclusion was based, was done with a packed column with 2500 packings which effect 0.21 theoretical plate per one packing. This number of theoretical plates was based on the fractionation of the system of benzene and carbon tetrachloride. By their fractionation of water, they obtained numbers between 250–400 from the fractionation of hydrogen isotopes, and applying these values, they concluded a value of 1.0056 as the relative volatility of H_2O^{16}/H_2O^{18}. The reason for the discrepancy between this value and our present value is not immediately clear. It seems probable, however, that their experiment was not based on true equilibrium of hydrogen isotopes. They used a continuous method for the fractional distillation, and the decrease of plate efficiency by such productive distillation may be more prominent for hydrogen isotopes than for oxygen isotopes, as was pointed out by Cohen[14]. In order to make applicable a value of around 1.004 for the relative volatility, the number of theoretical plates must be about 560, a value which does not seem improbable. If we use $0.12\times2500=525$ as the number of theoretical plates, we obtain 1.0043 as the relative volatility.

In conclusion, we do not find any fact which seems inconsistent to any great degree with our present result. Thus, by applying values of the natural abundance of D, O^{18} and O^{17} in normal water which are respectively 15.8, 224.7 and 21.9 in γ unit and of the relative volatility of $H_2O/HDO=\sqrt{1.052}$, and by assuming that the plate efficiency of the fractionation column is identical for hydrogen and oxygen isotopes, we conclude 1.0039 ± 0.0002 as the relative volatility of H_2O^{16}/H_2O^{18}.

Department of Chemical Engineering
Faculty of Engineering, Nagoya
University, Chigusa-ku, Nagoya

14) K. Cohen, *J. Chem. Phys.*, **8**, 588 (1940).

Benzylation of Acetylene. I. Formation of 3,4-Diphenyl-1-butyne and 3,4-Diphenyl-1,2-butadiene

By Teisuke Ando and Niichiro Tokura

(Received August 7, 1956)

Vaughn, Hennion, Vogt, and Nieuwland[1], in an attempted alkylation of acetylene by treating alkali metal acetylide (I) with various alkyl chlorides in liquid ammonia, observed that benzylacetylene (III) was not formed when benzyl chloride (II) was allowed to react with the acetylide.

The present writers carried out the same benzylation reaction and found that, instead of benzylacetylene (III), 3,4-diphenyl-1-butyne (IV) and an allenic compound, 3,4-diphenyl-1,2-butadiene (V), were formed.

To prepare the metal acetylide, lithium or sodium metal was dissolved in liquid ammonia and purified acetylene was passed through the solution until the blue color of the metal disappeared. The acetylide was allowed to react with benzyl chloride, the reaction product was taken up in ether, and the residue from the ethereal solution was fractionated under reduced pressure. The initial fraction of a small amout of unchanged benzyl chloride was followed by fractions A of b. p. 135°C (2 mmHg) and B of b. p. 190°C (2 mmHg) (total yield 10.3–34.6%), leaving a large amount of a residue which consisted of a viscous polymerized substance.

When lithium was used, the yields of A and B were 12.2% and 34.6% respectively, while sodium gave lower yields, A 0–5.2%

1) T. H. Vaughn, G. F. Hennion, R. R. Vogt and J. A. Nieuwland, *J. Org. Chem.*, **2**, 1 (1938).

and B 10.3–17.8%.

B is a yellowish, viscous liquid and forms a complex salt with silver nitrate, through which it can be purified and estimated. Thus, it has a terminal group $-C\equiv CH$ and the determination of residual silver in the complex salt and the liberated nitric acid during the complex formation gave a molecular weight 206 as a monoacetylenic compound. The structure of this substance was assumed to be

$$C_6H_5-CH_2-\underset{\displaystyle C_6H_5}{\underset{|}{CH}}-C\equiv CH. \qquad (IV)$$

Its infrared absorption spectrum exhibited a strong maximum at 3320 cm^{-1} due to stretching vibration of the terminal acetylenic bond and a weak one at 2120 cm^{-1} for a monosubstituted acetylene[2]. Catalytic reduction of B in the presence, of palladium carbon proceeded through a rapid absorption of 1 mole of hydrogen, and then a very slow absorption of one further mole of hydrogen. The product showed physical constants in good agreement with those of 1,2-diphenylbutane (VI)[3]. The infrared absorption for the unsaturated side-chain disappeared and a new absorption appeared at 1380 cm^{-1} due to methyl deformation[4]. Both the elementary analysis and the molecular refraction agreed with the theoretical values. Thus the structure of 3,4-diphenyl-1-butyne (IV) for B was concluded.

A is a colorless, clear, easily flowing liquid; it discolors bromine and potassium permanganate, but does not form a complex salt with silver nitrate. Its strong infrared absorptions at 1950, 1680, and 850 cm^{-1} showed it is an allene derivative[5]. As described in the experimental part, A is formed by the isomerization of B and this may be explained by assuming a structure of 3,4-diphenyl-1,2-butadiene (V) for A, which was ascertained by the oxidation of A with ozone to desoxybenzoin (VII).

It follows, therefore, that the reaction of the metal acetylide and benzyl chloride takes the following routes:

$$\underset{\text{(II)}}{C_6H_5CH_2Cl} + \underset{\text{(I)}}{NaC\equiv CH} \xrightarrow{\text{Liq. } NH_3}$$

$$\left[\underset{\text{(III)}}{C_6H_5-CH_2-C\equiv CH} \xrightarrow{NaC\equiv CH}\right.$$

$$\left[\underset{\displaystyle Na}{\overset{\displaystyle H}{\underset{|}{\overset{|}{C_6H_5-C-C\equiv CH}}}}\right] \xrightarrow{C_6H_5CH_2Cl}$$

$$C_6H_5-CH_2-\underset{\displaystyle C_6H_5}{\underset{|}{CH}}-C\equiv CH \xrightarrow{\text{isomerization}}$$

(IV)

$$C_6H_5-CH_2-\underset{\displaystyle C_6H_5}{\underset{|}{C}}=C=CH_2$$

(V)

$$IV \xrightarrow[\text{Pd-C}]{H_2} C_6H_5-CH_2-\underset{\displaystyle C_6H_5}{\underset{|}{CH}}-CH_2-CH_3$$

(VI)

$$V \xrightarrow{O_3} C_6H_5-CH_2-\underset{\displaystyle C_6H_5}{\underset{|}{C}}=O$$

(VII)

It is known that allenic compounds are formed in general in small amounts on heating acetylenic compounds with alkali hydroxide around 170°C[6], and a phenylbenzylallene, such as V, is comparatively easily formed from the isomeric acetylene at the room temperature even in the presence of such a weak base as ammonia.

Treatment of 3,4-diphenyl-2-butanone (VIII)[7] with phosphorus pentachloride followed by dehydrochlorination with potassium hydroxide[8] did not afford the acetylenic compound (IV) but almost the whole product was the allenic compound (V), which readily polymerized during distillation to give a large amount of a distillation residue.

$$C_6H_5-CH_2-\underset{\displaystyle C_6H_5}{\underset{|}{CH}}-COCH_3 \xrightarrow{PCl_5}$$

(VIII)

$$C_6H_5-CH_2-\underset{\displaystyle C_6H_5}{\underset{|}{\overset{\displaystyle Cl}{\underset{|}{\overset{|}{CH-C-CH_3}}}}} \xrightarrow{-HCl}$$

$$C_6H_5-CH_2-\underset{\displaystyle C_6H_5}{\underset{|}{\overset{\displaystyle Cl}{\underset{|}{\overset{|}{CH-C=CH_2}}}}} \xrightarrow{KOH}$$

2) L. J. Bellamy, "The Infra-red Spectra of Complex Molecules" John Wiley and Sons Inc., New York (1954), p. 49.
3) A. Klages and S. Heilmann, *Ber.*, **37**, 1452 (1904).
4) R. S. Rasmussen, *J. Chem. Phys.*, **16**, 712(1948).
5) W. J. Bailey and C. R. Pfeiffer, *J. Org. Chem.*, **20**, 97 (1955).
6) E. R. H. Jones, G. H. Whitham and M. C. Whiting, *J. Chem. Soc.*, **1954**, 3201; I. L. Jacobs, R. Akawie and R. G. Cooper, *J. Am. Chem. Soc.*, **73**, 1273 (1951).
7) M. M. Tiffeneau and M. J. Levy, *Bull. soc. chim. France*, **33**, 779 (1923).
8) C. Dufraisse and J. F. Viel, ibid., **37**, 817 (1925).

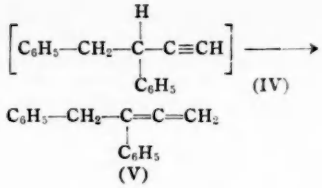

It was observed that 3,4-diphenyl-1-butyne (IV) was changed into 3,4-diphenyl-1,2-butadiene (V) merely by dissolving it in liquid ammonia and allowing the solution to stand overnight at the room temperature.

The formation of 3,4-diphenyl-1-butyne (IV) and of no benzylacetylene (III) in the reaction of metallic compounds of acetylene and benzyl chloride is analogous to the formation of 3,4-divinyl-1-butyne (X) in the reaction of a metal acetylide and allyl chloride (IX) in liquid ammonia.

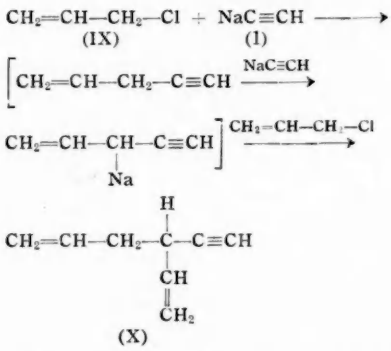

Reactions and properties of the acetylenic compound (IV) and its derivatives will be described elsewhere.

Experimental

Benzylation of Acetylene.—(1) Reaction of Lithium Acetylide and Benzyl Chloride.—Metallic lithium (1.7 g., 1/4 mole) was dissolved in 400 cc. of liquid ammonia, contained in a three-necked flask provided with a dry-ice reflux condenser and a stirrer, and maintained at $-50° \pm 5°$C in a dry-ice-ethanol bath. Acetylene, dried and purified by passage through concentrated sulfuric acid, soda lime, and phosphorus pentoxide, successively, was introduced into the solution with stirring until the blue color faded. It required about ten minutes. After stirring the solution for further ten minutes or so, 31 g. (1/4 mole) of benzyl chloride was added from a dropping funnel during about twenty-five minutes. The solution gradually acquired a pale pink color. When the mixture was stirred for 2.5 hr., it gradually became pale pinkish orange in color with increasing amount of a white precipitate. After

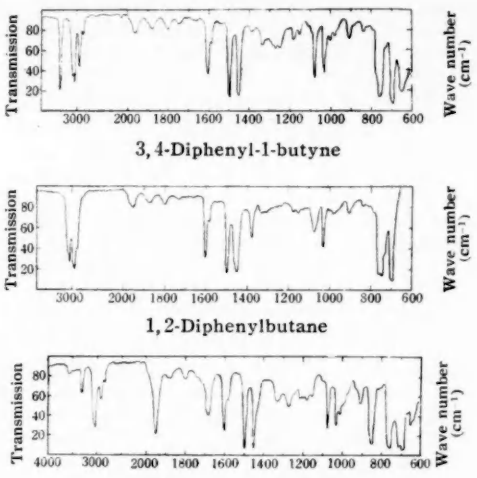

Fig. 1. Spectra were taken by a Perkin-Elmer Model 21 Infrared Spectrophotometer.

allowing the mixture to stand in an ice bath overnight, ammonia was allowed to evaporate and 100 cc. of water was added to the residue to dissolve the greyish white solid. Then an excess of 4 N hydrochloric acid was added to transform the by-product amine into the hydrochloride insoluble in ether, and the mixture was extracted with 200 cc. of ether. After filtration, the ethereal solution was washed successively with 4 N HCl and with water and dried over anhydrous sodium sulfate overnight. A small amount of hydroquinone was added to the ethereal solution, the ether was evaporated, and the residue was submitted to a low-pressure distillation in a nitrogen stream. Besides 1 g. of recovered benzyl chloride, b. p. 39–41°C/2 mmHg, the following fractions were obtained:

(A) Pale yellow liquid, b. p. 135–143°C/2 mmHg. 3.1 g. (12.2%).

(B) Yellowish brown viscous liquid, b. p. 185–190°C/2 mmHg, 8.9 g. (34.6%).

(C) Distillation residue, ca. 15 g.

B was identified with 3,4-diphenyl-1-butyne (IV) and A with 3,4-diphenyl-1,2-butadiene (V).

(2) Reaction of Sodium Acetylide and Benzyl Chloride.—Metallic sodium was dissolved in liquid ammonia under the same conditions as above and benzyl chloride was allowed to react with sodium acetylide so obtained. The yields of A and B from this reaction were as follows:

Expt. No.	Na (g.)	$PhCH_2Cl$ (g.)	Molar ratio Na/$PhCH_2Cl$	Yield A (g.)	A (%)	B (g.)	B (%)
1	46	253	1/1	0	0	35	16.9
2	12	126	1/2	5.4	5.2	10.6	10.3
3	12	31	2/1	0.8	3.1	4.6	17.8

Purification of Fraction B (3,4-Diphenyl-1-butyne (VI)[10].—To a solution of 5.5 g. of Fraction B, b. p. 185–190°C/2 mmHg, dissolved in 20 cc. of ethanol, a solution of 10 g. of silver nitrate dissolved in a mixture of 20 cc. of water and 40 cc. of ethanol was added, and the mixture was warmed for about 40 minutes on a water bath and allowed to stand overnight. The white precipitate was collected by filtration, washed with water to remove excessive silver nitrate and then with ethanol to remove the unchanged materials, and dried in a desiccator. Yield, 12 g.

A suspension of 12 g. of the silver complex salt in a 10% potassium cyanide solution was refluxed by heating on an oil bath, when an oily layer separated as the reaction proceeded. In ten hours' refluxing, the complex salt disappeared completely. After cooling, the mixture was extracted with ether, the ethereal layer was washed with water to neutral reaction, dried over anhydrous sodium sulfate and concentrated. The residue was distilled under a reduced pressure in nitrogen stream and in the presence of hydroquinone, to give 4.5 g. of a colorless, clear, viscous liquid, b. p. 190–192°C/2 mmHg, n_D^{25} 1.6040, d_{25}^{25} 1.0646. Mole Ref. Found: MR_D, 66.78. Calcd: 66.87.

Anal. Found: C, 92.86; H, 6.87. Calcd. for $C_{16}H_{14}$: C, 93.16; H, 6.84%. IR νmax: 3320 and 2120 cm^{-1}. Silver determination of the complex salt: 4.350 mg. of the substance gave an ignition residue (Ag) 1.988 mg. Calcd. for $C_{16}H_{13}Ag.AgNO_3$: 1.939 mg. Mol. wt., Found 194. Calcd. for $C_{16}H_{14}$: 206. Determination of HNO_3 produced during formation of silver complex salt[11]: 0.1691 g., and 0.1743 g. of the substance gave nitric acid equivalent to 10.67, and 11.00 cc., respectively, of 0.1 N NaOH. (f=0.7691). Mol. wt., Found: 206,206. Calcd. for $C_{16}H_{14}$: 206.

Catalytic Reduction of IV (Formation of 3,4-Diphenylbutane (VI).—A solution of 2 g. of IV in 100 cc. of methanol with the addition of 0.3 g. of palladium-carbon was submitted to reduction at ordinary temperature and pressure in a Willstätter apparatus. One mole of hydrogen was absorbed in twenty-five minutes while another mole of hydrogen in a longer time, fifteen hours being required in total. After removal of the catalyst, the solvent was evapolated, and the residue was submitted to vacuum distillation. The fraction of b, p. 153°C/11.5 mmHg, n_D^{17} 1.5882, agreed with the values of b. p. 152°C/11 mmHg and n_D^{18} 1.587 given for 1,2-diphenylbutane in the leterature[3]. Yield, 1.7 g.

Formation of 3,4-Diphenyl-1,2-butadiene (V) from 3,4-Diphenyl-2-butanone (VIII).—In order to change VIII, prepared by the method of Tiffeneau[7], to the acetylenic compound (IV) by the method of Dufraisse and Viel[8], VIII was treated successively with phosphorus pentachloride and with ethanolic potash. A solution of 17.4 g. of VIII dissolved in 35 cc. of petroleum ether was dropped into 25 g. of phosphorus pentachloride covered with 35 cc. of petroleum ether with stirring and the mixture was heated at 60°C for thirty hours. The mixture was then poured into ice water, extracted with ether, and ethereal layer was washed with water. After drying over anhyd. sodium sulfate, ether was evaporated and the residue was distilled under a reduced pressure, affording 10.3 g. of an oily substanc b. p. 156–158°C/5 mmHg. The oil was heated with 10% ethanolic potassium hydroxide for fifteen hours, and cooled, and ethanol was evaporated under a reduced pressure. The residue was extracted with ether, and the ethereal layer was washed with water to neutral reaction and dried over anhyd. sodium sulfate.

Distillation of the residue under a reduced pressure gave about 1 g. of V, b. p. 135–140°C/2 mmHg, and a minute amount of IV, b. p. 170–180°C 0.5 mmHg, with a distillation residue of a polymerized substance. V was identified by its infrared spectrum, exhibiting absorption maxima at 1950, 1680, and 850 cm^{-1}.

Formation of 3,4-Diphenyl-1,2-butadiene (V) from 3,4-Diphenyl-1-butyne (IV).—**(a) Allenation with Potassium hydroxide**[12].—A solution of 5 g. of IV dissolved in 100 cc. of 99% ethanol was added to a solution of 10 g. of potassium hydroxide dissolved in 10 g. of water with stirring, and the mixture was refluxed for six hours. Then, ethanol was evaporated under a reduced pressure, the residue was extracted with ether, and the ethereal layer was washed with water to neutral reaction. After drying over anhyd. sodium sulfate, the ether was evaporated and the residue was submitted to low-pressure distillation, giving 1 g. of colorless oil, b. p. 135°C/2 mmHg; I. R. νmax 1950, 1680 and 850 cm^{-1}. The rest remained in the flask as a residue.

(b) Allenation with Liquid Ammonia.—A solution of 5 g. of IV dissolved in 100 cc. of liquid ammonia in a pressure bottle was allowed to stand overnight, ammonia was allowed to evaporate, and the residue was extracted with ether. After washing with water and drying over anhyd. sodium sulfate, ether was evaporated and the residue was submitted to low-pressure distillation, giving 0.6 g. (12%) of a fraction, b. p. 135°C/2 mmHg, n_D^{18} 1.5992, 2.2 g. of another fraction, b. p. 140–195°C/2 mmHg, and 2 g. of a residue. The fraction b. p. 135°C/2 mmHg is the allene V, identified by its infrared absorptions at 1950, 1680 and 850 cm^{-1}. The fraction of b. p. 140–185°C/2 mmHg is a mixture of the allene V and the acetylene IV.

Ozonolysis of 3,4-Diphenyl-1,2-butadiene (V).—A solution of 2 g. of V dissolved in 100 cc. of ethyl acetate was cooled to −45°C and treated with ozone (0.021 mol./hr.) for one hour. Evaporation of the solvent from the reaction mixture gave a pale yellow oil, which was decomposed with 5 cc. of water and 20 cc. of 10% aqueous

10) M. Koulkes and I. Marszak, *Bull. soc. chim. France*, **1952**, 556.

11) G. Eglinton and M. C. Whiting, *J. Chem. Soc.*, **1953**, 3055.

12) A. Favorsky, *J. Prakt. Chem.*, **37**, 382 (1888).

sodium hydroxide and further oxidized with 10 cc. of 20% hydrogen peroxide.

On standing in a refrigerator overnight, the mixture gave a pale yellow solid, melting at 54–55.5°C. Yield, 1.2 g. (64%). Recrystallized from petroleum ether, it melted at 55–56°C, and showed no depression of the melting point in admixture with an authentic specimen of desoxybenzoin (VII)[13].

Summary

The reaction between benzyl chlorides and metal acetylides, prepared from metallic lithium and sodium in liquid ammonia resulted in the formation of new compounds, i. e. 3, 4-diphenyl-1-butyne and 3, 4-diphenyl-1, 2-butadiene. The benzylation of acetylene did not stop at benzylacetylene but another benzyl group was introduced to form 3, 4-diphenyl-1-butyne. 3, 4-Diphenyl-1, 2-butadiene was formed by the isomerisation of the butyne. This isomerisation occurred not only by the action of hot ethanolic potash but also in liquid ammonia at the room temperature. 3, 4-Diphenyl-1, 2-butadiene was readily polymerized by heat.

Infrared absorption spectra were measured by Prof. Kinumaki and his associates of this Institutes and the elementary analyses were made in the Laboratory of Shionogi Drug. Manufg. Co., Ltd. to whom the writers are deeply indebted. Thanks are also due to Miss Koko Miyaoka of this Laboratory for technical help.

Chemical Research Institute of Non-aqueous Solutions, Tohoku University, Sendai

13) C. F. H. Allen and W. E. Barker, *Org. Synth.*, **12**, 16 (1932).

Hydrogen Exchange and Isotope Effect on the Vinylation of Acetic Acid

By Noboru YAMADA

(Received November 19, 1956)

Introduction

As yet few investigations have been made as to the mechanism of the addition of reagent to the carbon triple bond, except that of the hydrogenation of acetylenic hydrocarbons[1]. The present investigation was undertaken to obtain some information about the mechanism of the addition to the triple bond. Vinyl acetate is synthetized by the addition of acetic acid to acetylene. By analogy with the addition of hydrogen halide to olefins it seems likely that the reaction takes place through the following process.

$$\text{(i)}\quad CH{\equiv}CH + H^+ \rightleftarrows CH_2{=}CH^+$$

$$\text{(ii)}\quad CH_2{=}CH^+ + CH_3COO^- \rightarrow CH_2{=}CH{\cdot}OCOCH_3 \qquad (1)$$

The initial step in the addition may be the donation of proton to acetylene by acetic acid to form an intermediate ion, (i), the latter then combining with acetate ion, (ii). This view suggested some ideas to the author, as follows. If (ii) is slow and rate-determining, acetylene may readily exchange its hydrogen with acetic acid in the course of reaction. However, if (i) is the slow step, the hydrogen exchange may hardly take place at all. Under this consideration the experiment of the deuterium exchange between acetylene and acetic acid-*d*, CH_3COOD, was undertaken. In the experiment acetylene and acetic acid-*d* were allowed to react in vapor phase with zinc acetate supported on active charcoal as catalyst at 160°C. In the course of reaction the change of deuterium concentration of acetylene was investigated. It appeared also possible to obtain some useful information about the reaction mechanism by the study of isotope effect on the reaction rate. The reaction rate was measured by a static method, and the effect of deuterium substitution on the reaction rate was studied.

1) G. C. Bond, "Catalysis," III, Reinhold Publishing Corp., New York, N. Y. (1955), p. 109.

Experimental

Materials.—G. R. glacial acetic acid was dried by vacuum distillation over phosphor pentoxide and used without farther treatment. Acetic acid-*d*, CH_3COOD, was prepared with acetic anhydrate and heavy water heating at 180°C. The heavy

water was obtained from Osaka University by courtesy of Prof. T. Titani and Prof. K. Hirota. The deuterium concentration of acetic acid-*d* was analyzed by burning it on cupric oxide and measuring the density of the water with a pressure sensitive buoy[2]. The deuterium concentration of the acetic acid-*d* was 96.2 atom % in hydroxyl hydrogen.

Acetylene was prepared with calcium carbide and water, and purified by the usual method. Dideuteroacetylene was prepared by the distillation of heavy water over calcium carbide following Lind's method[3]. Mass spectrometric analysis of the dideuteroacetylene showed that 8.1% of C_2HD was present, or 96.0 atom % in total deuterium concentration. The isotope analysis of acetylene was made in the Faculty of Science of Osaka University with the Hitachi MR-B type mass spectrometer.

Catalysts.—The zinc acetate catalyst supported on charcoal was prepared as follows. A proper amount of zinc acetate aqueous solution was absorbed into the active charcoal granules, Tsurumi Coal-GVAS, and they were dried at 110°C. Prior to use, the catalyst was evacuated a 170°C. Zinc acetate content of the catalyst used for the exchang experiment was 32% and that used for the isotope effect experiment was 28% in weight respectively.

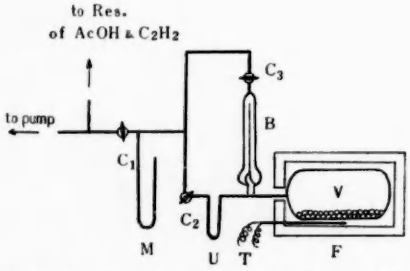

Fig. 1. Apparatus for the study of vinylation of acetic acid.

B	Bourdon gauge	M	manometer
C_1, C_2, C_3	stop cocks	T	thermocouple
		U	U tube
F	heater	V	reaction vessel

Apparatus and Procedure.—The main part of the apparatus is shown in Fig. 1. The glass reaction vessel, V, in which 18 g. of the catalyst had been contained, was evacuated at 160°C. A requisite amount of acetic acid-*d* was distilled into the U tube, U, in front of the reaction vessel, V, while U was cooled in liquid oxygen. Closing the stopcock, C_2, U was then warmed to room temperature, and the acetic acid-*d* was left to be adsorbed in the catalyst completely. Then acetylene was admitted into the reaction vessel through C_2. The succeeding pressure change with the reaction in the vessel was observed with the Bourdon gauge, B. The reaction temperature was kept at 160°C in the range of ±0.5°. After a definite time U was recooled in liquid oxygen, and the reaction was stopped. Acetylene was separated from the condensate in U by fractional distillation between −60° and −183°C. Prior to isotope analysis, acetylene was purified by repeated distillation through the traps at −60°C.

Results

I. Exchange of deuterium between acetylene and acetic acid-*d*.—In every run 0.2 cc. of acetic aid-*d* and about half of the equivalent moles of acetylene were admitted into the reaction vessel. The acetylene were admitted into the reaction vessel. The acetic acid-*d* used in this experiment contained 24.4 atom % of deuterium at the hydroxyl hydrogen. The total pressure was about 110 mmHg. at the start of every run. The results are given in Table I. In the fourth column of the table are shown the mole ratios of C_2HD and C_2H_2 in the acetylene samples, which were taken out in the course of vinylation by the procedure mentioned above. The formation of C_2HD indicated that the hydrogen exchange between acetylene and acetic acid-*d* occurred in the course of vinylation. As to the exchange rate, however, the reproducibility of the rates was hardly sufficient to make any kinetic analysis, for the observed ratios, C_2HD/C_2H_2, were not parallel with reaction time. It appears that the exchange rate increased with reaction time. It appears that the exchange rate increased with repetition of experiment. Some of the runs, which were carried out at 150°C, made no marked difference in the exchange rate to the other

TABLE I
DEUTERIUM EXCHANGE BETWEEN ACETYLENE AND ACETIC ACID-*d*

Run No.	Temp. (°C)	Reaction time (hr.)	C_2HD/C_2H_2
1	160	6	0.060
2	〃	12	0.110
3	〃	12	0.142
4	〃	15	0.191
5	〃	10.5	0.183
6	〃	3	0.170
7	150	3	0.182
8	〃	12	0.172
9	〃	6	0.162
10	〃	9	0.134
11*	160	21	0.094
12*	〃	12	0.108
13*	〃	6	0.182

* With active charcoal only.

2) T. Okamoto and M. Shindo, *J. Chem. Soc. Japan*, **57**, 9 (1936).
3) S. C. Lind, J. C. Jungers and C. H. Schiflett, *J. Am. Chem. Soc.*, **57**, 1032 (1935).

runs, which were carried out at 160°C. The runs from No. 11 to 13 were carried out with the active charcoal only, which contained no zinc acetate. In these runs no vinyl acetate was produced, but the exchange of deuterium occurred in a rate comparable to the other runs as is shown in Table I. The value of C_2HD/C_2H_2 at the exchange equilibrium can be estimated experimentally as about 1.8 from the data in Table I except No. 4, which was carried out under a somewhat different condition.

II. Deuterium isotope effect.—The rate of vinylation of acetic acid on the zinc acetate-charcoal catalyst is of the first order with respect to acetylene pressure[4], and in the presence of a definite and larger amount of acetic acid the reaction rate is approximately given by

$$-\frac{dP_a}{dt}=k_1P_a \qquad (2)$$

where P_a is the partial pressure of acetylene at any time t and k_1 is the first order rate constant. P_a is calculated approximately as the difference

$$P_a=P-P_b' \qquad (3)$$

where P is the total pressure of the reaction system at the time and P_b' is the adsorption equilibrium pressure of acetic acid before the admission of acetylene, or before the initiation of the reaction with acetylene. It has been assumed that in the beginning of reaction the decrease of acetic acid pressure with the reaction progress may be canceled by the increase of pressure of vinyl acetate produced. k_1 can be given by the slope of long P_a curve plotted against time as is shown in Fig. 2, where the results for a typical run are shown. The values of k_1 were used as the measure of deuterium isotope effect on the reaction of rate. Under a definite condition k_1 of the reaction of heavy acetylene and acetic acic-*d* was compared with that of the reaction of normal acetylene and acetic acid. The results at 160°C are given in Table II. In every run 0.27 cc. of acetic acid-*d* was used, and the initial pressure of acetylene was about 100 mmHg. The

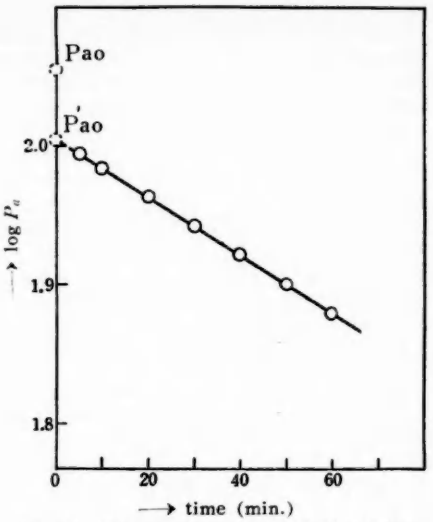

Fig. 2. The reaction rate of vinylation of acetic acid at 160°C.

runs of standard vinylation reaction with normal acetylene and acetic acid were performed before and after each run with the heavy reagents in order to confirm that the catalyst activity was not modified during this experiment. The results showed that the values of k_1 of the standard runs were always within $(3.6\pm0.1)\times10^{-3}$ min.$^{-1}$. In Table II the ratios, k_D/k_H, given in the fourth column are the ratios of k_1 of the reaction between the heavy reactants, of which the deuterium concentrations are given in the first and the second columns, and the k_1 of the reaction with the normal reactants. The ratios were always greater than unity and increased with the deuterium concentration of the reactants. The ratio was 1.6 for the reaction of almost wholly deuterated reactants, 96 atom %, at 160°C.

TABLE II

DEUTERIUM ISOTOPE EFFECT ON VINYLATION OF ACETIC ACID AT 160°C.

Deuterium Conc. atom %		$k_1\times10$	k_D/k_H
Acetylene	Acetic acid (in OH)		
0	0	3.6	
41	24	4.2	1.2
41	44	4.8	1.3
96	96	5.8	1.6

Discussion

Furukawa and Kozasa[5] investigated this vapor phase synthesis of vinyl acetate at

4) In another report*, it has been shown that the rate of vinylation of acetic acid on zinc acetate-charcoal catalyst is given by

$$-\frac{dp_a}{dt}=k\frac{p_a\,p_b}{(1+Kp_b)^2}$$

where p_a and p_b are the partial pressure of acetylene and that of acetic acid respectively. k is the rate constant and K is the equilibrium constant of adsorption of acetic acid on the catalyst.

* N. Yamada, *J. Chem. Soc. Japan (Pure Chem. Sect.)*, **78**, 252 (1957).

200° to 250°C. They noticed that the reaction rate is of the first order with respect to acetylene pressure and independent of acetic acid pressure. They presumed that the rate-determining step of this reaction is the adsorption of acetylene on the catalyst, and suggested that the reaction proceeds through acetylene-zinc acetate complex as intermediate. The author also studied the kinetics of this reaction at 160°C. Then it was concluded that the rate determining step is not the adsorption of acetylene, but is the reaction on the surface of the catalyst. Now the fact of the hydrogen exchange in the course of vinylation favors the above conclusion. If the adsorption was the slowest step and determined the reaction rate, acetylene would have little chance to exchange its hydrogen with acetic acid on the catalyst.

It has been shown that acetylene exchanges its hydrogen with acetic acid in the course of vinylation. This can be explained by accepting the already proposed mechanism (1) as that of the vinylation, and the step (ii) as the slow step. The hydrogen exchange was also found to occur between acetylene and acetic acid on the active charcoal, when no vinyl acetate was produced. If we assume that the exchange reaction on the charcoal proceeds through the same mechanism as that of the exchange on the zinc acetate catalyst, which has been presumed as (1), then the fact may suggest the following. The step (i) can proceed readily both from left to right and reversely, but the step (ii) cannot proceed so readily without zinc acetate catalyst. This argument makes it more probable that the step (ii) must be the rate-determining step.

We can find a great likeness between (1) and the mechanism of specific acid-catalyzed reaction as

$$\begin{aligned} &\text{(i)} \quad S + H^+ \rightleftarrows SH^+ \\ &\text{(ii)} \quad SH^+ \rightarrow \text{product} \end{aligned} \tag{4}$$

where S is the substrate. It has been found that most acid-catalyzed reactions proceed more readily in D_2O than in H_2O[5]. The isotope effect is caused by the pre-equilibrium (i) of (4). This means that if there is such a pre-equilibrium, the effect of the isotope mass makes the concentration of SD greater than that of SH under comparable conditions. If we find experimentally $k_D > k_H$ in an acid-catalyzed reaction, then an acid-base equilibrium must always be involved in the kinetic scheme. Now it has been found that there is such an isotope effect on vinyl acetate synthetic reaction as $k_D > k_H$.

The isotope effect obtained, $k_D/k_H = 1.6$, is of the same order as those found by other workers for acid-catalyzed reactions, $k_D/k_H = 1.3 \sim 3.0$[6]. It has not yet been fully ascertained whether vinylation reaction of organic acid with zinc acetate catalyst is an acid-catalyzed reaction[7]. However, since in the vinylation one of the reactants is an acid, it is reasonable to suppose that there exists such an acid-base equilibrium as (i) of (1). It should also be noted that usually the addition of reagents to the carbon-carbon triple bond requires a combination of a mercuric salt and a strong acid as catalyst. The fact of the hydrogen exchange between acetylene and acetic acid also favors this consideration. It may be concluded that by analogy to acid-catalyzed reaction the observed deuterium isotope effect supports the mechanism (1) as that of vinylation of acetic acid does.

In the previous papers the author reported the exchange of the acetate group between acetic acid, zinc acetate and vinyl acetate. It was shown that at 150°C acetate group exchange occurred rapidly between acetic acid and zinc acetate[8], but very slowly between acetic acid and vinyl acetate[9], and the exchange was not found between vinyl acetate and zinc acetate[10]. It is presumable that the exchange of the acetate group between acetic acid and zinc acetate proceeds through an intermediate complex as Norris[11] suggested

$$CH_3COOH + Zn(CH_3COO)_2 \rightleftarrows Zn(CH_3COO)_3 \cdot H \tag{5}$$

In other words the proton of acetic acid may easily transfer to one of the acetate groups of zinc acetate. This may be true also in the vinylation reaction of acetic acid on zinc acetate, and possibly then the transfer of proton from acetic acid to acetylene may also readily occur on the

5) J. Furukawa, H. Kozasa and S. Yamashita, *Chem. High Polymers* (Japan), **9**, 240 (1952).

6) K. B. Wiberg, *Chem. Rev.*, **55**, 718 (1955); R. P. Bell, "Advances in Catalysis," **IV**. Academic Press Inc. New York, N. Y. (1952), p. 184.

7) S. Otsuka, Y. Matumoto and S. Murahashi, *J. Chem. Soc. Japan (Pure Chem. Sect.)*, **75**, 798 (1954); S. Otsuka, ibid., **75**, 1115 (1954).

8) N. Yamada K. Suma and T. Takeuchi, ibid., **74**, 1018 (1953).

9) N. Yamada, T. Inokuchi and T. Takeuchi, ibid., **75**, 977 (1954).

10) N. Yamada, T. Inokuchi and T. Takeuchi, ibid., **75**, 1093 (1954).

11) E. A. Evance, J. L. Huston and T. H. Norris, *J. Am. Chem. Soc.*, **74**, 4985 (1952).

catalyst surface. This consideration leads to the more comprehensive picture of the reaction mechanism as shown below

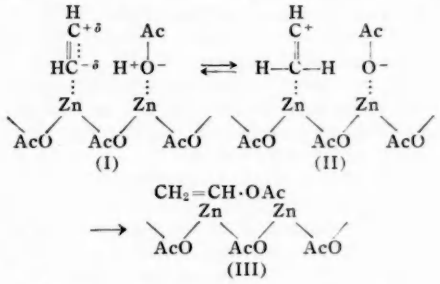

The kinetic study of this reaction[1] supports the mechanism of Hinshelwood type. That is to say, the reaction takes place between the acetylene molecules and the acetic acid molecules adsorbed on adjacent active points of the catalyst, presumably on adjacent zinc atoms. Acetylene an acetic acid may be linked to a zinc atom on the catalyst surface by coordination. It may result in electronic polarization of their molecules as (I) shows. The proton transfer may occur from acetic acid to the acetate ion of zinc acetate (acetate group exchange), or to acetylene (hydrogen exchange and vinylation). The step from (II) to (III) may be irreversible, for the acetate group exchange between vinyl acetate and zinc acetate was not found. As it has been mentioned, hydrogen exchange and isotope effect on the vinylation reaction of acetic acid indicate that the step (I)-(II) should be in pre-equilibrium and the step (II)-(III) should be the rate-determining step.

Summary

The mechanism of vinylation reaction of acetic acid was studied by the use of deuterium. The exchange of deuterium was found to occur between acetylene and acetic acid-*d* on zinc acetate-charcoal catalyst. The deuterium isotope effect of the reaction rate was also found, and the rate ratio, k_D/k_H, was 1.6 at 160°C. A mechanism of the reaction which contains a pre-equilibrium of intermediate ion formation, $CH{\equiv}CH + H^+ \rightleftarrows CH_2{=}CH^+$, $CH_2{=}CH^+ + CH_3COO^- \rightarrow CH_2{=}CH{\cdot}OCOCH_3$, was proposed and discussed.

The author wishes to express his sincere gratitude to Prof. T. Titani and Prof. K. Hirota of Osaka University, and also to Prof. T. Takeuchi of Toyama University for their invaluable help and encouragement during the course of this work. The author is indebted to Mr. Y. Kobayashi of Osaka University for mass spectrometric analysis.

Faculty of Literature and Sience
Toyama University, Toyama

*Studies on Antibiotics and Related Substances. V. Synthesis of 5-Methylenecyclopentanone-3-carboxylic Acid, an Antitumor Isomer of Sarkomycin**

By Sumio UMEZAWA and Mitsuhiro KINOSHITA

(Received December 15, 1956)

Recently, H. Umezawa and coworkers[1] obtained an antitumor substance, sarkomycin, from the fermentation broth of a *Streptomyces* similar to *S. erythrochromogenes*. Sarkomycin has not been isolated in a pure state, but Hooper et al.[2] reported that the main active principle is 2-methylenecyclopentanone-3-carboxylic acid. Therefore, it became interesting to synthesize analogues of methylenecyclopentanone-3-carboxylic acid. A brief communication[3]

* Presented before the Monthly Meeting of the Japan Antibiotic Research Association, at the Institute of Infectious Diseases, Tokyo, November 29, 1956.

1) H. Umezawa, T. Yamamoto, T. Takeuchi, T. Osato, Y. Okami, S. Yamaoka, T. Okuda, K. Nitta, K. Yagishita, R. Utahara and S. Umezawa, *Antibiotics and Chemotherapy*, **4**, 514 (1954).

2) I. R. Hooper, L. C. Cheney, M. J. Cron, O. B. Fardig, D. A. Johnson, D. L. Johnson, F. M. Palermiti, H. Schmitz and W. B. Wheatley, ibid., **5**, 585 (1955).

3) S. Umezawa and M. Kinoshita, *J. Antibiotics, Ser. A*, **IX**, 194 (1956).

has been given of the synthesis of an isomer of sarkomycin, 5-methylene-cyclopentanone-3-carboxylic acid which showed significant antitumor and antibacterial activities.

In the present paper, we report a more detailed study of the 5-methylene derivative and related compounds.

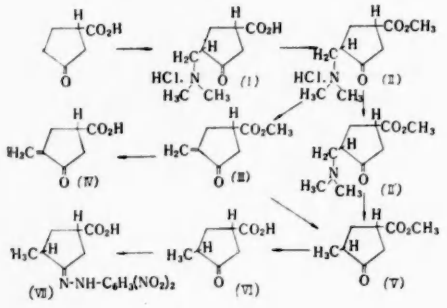

A mixture of cyclopentanone-3-carboxylic acid[4], paraformaldehyde, and dimethylamine hydrochloride, was fused to give 23% yield of 5-(dimethylaminomethyl)cyclopentanone-3-carboxylic acid hydrochloride (I), a Mannich base hydrochloride, m. p. 147–148°C (dec.). A common procedure with aqueous formaldehyde, dimethylamine hydrochloride, and cyclopentanone-3-carboxylic acid, gave also I. Esterification of I by the Fischer-Speier method with methanol gave methyl 5-(dimethylaminomethyl)cyclopentanone-3-carboxylate hydrochloride (II), m. p. 143–143.5°C (dec.), in 89% yield.

Degradation of the ester-hydrochloride (II) by vacuum distillation afforded a 76% yield of methyl 5-methylenecyclopentanone-3-carboxylate (III), m. p. 24–27°C, which, on standing in the absence of polymerization inhibitor, polymerized gradually.

Mild hydrolysis of III with dilute sulfuric acid in the presence of hydroquinone as an inhibitor followed by extraction with ethyl acetate and evaporation of the solvent in vacuo gave a crude product of 5-methylenecyclopentanone-3-carboxylic acid (IV), an almost colorless liquid, in 83% yield. After purification, IV was obtained as colorless needles melting at 67–74°C.

Structural proof of IV was obtained by hydrogenation of III with platinum catalyst in methanol solution to give 77% yield of methyl 5-methylcyclopentanone-3-carboxylate (V), b. p. 89–95°C (3 mmHg). Hydrolysis of V with dilute sodium hydroxide solution gave 5-methylcyclopentanone-3-carboxylic acid (VI) of b. p. 125–130°C (0.3 mmHg), which, by treatment with 2,4-dinitrophenylhydrazine, gave 2,4-dinitrophenylhydrazone (VII), m. p. 141–143°C, which did not depress the melting point of the authentic sample of the 2,4-dinitrophenylhydrazone of 5-methylcyclopentanone-3-carboxylic acid which was prepared by the synthetic route of Hope and Perkin[5].

Ozonolysis of methyl 5-methylenecyclopentanone-3-carboxylate (III) and of 5-methylenecyclopentanone-3-carboxylic acid (IV) gave formaldehyde (isolated as the methone derivative) as one of the products. This established the presence of the exomethylene group in III and IV, and thus the position of the double bond which was lost when III was hydrogenated to give methyl 5-methylcyclopentanone-3-carboxylate (V).

Moreover, catalytic hydrogenolysis of methyl 5-(dimethylaminomethyl)cyclopentanone-3-carboxylate (II'), b. p. 78–85°C (0.1 mmHg), which was obtained from II by treatment with dry ammonia in chloroform followed by filtration to remove ammonium chloride and finally by vacuum distillation, afforded the methyl 5-methylcyclopentanone-3-carboxylate (V), which was again led to 2,4-dinitrophenylhydrazone (m. p. 141–143°C) of 5-methylcyclopentanone-3-carboxylic acid (VI).

The infrared absorption characteristics (Fig. 1) of 5-methylenecyclopentanone-3-carboxylic acid (IV) were those typical of sarkomycin. The absorption at 6.09 μ was the evidence of a carbon-carbon double bond. The conjugated carbonyl absorption was found at 5.84 μ.

The ultraviolet absorption (Fig. 2, curve A) of IV in methanol solution showed a peak at 231 mμ suggesting an α, β-unsaturated ketone. The ultraviolet absorption (Fig. 2, curve B) of 5-methylcyclopentanone-3-carboxylic acid (VI) in methanol was

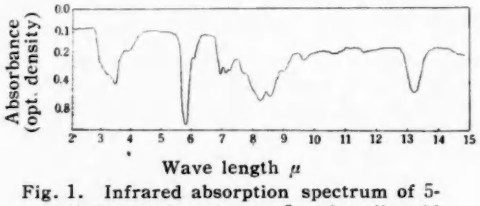

Fig. 1. Infrared absorption spectrum of 5-methylenecyclopentanone-3-carboxylic acid (Nujol)

4) F. W. Kay and W. H. Perkin, Jr., *J. Chem. Soc.*, **1906**, 1646.

5) E. Hope and W.H. Perkin, ibid., **1911**, 762.

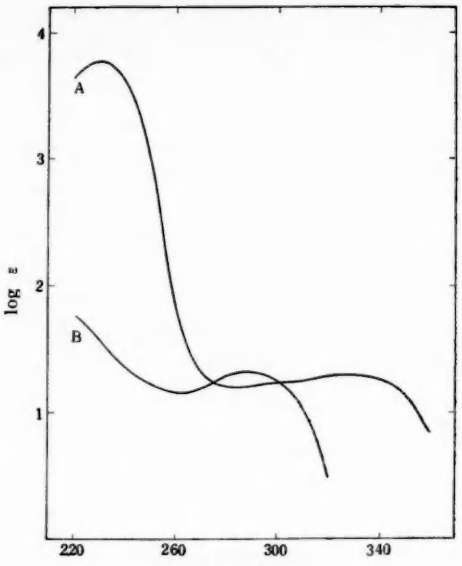

Fig. 2. Ultraviolet absorption spectra of 5-methylenecyclopentanone-3-carboxylic acid (IV, Curve A) and 5-methylcyclopentanone-3-carboxylic acid (VI, Curve B) in absolute methanol.

characterized by a carbonyl band near 285 mμ.

On treatment with methyl iodide, II' afforded in a quantitative yield a crystalline methiodide (VIII), m. p. 213°C (dec., sintered at 145°C.). However, the Hofmann degradation of VIII to obtain methylene derivative was unsuccessful.

Experimental

5-(Dimethylaminomethyl)cyclopentanone-3-carboxylic Acid Hydrochloride (I).—Cyclopentanone-3-carboxylic acid prepared by the route of Kay and Perkin[4] was condensed with formaldehyde and dimethylamine hydrochloride by the Mannich reaction.

Procedure A.—A mixture of 5.0 g. of cyclopentanone-3-carboxylic acid and 3.2 g. of dimethylamine hydrochloride was warmed on a water bath. To the resulting melt was added 1.18 g. of paraformaldehyde and then the mixture was stirred at 75-80°C for three hours and then evaporated under reduced pressure. The resulting syrup was dissolved in 10 cc. of hot absolute ethanol and a small amount of insoluble solid was removed by filtration. The solution was allowed to stand overnight in a refrigerator to separate the crystalline hydrochloride of Mannich base, which was collected, washed with absolute ethanol, and dried. M. p. 136-138°C (dec.). Yield, 2 g. (23%). Two recrystallizations from methanol afforded an analytical sample, m. p. 147-148°C (dec.), as a colorless prisms.

Anal. Found: C, 48.51; H, 6.91; N, 6.14. Calcd. for $C_9H_{15}O_3NCl$: C, 48.80; H, 7.22; N, 6.32%.

Procedure B.—A mixture of 2.0 g. of cyclopentanone-3-carboxylic acid, 1.2 cc. of aqueous 39% formaldehyde, and 1.27 g. of dimethylamine hydrochloride, was warmed at 75°C for four hours. The initial odour of formaldehyde disappeared. The resulting clear solution was evaporated under reduced pressure to give a viscous, pale-yellow oil, which was redissolved in 10 cc. of absolute ethanol by gentle warming and allowed to crystallize overnight in a refrigerator. The yield of crude crystals was 0.8 g.. On recrystallization from absolute methanol, an analytical sample of 5-(dimethylaminomethyl)cyclopentanone-3-carboxylic acid hydrochloride of m. p. 146-147°C (dec.) was obtained. Yield, 500 mg. (14%). When mixed with a sample prepared by procedure A described above, the melting point was unchanged.

Methyl 5-(dimethylaminomethyl)cyclopentanone-3-carboxylate Hydrochloride (II).—A mixture of 1.7 g. of 5-(dimethylaminomethyl)cyclopentanone-3-carboxylic acid hydrochloride (I) and 80 cc. of absolute methanol was saturated with dry hydrogen chloride and allowed to stand overnight. The methanol was removed by distillation at about 40°C under reduced pressure and the residue was dried in a desiccator. The resulting crystals were dissolved in a small quantity of methanol by gentle warming and the solution was diluted with absolute ether, whereupon there separated a crystalline precipitate of methyl 5-(dimethylaminomethyl)cyclopentanone-3-carboxylate hydrochloride, m. p. 138-140°C (dec.). Yield 1.6 g.. The crude crystals were redissolved in absolute methanol containing hydrogen chloride and recrystallization by addition of absolute ether gave colorless needles melting at 143-143.5°C (dec.).

Anal. Found: C, 50.84; H, 7.29; N, 5.80. Calcd. for $C_{10}H_{18}O_3NCl$; C, 50.95; H, 7.64; N, 5.95%.

Methyl 5-Methylenecyclopentanone-3-carboxylate (III).—A sample of 0.7 g. of methyl 5-(dimethylaminomethyl)cyclopentanone-3-carboxylate hydrochloride (II) was placed in a small round-bottom flask and heated at 145-150°C in an oil bath under highly reduced pressure (0.005 mmHg). Colorless crystals of methyl 5-methylenecyclopentanone-3-carboxylate were obtained in a receiver cooled in a dry ice- acetone bath. M. p. 24-27°C. Yield, 0.35 g. (76%). On standing at room temperature in the absence of polymerization inhibitor, this compound gradually polymerized and became less soluble in methanol or ethanol. The fresh product decolorized bromine in carbon tetrachloride rapidly.

Anal. Found: C, 62.34; H, 6.21. Calcd. for $C_8H_{10}O_3$: C, 62.32; H, 6.54%.

Ozonolysis of III.—A solution of 226 mg. of freshly prepared methyl 5-methylenecyclopentanone-3-carboxylate (III) in 10 cc. of ethyl acetate was treated with an approximately 2% by weight

ozone-oxygen mixture at 0°C at a rate of 500 cc. per minute for nineteen minutes. To the resulting pale-yellow solution was added 10 cc. of water and 300 mg. of zinc dust. The mixture was refluxed on a steam bath for thirty minutes. The reaction mixture was filtered while hot into a solution of 300 mg. of methone in 10 cc. of ethanol. Dilution with 20 cc. of water afforded needles, m. p. 186–187°C. Yield, 135 mg. (31%). Recrystallization from 80% ethanol gave pure crystals melting at 187–189°C. The melting point was undepressed on admixture with an authentic sample of formaldehyde methone of m. p. 189–190°C.

5-Methylenecyclopentanone-3-carboxylic Acid (IV).—A mixture of 997 mg. of freshly prepared methyl 5-methylenecyclopentanone-3-carboxylate (III), 20 cc. of 1.5 N sulfuric acid, and 3 mg. of hydroquinone (as an inhibitor), was stirred at 25–27°C for three hours to give a clear solution, which was adjusted to pH 2.0 with a saturated solution of sodium bicarbonate and extracted with three 10 cc. portions of ethyl acetate. After the extract had been dried over sodium sulfate, the ethyl acetate was removed by distillation under reduced pressure at 30–35°C to yield 5-methylenecyclopentanone-3-carboxylic acid, a pale-yellow liquid. Yield, 751, mg. (83%). On standing at room temperature in the absence of an inhibitor, this compound polymerized and gradually decreased in the antibacterial activity.

A freshly prepared sample of IV was dissolved in a small quantity of water, neutralized with sodium bicarbonate, and washed with ethyl acetate. Acidification and extraction with ethyl acetate followed by evaporation of the solvent in vacuo yielded colorless needles of IV melting at 67–74°C.

Anal. Found: C, 59.60; H, 5.81. Calcd. for $C_7H_8O_3$: C, 59.99; H, 5.75%.

The infrared spectrum (Fig. 1) of purified 5-methylenecyclo- pentanone-3-carboxylic acid (IV) in Nujol showed a peak at 6.09μ which is characteristic of the exocyclic methylene group in sarkomycin and had a conjugated carbonyl band at 5.84μ.

The ultraviolet spectrum (Fig. 2) of IV in methanol showed the presence of α, β-unsaturated ketone at 231 mμ (log. ε 3.76).

Ozonolysis of IV.—A solution of 200 mg. of freshly prepared 5-methylenecyclopentanone-3-carboxylic acid in 10 cc. of ethyl acetate was treated with ozone just as described in the ozonolysis of III. The yield of formaldehyde methone of m. p. 187–189°C was 113 mg. (28%). A mixed melting point determination carried out with an authentic sample of formaldehyde methone showed no change.

Hydrogenation of Methyl 5-Methylenecyclopentanone-3-carboxylate (III) to Methyl 5-Methylcyclopentanone-3-carboxylate (V).—A solution of 335 mg. of freshly prepared methyl 5-methylenecyclopentanone-3-carboxylate (III) in 2.5 cc. of methanol was shaken with 30 mg. of platinum oxide and hydrogen; 59 cc. (32.2°C, 754 mm.) of hydrogen was absorbed in fifteen minutes. After filtration, the filtrate was concentrated under reduced pressure to give a pale-yellow liquid. Fractional distillation in vacuo gave 260mg. (77%) of methylcyclopentanone-3-carboxylate of b. p. (bath temp.) 89–95°C (3 mm.).

5-Methylcyclopentanone-3-carboxylic Acid (VI).—A mixture of 558 mg. of methyl 5-methylcyclopentanone-3-carboxylate (V) in 1.5 cc. of 10% sodium hydroxide solution was stirred at room temperature for one hour. The resulting solution was acidified to pH 2.6 by addition of 1.5 N sulfuric acid, saturated with ammonium sulfate, and then extracted with ether. After the extract was dried over sodium sulfate, the ether was removed by distillation. Fractional distillation of the residue in vacuo gave a viscous liquid of 5-methylcyclopentanone-3-carboxylic acid, b. p. (bath temp.) 125–130°C (0.3 mm.). Yield, 340 mg. (66.8%). The 2,4-dinitrophenylhydrazone (VII) prepared by the general procedure melted at 141–143°C and did not depress the melting point of the authentic sample of the 2,4-dinitrophenylhydrazone of the 5-methylcyclopentanone-3-carboxylic acid which was prepared by the synthetic route of Hope and Perkin.[5]

Methyl 5-(Dimethylaminomethyl)cyclopentanone-3-carboxylate (II').—To a mixture of 710 mg. of methyl 5-(dimethylaminomethyl) cyclopentanone-3-carboxylate hydrochloride (II) and 5 cc. of chloroform was added 2.46 cc. of 1.23 N ammonia-chloroform solution, whereupon ammonium chloride immediately precipitated. The chloroform-layer containing the free ester-amine was separated and concentrated under reduced pressure. The oily residue was distilled in vacuo to give methyl 5-(dimethylaminomethyl)cyclopentanone-3-carboxylate, b. p. (bath temp.) 78–85°C (0.1 mmHg). Yield, 135 mg. The product had a weak smell of amine and was insoluble in water, soluble in dilute hydrochloric acid.

The reaction of II' with an excess of methyl iodide was exothermic and immediately afforded a crystalline methiodide (VIII) melting at 213°C (dec., sintered at 145°C) in a quantitative yield.

Anal. Found: N, 3.91 Calcd. for $C_{11}H_{20}O_3NI$: N, 4.11%.

However, the Hofmann degradation of VIII to obtain the methylene derivative was unsuccessful.

Hydrogenolysis of Methyl 5-(Dimethylaminomethyl)cyclopentanone-3-carboxylate (II).—A solution of 135 mg. of II' in 1.5 cc. of methanol was shaken with 15 mg. of platinum oxide and hydrogen; 25 cc. (26°C, 754.4 mmHg) of hydrogen was absorbed in twenty minutes. After filtration, the filtrate was concentrated under reduced pressure to give a crude product of methyl 5-methylcyclopentanone-3-carboxylate (IV), a fragrant, liquid. Yield, 95 mg..

The whole quantity of the crude product was hydrolyzed with 10% sodium hydroxide solution at room temperature and the after-treatment was carried out just as described above in the hydrolysis of V. A crude product of 5-methylcyclopentanone-3-carboxylic acid was obtained. Yield, 45 mg.. This was converted to the 2,4-dinitrophenylhydrazone, m. p. 139–142°C, which did not

depress the melting point of the authentic sample of 2,4-dinitrophenylhydrazone of VI.

Bioassays.—preliminary results have indicated that 5-methylenecyclopentanone-3-carboxylic acid (IV) possesses a potency of 12 units/mg. (in terms of sarkomycin potency) against *Staph. aureus* 209-P and about six times the potency against *Micrococcus flavus*. Methyl 5-methylenecyclopentanone-3-carboxylate (III) showed also a potency of 9.88 units/mg. (in 10% ethanol solution) against *S. aureus* 209-P and 11.2 units/mg. against *M. flavus*.

It is very interesting to find that IV possesses strong antitumor activities[6]. The minimum necessary concentration of IV for the anti-HeLa-cell effect was 5 mcg./cc.. Against cells of Ehrlich carcinoma, IV had a potency of 7.4 units/mg. (in terms of sarkomycin potency) by the cylinder plate method.[7] The daily intraperitoneal injection of 0.317 mg. of IV inhibited the ascites increase and prolonged the survival period of mice bearing ascites type of Ehrlich carcinoma by intraperitoneal route.

A detailed report on the biological activities of III and IV will be published elswhere.

6) Private communication from Prof. H. Umezawa of National Institute of Health, Tokyo.
7) S. Yamazaki, K. Nitta, T. Hikiji, M. Nogi, T. Takeuchi, T. Yamamoto and H. Umezawa, *J. Antibiotics*, **IX**, 135 (1956).

We are indebted to Prof. H. Umezawa, National Institute of Health, Tokyo, for antitumor assays.

Summary

1) 5-(Dimethylaminomethyl)cyclopentanone-3-carboxylic acid hydrochloride (I) has been synthesized from cyclopentanone-3-carboxylic acid by means of the Mannich reaction.

2) Methyl 5-(dimethylaminomethyl) cyclopentanone-3-carboxylate hydrochloride (II) has been degraded to give methyl 5-methylenecyclopentanone-3-carboxylate (III), which has been hydrolyzed into 5-methylenecyclopentanone-3-carboxylic acid (IV), an isomer of sarkomycin.

3) The structures of III and IV have been proven.

4) It has been found that III possesses significant antitumor and antibacterial activities and IV shows also antibacterial activities.

Department of Applied Chemistry
Engineering Faculty of
Keio University, Tokyo

*Effects of Mercerization on the Lateral Order Distribution of Cellulose**

By Yoshizo TSUDA and Sadataka MUKOYAMA

(Received November 24, 1956)

Introduction

In a previous paper[1] the authors have concluded that the fractional dissolution in sodium hydroxide solutions of various concentrations after methanolysis is the best method to obtain the lateral order distribution of cellulose. It is the purpose of the present paper to study the transition phenomena in the mercerization process using this method.

A number of investigators have studied the transition behavior in the mercerization process using the x-ray diffraction measurements[2], the moisture regain measurements[3,3] and the limit D. P. measurements[4].

In the mercerization process the phase transition of cellulose I into cellulose II accompanies a considerable decrystallization, which might have induced the discrepancy in the transition intervals observed with various measurements. So it is important to know the changes in the lateral order distribution in the mercerization process. In the present study this change was investigated with cotton linters pulp which shows a considerable change in the lateral order distribution.

1) Y. Tsuda and S. Mukoyama, This Bulletin, **29**, 748 (1956).
2) B.G. Rånby and H.F. Mark, *Svensk Papperstidning*, **10**, 374 (1955).
3) B. G. Rånby, *Acta Chem. Scand.*, **6**, 101 (1952).
4) L. Jörgensen and E. Ribi, *Nature*, **166**, 148 (1950).
* The main part of this paper was presented at the 9th Annual Meeting of the Chemical Society of Japan in April, 1956, Kyoto.

Experimental Procedure

a. Treatment with Sodium Hydroxide Solutions.—The pulp samples (1 g, powdered and bone-dried) were soaked at 20°C in 50 ml. of sodium hydroxide solutions for two hours. The pulps were recovered by suction on glass filter, washed with distilled water, N/2 acetic acid and distilled water again until they became acid-free. The samples were dried from alcohol.

b. Lateral Order Distribution.—The same method as described in the previous paper[1] was used.

c. Cellulosic Samples.—Cotton linters pulp and sulfite and sulfate wood pulps, the same samples as used in the previous study. BX yarn[5], a regenerated cellulose fibre of the highest lateral order among regenerated cellulose fibres[6].

Experimental Results and Discussion

Comparison of Lateral Order Distributions between Native and Mercerized Celluloses

In the previous paper it was shown that the lateral order distribution of cotton linters pulp is at higher order compared with wood pulps. But this difference is not observed between mercerized samples as shown in Fig. 1 and Fig. 2, at which the summative mass-order curves and lateral order distributions of both native and mercerized celluloses are shown. The distributions themselves become broad as a result of mercerization, and lower ordered portions of distributions increase. With regard to wood pulps the decrystallization accompanied by mercerization is characterized in the increase of lower ordered regions and the broadening of distributions, without appreciable changes in the lateral order of main ordered regions. However, mercerized cotton linters pulp has a similar distribution to that of wood pulp and thus the linters pulp loses its characteristic higher order after mercerization. These results mean that all of the mercerized celluloses exhibit the same lateral order distribution whatever their native origins may be. In order to compare them with regenerated cellulose fibres the lateral order distribution curve of BX yarn is also shown in Fig. 2. The lateral order of BX fibre, which is a regenerated cellulose fibre of the highest order is still lower than those of mercerized pulps, and the distribution of the former is broader than those of the latters. Therefore it will be concluded that the lateral order of regenerated cellulose is necessarily lower compared with that of native cellulose.

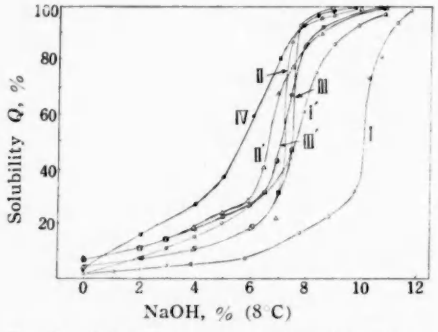

Fig. 1. Solubility curves of methanolyzed linters and sulfite and sulfate wood pulps both native and mercerized and methanolized BX yarn.
(I) native linters pulp
(I') mercerized linters pulp
(II) native sulfite wood pulp
(II') mercerized sulfite wood pulp
(III) native sulfate wood pulp
(III') mercerized sulfate wood pulp
(IV) BX yarn

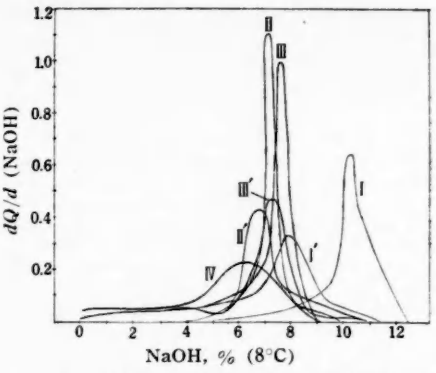

Fig. 2. Lateral order distribution curves of cotton linters and sulfite and sulfate wood pulps both native and mercerized and BX yarn.
(I) native linters pulp
(I') mercerized linters pulp
(II) native sulfite wood pulp
(II') mercerized sulfite wood pulp
(III) native sulfate wood pulp
(III') mercerized sulfate wood pulp
(IV) BX yarn

Variation of Lateral Order Distribution in the Process of Mercerization

As shown in Fig. 1 and Fig. 2, there is a remarkable variation of lateral order in the mercerization process with regard to

5) N. Drisch and L. Soep, *Text. Res. J.*, **23**, 513 (1953).
6) S. Mukoyama, *J. Soc. Textile Cellulose Ind.*(Japan). **12**, 772 (1955).

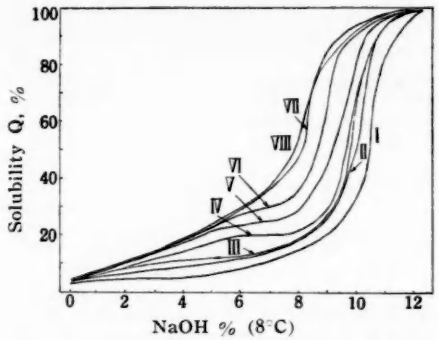

Fig. 3. Solubility curves of methanolized linters pulp pretreated with NaOH of following concentrations;
(I) original (II) 10% (III) 11% (IV) 12% (V) 13% (VI) 14% (VII) 15% (VIII) 17.5%

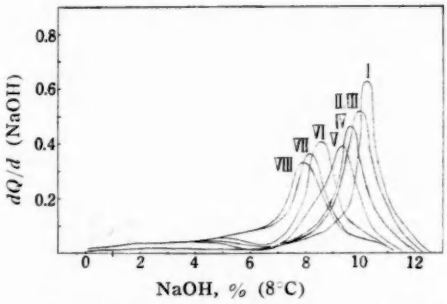

Fig. 4. Lateral order distribution curves of cotton linters pulp pretreated with NaOH of following concentrations.
(I) original (II) 10% (III) 11% (IV) 12% (V) 13% (VI) 14% (VII) 15% (VIII) 17.5%

cotton linters pulp but no appreciable variations with regard to wood pulps. Consequently as the sample for this study, cotton linters pulp was chosen. In Fig. 3 and Fig. 4 lateral order distributions of samples pretreated with sodium hydroxide solutions of various concentrations are shown. At 20°C no appreciable variation in distribution is observed up to the treatment with 10% NaOH solution. Up to the treatment with 13% NaOH solution no appreciable variations are observed in the lateral order of peak of distribution, but a successive broadening of the distribution toward the lower ordered portion can be observed with each treatment. It will be apparent in Fig. 3 and Fig. 4 that the main variation of lateral order distribution in the process of mercerization is induced by the treatment with NaOH solutions of the concentration of 13–15% at 20°C. This concentration interval of sodium hydroxide coincides with the interval which is necessary to induce phase transition. Thus the main variation of lateral order distribution is accompanied by the treatment with NaOH solutions of the concentration necessary to induce phase transition.

Here it will be possible to consider that the so-called decrystallization does not correspond to the lowering of the lateral order of the main highly ordered region but to the increase in the less highly ordered region. If these views are accepted, it will be concluded that the decrystallization is induced by the treatment with NaOH of lower concentration than that required to induce phase transition. This conclusion is consistent with the results obtained in the x-ray diffraction study as discussed in the previous paper[1].

Summary

Lateral order distributions of native and mercerized celluloses were compared and then the variation of distribution in the process of mercerization was investigated. It was concluded that mercerization generally induces broadening of distribution, and cotton linters pulp shows almost the same lateral order distribution after mercerization as those of wood pulps. The authors are grateful to Dr. K. Hoshino for permitting this publication.

Research Department of
Toyo Rayon Co., Ltd.
Otsu, Shiga-ken

Mikroanalyse mit Hilfe von Ionenaustauscherharzen. XII. Über den Nachweis in Tausendstelgammamenge vorhandenen Nickels mit Rubeanwasserstoffsäure[1]

Von Masatoshi FUJIMOTO

(Eingegangen am 2. November, 1956)

Einleitung

Zur qualitativen Mikroanalyse von den Ultramikroproben wie kosmischen Stauben, ist es wünschenswert, die möglichst empfindlichen Nachweismethoden anzuwenden, mit denen man selbst Tausendstelgammastoffmengen leicht prüfen kann.

In einer Reihe nachfolgender Mitteilungen unternimmt der Verfasser, mit den wohlbekannten, empfindlichen Reaktionen noch weit empfindlichere Nachweismethoden festzustellen.

In vorliegender Arbeit wurde in erster Linie eine ausserordentlich empfindliche Nachweismethode für Spurmenge des Nickels mit der Rubeanwasserstoffsäure (Dithioxamid)[2], durch Anwendung der farblosen und starksauren Kationenaustauscherharze festgestellt. Diese Methode beruht auf der Niederschlagbildung an der Grenzflächen zwischen Harz- und Lösungsphase, wie der Verfasser schon darüber genau mitgeteilt hat[3,4]. Die in der Probelösung vorhandenen Nickelionen lassen sich vorher als komplexe Hexaminkationen in die Kationenaustauscherharzphase sehr stark adsorbieren[5], und durch Zusatz der Rubeanwasserstoffsäurelösung entsteht ein dichter intensiv blauvioletter Niederschlag von Nickelkomplexe des Reagens gerade an der Grenzfläche zweier Phasen*[1], wobei sich infolgedessen die Reaktionsempfindlichkeit bemerkenswert erhöht.

Man kann auch die Begleitionen wie Kupfer(II) oder Kobalt(II), die auch gleichfalls mit dem genannten Reagens die stark sich färbenden stabilen Chelatverbindungen bilden und infolgedessen den gegenwärtigen Nachweis stark stören, durch Anwendung der Mikrosäule[6] starkbasischen Anionenaustauscherharzes aus einer stark salzsauren Lösung als Chlorkomplexanionen[7] vollkommen beseitigen.

Die in der gegenwärtigen Untersuchung benutzten Kationenaustauscherharze

Vier Arten farbloser und starksaurer Kationenaustauscherharze von verschiedenen Vernetzungsgraden, „1proz. DVB", „2.5proz. DVB", Dowex 50W-X8 und „20proz. DVB", und ein weisses und schwachsaures Harz, Amberlite IRC-50, wurden in der HR-Form angewandt[8].

Versuchsanordnung

Man versetzt auf einer weissen Tüpfelplatte einige Körnchen des farblosen Kationenaustauscherharzes mit je einem Tropfen der Probelösung und des Ammoniakwassers, und lässt sie eine Weile stehen. Dann fügt man dazu einen Tropfen verdünnter alkoholischer Lösung der Rubeanwasserstoffsäure und lässt sie nochmals einige Minuten stehen. Selbst bei Anwesenheit von Spurmenge des Nickels entsteht eine deutliche Violett- bzw. Violettblaufärbung, wenn die Probelösung keine Kupfer- und Kobaltsalze enthält*[2].

Massflüssigkeit und Reagenzien

1. Massflüssigkeit.—Aus derselben Stammlösung wie der in vorhergehender Mitteilung[1] wurde eine Reihe der Massflüssigkeit des Nickels durch Verdünnung mit 0.01 N Salzsäure hergestellt. Alle folgenden Untersuchungen über die besten Experimentalbedingungen wurden mit einer 0.01 N-salzsauren Lösung ausgeführt, deren 1 ccm genau 2.60 γ von Nickel enthielt.

2. Reagenzien.— (1) Alkoholische Stammlösung der Rubeanwasserstoffsäure: Man zerreibt

1) Die elfte Mitteilung: M. Fujimoto, Dieses Bulletin, **30**, 93 (1954).

2) Vgl. F. Feigl, „Spot Tests. I. Inorganic Applications," übersetzt von R. E. Oesper, 4. engl. Aufl., Amsterdam (1954), S. 145.

3) M. Fujimoto, Dieses Bulletin, **29**, 616 (1956).

4) M. Fujimoto, Dieses Bulletin, **30**, 87 (1957).

5) M. Honda, *Japan Analyst.* **3**, 132 (1954).

*1 Das Reagens wird von starkbasischen Anionenaustauscherharzen stark adsorbiert, aber diese waren hier nicht gut anzuwenden, denn nicht nur die stark gelbe Färbung der das Reagens adsorbierenden Harzkörnchen macht die Unterscheidbarkeit der Reaktion sehr schwierig, sondern auch der Niederschlag entsteht, statt an der Grenzfläche, anscheinend nur in der ganzen Lösungsphase.

6) M. Fujimoto, Dieses Bulletin, **29**, 595 (1956).

7) K. A. Kraus und G. E Moore, *J. Am. Chem. Soc.*, **75**, 1460 (1953).

8) M. Fujimoto, Dieses Bulletin, **29**, 600 (1956).

*2 Über die Trennung dieser störenden Kationen, vergleiche S. 277 ff.

gründlich 0.1 g von Kriställchen der extrareinen Rubeanwasserstoffsäure („Wako" zur Analyse) mit einem Glasstab, und erwärmt sie dann mit 20ccm von 99prozentigem Äthylalkohol unter jeweiligem, lebhaftem Umrühren bei etwa 50°C. Das Reagens löst sich allmählich und geht in eine orangerote, kolloidale Lösung über. Nach der Abkühlung fügt man zu dieser Lösung einige Menge des Alkohols bis zu genau 20 ccm. Die so erhaltene Reagenslösung hält gut, wenn man sie in einem wohl verstöpselten Gefäss im Dunkeln aufbewahrt.

(2) Ammoniakwasser: Käufliches extrareines 15 N Ammoniakwasser wurde vorbereitet.

Bestimmung der Bedingungen höchster Empfindlichkeit*3

1. Einfluss der Konzentration des angewandten Ammoniakwassers. — Zum gegenwärtigen Zwecke wurden Dowex 50W-X8 und 0.5prozentige Reagenslösung benutzt. Wie in Abb. 1 klar zu ersehen ist, sinkt die Intensität der Färbung an

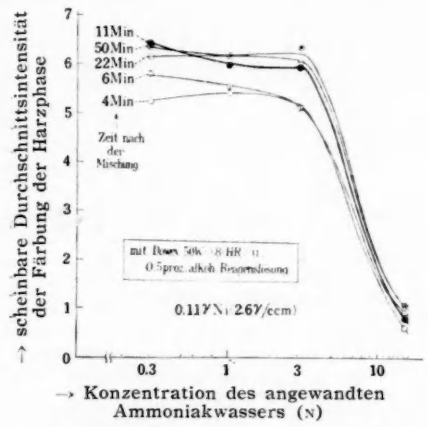

Abb. 1. Einfluss der Ammoniakwasserkonzentration.

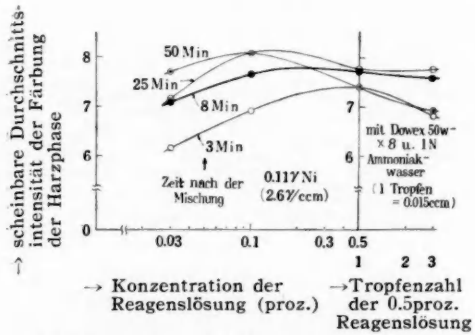
50 Min
25 Min
8 Min
3 Min
Zeit nach der Mischung
0.11γ Ni (2.6γ/ccm)
mit Dowex 50w-X8 u. 1N Ammoniakwasser (1 Tropfen = 0.015ccm)
→ scheinbare Durchschnittsintensität der Färbung der Harzphase
→ Konzentration der Reagenslösung (proz.)
→ Tropfenzahl der 0.5proz. Reagenslösung

Abb. 2. Einfluss der Reagenskonzentration.

*3 In bezug auf die halbquantitative Darstellungsweise von der scheinbaren Durchschnittsintensität der Färbung, vergleiche M. Fujimoto, Dieses Bulletin, **27**, 347 (1954); **29**, 567 (1956).

den Harzkörnchen erst nur dann stark ab, wenn die Konzentration des angewandten Ammoniakwassers höher als 3 N steigt. Im folgenden wurde daher 1 N Ammoniakwasser lediglich angewandt.

2. Einfluss der Konzentration der Reagenslösung.—Abb. 2 stellt den Einfluss der Reagenskonzentration auf die Färbungsintensität der Harzkörnchen, wobei Dowex 50W-X8 und 1 N Ammoniakwasser benutzt wurden. Mit 0.03prozentiger Lösung des Reagens ist die Färbung der Harzkörnchen etwas ungenügend und mit einer stärkeren als 0.5prozentigen Lösung sinkt sie allmählich mit der Zeit ab. Diese Entfärbungswirkung scheint mit dem steigenden Überschusse des Reagens zuzunehmen. So wählt man 0.1prozentige Reagenslösung als die am besten geeignete aus.

3. Einfluss der Harzart.—Die Resultate dafür werden in Abb. 3 zusammengestellt:

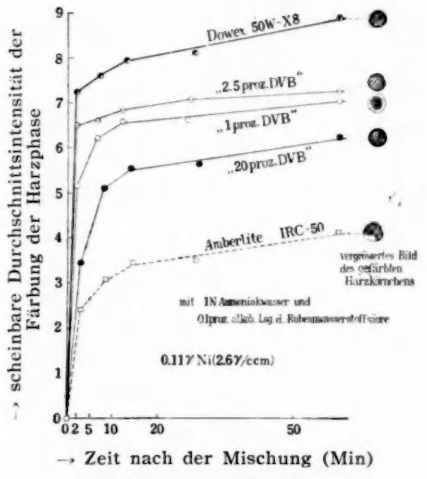
Dowex 50W-X8
„2.5proz. DVB"
„1proz. DVB"
„20proz. DVB"
Amberlite IRC-50
vergrößertes Bild des gefärbten Harzkörnchens
mit 1N Ammoniakwasser und 0.1proz. alkoh. Lsg. d. Rubeanwasserstoffsäure
0.11γ Ni (2.6γ/ccm)
→ scheinbare Durchschnittsintensität der Färbung der Harzphase
→ Zeit nach der Mischung (Min)

Abb. 3. Einfluss der Harzart.

Wie die genannte Abbildung uns zeigt, übt der Vernetzungsgrad des Harzes auf die Intensität sowie auf den Zustand der Färbung der Harzkörnchen einen beträchtlichen Einfluss aus. Diese Tatsache lässt sich dadurch erklären, dass die Affinität der Nickel(II)-amminkomplexkationen auf das Kationenaustauscherharz mit steigendem Vernetzungsgrade bedeutend zunimmt, und dass eine Art der Adsorption des Reagens ein wenig innerhalb der Harzkörnchen stattfindet, deren Ursachen bis jetzt nicht erklärlich ist. Man benutzt Dowex 50W-X8 (8prozentig vernetztes Harz) als die beste Harzprobe.

Es ist auch interessant, dass die Färbung der Harzphase sich hierbei schon 2 Min nach dem Zusatze des Reagens auf beinahe konstante Intensität erstreckt. Diese Tatsache bedeutet, dass das vorher in die Harzphase adsorbierte Nickel an der Grenzfläche zweier Phasen mit dem Reagens reagiert und, infolge der Entstehung der dicken Niederschlagschicht, keine Nickelionen sich weiter in die Harzphase adsorbieren lassen.

4. Einfluss der Salzkonzentration der Probelösung. — Wegen der beträchtlich starken Affinität der komplexen Nickel(II)-amminkationen auf die Kationenaustauscherharze[5] wird die Färbungsintensität der Harzphase von der Salzkonzentration der Versuchslösung nur geringfügig beeinflusst (vgl. Abb. 4). Es ist aber wünschenswert, wenn möglich, mit der Probelösung, deren Salzkonzentration niedriger als 1 N reguliert wird, den Nachweis auszuführen.

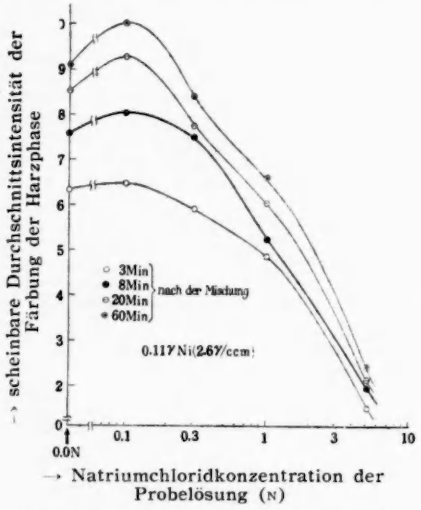

Abb. 4. Einfluss der Salzkonzentration.

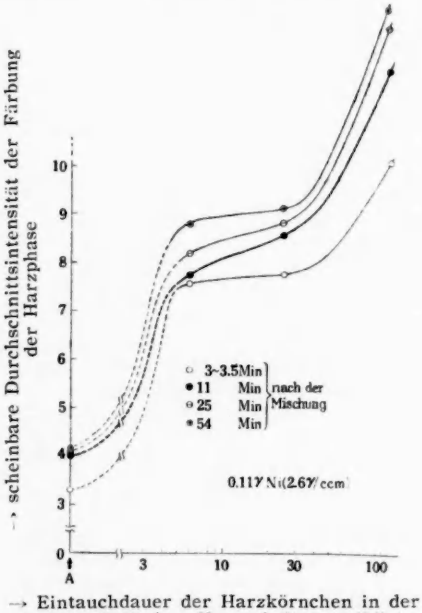

Abb. 5. Einfluss der Eintauchdauer der Harzkörnchen in der ammoniakalischen Versuchslösung auf die Färbungsintensität der Harzphase.

5. Einfluss der Eintauchdauer der Harzkörnchen in der ammoniakalischen Probelösung. — Versuchsweise wurde der genannte Einfluss untersucht. Wie der Verlauf der Kurven von Abb. 5 zeigt, verstärkt sich die Färbung der Harzkörnchen allmählich mit der Eintauchdauer in der ammoniakalischen Probelösung. Soweit es die Umstände erlauben, empfiehlt es sich, die Harzkörnchen möglichst lang in der ammoniakalischen Probelösung einzutauchen, aber, vom praktischen Standpunkt aus, sei das 5 Min lange Eintauchen der Harzkörnchen in die Versuchslösung genügend.

6. Bedingungen höchster Empfindlichkeit. — Das folgende beste Verfahren wurde aus der obigen Untersuchungen genau festgestellt:

„Man versetzt auf einer weissen Tüpfelplatte einige Körnchen des farblosen, starksauren und mittelmässig vernetzten Kationenaustauscherharzes wie Dowex 50W-X8 mit je einem Tropfen der Probelösung und 1 N Ammoniakwassers, und lässt sie etwa 5 Min stehen. Wenn die Salzkonzentration der Probelösung sehr hoch ist, so empfiehlt es sich, diese durch Zusatz von destilliertem Wasser bis zu niedriger als 1 N zu verdünnen. Dann fügt man einen Tropfen 0.1prozentiger alkoholischer Lösung der Rubeanwasserstoffsäure dazu, und nach 2 oder 3 Min beobachtet man eine auf der Harzkörnchen entstandene Violett- bzw. Violettblaufärbung mit einer Lupe."

Bestimmung der Erfassungsgrenze

Wie aus dem Verlaufe der Kurven von Abb. 6 klar zu ersehen ist, ist die hier festgestellte neue Nachweismethode ausserordentlich empfindlich; d. h. deren Erfassungsgrenze ist so klein wie 0.0021 γ Nickel unter Grenzkonzentration $1 : 1.9 \times 10^7$. Diese Menge entspricht 0.02prozentigem Nickelgehalt in 10 γ Probe.

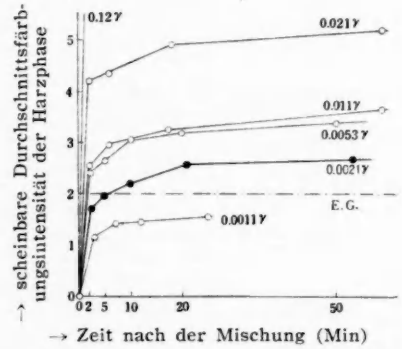

Abb. 6. Bestimmung der Erfassungsgrenze.

Einflüsse der Begleitionen

Die Ergebnisse dafür wurden in Tabelle I gesamt dargestellt:

TABELLE I

EINFLÜSSE DER BEGLEITSTOFFE

Begleitstoffe	benutzter Verbindungstypus	Farbton der Harzphase*	Menge der Begleitstoffe	nachweisbare Nickelmenge	Grenzverhältnis	Bemerkungen**
Ti(IV)	$TiOSO_4$	bräunlich gelb	100 γ	0.0042 γ	$1:2.4\times10^4$	—
V(V)	NH_4VO_3	gräulich hellgrün	59 γ	0.0074 γ	$1:8\times10^3$	—
Cr(III)	$KCr(SO_4)_2$	grasgrün	2 γ	0.011 γ	$1:1.9\times10^2$	Cr(III)≦0.005proz.
Mn(II)	$MnSO_4$	beinahe farblos	320 γ	0.0042 γ	$1:7.6\times10^4$	—
Fe(III)	$FeCl_3$	farblos	20 γ	0.011 γ	$1:1.9\times10^3$	*a*, *b*, Fe(III) ≦0.05proz.
〃	〃	farblos	2000 γ	0.0042 γ	$1:4.7\times10^5$	*c*
Co(II)	$Co(NO_3)_2$	gelbbraun	0.05 γ	0.018 γ	1:2.8	Co(II)≦0.0002proz.
〃	〃	farblos	424 γ	0.0044 γ	$1:9.6\times10^4$	*c*
Cu(II)	$CuSO_4$	schmutzig dunkelgrün	0.1 γ	0.011 γ	1:9	Cu(II)≦0.0005proz.
〃	〃	farblos	1600 γ	0.0042 γ	$1:3.8\times10^5$	*c*
Zn(II)	$ZnSO_4$	hellgrau	96 γ	0.0042 γ	$1:2.3\times10^4$	Zn≦0.3proz.
Cd(II)	$CdSO_4$	farblos	160 γ	0.0042 γ	$1:3.7\times10^4$	Cd≦0.5proz.
Hg(II)	$Hg(NO_3)_2$	farblos	27 γ	0.007 γ	$1:3.9\times10^3$	Hg≦0.1proz.
Cr(VI)	$K_2Cr_2O_7$	hellgelb	360 γ	0.0021 γ	$1:1.7\times10^5$	—
Mo(VI)	$(NH_4)_2MoO_4$	hellgrau	390 γ	0.0042 γ	$1:9.2\times10^4$	—
W(VI)	Na_2WO_4	farblos	76 γ	0.0021 γ	$1:3.6\times10^4$	W≦0.2proz.
U(VI)	$(UO_2)(CH_3CO_2)_2$	lebhaft zitronengelb	320 γ	0.0042 γ	$1:7.6\times10^4$	*a*
Pb(II)	$Pb(NO_3)_2$	hellbraun	25 γ	0.011 γ	$1:2.4\times10^3$	Pb≦0.06proz.
Bi(III)	$Bi(NO_3)_3$	hellbraun	360 γ	0.0021 γ	$1:1.7\times10^5$	*a*
Sb(III)	$SbCl_3$	farblos	32 γ	0.0048 γ	$1:6.7\times10^3$	—
Sn(IV)	$SnCl_4$	farblos	72 γ	0.0021 γ	$1:3.4\times10^4$	Sn≦0.2proz.
Al(III)	$Al(NO_3)_3$	farblos	270 γ	0.011 γ	$1:2.5\times10^4$	—
F^-	KF	farblos	2800 γ	0.0021 γ	$1:1.4\times10^6$	—
PO_4^{3-}	Na_2HPO_4	farblos	640 γ	0.007 γ	$1:9\times10^4$	—
$C_2O_4^{2-}$	Oxalsaures Ammonium	farblos	450 γ	0.0021 γ	$1:2.2\times10^5$	—
$C_4H_4O_6^{2-}$	Seignettesalz	farblos	840 γ	0.0042 γ	$1:2.0\times10^5$	—
$C_6H_5O_7^{3-}$	Zitronensaures Ammonium	hellgrau?	1100 γ	0.007 γ	$1:1.6\times10^5$	—

* Farbton hervorgerufen nur durch die Begleitstoffe.

** *a*: Ein Blindversuch wurde hier nebeneinander durchgeführt.
b: Die Harzkörnchen wurden von orangebraunem Niederschlag bedeckt.
c: Nach dem Zusatze konzentrierter Salzsäure wurde die Probelösung in eine Mikrosäule starbasischen Anionenaustauscherharzes durchgelassen, um diese Begleitstoffe völlig zu beseitigen.

Chrom(III)-, Eisen(III)-, Kobalt(II)-, Kupfer(II)-, Blei(II)- und Antimon(III)-salze stören den Nachweis beträchtlich. Die Störung des Chroms(III) kann man durch Oxydation zur Chromate oder Bichromate[9] leicht beseitigen. Der höchst schädliche Einfluss der Eisen(III)-, Kobalt(II)- und Kupfer(II)-salze wurde in solcher Weise wie es im nachfolgenden Abschnitt genau beschrieben wird, leicht beseitigt.

Trennung der Eisen(III)-, Kobalt(II)- und Kupfer(II)-salze als Chlorkomplexanionen durch Anwendung der Mikrosäule des starkbasischen Anionenaustauscherharzes

Da hier nur die Nickelsalze sich gar nicht aus der stark salzsauren Lösung von starkbasischen Anionenaustauscherharzen adsorbieren lassen, kann man die höchst schädliche Störung der Übergangselemente wie Eisen(III), Kobalt(II), oder Kupfer(II) durch chromatographische Anwendung der Mikrosäule des starkbasischen und fein pulverisierten Anionenaustauscherharzes wie folgt völlig beseitigen.

Man stellt mit geringer Menge des starkbasischen Anionenaustauscherharzes, Dowex 1-X10 (RC1-Form, 100 bis 200 Maschen), eine kleine Harzsäule (0.3 cm Durchmesser und etwa 3 cm Länge)[*4] auf[6], und man reguliert vorher die Bedingungen des Harzes, indem man durch die Säule etwa zehn Tropfen 12 N Salzsäure (zur Analyse; u. dgl.) durchlaufen lässt. Man bringt

9) In bezug auf das mikrochemische Oxydationsverfahren für Chrom(III)-salze, vergleiche M. Fujimoto, Dieses Bulletin, **27**, 347 (1954).

[*4] Sie entspricht der Austauschkapazität von etwa 0.4 Milliäquivalente der Anionen.

danach einige Tropfen der Probelösung auf das Ende eines Blattes Objektglases und unter Umschütteln erhitzt sie allmählich über einem Mikrobrenner[10] bis zum beinahen Trocknen. Dann extrahiert man diesen Rückstand mit zwei oder drei Tropfen 12 N Salzsäure, und mit einer kleinen Kapillarpipette (1 Tropfen = 0.02ccm) fügt man diese stark salzsaure Lösung auf die obengenannte Mikroharzsäule stückweise hinzu (etwa 0.01 ccm/Min). Man sammelt das hier erhaltene Eluat in einer Vertiefung der Tüpfelplatte an. Die in der Probelösung vorhandenen Eisen(III)-, Kobalt(II)- und Kupfer(II)-salze werden nach der genannten Reihenfolge, von dem oberen Ende der Harzsäule nach unten, als chromgelbe, grünblaue und orangegelbe Bänder adsorbiert. Schliesslich drängt man mit etwa 0.2 ccm 12 N Salzsäure nur das Nickel(II) aus der Säule heraus, dann erwärmt man eine Weile die obige Tüpfelplatte auf einem Wasserbade, um die überschüssige Salzsäure verdampfen zu lassen, und versetzt den hier erhaltenen Rückstand mit zwei Tropfen heissen destillierten Wassers. Nach der Abkühlung kann man den Nachweis des Nickels mit dieser wässerigen Lösung ohne Störung durchführen. Die gebrauchte Harzsäule wird zuerst mit 1 ccm 0.5 N Salzsäure in die RCl-Form zurückgeführt und dann mit Wasser völlig gewaschen. Man kann auch die Zinn(IV)-, Antimon(III)-, Zink- und Quecksilber(II)-salze usw. in obenerwähnter Weise völlig beseitigen.

Zusammenfassung

1. Die farblosen, starksauren und mittelmässig vernetzten Kationenaustauscherharze werden zur wohlbekannten Niederschlagbildungsreaktion zwischen den Nickelsalzen und der Rubeanwasserstoffsäure angewandt, und eine ausserordentlich empfindliche Nachweismethode wird neu und gründlich durch Beschränkung der Fällungsstelle an der Grenzfläche zwischen Harz und Lösungsphase festgestellt.

2. Die besten Experimentalbedingungen für obengenannte Nachweismethode werden genau bestimmt durch ausführliche Untersuchung über die verschiedenen Faktoren, wie die Konzentration des Ammoniakwassers und des Reagens, Sorte und Vernetzungsgrad der Harze, Salzkonzentration an der Probelösung, Eintauchdauer der Harzkörnchen in der ammoniakalischen Probelösung, u. s. w..

3. Die Einflüsse verschiedenartiger fremder Ionen werden ausführlich untersucht und die schädliche Störung der Eisen(III)-, Kobalt(II)- und Kupfer(II)-salze wird durch chromatographische Anwendung der Mikrosäule starkbasischen Anionenaustauscherharzes raffiniert beseitigt.

Zum Schluss möchte der Verfasser Herrn Prof. Dr. E. Minami für seine zahlreichen wertvollen Ratschläge über die vorliegende Untersuchung seinen herzlichsten Dank aussprechen.

Für die Harzproben, „1proz. DVB", „2.5-proz. DVB" und „20proz. DVB" ist der Verfasser Herrn Prof. Dr. A. Kawamura an der Landwirtschaftlichen und Technischen Universität zu Tokyo zu grossem Dank verpflichtet.

Laboratorium der analytischen Chemie,
Chemisches Institut der
wissenschaftlichen Fakultät,
Universität zu Tokyo, Hongo, Tokyo

10) A. A. Benedetti-Pichler, „Introduction to the Microtechnique of Inorganic Analysis," 1. Aufl., New York (1942), S. 8.

Mikroanalyse mit Hilfe von Ionenaustauscherharzen. XIII. Über den Nachweis in Tausendstelgammamenge vorhandenen Kobalts mit Nitroso-R-salze[1]

Von Masatoshi FUJIMOTO

(Eingegangen am 5. November, 1956)

Einleitung

Bei der vorliegenden Arbeit, stellte der Verfasser über die für Kobalt ausserordentlich empfindlichen Nachweismethoden Untersuchungen an.

Es wurde das Nitroso-R-salz (1-Nitroso-2-Oxynaphthalin-3, 6-Disulfonsaures Natrium)[2] als ein Vertreter der auf Kobalt

1) Die zwölfte Mitteilung: M. Fujimoto, Dieses Bulletin, **30**, 274 (1957).

2) Vgl., z. B., I. Mellan, „Organic Reagents in Inorganic Analysis," Philadelphia, (1941), S. 332, sowie. E. B. Sandell, „Colorimetric Determination of Traces of Metals," 2. Aufl., (1950) New York, S. 274.

sehr empfindlich einwirkenden Reagenzien angewandt. Die stark sich färbenden Chelatanionen, die das Nitroso-R-salz, unter geeignetem pH-Werte der Versuchslösung, mit den Kobalt(II)-salzen bildet, werden von den farblosen und starkbasischen Anionenaustauscherharzen so stark adsorbiert, dass die Intensität der in der Harzphase entstandene intensive Rotfärbung gar nicht von der Salzkonzentration der Probelösung beeinflusst wird. Die Färbung der Harzphase ist infolgedessen entschieden stärker als die der Lösungsphase und die Reaktionsempfindlichkeit wird auffallend erhöht.

Die Reagensanionen werden dabei von den genannten Harzen gleichfalls stark adsorbiert und färben diese Phase lebhaft grünlich gelb. Wegen dieses intensiven grüngelben Hintergrundes vom Reagens wird der Nachweis besonders dann beträchtlich unsicher, wenn es sich um eine sehr geringe Menge des Kobalts handelt. Dieser Nachteil wurde jedoch dadurch leicht überwunden, dass man die Harzkörnchen, nach der Bildung betreffender Chelatanionen in der Harzphase, mit verdünnter Salpetersäure eine Weile kocht und dadurch nur das überschüssige Reagens vollständig zersetzt. Dieses Verfahren ist nicht nur zur Erhöhung der Reaktionsempfindlichkeit sehr geeignet, sondern auch zur Beseitigung der Störung von verschiedenartigen fremden Kationen wie Nickel(II), Kupfer(II) usw., die gleichfalls mit dem genannten Reagens die stark sich färbenden Chelatanionen bilden.

Massflüssigkeit und Reagenzien

1. Massflüssigkeit.— Man stellte eine Stammlösung des Kobalts dar, indem man das nickel- und eisenfreie Kobalt(II)-nitrat in 0.01 N Salpetersäure eintrug. 1 ccm dieser Stammlösung enthielt genau 5.74 mg von Kobalt*1. Eine Reihe der Massflüssigkeiten des Kobalts wurde aus dieser Stammlösung durch Verdünnung mit 0.01N Salpetersäure hergestellt. Alle folgende Untersuchungen über das beste Verfahren wurden mit einer 0.01N-salpetersauren Lösung ausgeführt, deren 1 ccm genau 5.74 γ von Kobalt enthielt.

2. Anionenaustauscherharze.—Um den Einfluss der Vernetzungsgrade der Harze auf die Färbungsintensität der Harzphase miteinander zu vergleichen, wurden hier die käuflichen, farblosen und starkbasischen Harze, Dowex 1-X1, -X2, -X4 und -X8, in der RCl-Form angewandt. Überdies wurde ein beinahe farbloses und mittelstarkbasisches Harz, Amberlite XE-114 (RCl-Form), ebenfalls angewandt.

3. Reagenzien. — (1) 2prozentige wässerige Stammlösung des Nitroso-R-salzes : Man löst 0.4 g des käuflichen extrareinen Nitroso-R-salzes (zur Analyse) in eine kleine Menge destillierten Wassers auf und verdünnt diese mit destilliertem Wasser genau zu 20 ccm.

(2) 4 N wässerige Lösung des Natriumacetats als Pufferlösung: Aus dem extrareinen Reagens (zur Analyse) stellt man diese Stammlösung her. Deren pH-Wert war genau 8.20.

(3) 2 N Salpetersäure.—Aus der käuflichen, extrareinen Salpetersäure bereitet man diese Lösung vor.

Bestimmung der Experimentalbedingungen höchster Empfindlichkeit*2

1. Einfluss der Ordnung der Versetzung von Reagenzien und Probelösung. — Auf dem in Tabelle I beschriebenen Wege, wurde der Einfluss der Versetzungsordnung der Reagenzien usw. auf die Färbungsintensität der Harzphase untersucht, wobei Dowex 1-X1 (RCl-Form), 0.05prozentige Lösung des Nitroso-R-salzes und 4 N Lösung des Natriumacetats als Pufferlösung angewandt wurden.

Wie Abb. 1 uns zeigt, üben die hier ausgewählten Faktoren auf die Färbungsintensität keinen

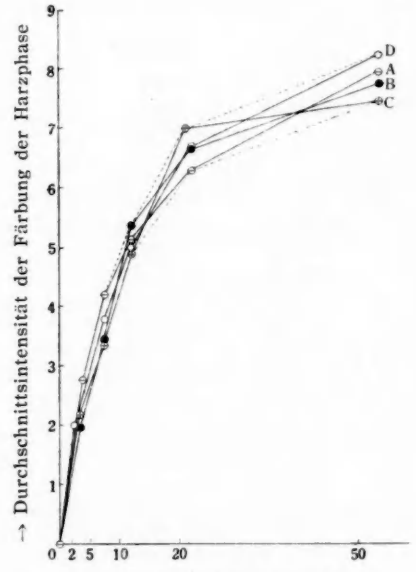

Abb. 1. Gegenüberstellung der veschiedenen Ordnung der Versetzung von Probe- und Reagenslösungen (Vgl. Tablle I).

*1 Die Menge des in der obengenannten Stammlösung vorhandenen Kobalts wurde durch komplexometrische Titration mit 0.01 M Massflüssigkeit von Äthylendiamintetraessigsaurem Dinatrium und Murexid als Metallindikatorgenau bestimmt.

*2 In bezug auf die schematische, halbquantitative Darstellungsweise von der scheinbaren Durchschnittsintensität der Färbung der Harzphase, vergleiche M. Fujimoto, Dieses Bulletin, **27**, 347 (1954); **29**, 567(1956).

TABELLE I

VERSCHIEDENE BEDINGUNGEN VON ABB. 1

Verfahren	Zeichen der Kurve	Inhaltsangabe des Verfahrens
A	⊖	RCl*+Probelsg.**—(5 Min)→+0.05proz. Lsg. des Nitroso-R-salzes+4N Lsg. des CH_3COONa
B	●	RCl+0.05proz. Lsg. des Nitroso-R-salzes—(5 Min)→+4N Lsg. des CH_3COONa+Probelsg.
C	⊕	RCl+4N Lsg. des CH_3COONa—(5 Min)→+0.05proz. Lsg. des Nitroso-R-salzes+Probelsg.
D	○	Probelsg.+0.05proz. Lsg. des Nitroso-R-salzes—(5 Min)→+4N Lsg. des CH_3COONa+RCl

* RCl bedeutet hier Dowex 1-X1 von RCl-Form.

** 1 Tropfen der obengenannten Probelösung enthält 0.21 γ Kobalt (5.74 γ/ccm).

TABELLE II

EINFLÜSSE DER BEGLEITSTOFFE

Begleitstoffe	benutzter Verbindungstypus	Farbton der Harzphase*	Menge der Begleitstoffe	nachweisbare Kobaltmenge	Grenzverhältnis	Bemerkungen**
Ti(IV)	$TiOSO_4$	sehr hell gelb	100 γ	0.0046 γ	$1:2.2\times10^4$	*a*
V(V)	NH_4VO_3	sehr hell gelb	70 γ	0.0029 γ	$1:2.4\times10^4$	—
Cr(III)	$KCr(SO_4)_2$	farblos	350 γ	0.0029 γ	$1:1.2\times10^5$	*b*
Mn(II)	$MnSO_4$	gelb	2600 γ	0.0029 γ	$1:9\times10^5$	—
Fe(III)	$FeCl_3$	farblos	35 γ	0.0029 γ	$1:1.2\times10^4$	Fe(III)≦0.1proz.
Fe(II)	Mohrsches Salz	farblos	350 γ	0.0029 γ	$1:1.2\times10^5$	*b*
Ni(II)	$NiCl_2$	hellorangegelb	300 γ	0.0057 γ	$1:5.3\times10^4$	*b*, *c*, *d*
Cu(II)	$CuSO_4$	hellorangegelb	320 γ	0.0046 γ	$1:7.0\times10^4$	*b*, *c*, *d*
Zn(II)	$ZnSO_4$	hellbraungelb?	270 γ	0.0076 γ	$1:3.5\times10^4$	—
Cd(II)	$CdSO_4$	hellgelb	1600 γ	0.0046 γ	$1:3.5\times10^5$	—
Hg(II)	$Hg(NO_3)_2$	farblos	350 γ	0.0029 γ	$1:1.2\times10^5$	—
Cr(VI)	$K_2Cr_2O_7$	gelb	3.2 γ	0.0046 γ	$1:7\times10^2$	Cr(VI)≦0.01proz.
〃	〃	hellgelb	320 γ	0.0046 γ	$1:7\times10^4$	*e*
Mo(VI)	$(NH_4)_2MoO_4$	hellorange	67 γ	0.0057 γ	$1:1.2\times10^4$	*d*, Mo≦0.2proz.
W(VI)	Na_2WO_4	weiss***	330 γ	0.0046 γ	$1:7.2\times10^4$	—
U(VI)	$UO_2(CH_3COO)_2$	farblos	350 γ	0.0029 γ	$1:1.2\times10^5$	—
Pb(II)	$Pb(NO_3)_2$	hellorangegelb	320 γ	0.0046 γ	$1:7\times10^4$	*d*
Sn(IV)	$SnCl_4$	farblos	295 γ	0.0029 γ	$1:1\times10^5$	*f*
Ge(IV)	GeO_2	hellgelb	25 γ	0.0029 γ	$1:8.8\times10^3$	*d*
Sb(III)	$SbCl_3$	hellorange	320 γ	0.0048 γ	$1:7\times10^4$	*a*, *b*
Bi(III)	$Bi(NO_3)_3$	gelb	200 γ	0.011 γ	$1:1.8\times10^4$	Bi≦1proz.
Al(III)	$Al(NO_3)_3$	farblos	350 γ	0.0029 γ	$1:1.2\times10^5$	Al≦1proz.
HPO_4^{2-}	Na_2HPO_4	hellgelb	1700 γ	0.0029 γ	$1:6\times10^5$	—
$C_2O_4^{2-}$	Oxalsaures Ammonium	sehr hell gelb	720 γ	0.0046 γ	$1:1.6\times10^5$	—
$C_4H_4O_6^{2-}$	Seignettesalz	farblos	920 γ	0.0029 γ	$1:3.2\times10^5$	—
$C_6H_5O_7^{3-}$	Zitronensaures Ammonium	farblos	1400 γ	0.0029 γ	$1:4.8\times10^5$	—

* Farbton der Harzphase hervorgerufen nur durch die Begleitstoffe.

** *a*: 2 bzw. 3 Tropfen der 4N Lösung des Natriumacetats wurden angewandt.
b: 2 bzw. 3 Tropfen der 2N Salpetersäure wurden hinzugefügt.
c: 0.5proz. Reagenslösung wurde angewandt.
d: Erst dann, wenn man neben Blindversuche miteinander durchführt, wurde die Anwesenheit des Kobalts nachgewiesen.
e: Durch eine Mikroharzsäule von Dowex 1-X4 (4 mm×15 mm: RCl-Form) wurde eine grosse Menge der Chromate völlig beseitigt[3].
f: Gibt es Kobalt in der Probelösung, so färben sich die Harzkörnchen intensiv gelb.

*** Die Harzkörnchen trüben sich milchweiss.

3) M. Fujimoto, Dieses Bulletin, **29**, 595 (1956).

Einfluss aus, und es scheint, dass das vorherige 5 Min lange Eintauchen der Harzkörnchen in die Reagenslösung usw. auf die Färbung der Harzphase gar nicht befördernd einwirkt. Aus diesem Grunde hat der Verfasser von nun an das Verfahen „B" als geeignetstes solcher Verfahren ausgewählt und nach diesem alle folgende Vergleichungen von verschiedenen Faktoren durchgeführt.

2. Einfluss der Konzentration der Reagenslösung. — Um den Einfluss des überschüssigen Reagens auf die Menge der in die Harzphase adsorbierten Chelatanionen zu erkennen, wurde eine Reihe der Versuche mit den Reagenslösungen von verschiedenen Konzentrationen durchgeführt. Wie in Abb. 2 klar zu ersehen ist, sinkt die Intensität der Färbung der Harzphase mit der steigenden Reagenskonzentration stark ab, d. h., die Menge der in die Harzphase adsorbierten Chelatanionen wird von der Reagenskonzentration beträchtlich beeinflusst. Infolgedessen wurde nur 0.05prozentige Lösung des Nitroso-R-salzes, in Betracht der Unterscheidbarkeit gegen den Blindversuch, angewandt.

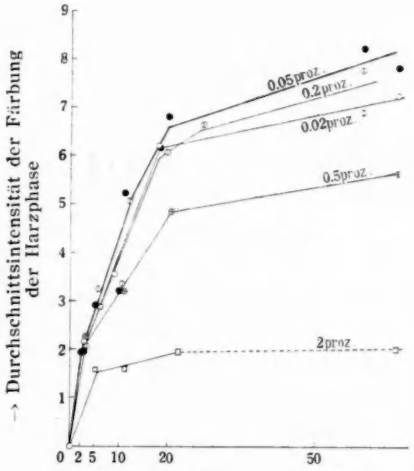

Abb. 2. Einfluss der Konzentration der Nitroso-R-salzlösung auf die Unterscheidbarkeit der Färbung der Harzphase nach dem Verfahren B von Abb. 1.

3. Einfluss der Konzentration der Natriumacetatlösung.— Wie Abb. 3 uns zeigt, übt die Konzentration des Natriumacetats als Pufferlösung auf die Färbungsintensität der Harzphase keinen Einfluss aus. Vom Standpunkt deren Pufferwirkung jedoch aus, empfiehlt es sich, mindestens 0.3 N Lösung des Acetats anzuwenden.

4. Einfluss der Harzart.—Die Färbungsintensität der Harzphase nimmt stark mit dem steigenden Vernetzungsgrade ab, wie man in Abb. 4 deutlich ersehen kann. Mittelstarkbasisches Harz, Amberlite XE-114, ist geeignet, wenn auch die Harzphase sich etwa langsam färbt. Ein

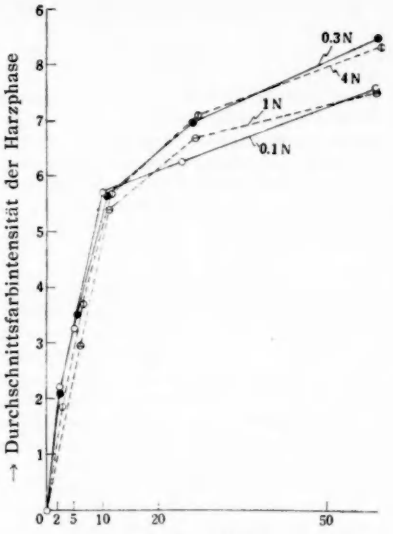

Abb. 3. Einfluss der Natriumacetatkonzentration auf die Färbungsintensität der Harzphase nach dem Verfahren „B" in Abb. 1.

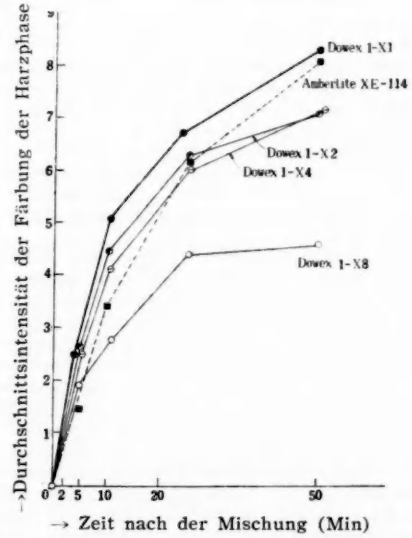

Abb. 4. Einfluss des Vernetzungsgrads der Harze auf die Färbungsintensität der Harzphase.

niedrig vernetztes Harz, Dowex 1-X1, wurde als das beste ausgewählt.

5. Einfluss der Salzkonzentration der Probelösung. — Wie bereits aus der Tatsache vom Abschnitt 3. leicht zu erwarten ist, wird die

Färbung der Harzphase durch Zusatz des Neutralsalzes wie Natriumchlorids gar nicht beeinflusst (vgl. die dicken, gestrichelten Linien von Abb. 5).

6. Ausgeprägte Erhöhung der Empfindlichkeit durch Zersetzung überschüssiges, in der Harzphase vorhandenes Reagens mit Salpetersäure.—Es wurde schon mitgeteilt, dass nur das Kobalt(II)-chelat durch Kochen mit verdünnter Salpetersäure unverändert bleibt, während die Eisen(III)-, Nickel(II)- und Kupfer(II)-chelate durch diese Behandlung leicht zersetzt werden[2]. Mit Rücksicht darauf, dass die Färbung der Harzphase von der Salzkonzentration der Probelösung kaum beeinflusst wird, untersuchte der Verfasser darüber, welchen Einfluss das genannte Verfahren auf die Färbung der Harzphase ausübt. Die Resultate werden in Abb. 6 zusammengestellt. Wenn das genannte Zersetzungsverfahren nicht angewandt wird, so färben sich die Harzkörnchen nach dem Verlauf der Kurve-A. Die Färbungsintensität der Harzphase nimmt dann merklich zu, wie in den Kurven-B und -C beschrieben, wenn man die Harzkörnchen 3 oder 8 Min nach der Bildung des Chelats in der Harzphase, mit einem Tropfen 2 N Salpetersäure auf einem Wasserbad etwa 3 Min erhitzt. Die intensive, von überschüssigem Reagens hervorgerufene Grüngelbfärbung der Harzphase verschwinden dabei vollständig. Die Kurve-D zeigt den Färbungsverlauf in dem Fall, wo man, erst nach dem Erhitzen des Gemisches der Probelösung, der Reagenslösung und der Pufferlösung mit einem Tropfen der 2 N Salpetersäure, die Harzkörnchen hinzufügt. Von diesen Resultaten aus betrachtet, ist es wünschenswert, dass man, etwa 5 Min nach der Bildung des betreffenden Chelats in der Harzphase, das Reaktionsgemisch zusammen mit 2 N Salpetersäure etwa 3 Min kocht.

7. Das empfehlenswerteste Verfahren.—Alles Obenerwähnte zusammengenommen, kann man wie folgt das beste Nachweisverfahren feststellen:—

„Auf einer weissen Tüpfelplatte versetzt man einige Körnchen des farblosen, starkbasischen und niedrig vernetzten Anionenaustauscherharzes wie Dowex 1-X1, mit je einem Tropfen 0.05prozentiger Lösung des Nitroso-R-salzes, 0.3N Lösung des Natriumacetats und der Probelösung. Nach 5 Min langem Stehenlassen fügt man zu diesem Gemische einen Tropfen 2 N Salpetersäure, erhitzt auf einem Wasserbad etwa 3 Min lang und lässt dieses abkühlen. Je nach dem Kobaltgehalt von der Probelösung, entsteht in der Harzphase eine mehr oder weniger intensive Rotfärbung. Wenn die Menge des Kobalts sehr gering ist, so empfiehlt es sich, einen Blindversuch daneben durchzuführen."

Bestimmung der Erfassungsgrenze

Die Resultate der für veschiedene Kobaltmengen ausgeführten Versuche werden in Abb. 7 zusammengestellt. Die Erfassungsgrenze ist 0.0029 γ unter Grenzkonzentration $1 : 1.4 \times 10^7$. Diese entspricht etwa 0.03prozentigem Kobaltgehalt in 10 γ Probe.

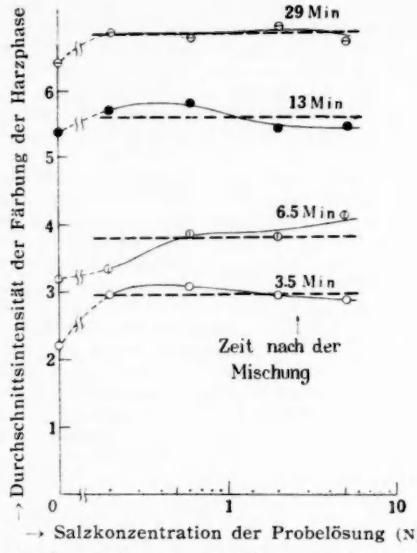

Abb. 5. Einfluss der Salzkonzentration der Probelösung auf die Färbungsintensität der Harzphase.

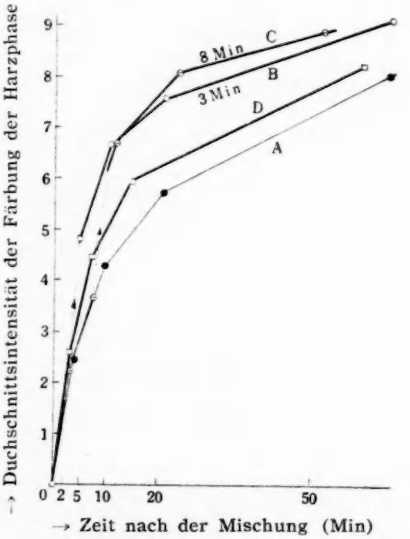

Abb. 6. Wirksamkeit des Zusatzes von Salpetersäure.

-·-·- bedeutet das 3 Min lange Erhitzen des Gemisches mit 1 Tropfen der 2 N Salpetersäure bei 100°C

—— ist der Verlauf vor dem Zusatze der 2 N Salpetersäure

—— ist der Verlauf nach dem Erhitzen mit der 2 N Salpetersäure

Einflüsse der Begleitstoffe

Die Resultate stehen in Tabelle II (S. 280). Die Störung der Nickel(II)- und Kupfer(II)-salze wurde leicht durch Erhitzen mit überschüssiger 2 N Salpetersäure beseitigt. Nur die Eisen(III)-salze beeinträchtigen etwas den Nachweis. Die hier fest gestellte Nachweismethode ist daher entschieden spezifisch.

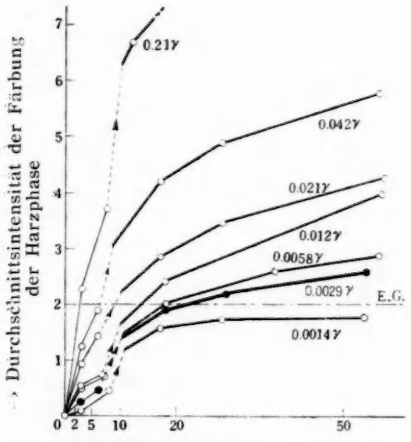

Abb. 7. Bestimmung der Erfassungsgrenze

In bezug auf die hier angewandten Zeichen, vegleiche Abb. 6.

Zusammenfassung

1. Die Empfindlichkeit der Farbenreaktion zwischen den Kobaltsalzen und dem Nitroso-R-salze wird durch einfache Anwendung farblosen, starkbasischen und niedrig vernetzten Anionenaustauscherharzes auffallend erhöht, womit eine neue und ausserordentlich empfindliche Tüpfelmethode zum Nachweis spurweise vorhandenen Kobalts ganzlich festgestellt wird.

2. In gleicher Weise, wie in den vorhergehenden Mitteilungen genau beschrieben, wird das empfehlenswerteste Verfahren genau festgestellt. Die Anwendung verdünnter Salpetersäure ist dabei sehr geeignet, nicht nur zur Erhöhung der Reaktionsempfindlichkeit, sondern auch zur Zersetzung der den Nachweis störenden, stark sich färbenden Chelate von Nickel(II), Kupfer(II) usw.

Zum Schluss möchte der Verfasser Herrn Prof. Dr. E. Minami für seine wertvollen Ratschläge über die gegenwärtige Untersuchung seinen herzlichsten Dank aussprechen.

Laboratorium der analytischen Chemie,
Chemisches Institut der
wissenschaftlichen Fakultät,
Universität zu Tokyo, Hongo, Tokyo

Mikroanalyse mit Hilfe von Ionenaustauscherharzen. XIV. Über den Nachweis in Tausendstelgammamenge vorhandenen Eisens mit 2, 2'-Bipyridyl[1]

Von Masatoshi FUJIMOTO

(Eingegangen am 5. November, 1956)

Einleitung

Es wurde in der vorliegenden Arbeit über eine empfindliche Farbenreaktion[2] zwischen den Eisen(II)-salzen und 2, 2'-Bipyridyl untersucht. Die intensiv sich färbenden Eisen(II)-Bipyridylchelatkationen werden von den farblosen Kationenaustauscherharzen stark adsorbiert und geben dieser Phase eine entschieden deutliche Rotfärbung, mit deren Hilfe man einen ausserordentlich empfindlichen Nachweis des Eisens ausführen kann.

Versuchsanordnung

Man bringt auf eine weisse Tüpfelplatte nacheinander einige Körnchen des farblosen Kationenaustauscherharzes, und je einen Tropfen der Probelösung, verdünnter Lösung des Hydroxylaminhydrochlorids und der des Natriumacetats als Pufferlösung und verdünnter alkoholischer Lösung des 2, 2'-Bipyridyls, danach beobachtet

1) Die dreizehnte Mitteilung: M. Fujimoto, Dieses Bulletin, **30**, 278 (1957).

2) Vgl., z. B., M. L. Moss und M. G. Mellon, *Ind. Eng. Chem., Anal. Ed.*, **14**, 862 (1942).

man eine in der Harzphase entstandene Rotfärbung mit einer Lupe.

Massflüssigkeit und Reagenzien

1. Massflüssigkeit.—Aus derselben Stammlösung des Eisen(III)-chlorids wie der in der siebenten Mitteilung[3] wurde eine Reihe der Massflüssigkeit durch Verdünnung mit extrareiner 0.01N Salzsäure hergestellt. Bei den folgenden Vergleichungen verschiedener Experimentalfaktoren wurde eine 0.01N-salzsaure Lösung angewandt, deren 1 ccm genau 10 γ von Eisen(III) enthielt.

2. Kationenaustauscherharze.—Die farblosen und starksauren Harze von verschiedenen Vernetzungsgraden wurden angewandt, um den Einfluss des Vernetzungsgrades zu untersuchen. Diese sind „1proz. DVB", „2.5proz. DVB", Dowex 50W-X8, Dowex 50W-X12 und „20proz. DVB"[4]. Ein käufliches Kationenaustauscherharz von Phosphonsäuretypus, Duolite C-60, wurde gleichfalls angewandt. Vor dem Gebrauch wurden alle diese Harze mit destillierter Salzsäure gründlich gewaschen, um die Spurmenge des Eisens völlig zu beseitigen, und mit destilliertem Wasser ausgewaschen.

3. Reagenzien.—Hierbei muss man vorher besonders sorgfältig prüfen, dass alle die hier anzuwendenden Reagenzien das Eisen nicht selbst in Spurmenge enthalten.

(1) 2prozentige alkoholische Stammlösung des 2, 2'-Bipyridyls: Man löst 0.1 g käuflichen extrareinen 2, 2'-Bipyridyls (Wakō, „zur Analyse") in 5 ccm Äthylalkohol.

(2) 10prozentige Stammlösung des Hydroxylaminhydrochlorids: Man löst 3 g eisenfreies Reagens (zur Analyse) in 30 ccm destillierten Wassers. Diese Lösung wird zur Reduktion des Eisens(III) angewand.

(3) 4N wässerige Lösung des Natriumacetats als Pufferlösung: Dieselbe Stammlösung wie die der vorhergehenden Mitteilung[1] wurde angewandt.

Bestimmung der Experimentalbedingungen höchster Empfindlichkeit*1

1. Einfluss des Vernetzungsgrades von den Harzen.—Hier wurden 10prozentige Lösung des Hydroxylaminhydrochlorids, 1N Lösung des Natriumacetats und 2prozentige alkoholische Lösung des 2, 2'-Bipyridyls als die Vertreter angewandt. Die Resultate dafür stehen in Abb. 1:

Die Harzphase färbt sich dann am stärksten, wenn man „2.5proz. DVB" verwendet. Bei den hoch vernetzten Harzen wird die Färbung der Harzphase beträchtlich geschwächt. Duolite C-60 war für den vorliegenden Zweck ungeeignet.

2. Einfluss der Reagenskonzentration.—Hier wurde das Harz, „2.5proz. DVB" angewandt. Der Einfluss der Konzentration des benutzten

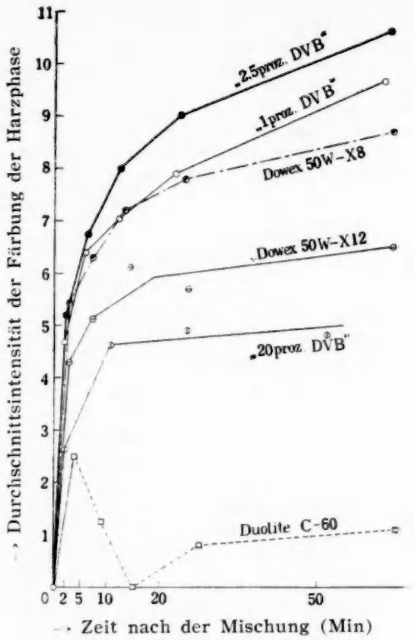

Abb. 1. Einfluss der Harzart.

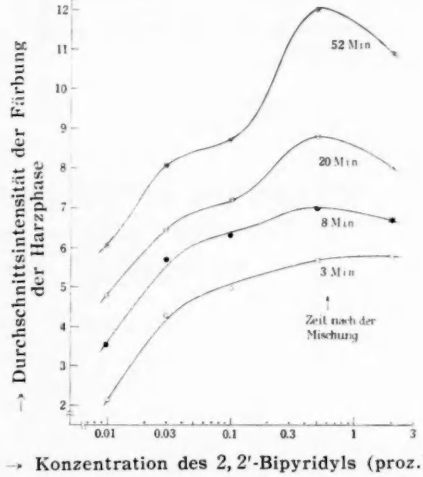

Abb. 2. Einfluss der Konzentration des 2, 2'-Bipyridyls.

2, 2'-Bipyridyls auf die Färbungsintensität der Harzphase wurde in Abb. 2 dargestellt. Wie daraus leicht zu erkennen ist, verstärkt sich die Färbung der Harzphase mit der steigenden Reagenskonzentration allmählich, bis sie bei etwa 0.5-Prozent. das Maximum beträgt, und dann wird sie etwas schwächer. Im folgenden wurde daher 0.5prozentige Reagenslösung angewandt.

3) M. Fujimoto, Dieses Bulletin, **29**, 776 (1956).
4) Vgl. M. Fujimoto, Dieses Bulletin, **29**, 600 (1956).
*1 In bezug auf die schematische, halbquantitative Darstellungsweise von der scheinbaren Durchschnittsintensität der Färbung der Harzphase, vergleiche M. Fujimoto, Dieses Bulletin, **27**, 347 (1954); **29**, 567 (1956).

3. Einfluss der Konzentration des benutzten Hydroxylaminhydrochlorids. — Die Resultate dafür stehen zusammengefasst in Abb. 3, aus welcher man 3prozentige Lösung als die am geeignetste auswählen kann.

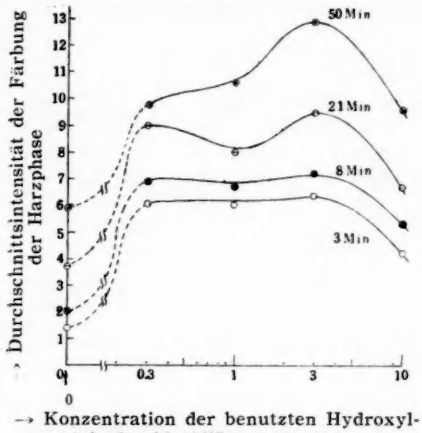

→ Konzentration der benutzten Hydroxylaminhydrochloridlösung (proz.)

Abb. 3. Einfluss der Konzentration des Hydroxylaminhydrochlorids.

Hierbei ist sehr interessant, dass, selbst bei Abwesenheit von Hydroxylamin, die betreffende Rotfärbung in der Harzphase deutlich entsteht. Mit Rücksicht auf die Tatsache, dass die Lösungsphase sich bei Abwesenheit von Hydroxylamin dann gar nicht rot färbt, wenn man keine Harzkörnchen hinzufügt, könnte man vermuten, dass das anfangs in der Harzphase entstandene Eisen(III)-2, 2'-Bipyridyl von den häufig als die Begleiter in der Kationenaustauscherharzphase vorhandenen, ungesättigten Gruppen zum entsprechenden Eisen(II)-chelat einigermassen leicht reduziert werden.

4. Einfluss der Konzentration der in der Probelösung vorhandenen Salze. — Hierbei wurden die am besten geeigneten Reagenzien, d. h., „2.5proz. DVB" (HR-Form), 0.5prozentige Lösung des 2, 2'-Bipyridyls und 3prozentige Lösung des Hydroxylaminhydrochlorids angewandt. Die Färbung der Harzphase nimmt mit der steigenden Salzkonzentration der Probelösung allmählich ab, wie man in Abb. 4 ersieht, aber man kann selbst mit der Probelösung, deren Salzkonzentration so hoch wie 5N liegt, den Nachweis mit befriedigender Empfindlichkeit ausführen.

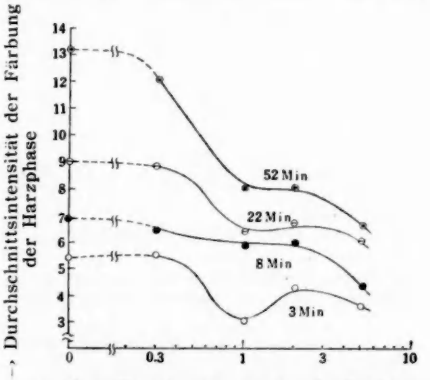

→ Konzentration des in der Probelösung vorhandenen Natriumchlorids (N)

Abb. 4. Einfluss der Salzkonzentration.

5. Das empfehlenswerteste Verfahren.—Alles Obenerwähnte zusammengenommen, kann man das am besten geeignete Verfahren wie folgt feststellen:—

„Auf einer weissen Tüpfelplatte versetzt man einige Körnchen des farblosen, starksauren und niedrig vernetzten Kationenaustauscherharzes, mit je einem Tropfen der Probelösung, 3prozentiger Lösung des Hydroxylaminhydrochlorids, 1N Lösung des Natriumacetats als Pufferlösung und 0.5prozentiger alkoholischer Lösung des 2, 2'-Bipyridyls, und deckt dieses Gemisch mit einer Glasscheibe, um das ganze System vor dem in der Luft vorhandenen Staub zu beschützen. Einige Minuten nach der Mischung beobachtet man mit einer Lupe eine Rotfärbung, die die Harzkörnchen bei Anwesenheit von Eisen liefern. Handelt es sich um sehr geringe Menge des Eisens, empfiehlt es sich, einen Blindversuch nebenbei durchzuführen".

Bestimmung der Erfassungsgrenze

Die Ergebnisse dafür werden in Abb. 5 dargestellt. Die Erfassungsgrenze 0.0025 γ von Eisen unter Grenzkonzentration $1:1.6\times10^7$ wurde hier bestimmt. Diese Erfassungsgrenze entspricht 0.025prozentigem Eisengehalt in 10 γ Probe.

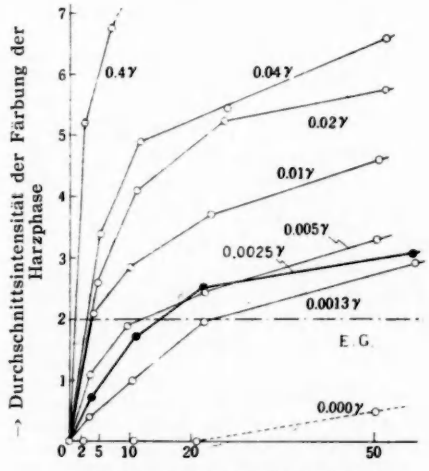

→ Zeit nach der Mischung (Min)

Abb. 5. Bestimmung der Erfassungsgrenze.

Wie bereits im vorhergehenden Abschnitt darauf hingewiesen, muss man hier die Tüpfelplatte

mit einer Glasscheibe fest schliessen, um keinen Staub eindringen zu lassen. Von Bedeutung ist dieses Verfahren besonders dann, wenn es sich um die Spurmenge des Eisens in der Probelösung handelt, denn selbst eine so kleine Menge Eisen, wie in dem in der Luft spurweise vorhandenen Staub enthalten ist, gibt der Harzphase eine deutliche Rotfärbung.

Einflüsse der Begleitionen

Wie in Tabelle I zusammengestellt, ist die gegenwärtige Nachweismethode entschieden spezifisch, ausser dass Kupfer(II)- und Kobalt(II)-salze ein wenig den Nachweis stören.

TABELLE I

EINFLÜSSE DER BEGLEITSTOFFE

Begleitstoffe	benutzter Verbindungstypus	Farbton der Harzphase*	Menge der Begleitstoffe	nachweisbare Eisenmenge	Grenzverhältnis	Bemerkungen**
Ti(IV)	$TiOSO_4$	farblos	100 γ	0.004 γ	$1:2.5\times10^4$	*a, b*
V(V)	NH_4VO_3	hellgelbbraun?	70 γ	0.0025 γ	$1:2.8\times10^4$	——
Cr(III)	$KCr(SO_4)_2$	grauviolett	64 γ	0.004 γ	$1:1.6\times10^4$	*c, d,* Cr(III)≦0.2proz.
Mn(II)	$MnSO_4$	farblos	1580 γ	0.0025 γ	$1:6.3\times10^5$	——
Co(II)	$Co(NO_3)_2$	dunkelgelb	11 γ	0.007 γ	$1:1.6\times10^3$	*c, d,* Co≦0.02proz.
Ni(II)	$NiCl_2$	hellgrün	1400 γ	0.004 γ	$1:3.5\times10^5$	*c, e*
Cu(II)	$CuSO_4$	hellgraugrün	17.5 γ	0.0025 γ	$1:7\times10^3$	*c,* Cu≦0.05proz.
〃	〃	weissbraun	135 γ	0.007 γ	$1:1.9\times10^4$	*d, f*
Zn(II)	$ZnSO_4$	farblos	200 γ	0.01 γ	$1:2\times10^4$	*a*
Cd(II)	$CdSO_4$	etwas milchweiss	1400 γ	0.0057 γ	$1:2.5\times10^5$	*a*
Hg(II)	$Hg(NO_3)_2$	farblos	160 γ	0.004 γ	$1:4\times10^4$	Hg(II)≦0.5proz.
Cr(VI)	$K_2Cr_2O_7$	hellbraungrau	64 γ	0.004 γ	$1:1.6\times10^4$	*c, d,* Cr(VI)≦0.2proz.
Mo(VI)	$(NH_4)_2MoO_4$	gelb (etwas getrübt)	390 γ	0.004 γ	$1:9.8\times10^4$	*c*
W(VI)	Na_2WO_4	farblos	360 γ	0.0025 γ	$1:1.4\times10^5$	——
U(VI)	$UO_2(CH_3COO)_2$	hellbraun	350 γ	0.0025 γ	$1:1.4\times10^5$	——
Pb(II)	$Pb(NO_3)_2$	farblos	2200 γ	0.0025 γ	$1:8.8\times10^5$	——
Sn(IV)	$SnCl_4$	farblos	300 γ	0.0025 γ	$1:1.2\times10^5$	——
Ge(IV)	GeO_2	farblos	25 γ	0.0025 γ	$1:1\times10^4$	——
Sb(III)	$SbCl_3$	farblos	320 γ	0.004 γ	$1:8\times10^4$	——
Bi(III)	$Bi(NO_3)_3$	farblos	3200 γ	0.004 γ	$1:8\times10^5$	*c, g*
Al(III)	$Al(NO_3)_3$	farblos	1700 γ	0.004 γ	$1:4.2\times10^5$	——
Be(II)	$BeCl_2$	farblos	180 γ	0.0025 γ	$1:7.2\times10^4$	——
F^-	KF	farblos	650 γ	0.01 γ	$1:6.5\times10^4$	*h*
Br^-	KBr	farblos	7000 γ	0.0025 γ	$1:2.8\times10^6$	——
J^-	KJ	farblos	20000 γ	0.004 γ	$1:5\times10^6$	*a*
PO_4^{3-}	Na_2HPO_4	farblos	1700 γ	0.0025 γ	$1:6.8\times10^5$	——
NO_2^-	$NaNO_2$	farblos	340 γ	0.0025 γ	$1:1.4\times10^5$	——
$C_2O_4^{2-}$	Oxalsaures Ammonium	farblos	260 γ	0.007 γ	$1:3.8\times10^4$	——
$C_4H_4O_6^{2-}$	Seignettesalz	farblos	920 γ	0.0025 γ	$1:3.7\times10^5$	——
$C_6H_5O_7^{3-}$	Zitronensaures Ammonium	farblos	1400 γ	0.0025 γ	$1:5.6\times10^5$	——

* Farbton der Harzphase hervorgerufen nur durch die Begleitstoffe.

** *a*: Die Probelösung wurde hier vor dem Zusatze der Reagenzien mit 3 bzw. 5 Tropfen destillierten Wassers verdünnt.

b: 3 Tropfen der 1N Lösung des Natriumacetats wurden beigefügt.

c: Erst dann, wenn der genannte Nachweis neben Blindversuche miteinander durchgeführt wurde, wurde die Anwesenheit des Eisens nachgewiesen.

d: Bei diesen Fällen wurden 2 Tropfen 2prozentiger Lösung des 2, 2'-Bipyridyls angewandt.

e: Wenn kleinste Menge des Eisens in der Probelösung enthalten ist, färben sich die Ränder der Harzkornchen hell kirschrot.

f: Nach dem Zusatze der 2M Kaliumjodidlösung nud 20prozentiger Natriumthiosulfatlösung zur Probelösung wurden die Reagenzien hinzugefügt.

g: Der hier gebildete weisse kristalline Niederschlag lieferte auch bei Anwesenheit des Eisens schöne Pfirschfarbe.

h: Vor dem Zusatze der Reagenzien wurde die Probelösung mit 1 Tropfen 33prozentiger Essigsäure versetzt.

Zusammenfassung[*2]

1. Durch einfache Anwendung von farblosen, starksauren, niedrig vernetzten und eisenfreien Kationenaustauscherharzen, nimmt die Empfindlichkeit und Selektivität der Farbenreaktion zwischen Eisen(II)-salzen und 2,2'-Bipyridyl beträchtlich zu, und eine ausserordentlich empfindliche und spezifische Nachweismethode für Spurmenge des Eisens wird neu festgestellt.

2. Die besten Experimentalbedingungen werden genau festgestellt durch ausführliche Untersuchung über die Einflüsse von der Harzart, sowie der Konzentration des Reagens, des Hydroxylaminhydrochlorids und der in der Probelösung vorhandenen Salze. Die Einflüsse fremder Ionen werden dabei gründlich untersucht.

[*2] Der Verfasser gibt hierbei einer ganzen Reihe der neuen Nachweismethoden mit Hilfe von Ionenaustauscherharzen einen passenden Namen „Harztüpfelmethode".

Zum Schluss möchte der Verfasser Herrn Prof. Dr. E. Minami für seine zahlreichen wertvollen Ratschläge über die vorliegende Untersuchung seinen herzlichsten Dank aussprechen.

Für die Harzproben, „1proz. DVB", „2.5-proz. DVB" und „20proz. DVB", ist der Verfasser Herrn Prof. Dr. A. Kawamura an der Landwirtschaftlichen und Technischen Universität zu Tokyo zu grossem Dank verpflichtet.

Laboratorium der analytischen Chemie,
Chemisches Institut der
wissenschaftlichen Fakultät,
Universität zu Tokyo Hongo, Tokyo

Studies on the Chemical Constitution of Agar-agar. XX[1]*. Isolation of a Tetrasaccharide by Enzymatic Hydrolysis of Agar-agar*[2]

By Choji Araki and Kiyoshi Arai

(Received December 1, 1956)

Araki has suggested that agarose, the main polysaccharide of agar, is composed of 1,3-linked β-D-galactopyranose and 1,4-linked 3,6-anhydro-α-L-galactopyranose, the residues being alternately repeated to form a chain[3]. The structure suggested has been based on the chemical composition of agar, the identification of the scission products of methylated agarose[4,5], the isolation of agarobiose (4-*O*-β-D-galactopyranosyl-3,6-anhydro-L-galactose) and its derivatives from the products of partial acid hydrolysis[6], mercaptolysis[7] and methanolysis[8] of agar, and the isolation of neoagarobiose (3-*O*-3,6-anhydro-α-L-galactopyranosyl-D-galactose) from the products of enzymatichydrol ysis of agar[9]. In the last-mentioned process, the extract of an agar-digesting bacterium *Pseudomonas kyotoensis* was used as an enzyme solution, and a mixture of four oligosaccharides resulted. The mixture was resolved into its components by chromatography on a charcoal column, and neoagarobiose was eluted from the column with 7.5% ethanol. This paper is concerned with a tetrasaccharide, which has been eluted from the same column with 17.5% ethanol.

The tetrasacccharide, constituting a predominant quantity (40%) among the hydrolysates, forms a crystalline tetrahydrate having the composition $C_{24}H_{38}O_{19}\cdot 4H_2O$, when crystallized from a mixture of methanol and ethanol. The fully acetylated and methylated derivatives have also been obtained as crystals having the respective compositions $C_{24}H_{28}O_{19}(COCH_3)_{10}\cdot 2H_2O$ and $C_{24}H_{28}O_9(OCH_3)_{10}$. The tetrasaccharide has been shown to be *O*-3,6-anhydro-α-L-galactopyranosyl-(1→3)-*O*-β-D-

1) Part XIX: S. Hirase, This Bulletin, **30**, 68, 70, 75 (1957).
2) The main part of this paper was presented at the 9th Annual Meeting of the Chemical Society of Japan held in Kyoto on April 3, 1956.
3) C. Araki, This Bulletin, **29**, 543 (1956); *Memoirs of the Faculty of Industrial Arts, Kyoto Technical Univ.*, **5**, 21 (1956).
4) C. Araki *J. Chem. Soc. Japan*, **58**, 1362 (1937).
5) C. Araki, ibid., **61**, 775 (1940).
6) C. Araki, ibid., **65**, 533, 627 (1944).
7) S. Hirase and C. Araki, This Bulletin, **27**, 105 (1954).
8) C. Araki and S. Hirase, ibid., **27**, 109 (1954).
9) C. Araki and K. Arai, ibid., **29**, 339 (1956).

galactopyranosyl-(1→4)-*O*-3,6-anhydro-α-L-galactopyranosyl-(1→3)-D-galactose(I), or in a simpler expression 4′-*O*-β-neoagarobiosyl neoagarobiose. The linkages involved provide a strong evidence to support the foregoing structure of agarose suggested by one of the authors.

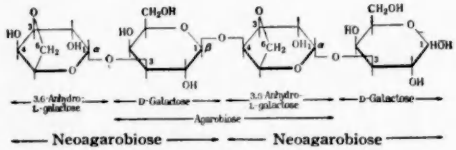

(I) Neoagarotetraose

The structure (I) has ben assigned for the following reasons. Complete methanolysis of the tetrasaccharide afforded 3,6-anhydro-L-galactose dimethylacetal and methyl D-galactoside in an equal molar proportion, indicating that the tetrasaccharide is composed of two moles each of 3,6-anhydro-L-galactose and D-galactose. On reduction of the tetrasaccharide with sodium borohydride, a corresponding glycitol was obtained, which on methanolysis yielded dulcitol together with 3,6-anhydro-L-galactose dimethylacetal and methyl D-galactoside, establishing thereby the reducing end of the parent tetrasaccharide as a D-galactose residue. When the tetrasaccharide was subjected to hydrolysis with the enzyme extract of *P. kyotoensis*, the sole product that could be detected and isolated was neoagarobiose. This evidence suggests that the tetrasaccharide is neoagarobiosyl-neoagarobiose involving two 1→3 linkages. On mild hydrolysis of the tetrasaccharide with 0.04 N-oxalic acid solution, there were obtained equal molar quantities of 3,6-anhydro-L-galactose, D-galactose and agaro- biose, the separation being effected by charcoal chromatography. Identification of the last disaccharide proves the presence of the 1→4 linkage in the parent tetrasaccharide molecule. Thus it is possible to assign the structure(I) to the tetrasaccharide isolated.

The structure(I) has been supported also by the identification of the cleavage fragments of the methylated tetrasaccharide. Complete methanolysis of the fully methylated tetrasaccharide afforded a mixture of the following fragments, which were separated on a charcoal column: (a) 2-*O*-methyl-3,6-anhydro-L-galactose derivatives, identified after hydrolysis and bromine oxidation as methyl 2-*O*-methyl-3,6-anhydro-L-galactonate and also as its corresponding amide, (b) 2,4-di-*O*-methyl-3,6-anhydro-L-galactose dimethylacetal, identified after hydrolysis and bromine oxidation as 2,4-di-*O*-methyl-3,6-anhydro-L-galactonic acid and its amide, and (c) methyl 2,4,6-tri-*O*-methyl-D-galactoside, identified after hydrolysis as a crystalline sugar and its anilide.

A general nomenclature is suggested here for the oligosaccharides produced by partial break down of agarose and a similar polysaccharide. The prefix "agaro" is added to an oligosaccharide whose non-reducing end is presented by D-galactopyranose. Thus the name agarobiose was assigned to a disaccharide 4-*O*-β-D-galactopyranosyl-3,6-anhydro-L-galactose[6]. While, the prefix "neoagaro" is added to an oligosaccharide whose non-reducing end is presented by 3,6-anhydro-L-galactopyranose. Thus the name neoagarobiose was assigned to a disaccharide 3-*O*-3,6-anhydro-α-L-galactopyranosyl-D-galactose[9]. On this basis the tetrasaccharide investigated in this paper is termed neoagarotetraose.

From the fact that neoagarobiose and neoagarotetraose resulted from agar by the action of the enzymes of an agar-digesting bacterium, and also that neoagarotetraose is hydrolysed by the same enzymes to yield neoagarobiose, it may possibly be assumed that agarose is hydrolysed by the enzymes at its occasional 1→4 β-D-galactoside linkages to yield higher homologues of neoagaro-oligosaccharides, which are in turn hydrolysed at their 1→4 linkages to form neoagarobiose as the lowest fragement.

Experimental

General Procedure.—Evaporation and concentration were carried out under reduced pressure below 40°. All the melting points are uncorrected. Unless otherwise stated the specific rotation was measured in the aqueous solution with a 1 dm. tube. The paper chromatograms were irrigated with *n*-butanol-acetic acid-water (4 : 1 : 2 v/v) in the ascending manner and were sprayed with an *o*-aminophenol reagent[10]. For the charcoal chromatography, there was used active carbon Shirasagi[11], which was not mixed with Celite.

Neoagarotetraose.—A part (2.0 g.) of the 17.5% ethanol eluate, $[\alpha]_D$+1.1°, obtained in Part XVIII[9], was dissolved in a few drops of water, and methanol was added while heating to form insoluble precipitates, which were subsequently removed by filtration. Then absolute ethanol (nearly equal in volume to that of the

10) S. Hirase, C. Araki and S. Nakanishi, ibid., **26**, 183 (1953).
11) Product of Takeda Pharmaceutical Industries, Ltd., Osaka.

methanol used) was added to the filtrate while boiling until the solution became slightly turbid, and the resulting solution was kept in a refrigerator. The crystals deposited were filtered and washed successively with ethanol-methanol (2 : 1), ethanol and ether; yield 0.8 g. The filtrate and washings were combined and evaporated, when the second crop of the crystals was obtained; yield 0.6 g.

The two crops of the recrystals were combined and recrystallized by dissolving in hot methanol, adding twice the volume of ethanol while boiling, and then keeping the solution in a refrigerator. Neoagarotetraose was deposited as colorless fine crystals, which were filtered and washed successively with ethanol-methanol (2 : 1), ethanol and ether; yield 0.50 g. It sintered at 190°, melted at 214–218° under decomposition, and had a specific rotation $[\alpha]_D^{21}$ −3.9° (after twenty four hours, *c* 1.0). It gave on a paper chromatogram a spot whose R_{gal} value[9] was 0.71, and showed a reducing power 27.85% of D-galactose. The analysis of the sample dried at 100° in vacuo over phosphorus pentoxide showed that it was a tetrahydrate.

Anal. Found: C, 40.98; H, 6.60. Calcd. for $C_{24}H_{38}O_{19}\cdot 4H_2O$: C, 41.10; H, 6.55%.

The mother liquor of the recrystallization was diluted with methanol and again evaporated to form hygroscopic crystals, which sintered at 98°, melted at 104–107°, had a specific rotation $[\alpha]_D^{22}$ −2.8° (1.0), and which gave a spot with R_{gal} value 0.71 on a paper chromatogram. The analysis of the sample dried at 65° in vacuo over phosphorus pentoxide indicated that it was a dihydrate.

Anal. Found: C, 43.07; H, 6.42. Calcd. for $C_{24}H_{38}O_{19}\cdot 2H_2O$: C, 43.10; H, 6.31%.

Deca-*O*-acetylneoagarotetraose.—Neoagarotetraose (1.0 g.) in pyridine (20 cc.) was acetylated with acetic anhydride (7.0 g), which was added dropwise under ice cooling. After being left at room temperature (18–19°) for seventy-two hours, the reaction solution was poured with stirring into ice-water (120 cc.), and crystals of the acetate formed were filtered and washed with ice-water; yield 1.0 g.; m. p. 115–116°. Recrystallization was effected first from *n*-butanol and then from methanol-ethanol; m. p. 121°; $[\alpha]_D^8$ −15.8° (chloroform, *c* 1.0) and −11.8° (methanol, *c* 1.0).

Anal. Found: C, 49.15; H, 5.74: CH_3CO, 41.58. Calcd. for $C_{24}H_{28}O_{19}(COCH_3)_{10}\cdot 2H_2O$: C, 49.10; H, 5.72; CH_3CO, 40.00%.

Methyl Nona-*O*-methyl-β-neoagarotetraoside.—A methylation of neoagarotetraose (2.0 g.) was carried out first under ice cooling and then at room temperature (24–25°) over three days in the same manner as in the case of neoagarobiose[9], using dimethylsulfate (63 cc., total) and 32% potassium hydroxide solution (150 cc., total). After completion of the reaction, the reaction mixture was filtered to remove the precipitated potassium sulfate and the filtrate was extracted four times with chloroform (200 cc., total). The extracts were combined, washed once with water, dried over sodium sulfate, and evaporated to a syrup (2.5 g.), which on dissolution in ether and evaporation afforded a semi-solid (2.28 g., OCH_3 36.1%). It was then twice methylated with methyl iodide (25 g.) and silver oxide (15 g.), and the final product was obtained by extraction with ether and subsequent evaporation as a crystalline mass (2.0 g., OCH_3 40.5%), which was triturated with ether. The separated crystals were then filtered; yield 0.48 g.; m.p. 164°. An additional crop was obtained from the filtrate by adding petroleum ether (45–53°) and keeping in a refrigerator; yield 0.72 g.; m. p. 163–164°. The crystals obtained were combined, recrystallized from methanol and washed with ether; m. p. 167°; $[\alpha]_D^{19}$ −87.6° (chloroform, *c* 1.0) and −85.9° (methanol, *c* 1.0). The negative values of the rotation indicate that it is a β-anomer of the methylated neoagarotetraoside.

Anal. Found: C, 52.90; H, 7.64; OCH_3, 40.37; m. w. (Rast), 768. Calcd. for $C_{24}H_{28}O_9(OCH_3)_{10}$: C, 53.12; H, 7.53; OCH_3, 40.27%; m. w., 770.

Methanolysis of Neoagarotetraose.—Neoagarotetraose (1.0 g.) in 4% methanolic hydrogen chloride (50 cc.) was heated under reflux until the optical rotation of the solution reached a constant value: $[\alpha]_D$ −25.0° (initial)→+32.0° (final). After fifteen hours the solution was neutralized with silver carbonate, filtered and evaporated to a syrup (1.15 g.). Paper chromatographic examination showed that the syrup was a mixture of 3,6-anhydro-L-galactose dimethylacetal and methyl D-galactoside. A part (1.0 g.) of the mixture was separated into its components on a powdered filter paper column in the manner previously reported from this laboratory[8,9].

3,6-Anhydro-L-galactose Dimethylacetal.—This substance was eluted from the column with *n*-butanol saturated with water, and was obtained as a colorless syrup on evaporation; 0.50 g.; $[\alpha]_D^{25}$ −31.1° (*c* 0.9); OCH_3, found: 29.62% (calcd. for $C_6H_{10}O_4(OCH_3)_2$: 29.81%). It showed a strong Seliwanoff's ketose reaction and gave on a paper chromatogram a spot corresponding to 3,6-anhydro-L-galactose dimethylacetal. Identification was carried out in the usual manner by hydrolysis to a reducing sugar, which was then converted to 3,6-anhydro-L-galactose diphenylhydrazone[12]; m. p. 153°; $[\alpha]_D^{23}$ −34.6° (initial, methanol, *c* 1.4).

Anal. Found: N, 8.61. Calcd. for $C_{15}H_{20}O_4N_2$: N, 8.53%.

Methyl D-Galactoside.—After removal of the 3,6-anhydro-L-galactose dimethylacetal from the column, methyl D-galactoside was eluted with 80% aqueous methanol, and was obtained as a syrup (0.48 g.) on evaporation. Crystallization from methanol-acetone-(1 : 2) afforded methyl α-D-galactoside monohydrate: m. p. and mixed m. p. 108–109°; $[\alpha]_D^{23}$ +180.5° (*c* 1.0); OCH_3, found: 14.73% (calcd. for $C_7H_{14}O_6\cdot H_2O$: 14.62%).

Reduction and Methanolysis of Neoagarote-

12) C. Araki, *J. Chem. Soc. Japan*, **65**, 725 (1944).

traose.—A solution of neoagarotetraose (1.50 g.) in water (30 cc.) was combined with a solution of sodium borohydride (0.15 g.) in water (10 cc.), and the resulting solution was left at room temperature (7°) withoccasional shaking for two and a half hours, at which time the solution showed no longer reducing power. It was then carefully neutralized with 0.25 N-aqueous acetic acid under ice cooling, and evaporated to dryness. Crude neoagarotetra-itol, obtained as an amorphous material (1.65 g.), was crystallized from methanol-ethanol (1 : 1); m. p. 60–63°; $[\alpha]_D^{11}$ −32.0° (*c* 1.3, *l* 0.5).

The above glycitol (1.60 g.) in 4% methanolic hydrogen chloride (100 cc.) was heated under reflux until the optical rotation of the solution reached a constant value ($[\alpha]_D$ −25.0° → +3.1°) After eighteen hours the solution was neutralized with silver carbonate, filtered and evaporated to give a syrupy mixture (1.45 g.) of the following three products, which were separated by chromatography.

*3,6-Anhydro-*L*-galactose Dimethylacetal.*—The above mixture was placed on a starch column (4.5×25 cm.) and eluted with *n*-butanol saturated with water. The eluate showing the optical rotation in the negative direction was evaporated to dryness, 3,6-anhydro-L-galactose dimethylacetal being obtained as a colorless syrup; yield 0.60 g; $[\alpha]_D^{22}$ −29.8° (*c* 0.9); OCH_3, found: 28.8% (calcd. for $C_6H_{10}O_4(OCH_3)_2$: 29.81%). It was identified in exactly the same manner as that above-mentioned.

Methyl D*-Galactoside.*—The chormatographic column was then eluted with *n*-butanol-ethanol-water (4 : 1 : 2), and the eluate showing the optical rotation in the positive direction was evaporated to dryness. Methyl D-galactoside was obtained as a syrup (0.40 g.) and was identified in exactly the same manner as that above-mentioned.

Dulcitol.—The elution with the same solvent was continued and the eluate (200 cc.) showing no optical rotation was concentrated to a syrup (0.20 g.). Then the eluant was changed to 80% aqueous methanol and the eluate (200 cc.) was concentrated to a syrup (0.20 g.). The syrups obtained were combined and subjected to crystallization from methanol, affording dulcitol; yield 0.20 g.; m. p. 186–187°, not depressed on admixture with an authenic sample; $[\alpha]_D^9 \pm 0°$ (*c* 1.0).

Anal. Found: C, 39.55; H, 7.42. Calcd. for $C_6H_{14}O_6$: C, 39.56; H,7.75%.

Hydrolysis of Neoagarotetraose with 0.04 N-Oxalic Acid.—Neoagarotetraose (1.50 g.) in 0.04 N-oxalic acid solution (100 cc.) was heated in a boiling water bath, the progress of the hydrolysis being followed polarimetrically: $[\alpha]_D$ −1.7° (initial), −4.0° (15 min.), −3.3° (30 min.), −2.7° (1 hr.), +0.7° (1.5 hr.), +5.5° (2 hr.), +6.0 (2.5 and 3 hr., constant). After three hours the acid was removed by neutralization with calcium carbonate and filtration, the filtrate was concentrated to a syrup, which was then extracted with methanol, and the extract was again concentrated to give a light yellow syrup (1.50 g.). When chromatographed on a paper, it showed a brown spot corresponding to galactose, and two yellow with tails spots, the centres of which had the respective R_{gal} values 2.07 and 3.10, corresponding to agarobiose and 3,6-anhydro-galactose, respectively. The separation of the mixture was effected by the charcoal chromatography of Whistler and Durso[13].

A 10% aqueous solution of the syrup (1.50 g.) was placed on a charcoal column (3.3×7.0 cm.) and eluted with water and with successive higher concentrations of ethanol in water. The eluate (30 cc. per fraction) was examined both polarimetrically and paper chromatographically, and the fractions containing the same material were combined and evaporated to recover the material. The result is given in Table I, and the yields cited indicate the presence of D-galactose, 3,6-anhydro-L-galactose and agarobiose in the approximate mcle ratio 1 : 1 : 1. The identification of each product was carried out in the manner described below.

D*-Galactose.*—Fraction I, which completely solidified, was recrystallized from methanol, affording D-galactose; yield 0.25 g.; m. p. 166–167°; $[\alpha]_D^6$ +96.5° (initial) → +79.5° (after twenty four hours, *c* 1.0).

Anal. Found: C, 40.15; H, 6.89. Calcd. for $C_6H_{12}O_6$: C, 40.00; H, 6.67%.

The filtrate of the recrystallization was concentrated to a syrup, which afforded D-galactose phenylosazone on treatment with phenylhydrazine in the presence of acetic acid; m. p. and mixed

TABLE I

CHROMATOGRAPHIC SEPARATION OF THE HYDROLYSATES OF NEOAGAROTETRAOSE WITH 0.04 N-OXALIC ACID SOLUTION

Fraction	I	II	III	IV	V	VI	VII
Eluted by	W	W	2.5%E	5.0%E	7.5%E	10%E	17.5%E
Volume (cc.)	330	420	360	570	450	420	450
$[\alpha]_D$(°)	+53.7	−18.8	−15.6	−7.8	−17.5	−2.8	−3.0
Yield (g.)	0.35	0.20	0.13	0.41	0.17	0.05	0.08
Component identified	D-Galactose	3,6-Anhydro-L-galactose		Agarobiose		Neoagarotetraose unchanged	

W: Water, E: Ethanol

13) R. L. Whistler and D. F. Durso, *J. Am. Chem. Soc.*, **72**, 677 (1950).

m. p. 187–188°; N, found: 15.63% (calcd. for $C_{14}H_{22}O_4N_4$: 15.70%).

3,6-Anhydro-L-galactose.—Fractions II and III showed a distinct Seliwanoff's ketose reaction and reduced a Fehling's solution at room temperature. The phenylosazone prepared therefrom agreed with 3,6-anhydro-L-galactose phenylosazone[12]; m. p. and mixed m. p. 216–217°; $[\alpha]_D^6$ −65.3° (initial) → −37.6° (after twenty four hours, pyridine-ethanol (2 : 3), *c* 0.5, *l* 0.5).

Anal. Found: N, 16.62. Calcd. for $C_{18}H_{20}O_3N_4$: N, 16.46%.

Agarobiose.—Fractions IV and V showed a Seliwanoff's reaction and reduced a Fehling's solution at room temperature. The phenylosazone prepared therefrom agreed with agarobiose phenylosazone[6]; m. p. 218–219°; $[\alpha]_D^6$ −155.7° (initial) → −137.6° (after forty eight hours, pyridine-ethanol (2 : 3), *c* 0.6, *l* 0.5).

Anal. Found: N, 11.23. Calcd. for $C_{24}H_{30}O_5N_4$: N, 11.15%.

Neoagarotetraose Recovered.—Fractions VI and VII did not reduce a Fehling's solution at room temperature and gave on a paper chromatogram a single spot corresponding to neoagarotetraose (R_{gal} 0.71), proving thereby to be an unchanged material.

Hydrolysis of Neoagarotetraose with Enzymes.—The enzyme solution used for the following experiments was prepared on a 100 cc. scale from *P. kyotoensis* exactly in the same manner as that reported in Part XVIII[9]. Twenty five cc. of the solution was buffered with N/15-potassium dihydrogen phosphate (10 cc.) and was diluted with water to 40 cc., and a drop of toluene was added, the pH value of the resulting solution being 5.6. Three similar batches were prepared: (A) with addition of neoagarotetraose (0.5 g.), (B) with addition of neogarotetraose (0.5 g.) after being heated to kill the enzymes, and (C) without addition of neoagarotraose. These were kept at 40° in an incubator, and aliquotes (2.0 cc.) were periodically withdrawn to determind the reducing power by Bertrand's method (table II). Only the batch A showed an increase in the reducing power, corresponding to 21.8% hydrolysis.

After forty eight hours, batches A and C were respectively heated for five minutes in a boiling water bath to stop the reaction. All the batches were separately concentrated, the residues were repeatedly extracted with hot methanol, and the extracts were again evaporated to dryness. The resulting syrups weighed (A) 0.40 g., (B) 0.40 g. and (C) 0.10g., respectively. Paper chromatographic examination indicated that syrup A was a mixture of neoagarobiose and neoagarotetraose, syrup B contained neoagarotetraose only, and the syrup C contained neither of them, proving thereby that the neoagarobiose in the syrup A was derived by the hydrolysis of neoagarotetraose with enzymes.

For the isolation of the neoagarobiose, the experiment A was repeated five times, and the combined syrups (2.4 g.) were chromatographed on a charcoal column (4.5×10 cm.) in a manner similar to the separation of the acid-hydrolysates of neoagarotetraose, the result being shown in Table III.

Fraction I was chiefly inorganic substances. Fraction II gave on a paper chromatogram a spot (R_{gal} 1.15) corresponding to neoagarobiose, fraction III two spots (R_{gal} 1.15 and 0.71) corresponding to neoagarobiose and neoagarotetraose, and fractions IV, V and VI a spot (R_{gal} 0.71) corresponding to neoagarotetraose, respectively. The identification was carried out as follows.

Neoagarobiose.—Fraction II was amorphous powders, a part (0.25 g.) of which was dissolved in a few drops of water, twice its volume of methanol was added while heating, the solution was filtered, and additional methanol was added to the filtrate while heating. When the resulting solution was kept in a refrigerator, neoagarobiose

TABLE II

HYDROLYSIS OF NEOAGAROTETRAOSE WITH ENZYMES*

	Initial	8 hr.	24 hr.	32 hr.	48 hr.	±**
A	170.4	184.0	195.0	198.5	207.6	+37.2
B	176.4	179.0	182.9	179.0	167.6	−8.8
C	6.9	8.1	10.9	9.2	10.2	+3.3

A: A buffered enzyme solution (40 cc.) + neoagarotetraose (0.5 g.).
B: A buffered enzyme solution (40 cc.) killed + neoagarotetraose (0.5 g.).
C: A buffered enzyme solution (40 cc.) only.
* The figures are indicated by Bertrand's copper value (mg.), calculated for the whole solution (40 cc.).
** An increase or decrease in copper value after 48 hr.

TABLE III

CHROMATOGRAPHIC SEPARATION OF ENZYMATIC HYDROLYSATES OF NEOAGAROTETRAOSE

Fraction	I	II	III	IV	V	VI
Eluted by	W	5%E	7.5%E	10%E	15%E	17.5%E
Volume (cc.)	640	750	1230	480	1050	720
Yield (g.)	0.1	0.30	0.25	0.25	1.20	0.25
$[\alpha]_D$ (°)	±0	+16.5	−0.9	−1.8	−2.9	−3.0

W: Water, E: Ethanol.

was deposited; yield 0.15 g.; m. p. 202–203°, not depressed on admixture with an authentic sample[9]; $[\alpha]_D^{15}$ +25.0° → +22.5° (*c* 1.1).

Anal. Found: C, 44.25; H, 6.33. Calcd. for $C_{12}H_{20}O_{10}$: C, 44.44; H, 6.22%.

The filtrate from the above crystals was concentrated to a syrup, which was then treated with phenylhydrazine in the presence of acetic acid. The phenylosazone obtained had m. p. 198–199°, not depressed on admixture with neoagarobiose phenylosazone[9].

Anal. Found: N, 11.37. Calcd. for $C_{24}H_{30}O_5N_4$: N, 11.15%.

Neoagarotetraose Recovered.—All the fractions IV, V and VI were amorphous powders, which on acetylation with acetic anhydride and pyridine gave neoagarotetraose deca-acetate, m. p. 120–121°, not depressed on admixture with the sample described earlier.

Methanolysis of Methyl Nona-*O*-methyl-β-neoagarotetraoside.—The methylated tetraoside (1.70 g.), described earlier, was dissolved in 4% methanolic hydrogen chloride (100 cc.) and the solution was heated under reflux until the optical rotation of the solution reached a constant value ($[\alpha]_D$ −39.9° → +32.4°). After seventeen hours the solution was neutralized with silver carbonate, filtered and evaporated to a syrup, which was then dried by dissolution in ether and re-evaporation; yield 1.60 g.; OCH_3, found: 44.5%.

Separation of the Methanolysates by Charcoal Chromatography.—A 10%aqueous solution of the above methanolysates (1.60 g.) was placed on a charcoal column (3.5×10 cm.) and eluted with water and with successive higher concentrations of ethanol in water. The eluates were collected at 30 cc. intervals, and the fractions showing the same content were combined and concentrated to dryness (Table IV). The eluates with water (450 cc.) and with 2.5% ethanol (first 750 cc.) were discarded, since they left nothing on evaporation. The compounds recovered by evaporation were identified in the manner described below.

a) 2-*O*-Methyl-3, 6-anhydro-L-galactose Part.—Fractions I and II, showing a distinct Seliwanoff's reaction, were proved to be derivatives of 2-*O*-methyl-3, 6-anhydro-L-galactose by the conversion into the following crystatalline compounds.

Methyl 2-O-Methyl-3, 6-anhydro-L-galactonate.—A part (0.27 g.) of the fraction I was hydrolysed with 3% hydrobromic acid (6 cc.) in the boilng water bath for ten minutes, and was then oxidized with bromine (0.4 cc.), which was dropped into the hydrolytic solution kept at 40° during four hours. After being left overnight room temperature, the reaction solution was aerated to remove excess bromine, neutralized with silver carbonate, filtered before and after treatment with hydrgen sulfide, and evaporated to a syrup, which solidified on dissolution in methanol and evaporation; yield 0.23 g.

The oxidation product obtained above was esterified by heating in 4% methanolic hydrogen chloride for five hours. The methyl ester, isolated in the usual manner, was separated from a syrupy contaminant by tiling; yield 0.25 g.; m. p. 85–86°. Recrystallization from benzene afforded pure methyl 2-*O*-methyl-3, 6-anhydro-L-galactonate[5]; yield 0.17 g.; m. p. 91°, not depressed on admixture with an authentic specimen; $[\alpha]_D^{24}$ −61.6° (*c* 0.8, *l* 0.5).

Anal. Found: C, 46.79; H, 6.68; OCH_3, 29.1. Calcd. for $C_6H_5O_4(OCH_3)_2$: C, 46.58; H, 6.85; OCH_3, 30.12%.

2-O-Methyl-3, 6-anhydro-L-galactonamide.—The methyl ester obtained above was converted in the usual manner into an amide[5]; m. p. 170–171°; $[\alpha]_D^{23}$ −74.3° (*c* 2.3, *l* 0.5).

Anal. Found: N, 7.15; OCH_3, 16.22. Calcd. for $C_7H_{13}O_5N$: N, 7.33; OCH_3, 16.23%.

b) 2, 4, 6-Tri-*O*-methyl-D-galactose Part.—Solid fractions III and IV were methyl 2, 4, 6-tri-*O*-methyl-D-garactoside, contaminated by a small amount of methyl 2-*O*-methyl-3, 6-anhydro-L-galactoside,which was removed as follows. The two fractions were combined and treated with N/50-sulfuric acid in a boilng water bath for two hours to hydrolyse the contaminant, and then the solution was neutralized with barium carbonate, filtered and evaporated to dryness. The resulting residue (0.70 g.), which solidified on dissolution in methanol and re-evaporation, was extrated with boiling petroleum ether (b. p. 45–55°). On cooling the extract afforded crystals of methyl 2, 4, 6-tri-*O*-methyl-D-galactoside; yield 0.40 g.; m. p. 70–72°; $[\alpha]_D^{23}$ +54.2° (*c* 1.8); OCH_3, found: 51.37% (calcd. for $C_6H_9O_2(OCH_3)_4$: 52.54%). Evaporation of the mother liquor afforded an additional crop (0.25 g.).

2, 4, 6-Tri-O-methyl-D-galactose.—The above

TABLE IV

CHROMATOGRAPHIC SEPARATION OF THE METHANOLYSATES OF METHYLATED NEOAGAROTETRAOSIDE

Fraction	I	II	III	IV	V	VI	VII
Eluted by	2.5%E	5%E	5%E	7.5%E	7.5%E	10%E	10%E
Volume (cc.)	600	600	750	660	600	600	600
Yield (g.)	0.30	0.06	0.48	0.20	0.15	0.22	0.05
n_D^{25}	1.4647	1.4655	solid	solid	1.4539	1.4526	1.4500
OCH_3 (%)	32.6	33.5	47.8	49.0	49.0	48.3	49.3
$[\alpha]_D^{25}$ (°)	−29.6	+34.2	+73.9	+63.2	+50.3	+26.1	+54.0

E: Ethanol — 2-*O*-Methyl-3, 6-anhydro-L-galactose part — 2, 4, 6-Tri-*O*-methyl-D-galactose part — 2, 4-Di-*O*-mehyl-3, 6-anhydro-L-galactose part

methyl glycoside (0.40 g.) was hydrolysed with N-sulfuric acid (12 cc.) in the usual manner. The resulting 2,4,6-tri-*O*-methyl-D-galactose was crystallized from ether; yield 0.25 g.; m. p. 97–98°. Recrystallization from the same solvent afforded a pure specimen; yield 0.20 g.; m. p. 113–114°, not depressed on admixture with an authentic sample[4]; $[\alpha]_D^{30}$ +111.7° (initial) → +91.3° (after twenty four hours, *c* 1.7).

Anal. Found: C, 48.65; H, 8.27; OCH_3, 41.20. Calcd. for $C_6H_9O_3(OCH_3)_3$: C, 48.65; H, 8.11; OCH_3, 41.89%.

2,4,6-Tri-O-methyl-L-phenyl-D-galactosylamine.—The above sugar was treated with aniline in the usual manner to give an anilide[4]; m. p. 172–173°; $[\alpha]_D^{31}$ −81.5° (initial) → +38.6° (after forty eight hours; acetone, *c* 1.4, *l* 0.5).

Anal. Found: N, 4.78; OCH_3, 31.54. Calcd. for $C_{15}H_{23}O_5N$: N, 4.71; OCH_3, 31.31%.

e) **2,4-Di-*O*-methyl-3,6-anhydro-L-galactose Part.**—Fractions V, VI and VII were fairly positive to Seliwanoff's test and gave on a paper chromatogram a yellow spot corresponding to 2,4-di-*O*-methyl-3,6-anhydro-L-galactose dimethylacetal.

2,4-Di-O-methyl-3,6-anhydro-L-galactonic Acid.—The fractions VI and VII were combined and a part (0.25 g.) of the resulting mixture was hydrolysed and then oxidized in exactly the same manner as that described for 2-*O*-methyl-3,6-anhydro-L-galactose derivatives. The oxidation product (0.18 g.) was crystallized from ethyl acetate; m. p. 150°, not depressed on admixture with 2,4-di-*O*-methyl-3,6-anhydro-L-galactonic acid[14]; $[\alpha]_D^{17}$ −61.4° (*c* 1.2, *l* 0.5).

Anal. Found: C, 46.34; H, 6.86; OCH_3, 29.66. Calcd. for $C_6H_9O_4(OCH_3)_2$: C, 46.58; H, 6.85; OCH_3, 30.15%.

2,4-Di-O-methyl-3,6-anhydro-L-galactonamide. The above acide (0.1 g.) was esterified with boiling 4% methanolic hydrogen chloride (3 cc.) and the methyl ester obtained was further converted to the amide[14] in the usual manner; m. p. 150°; $[\alpha]_D^{24}$ −73.4° (*c* 1.3, *l* 0.5).

Anal. Found: N, 6.95; OCH_3, 29.65. Calcd. for $C_5H_{13}O_5N$: N, 6.83; OCH_3, 30.25%.

14) C. Araki, *J. Chem. Soc. Japan*, **61**, 503 (1940).

Summary

1. A tetrasaccharide, forming a crystalline tetrahydrate, has been isolated from the products of enzymatic hydrolysis of agar. Its fully acetylated and methylated derivatives have also been obtained as crystals.

2. Identification of both monosaccharide and disaccharide constituents has led to the assignment of the structure, *O*-3,6-anhydro-α-L-galactopyranosly-(1→3)-*O*-β-D-galactopyranosyl-(1→4)-*O*-3,6-anhydro-α-L-galactopyranosyl-(1→3)-D-garactose, to the tetrasaccharide isolated. The structure has been supported also by methylation data.

3. The tetrasaccharide has been termed neoagarotetraose, based on the general nomenclature suggested for oligosaccharides derived from agarose and a similar polysaccharide.

4. A probable course has been assumed for the enzymatic degradation of agarose.

The authors are indebted to Mr. N. Nakata for assistance in this study and to Mr. S. Hirase for help in the preparation of the manuscript. This study has been aided by the Grant for Fundamental Scientific Research from the Ministry of Education, for which our thanks are also expressed.

Institute of Chemistry, Faculty of Industrial Arts, Kyoto Technical University, Matsugasaki, Kyoto

Photo-dichroism of Printed-out Silver. II. Theoretical Consideration of the Mechanism from the point of View that the Phenomenon of Photo-dichroism would be an Anisotropic Herschel effect

By Isao KAMIYA

(Received July 12, 1956)

In the previous paper[1], the author has reported some experimental evidences in favor of the view that the phenomenon of photo-dichroism of printed-out silver is an anisotropic Herschel effect.

In the present paper, the author carries out the theoretical consideration of the same subject and proposes the mechanism by which the films of printed out silver being exposed to polarized light become anisotroric in their optical nature.

According to the theory, the value of photo-dichroism would be given by the formula which is the function of the time of exposure, energy of exposing light, temperature and the wave length of observed light. Thus, the quantitative expression of the phenomenon, which has not been reported up to the present, can be undertaken.

Consideration

Mott and Gurney[2] have proposed the following explanation of the mechaism of of Herschel effect.

When a previously illuminated film (in which the latent image is contained) is exposed to red light, the action of the light will remove electrons from the latent image (paticles of metallic silver) into conduction band of silver halide. The silver speck then carries a positive charge. This will cause an electrolytic current, consisting of silver ions, to flow from the latent image into the silver halide crystals. The silver speck thus will be gradually destroyed.

When a surface of metallic silver is exposed obliquely, as shown in Fig. 1, to polalized light of which the electric vector is in the plane of incidence, the number of inner-photo-electrons (say $J_{\parallel}$) is given by the following formula[3],

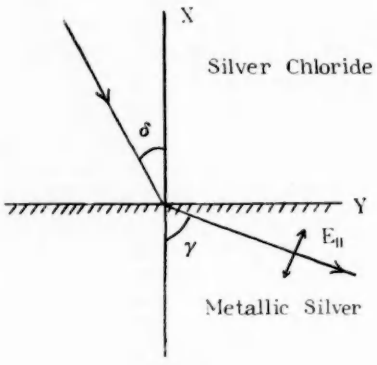

Fig. 1.

$$J_{\parallel}=\frac{R_0}{h\nu}\frac{\sin^2\gamma\sin^2\delta}{\sin^2(\gamma+\delta)\cos^2(\delta-\gamma)}\times\left(1-\sqrt{(\phi-\chi)/h\nu}\right)\left[1+\frac{3}{2}\times(2-\cos^2\gamma)\{\sqrt{(\phi-\chi)/h\nu}+(\phi-\chi)/h\nu\}\right] \quad (1)$$

by the light of which the electric vector is perpendicular to the plane ($J_{\perp}$),

$$J_{\perp}=\frac{R_0}{h\nu}\frac{\sin^2\gamma\cos^2\delta}{\sin^2(\gamma+\delta)}\left(1-\sqrt{(\phi-\chi)/h\nu}\right)\times\left[1-\frac{1}{2}\{\sqrt{(\phi-\chi)/h\nu+(\phi-\chi)/h\nu}\}\right] \quad (2)$$

where ϕ is the work function of metallic silver, χ is the electron affinity of silver chloride, $h\nu$ is the energy of exposiog light and δ and γ are the angles of incidence and refraction. R_0 is to be given as,

$$R_0=A(\varepsilon+A)[1-\epsilon\exp\{-(\varepsilon+A)d\}]$$

where A is the fraction of absorbed quanta contributing to remove the electrons and ε is that on other processes and d is the thickness of the metal.

In fact, there would be a great many such surfaces of metallic silver in the film of printed-out silver and the normals

1) I. Kamiya, This Bulletin, **30**, 6 (1957).
2) N. F. Mott and R. F. Gurney, "Electronic. Processes in Ionic Crystals," Oxford Press (1950), p. 243.
3) I. Kamiya, *J. Chem. Scc. Japan*, **76**, 960 (1955).

of these surfaces would orientate in all directions.

The number of inner-photo-electrons for arbitrary surfaces can be calculated in the following ways.

Let x be the direction of incident parallel beam of which the electric vector is in xy-plane (y being perpendicular to x) and z be the direction being perpendicular to x and y.

Then, if the direction cosines of the normal to this surface are $\cos\alpha$, $\sin\alpha\cos\beta$, and $\sin\alpha\sin\beta$ with respect to x, y and z, and y and z axes are rotated by β on yz-plane, let two new axes be called to y' and z' axes, then the xy'-plane will be the plane of incidence and xz'-plane will be the plane being perpendicular to the plane of incidence (Fig. 2).

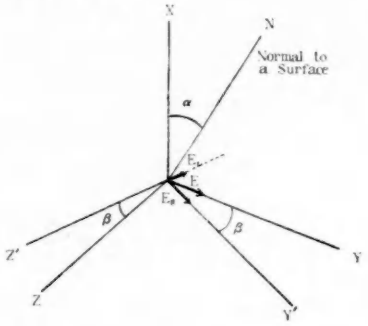

Fig. 1.

The electric vector of exposing light is divided into two components, one of which is in xy'plane (say $\boldsymbol{E}_{\parallel}$), and the other in xz'-plane (say $\boldsymbol{E}_{\perp}$).

Thus, the number of inner-photo-electrons due to $\boldsymbol{E}_{\parallel}$ can be obtained by the same method as before, that is,

$$J_{\parallel}' = \frac{R_0}{h\nu}\frac{\sin^2(\alpha+\alpha')\cos^2(\alpha-\alpha')}{\sin^2\alpha\sin^2\alpha'}\times\left(1-\sqrt{(\phi-\chi)/h\nu}\right)\times\left[1+\frac{3}{2}(2-\cos^2\alpha')\{\sqrt{(\phi-\chi)/h\nu}+(\phi-\chi)/h\nu\}\right]\boldsymbol{E}_{\parallel}^2 \quad (3)$$

and to $\boldsymbol{E}_{\perp}$,

$$J_{\perp}' = \frac{R_0}{h\nu}\frac{\sin^2\alpha\cos^2\alpha'}{\sin^2(\alpha+\alpha')}\left(1-\sqrt{(\phi-\chi)/h\nu}\right)\times\left[1-\frac{1}{2}\{\sqrt{(\phi-\chi)/h\nu}+(\phi-\chi)/h\nu\}\right]\boldsymbol{E}_{\perp}^2 \quad (4)$$

where α and α' are the angles of incidence and refraction. The relation between α and α' will be given as,

$$n_1\sin\alpha = n_2\sin\alpha'$$

in which n_1 is refractive index of silver chloride and n_2 is that of metallic silver.

Then, the total number of such electrons for all particles due to each component are given by the following formula,

To $\boldsymbol{E}_{\parallel}$,

$$J_{\parallel\,\mathrm{Tol}} = \int_0^{\pi}\int_0^{\pi/2}\frac{R_0}{h\nu}\left(1-\sqrt{(\phi-\chi)/h\nu}\right)\times\frac{\sin^2\alpha\sin^2\alpha'}{\sin^2(\alpha+\alpha')\cos^2(\alpha-\alpha')}\times\left[1+\frac{3}{2}(2-\cos^2\alpha')\{\sqrt{(\phi-\chi)/h\nu}+(\phi-\chi)/h\nu\}\right]\cos^2\beta\,d\alpha'd\beta \quad (5)$$

and to $\boldsymbol{E}_{\perp}$,

$$J_{\perp\,\mathrm{Tol}} = \int_0^{\pi}\int_0^{\pi/2}\frac{R_0}{h\nu}\left(1-\sqrt{(\phi-\chi)/h\nu}\right)\times\frac{\sin^2\alpha\cos^2\alpha'}{\sin^2(\alpha+\alpha')}\times\left[1-\frac{1}{2}\{\sqrt{(\phi-\chi)/h\nu}+(\phi-\chi)/h\nu\}\right]\sin^2\beta\,d\alpha'd\beta \quad (6)$$

where, for simplicity, the electric vector is taken to be a unit, so that $\boldsymbol{E}_{\parallel}=\cos\beta$ and $\boldsymbol{E}_{\perp}=\sin\beta$. Then, it is furthr put that n_2 is equal to $n_1/10$*, R_0 is independent on α'.

To these approximations, $J_{\parallel\,\mathrm{Tol}}$ and $J_{\perp\,\mathrm{Tol}}$ cnn be calculated by means of approximation integration using trapezoidal rule,

$$J_{\parallel\,\mathrm{Tol}} \fallingdotseq \frac{1-\sqrt{(\phi-\chi)/h\nu}}{h\nu}[0.13+0.27\{\sqrt{(\phi-\chi)/h\nu}+(\phi-\chi)/h\nu\}]R_0 \quad (7)$$

$$J_{\perp\,\mathrm{Tol}} \fallingdotseq \frac{1-\sqrt{(\phi-\chi)/h\nu}}{h\nu}[0.09-0.05\{\sqrt{(\phi-\chi)/h\nu}+(\phi-\chi)/h\nu\}]R_0 \quad (8)$$

After the absorption process, the silver specks will be gradually destroyed by the mechaism proposed by Mott and Gurney.

* The refractive indexes of metallic silver, silver chloride and silver bromide for $\lambda=656\,m\mu$ are given as 0.25, 2.05 and 2.23 respectively. J. W. Mellor, "A Comprehensive Trea- tise on Inorg. and Theor. Chem." Vol. III (1930), pp. 331, 396 and 421.

In order to calculated the rate of destruction of silver specks, it is assumed that the rate will depend on the concentration gradient of silver ions.

When the film in which n_0 particles of metallic silver have been contained is exposed to polarized red light, the number of silver ions produded in t minutes is given by the following formula, since the number of such ions is equal to that of inner-photo-electrons,

$$\left.\begin{aligned} n_{\parallel}' &= n_0\{1-\exp(-J_{\parallel \mathrm{Tol}}\cdot t)\} \quad \text{to } \boldsymbol{E}_{\parallel}, \\ n_{\perp}' &= n_0\{1-\exp(-J_{\perp \mathrm{Tol}}\cdot t)\} \quad \text{to } \boldsymbol{E}_{\perp}. \end{aligned}\right\} \tag{9}$$

Now, let dn be the amount of silver ions self-diffusing into silver chloride in time of dt, then this is shown as,

$$\mathrm{d}n = D\cdot S\cdot \Delta C \mathrm{d}t \tag{10}$$

where, S the contact area between silver ion and silver chloride, ΔC is the concentration gradient of these ions and D is diffusion constant.

In (10), it is further assumed that, S is independent on exposing time and ΔC is propotional to the number of producing ions by the assumption made before, then,

$$\Delta C = k\mathrm{d}[n_0\{1-\exp(-J_{\mathrm{Tol}}\cdot t)\}]/\mathrm{d}t$$
k: constant.

With this consideration, the remainded number of colloidal particles of metallic silver after t minutes' exposure is given,

$$n_{\parallel \mathrm{R}} = n_0 - \int_0^t DSk\mathrm{d}\{1-\exp(-J_{\parallel \mathrm{Tol}}\cdot t)\}/\mathrm{d}t\cdot \mathrm{d}t = n_0[1-DSk\{1-\exp\times(-J_{\parallel \mathrm{Tol}}\cdot t)\}] \quad \text{to } \boldsymbol{E}_{\parallel}, \tag{11}$$

$$n_{\perp \mathrm{R}} = n_0[1-DSk\{1-\exp(-J_{\perp \mathrm{Tol}}\cdot t)\}] \quad \text{to } \boldsymbol{E}_{\perp}. \tag{12}$$

Now, it may be taken that,

$$D = D_0\exp(-U/RT)$$

where, U is the diffusion energy of silver ion at the temperature of T° K, R is gas constant and D_0 is a constant, so that (11) and (12) will be, putting $K = D_0Sk$,

$$n_{\parallel \mathrm{R}} = n_0[1-K\{1-\exp(-J_{\parallel \mathrm{Tol}}\cdot t)\}\times\exp(-U/RT)] \tag{13}$$

$$n_{\perp \mathrm{R}} = n_0[1-K\{1-\exp(-J_{\perp \mathrm{Tol}}\cdot t)\}\times\exp(-U/RT)] \tag{14}$$

Now, if we measure the absorption of of the film, which has been exposed to polarized red light, with the light of which the electric vector is the same direction as that of exposed light, the intensity of the light after passing through the film is,

$$I_{\parallel} = I_0\exp\{-(\lambda_{\parallel}n_{\parallel \mathrm{R}} + \lambda_{\perp}n_{\perp \mathrm{R}})\} \tag{15}$$

with the light of which the electric vector is perpendicular to that of exposed light,

$$I_{\perp} = I_0\exp\{-(\lambda_{\perp}n_{\parallel \mathrm{R}} + \lambda_{\parallel}n_{\perp \mathrm{R}})\} \tag{16}$$

where, $\lambda_{\parallel}$ is the absorption coefficient when the electric vector of observed light is in the plane of incidence and $\lambda_{\perp}$ is that when the electric vector is perpendicular to the plane.

The value of photo-dichroism ($\boldsymbol{D}$) is defined[4] as,

$$\boldsymbol{D} = \ln I_{\parallel} - \ln I_{\perp} \tag{17}$$

hence, putting (15) and (16) into (17), we obtain as,

$$\boldsymbol{D} = (\lambda_{\parallel} - \lambda_{\perp})(n_{\perp \mathrm{R}} - n_{\parallel \mathrm{R}}) \tag{18}$$

Then, from (8), (9), (13) and (14), (18) is written as,

$$\boldsymbol{D} = n_0K(\lambda_{\parallel} - \lambda_{\perp}) \times [e^{-(1-\sqrt{(\phi-x)/h\nu})/k\nu\{0.09-0.05\sqrt{\sqrt{(\phi-x)/h\nu}+(\phi-x)/h\nu}\}R_0t} - e^{-(1-\sqrt{(\phi-x)/h\nu})/k\nu\{0.13+0.27\sqrt{\sqrt{(\phi-x)/h\nu}+(\phi-x)/h\nu}\}R_0t}] \times\exp(-U/RT) \tag{19}$$

TABLE I

THEORETICAL AND EXPERIMENTAL VALUES OF DICHROISM AGAINST THE TIME OF EXPOSURE

Wave length of measuring light (mμ)	Time of exposure (Min.) Parameters $n_0K(\lambda_{\parallel}-\lambda_{\perp})\exp(U/RT)$.	5 obs.	5 calcd.	15 obs.	15 calcd.	30 obs.	30 calcd.	60 obs.	60 cald.
680	135.4	18	15.2	38	39.7	62	65.4	83	91.4
640	353.5	45	39.6	114	103.7	159	170.8	205	238.4
620	444.9	62	65.4	136	145.2	227	239.1	334	333.9
540	−309.8	—	−37.8	—	−80.8	−152	−148.6	−206	−210.7
520	−227.2	−26	−25.5	—	−66.6	−103	−109.7	−162	−153.3

4) F, Weigert, *Z. Phys. Chem.*, **B3**, 389 (1929).

As seen from (19), D depends on the time of exposure (t), energy of exposing light ($h\nu$), temperature (T) and the wave length of measuring light. ($\lambda_{\parallel}-\lambda_{\perp}$).

With the experimental condition, we put $h\nu=1.8$ eV. and assume that $\phi-\chi$ is 1 eV[2]. and R_0 is equal to 1/2**, then (19) is deduced to be,

$$D=n_0K(\lambda_{\parallel}-\lambda_{\perp})\{\exp(-0.026\,t)-\exp(-0.002\,t)\}\exp(-U/RT) \quad (20)$$

In (20), if T is constant, D is the function of t and ($\lambda_{\parallel}-\lambda_{\perp}$). Thus, by taking ($\lambda_{\parallel}-\lambda_{\perp}$) to be the suitable parameter which is the function of the wave length of observed light, D can be plotted against t. These results are shown in Table I, where, it is found that the theoretical is in fairly good agreement with the experimental.

Furthermore, according to the author's theory, the activation energy of this dichroic change is explained as the diffusion energy of silver chloride, which has been known to be about 7000 cal/mol[5]. In the previous paper, the activation energy has been found to be of the order 7000 cal/mol[1].

From these evidences, it would be said that the author's theory might be permissible.

As has been shown, the parameter method can explain the behavior of dichroism against the time of exposure. This method, however, is not pemissible to solve the values observed with the light of which the wave lengths are in the region between 550 and 580 mμ. As illustrated in Fig. 3, the continuous curves obtained by means of the parameter method are in good agreement with experimental results in the region more than 580 mμ and less than 550 mμ. (being shown as triangle points). This agreement, however, is not satisfactory in the region between 550 and 580 mμ as seen in Fig. 3 (dotted lines).

This will probably be due to the fact that the values of ($\lambda_{\parallel}-\lambda_{\perp}$) are not independent to the time of exposure. This is to be discussed in the next paper.

It has been found that, when the film is exposed to the light of which the wave length is 630 mμ, the value which is observed with this wave length is larger than that with any other wave length, and if exposed to green light, the value

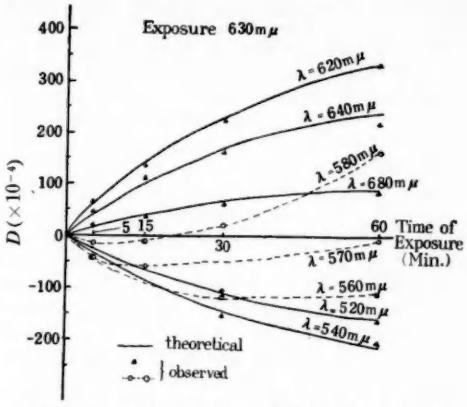

Fig. 3. The curves of theoretical and experimental values of D against the time of exposure.

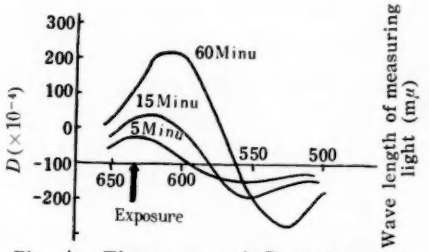

Fig. 4. The curves of D against the wave length of measuring light for exposure to 630 mμ.

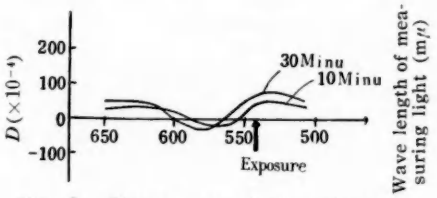

Fig. 5. The curves of D against the wave length of measuring light for exposure to 540 mμ.

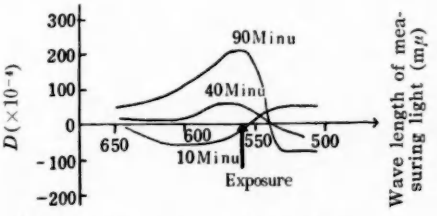

Fig. 6. The curves of D against the wave length of measuring light for exposure to 560 mμ.

5) Ref, (2) p. 47.

** Being A equal to π, R_0 is to be 1/2 for larger value of α.

observed with green light is maximum and so on. In Figs. 4, 5 and 6, the observed values of dichroism with various wave lengths are shown for the films which are exposed to 630, 540 and 500 mμ respectively, in which the ordinates denote the degree of dichroism and the abscissa the wave length of observed light.

This phenomenon is termed "Color adaptation of photo-dichroism.

The phenomenon of photo-dichroism shows further peculiar behavior. The maximum point, corresponding to color adaptation, is shifted to a shorter wave length region by increasing the exposure. The values in the green region become negative for the film which is exposed to red light, whereas the values in red region become negative for one exposed to green light. These are shown in Figs. 4 and 5. This is called "Inversion effect of photo-dichroism."

Every kind of behavior can not be solved by means of the parameter method. That is, it is recessary to study the variation of $(\lambda_{\parallel}-\lambda_{\perp})$ in order to investigate these complicated kinds of behavior.

From the above point of view, the author is going to investigate the absorption spectra of the films of printed-out silver in various conditions so that these kinds of behavior may be explained by the changing of absorption coefficients.

The author wishes to express his thanks to the late Prof. J. Shidei and Dr. D. Yamamoto for their kind advice.

Department General Education, Nagoya University, Nagoya

Photo-dichroism of Printed-out Silver. III. Absorption Spectra and Dichroism

By Isao KAMIYA

(Received August 9, 1956)

According to the theory which has been developed by the author, the phenomenon of photo-dichroism is probably an anisotropic Herschel effect and when the film of printed-out silver is exposed to linear polarized red light of energy 1.8 eV. for t minutes at $T°$ K, the value of dichroism is given by the following equation,

$$D=n_0K(\lambda_{\parallel}-\lambda_{\perp})\{\exp(0.002\,t)-\exp(-0.026\,t)\}\exp(-U/RT) \qquad (1)$$

where $\lambda_{\parallel}$ and $\lambda_{\perp}$ are the absorption coefficients of the lightof which the electric vectors are in the plane of incidence and perpendicular to the plane. (This plane is constructed with the incident ray and the normal to the surface of colloidal silver). U is activation energy, R is gas constant and n_0K is constant.

When T is constant, with suitable values of parameter $n_0Ke^{-U/RT}(\lambda_{\parallel}-\lambda_{\perp})$, (1) gives curves of D against the time of exposure closely resembling the experimental results, as has been shown in a previous paper[1]. The method of calculating D with the parameter has been called the parameter method.

This parameter method, however. was not acceptable to calculate the values observed with the light of which wave lengths are in the region between 580 mμ and 550 mμ.

This is probably due to the fact that $(\lambda_{\parallel}-\lambda_{\perp})$ is no longer taken to be independent of the time of exposure in this case.

Moreover, the treatment using this method did not say anything about the complicated phenomena such as *Color-adaptation* and *Inversion effect*, for, in order to explain these phenomena, the variation of $(\lambda_{\parallel}-\gamma_{\perp})$ under the action of exposing light must be considered.

From this point of view, the author has investigated the question if the variation of absorption spectrum of the film of printed-out silver is found when exposed to red or orenge light.

Actually, there appeared a new absorption spectrum in the film after prolonged exposure to red or orange light.

A possible explanation of this appearance of the new absorption spectrum could

1) I. Kamiya, This Bulletin, **30**, 294 (1957).

be given when it is assumed that the process would be an anisotropic Herschel effect.

It has been also found that the absorption difference curve by subtracting the absorption curve of an exposed film from of an unexposed one is very similar to the obsorved spectral dispersion curve of dichoroism. Then the author has been able to explain the processes of *Color-adaptation* and *Inversion effect* as well as of the peculiar behavior of the values of dichroism observed with the light of which the wave lengths are in the region between 580 mμ and 550 mμ, which is his main purpose in this paper, assuming that the phenomenon of photo-dichroism would be a results of difference in absorption of two systems, one is that before exposure and the other is that after exposure.

Experimental

The films of Valenta's emulsion were prepared by the same method as described by Weigert[2].

One of these was washed by water so that it was almost free from all soluble silver salts (such as silver nitrate and organic silver compounds), let this plate be called "washed plate". The other was unwashed: called "unwashed plate".

Then, the absorption curves were measured by use of Beckmann-type spectrophotometer under various conditions as the following:

1. The absorption curve of washed plate of printed-out silver which had been illuminated with ultra-violet light of Hg-lamp was measured, and after that time that of the washed plate after being exposed to strong natural red light (630 mμ) was measured. The measurements are shown in Fig. 1, where the continuous line (a) and broken one (b) denote the absorption curves before and after exposure respectivery.

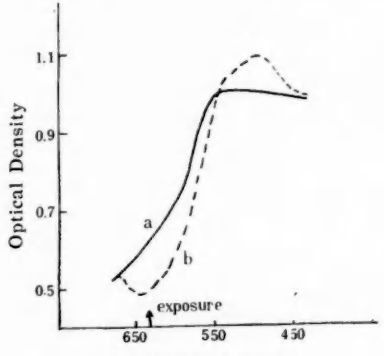

Fig. 1. Absorption curves of washed plate.
a: before exposure,
b: after exposure to 630 mμ.

A five ampere carbon are and glass filter of 620–640 mμ spectral region (Shimazu, No. 63) were used as exposing red light source.

2. The curves of the unwashed plate were also measured under the same conditions as that of the washed plate by the same way as described above, which are shown in Fig. 2, where the descriptions are the same as those in Fig. 1. As shown in Fig. 1 and Fig. 2. there can be seen the remarkable *Color-adaptation*, that is, the plates which have been exposed to red light are transparent in red light.

The curves obtained under other conditions (such as under exposure to orange light) are to be shown in the next section.

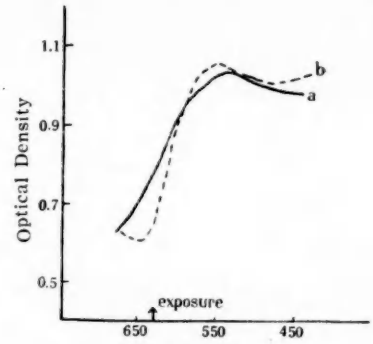

Fig. 2. Absorption curves of unwashed plate.
a: before exposure,
b: after exposure to 630 mμ.

Discussion

After per-illumination with ultra-violet light, the film of Valenta's emulsion which bad been almost transparent turned brown at first, then became dark red.

This coloring metter, a new absorption band appearing in visible region, is attributed to the formation of colloidal particles of metallic silver[3].

According to Freundlich[4], the absorption spectra of colloidal particles of metallic siver depend on the dimensions of these particles and the maxima of the spectra shift to the shorter wave length side as the dimension become smaller. In Table I, the relation between diameters of the perticles and transmitted light is illustrated.

As seen in Fig. 1 and 2, the transparency of red light increases after exposed to red light (*Color-adaptation*).

2) F. Weigert, *Ann. Physik*, **63**, 685 (1920).

3) R. Hilsch and R. W. Pohol, *Z. Phys.*, **77**, 42 (1933).

4) H. Freundlich, "Kapillarchemie", **I**, Leipzig (1932). P. P. 32.

TABLE I
RELATION BETWEEN DIAMETER AND TRANSMITTED LIGHT OF COLLOIDAL SILVER PARTICLES

Diameter of colloidal silver particles in mμ	Transmitted light
25—35	red
35—45	red—violet
50—60	blue—violet
70—80	blue

This may be due to the following mechanism.

When the particles of metallic silver are exposed to red light, the comparative large particles which are sensitive to red light will absorb the light and be destroyed causing Herschel effect so that the transparency in red light increases[1].

Tallert[5], in the study of Herschel effect, has concluded that colloidal particles of metallic silver do nothing but break up into smaller and more numerous parts by Herschel effect. On account of this, the opacity of the film increases in green region by such re-distributed particles which are the most sensitive to green light.

Next, if the absorption difference curve by substructing the absorption curve of exposed film from that of non-exposed one is made, i. e. the curve of (b)—(a) in Fig. 1 or 2, this is almost similar to the spectrometric dichroism curve.

In Figs. 3 and 4, the difference curves and observed dichroism curves of the washed plate and the unwashed plate are shown, where the upper curve donotes the dichroism curve and the lower the difference curve. The dichroism and difference curves of unwashed plate are almost similar to those of washed plate, but are displaced somewhat in the direction of the long wave length side.

This might be due to the difference of absorption spectra between washed and unwashed plates.

This similarity is also found when the film is exposed to strong orange light (580 mμ). The absorption curves after and before exposure are shown in Fig. 5, where

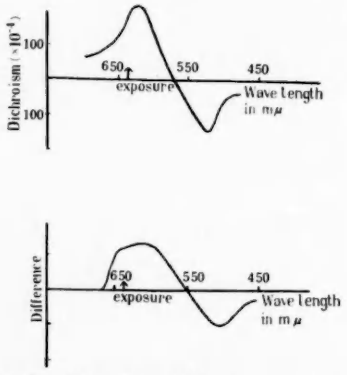

Fig. 3. Absorption difference curve and dichroism curve of washed plate when exposed to 630 mμ.

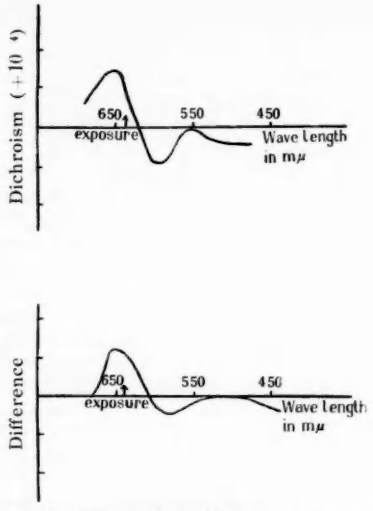

Fig. 4. Absorption difference curve and dichroism curve of unwashed plate when exposed to 630 mμ.

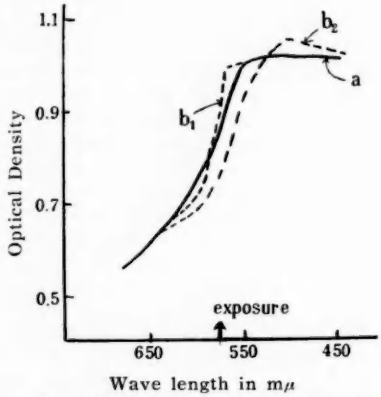

Fig. 5. Absorption curves of washed plates.
a: before exposure-
b_1: after 20 minutes' exposure,
b_2: after 90 minutes' exposure to 580 mμ.

5) H. Tallert, *Z. phys. Chem.*, **140**, 355 (1929).

(a) is the absorption curve of the washed plate before exposure, (b_1) and (b_2) are those after exposure for 20 and 90 minutes. Thus the absorption difference curves for 20 and 90 minutes' exposure were obtained as before.

In Fig. 5, these difference curves are shown. It is found that these curves are fairly analogous to dichroism curves (when exposed to linear polarized orange light), which are shown in Fig. 6.

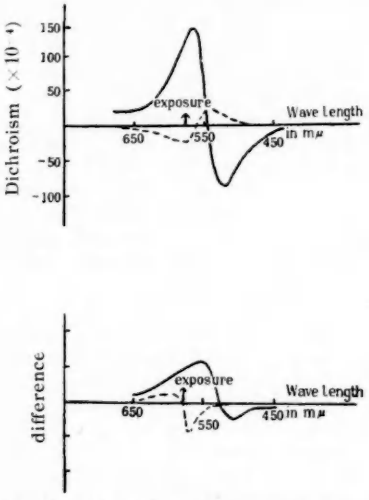

Fig. 6. Absorption difference curve and dichroism curve of washed plate when exposed to 580 mμ.
---: after 20 minutes' exposure,
——: after 90 minutes' exposure.

A five ampere carbon arc and a glass filter of 580 mμ and 600 mμ spectral region were used as orange light source.

It should be noticed here that the absorption difference curve is not color-adaptable in the beginning of exposure as the dichroism curve also is.

These results should be kept in mind for it proves to be explained that the photo-dichroism may be a results of difference in absorption between, after and before exposure.

From such a point of view, it is to be assumed that the absorption coefficients of the film before and after exposure might be similar to $a_\perp$ and a respectively if the vectrial absorption coefficient having component $a_\perp$ and a is perpendicular and parallel to the electric vector of exposing light.

In the previous paper[2], the author has described the phenomenon that the values of dichroism observed using the light of which the wave lengths are in the region between 580 mμ and 550 mμ can not be explained by the parameter method.

By the above assumption, the question, what causes this behavior, can be answered by considering the following mechanism.

The absorption curve of Valenta's plate is to be taken as (a) in Fig. 1 and if the same plate is exposed to red light, the colloidal perticles of metallic silver which are sensitive to red light are re-distributed causing Herschel effect; at the first step of the process the destruction would occur a little as shown as (b_1) in Fig. 7. By increasing exposure, the absorption will change from (b_1) to (b_2) and then to (b_3) in Fig. 7 owing to the fact that further destruction takes place.

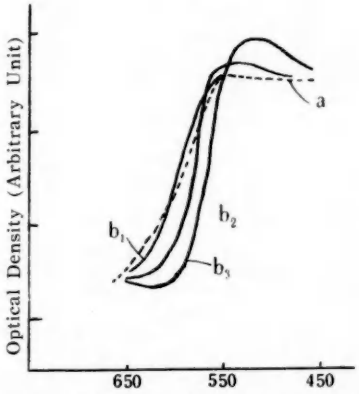

Fig. 7. Schematic changes of absorption curve by increasing exposure to red light.
a: before exposure
b_1, b_2, b_3: after exposure.
The curve will be changed b_1, b_2 and b_3 by exposing.

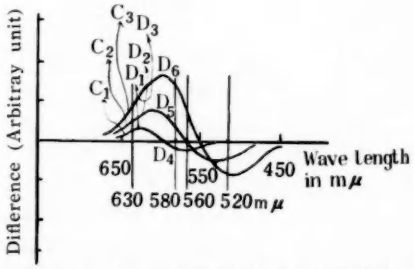

Fig. 8. Schematic absorption difference curve under various time of exposure to red light.
The curve will be changed as c_1, c_2 and c_3 by exposing.

From (a) and (b_1), (b_2), (b_3), the absorption difference curves in each case can be obtained, which are shown as (c_1), (c_2) and (c_3) in Fig. 8.

If the absorption difference curves are treated as dichroism curves, the theoretical values of dichroism against the time of exposure can be obtained by the following method.

When the lines perpendicular to abscissa at the points of 630 mμ, 570 mμ, 560 mμ and 520 mμ are drawn, and the crossing points of these lines to the absorption difference curves in Fig. 8 are denoted as D_1, D_2, D_3, D_4……, these points will be taken as the values of dichroism against the time of exposure and thus semi-quantitative curves observed with 630 mμ, 570 mμ, 560 mμ and 520 mμ can be obtained, which are illustrated in Fig. 9.

The experimental dichroism curves against the time of exposure measured with 630 mμ, 570 mμ, 560 mμ and 520 mμ are also shown in Fig. 10.

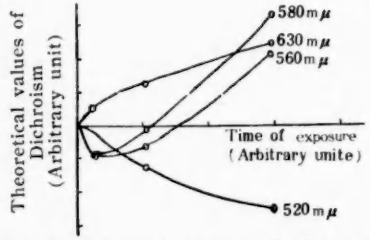

Fig. 9. Schematic change of absorption difference values against the time of exposure under various wave length of measuring light.

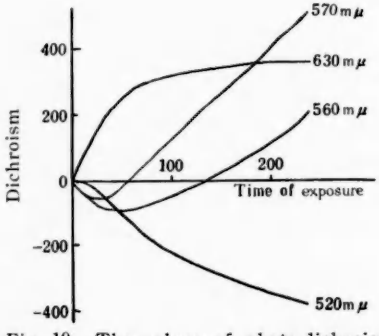

Fig. 10, The values of photo-dichroism against the time of exposure under various wave length of measuring light.

It will be seen that the experimental curves correspond to th theoretical. Thus, it can be concluded that when the film of Valenta's emulsion is exposed to 630 mμ, the comparative large particles which are sensitive to the light will be destoyed and broken up into smaller particles which are sensitive to green light, so that the absorption of the film after exposure to the light will be decreased in the red and increased in the green region, and thus the parameter method is useful.

On the other hand, the amount of colloidal silver which is sensitive to orange light will be increased at the beginning of exposure to 630 mμ because some of collidal particles which are sensitive to red light will change to somewhat smaller particles, so that the values of dichroism are negative when observed with orange light at first, where-by for a long-time exposure the number of the particles which are sensitive to orange light will be descreased because these particles would be sensitive and destroyed more or less when exposed to red light, so that the values turned to positive for a long time.

This is the answer to the question why the parameter method is not useful to explain the behavior of the values observed with the light of which the wave lengths are in the region between 580 mμ and 550 mμ.

From these evidences, the conclusion that the phenomenon of photo-dichoroism of printed-out silver would be produced by the same mechanism as that of Herschel effect might be permissible.

However, the question why the difference curve is analogous to that of dichroism has not been discussed.

Unfortunately, the absorption difference curve obtained by exposure with blue light was too different from the dichroism curve to make such a simple assumption.

This is probably due to the following possible events.

When the film is exposed to blue light, the photolytic process may take place to produce the colloidal particles of metallic silver or *Induced photo-dichoroism* may be caused in the system.

On this reason, the discussion has to be limited to the case when the film is exposed to red or orange light by which the photolysis or *Induced photo-dichoroism* does not occur.

The author wishes to express his thanks to the late Prof. J. Shidei and Dr. D. Yamamoto for their kind advice.

Department of General Education, Nagoya University, Nagoya

SHORT COMMUNICATIONS

Polarographic Determinations of Minute Quantities of Lead in High-Purity Electrolytic Zinc Using the Rotated Dropping Mercury Electrode

By Nobuyuki TANAKA and Toshiko KOIZUMI

(Received December 12, 1956)

The polarographic method with a dropping mercury electrode (DME) has been widely employed for the determination of minute quantities of lead contained in high-purity electrolytic zinc. The method, though fairly accurate, is often questioned because of its insufficient sensitivity. Recently W. Stricks and I. M. Kolthoff devised a new electrode in polarography, called rotated dropping mercury electrode (RDME), and reported an extensive fundamental work on the characteristics of the electrode and also on the polarography at the electrode[1]. Because of its high sensitivity, the RDME has been applied to the polarographic determination of minute quantities of lead contained in high-purity electrolytic zinc.

The electrode used in this study was similar to that reported by Stricks and Kolthoff[1], which was driven by means of a synchronous motor (Type A, provided with gears for speeds of 100, 150, 200, 300 r. p. m., constructed by Yanagimoto Co.), and had the characteristics of 4.957 mg./sec. for m and 7.22, 5.72 and 3.54 sec. for t at 100, 150 and 200 r. p. m., respectively, being measured in deaerated 0.1 M potassium chloride solution at 40.0 ± 0.1 cm. of mercury head with open circuit. A saturated calomel electrode was used for a reference electrode. Current-voltage curves were measured with Yanagimoto pen-recording polarograph Model PB-4. All measurements were carried out in a thermostat of 25° ± 0.1°C.

Current-voltage curves were obtained with various concentrations of lead in deaerated 0.1 M and 1 M sodium chloride solutions containing 5×10^{-6} M polyoxyethylene lauryl ether (LEO) as a maximum suppressor. A proportionality was obtained between the concentration of lead and the limiting current. The best reproducibility was found at 100 r. p. m. as shown in Table I, although the i_l/c value was the highest at 150 r. p. m.

TABLE I

LIMITING CURRENTS OF LEAD IONS IN 0.1 M KCl − 5×10^{-6} M LEO

Conc. of Pb(II), M	i_l, μ amp.	i_l/c, μ amp./10^{-4} M
2.94×10^{-7}	0.017_2	5.8_2
0.979×10^{-6}	0.057_5	5.8_4
2.94×10^{-6}	0.172	5.8_3
0.979×10^{-5}	0.573	5.86
2.94×10^{-5}	1.70_4	5.80
0.979×10^{-4}	5.71	5.83
2.94×10^{-4}	17.03	5.80

In deaerated 1 M zinc chloride solutions containing 5×10^{-6} M LEO the i_l/c value for lead was also found constant in the concentration range investigated, but somewhat smaller than those in 0.1 M and 1 M potassium chloride solutions. High-purity electrolytic zinc was dissolved in concentrated hydrochloric acid and the excess of the acid was removed by evaporation. The residue was dissolved into distilled water containing 5×10^{-6} M LEO to make 1 M in concentration in regard to zinc chloride. The concentration of lead was determined directly from the i_l/c value obtained for lead in 1 M zinc chloride and also by the standard addition method. In Table II are given some of the results obtained, which

TABLE II

LEAD CONTENT IN HIGH-PURITY ELECTROLYTIC ZINC

Sample	Content of Lead found, %	
	from the i_l/c value	by standard addition method
No. 1	0.0007_1	0.0007_1
No. 4	0.0012_0	0.0011_8
No. 6	0.0015_8	0.0015_4
No. 8	0.0013_7	0.0013_6
No. 9	0.0011_7	0.0011_2
No. 10	0.0001_3	0.0001_3

contain the determination of lead down to 0.0001 % in content of electrolytic zinc. Further studies on the characteristics of the RDME and on other applications will be reported in subsequent publications.

The authors would like to express their gratitude to Dr. I. M. Kolthoff for his advice in this study. They also thank

1) W. Stricks and I. M. Kolthoff, *J. Am. Chem. Soc.*, **78**, 2085 (1956); See also, Nobuyuki Tanaka, *J. Japan. Chem.*, **10**, 814 (1956).

the Ministry of Education for the financial support of this research.

Department of Chemistry
Faculty of Science
Tohoku University, Sendai

Structure of Compound A, a Hydrolysis Product of Roseothricin A

By Toshio GOTO,* Yosimasa HIRATA,* Seigo HOSOYA** and Nobuhiko KOMATSU**

(Received November 10, 1956)

Roseothricin is a streptothricin-like complex antibiotic, produced by *Streptomyces Roseochromogenus*[1] and has been separated into three components, roseothricin A, B and C, by means of ion exchange chromatography[2]. Chemical investigations have been undertaken on roseothricin A.

Acid hydrolysis of roseothricin A afforded two β-amino acids, β-lysine (I) and roseonine (II), as reported previously,[3] and a glucosamine-like sudstance (III) with properties as follows: crystalline hydrochloride, dec. p. 145–155°C, paper chromatography BuOH : AcOH : H_2O (4 : 1 : 1) Rf. 0.33 (glucosamine 0.33, chondrosamine 0.25), collidine 0.44 (G. 0.43, C. 0.35), phenol : NH_3 0.74 (G. 0.70, C. 0.64), AcOEt : pyridine : H_2O (2 : 1 : 2) 0.86 (G. 0.87), Me COEt 0.03 (G. 0.03), Fehling, triphenyltetrazolium, ninhydrin, Elson-Morgan and Tollens reactions are positive like glucosamine; $\nu_{max.}^{KBr}$ (III. HCl) 1605 m, 1498m, 1404m, 1332 w, 1319 w, 1253 w, 1230 w, 1149 m, 1121s, 1100 s, 1070 s, 1040 s cm^{-1} (s: strong, m: medium, w: weak). The infrared spectrum is slightly different from that of glucosamine, but bands at 1605 and 1498[4] due to a primary amino group are present and the shape of the absorption at 1100-1000 (alcoholic hydroxyl) is very similar to that of glucosamine. It is almost indistinguishable from glucosamine by means of paper chromatography, and these facts together with the analytical data of compound A strongly suggest that substance III is a stereoisomer of glucosamine.

Compound A, colorless needles, dec. p. 215–220°C, which consists of II and III, was obtained as one of the acid hydrolysis products of roseothricin A. Counter current distribution (CCD) (BuOH : MeOH: AcOH : H_2O, 18 : 2 : 1 : 19) of the partial DNP (2, 4-dinitrophenyl) product of compound A afforded two peaks at K=0.16 and 9.0, as measured by the absorption at 350 mμ. From the number of the peaks it may be deduced that two amino groups capable of being DNP-ated exist in one molecule of compound A. The product of complete DNP-ation, DNP-compound A, m. p. 192–196°C (dec.), had an $E_{1\,cm.}^{1\%}$ value of 306 at 350 mμ[5] and the molecular wight calculated on the assumption of the presence of twe amino groups is ca. 682.[6] Analytical, pKa', I. R., and other data point to 1 : 1 ratio of II and III in the compound A. Found: C, 32.65; H, 6.25; N, 16.12. Calcd. for $C_{24}H_{44}O_{13}N_{10}$. 6HCl (2 moles each of II and III minus $3H_2O$; mol. wt., 680.67[6]) : C, 32.05; H. 5.60; N, 15.57%. Compound A has eight pKa's; to at ca. 2.4 (II-CO_2H), to at 6.5 (III-NH_3^+),[7] two at 8.9 (II β-NH_3^+) and two at 10.4 (II guanidinium). The mol. wt. obtained from this potentiometric curve is ca.645.[6] $\nu_{max.}^{KBr}$ (compound A. HCl) 1732 m (-CO_2H[8]), 1658 s (sym. trisubstituted guanidine band[9]), 1609 m, and 1490 m, br (-NH_3^+ of both II and III), 1405 m, 1388 m, 1220 m, br, 1075 s, and 1054 s, cm^{-1} (br: broad). Since 5.96 moles of periodate are consumed by 1 mole of compound A, it is suggested that C_2-NH_2, C_3-and C_4-OH of III, and the β-NH_2 and OH of II in compound A may all be free.

1) S. Hosoya, M. Soeda, N. Komatsu, S. Imamura, M. Iwasaki, Y. Sonoda and K. Okada, *Jap. J. Exptl. Med.*, **20**, 121 (1949); *J. Antibiotics*, **3**, (4), 217 (1950).
2) Y. Saburi, *J. Antibiotics*, **6**, (8), 402 (1953).
3) K. Nakanishi, T. Ito, M. Ohashi, I. Morimoto and Y. Hirata. *J. Am. Chem. Soc.* **76**, 2843 (1954); This Bulletin, **27**, 539 (1954); ibid., submitted for publication.
4) K. Nakanishi, T. Goto, M. Ohashi, this Bulletin, submitted for publication.
5) Calculation was made as ε=15500 (at 350 mμ) per one mole of DNP group.
6) Molecular weight as free base.
7) The reason that these amino groups are not DNP-ated, is that rate of DNP-ation of III-NH_2 is much slower than that of II β-NH_2, and DNP-ation of III-NH_2 is prevented by precipitation of DNP-compound A.
8) The fact that it is not an ester may be deduced from the following. When trimethylamine is added to compound A and the mixture is immediately evaporated to dryness, this band is absent and a band at ca. 1600 cm^{-1} due to a carboxylate group is seen. Furthermore, this band is absent in DNP-compound A; similar to the case of DNP-roseonine, this is due to the fact that the guanidine portion cannot be DNP-ated and forms an intramolecular salt with this carboxyl group. This corresponds to the two pka' values at 2.4.
9) N N'-Disubstituted guanidine hydrochlorides possess, two strong absorptions at 1680 and 1600 cm^{-1} (roseonine-2HCl, 1682, 1581), whereas N. N', N''-trisubstituted guanidine hydrochlorides possess only one strong absorption at ca. 1650 cm^{-1}. On the other hand, N, N, N'-trisubstituted guanidine hydrochlorides show three bands at 1650s, 1620s, and 1570m cm^{-1}. Hence the guanidine group in compound A is symmetrically trisubstituted, i. e., the 2'-amino group is linked to some other group (T. Goto, K. Nakanishi, this Bulletin, submitted for publication).

Compound A, therefore, contains a N-glucoside linkage; the Elson-Morgan reaction is positive, but the Fehling reaction is negative, and the tetrazolium reaction becomes positive after longer heating period than that of III. The strong electron attractive effect of the guanidinium ion probably accounts for the lower pKa' of compound A (6.5) than that of III (7.8). The fact that the linkage between II and III

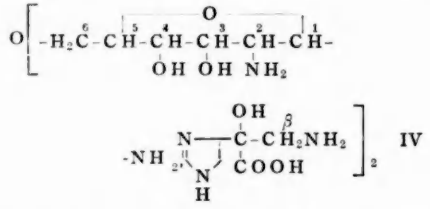

IV

is more stable under acidic conditions than alkaline is also explicable in terms of this effect. Compound A is extremely resistant towards acid hydrolysis; i. e., no appreciable hydrolysis occurred upon heating for 22 days with concentrated hydrochloric acid at 34°, and ca. 15% was hydrolysed upon heating for 11 days with 20% hydrochloric acid at 50°. This difficulty in hydrolysis points to the absence of an acetal linkage. Ester or amide bands were not observable in the region 1750–1500 cm^{-1}. These together with the amount of periodic acid consumption suggested that a primary hydroxyl group participates in an ether linkage. We wish to present IV for compound A.

We wish to thank Dr. K. Nakanishi for his advice in this research, and the Sanyo Pharmaceutical Co. for preparing a portion of roseothricin.

*Chemical Institute, Nagoya University Chikusa, Nagoya
**Institute for Infectious Diseases, Tokyo Univ., Minato. Tokyo

Papers Published in the Journal of the Chemical Society of Japan, Pure Chemistry Section

(Printed in Japanese)

Vol. 78, No. 2 (February, 1957)

H. KAKIYAMA: Monolayer Studies of Tanning Effect. I.

K. KURODA: X-ray Study of Two Component Mixture of Fatty Acid Amides.

T. KOTSUKA: Studies on the Cohesion of the Ideal Liquid. I~II.

K. SAKAI: Physico-Chemical Properties of Fused Salts. VIII.

S. SHISHIDO et al.: The Spinnability of Liquids. I.

H. TSUBOMURA: Electronic Structures of the Heterocyclic Compounds. I.

M. HAYASHI: Skeletal Deformation Vibrations and Molecular Forms of *n*-Pentane Type Molecules.

K. MIURA et al.: Surface Films of Nucleic Acid.

S. MIYAZAKI et al.: Studies on the Decompositions of H_2O by High Frequency Glow Discharge. I.

S. MIYAZAKI et al.: Studies on the Decomposition of NH_3 Gas by High Frequency Glow Discharge. II.

N. YAMADA: Kinetics of Vinyl Acetate Vapor Phase Synthesis.

N. YUI et al: Concentration of Acid Mixtures and their pH. II.

T. INOUE et al.: The Reduction of Potassium Permanganate by Potassium Amide and Disproportionation of Potassium Manganate to Potassium Permanganate and Manganese Dioxide in Liquid Ammonia.

I. HOSOKAWA et al.: Chemical Studies on the Shallow Deposits. IV.

K. WATANABE: Studies on the Platinum Group. IX.

H. NAGAI: Precipitation Paper Chromatography of Inorganic Cations with 8-Quinolinol. IV.

K. IKEDA: Isomerism and polymorphism of *p*-Nitro-*p'*-Methoxy-Dibenzoylmethane Enol-ethers.

K. IKEDA: Isomerism and Polymorphism of Dibenzoylmethane Enol-ethers. III.

E. IWATA: On the *o*-, *m*- and *p*-Substitution Reaction. VIII~X.

T. KUBOTA: Spectrochemical Studies on the Molecular Complexes of Pyridine 1-Oxide and Its Methyl Derivatives with Iodine.

H. SASAKI: A Synthesis of DL-Serine.

T. SIMADATE et al.: Synthesis of Adenosine.

M. TAKATORI et al.: Studies of Flavanone. XX.

Y. NAKAYAMA et al.: γ-Methyleneglutamic Acid. II.

K. MAYUMI et al: Study on the Vinylidene Chloride Resin. VI~VII.

J. MIYAMOTO et al.: On the Cobalt Metabolism of Micro-organism. III.

S. MOROSAWA: On the Portion Assumed to be Tetrodonin by Tahara in the Ovaries of Globefish.

T. YAMASAKI: On the Reaction between Phosphorus Pentasulfide and Aromatic Alcohol.

H. YŪKI et al.: On the Synthesis of Polytyrosine.

H. YŪKI et al.: Synthetic Amphoteric Polypeptides. VII~VIII.

D. YAMAMOTO: On the Creeping of Decalin Solution.

E. KUROSAWA: A New Method for the Preparation of Acylhydroquinones.